DETECTION OF SUBTLE IMMUNE DEFECTS IN INDIVIDUALS AT RISK OF PNEUMOCOCCAL DISEASE

Thesis submitted by
Furaha Florence Asani

For

The degree of Doctor of Philosophy

Department of Infection, Immunity and Cardiovascular
Disease
The Medical School
Faculty of Medicine, Dentistry and Health

October 2017

For Dr. Roger Kalume Asani

And

Professor Andy Heath

Who were two great men of Science.

SUMMARY

Immunocompromised individuals are at increased risk of developing invasive pneumococcal disease (IPD). We have previously shown that IPD sufferers have defective *in vitro* B-cell responses to a T-independent antigen mimic (αδdex), relative to healthy controls. We hypothesized that similar defects will be found in HIV-infected individuals, who continue to be at greater risk of IPD despite antiretroviral therapy, and in Monoclonal Gammopathy of Undetermined Significance (MGUS) patients.

Lymphocytes enriched from whole blood were cultured with αδdex alone and combined with anti-CD3, to assess both direct T- and B-cell effects, and T-cell help to B-cells. T- and B-cell activation and proliferation were assessed using standardised flow cytometry. B-cell subsets were stratified by CD19, CD10, CD20, CD21 and CD27 into plasmablasts, activated memory cells, resting memory cells, naive, and tissue-like memory cells.

Results from 16 HIV-infected individuals [mean CD4 count 677.63/mm^3, undetectable viral loads] showed no change in overall CD19+ B-cell activation but increased proliferation upon T-cell-helped pneumococcal-stimulation, compared to age-, sex- and ethnicity-matched controls. However, αδdex elicited significantly higher ($p \leq 0.05$) activation in plasmablasts in HIV-infected individuals compared to healthy controls. Furthermore, MGUS patients expressed significantly lower CD25 on CD8+ T-cells compared to healthy controls, following stimulation with anti-CD3 and anti-CD28 ($p \leq 0.01$). Age, sex and ethnicity were also found to influence T- and B-cell responses to polyclonal-stimulation in healthy individuals.

Although activation of CD19+ B-cells was similar between HIV-infected adults and healthy controls, polyclonal B-cell stimulation reveals a persisting hyperactivation defect in the plasmablast B-cell compartment in HIV infection despite virological suppression. The findings in this study may indicate impaired immune control of pathogens such as *S. pneumoniae* in immunocompromised individuals.

Thank you,

To the Teachers

Not one word has ever been wasted. Those that have gone unused in the stories carved in Science have been used through other creative mediums. And all these stories have needed telling.

To the Tempest

Ars longa, vita brevis. Life and death fall within the continuum of existence. And legacies and energies and Trinities will forever hold us as one. We may be broken multiple times but life is the Art of putting together broken pieces into beautiful new forms.

To the Temples

From the chimes of the town hall that sang me lullabies to the various homes that have shrouded me with safety. The inanimate are often the best of friends.

And finally, to the Testimony ahead.

'The best is yet to come...'
-   Carolyn Leigh

Chapter One

Chapter Six

αδdex	Anti-IgD conjugated dextran
AIDS	Acquired Immune Deficiency Syndrome
AM	Activated Memory Cells
APC	Antigen presenting cell
APO-1	Apoptosis antigen-1
ART	Antiretroviral Therapy
ASC	Antibody-secreting cell
BAL	Broncheoalveolar lavage
BCR	B-cell receptor
cART	Combination Antiretroviral Therapy
CD	Cluster of Differentiation
CDC	Centers for Disease Control and Prevention
CFSE	Carboxyfluorescein diacetate succinimidyl ester
CRM_{197}	Non-toxic Diphtheria toxin mutant
FACS	Fluorescence activated cell sorting
FCRL4	Fc receptor-like protein 4
FMO	Fluorescence-Minus-One
FSC-A	Forward scatter area
GALT	Gut-associated lymphoid tissue
HAART	Highly Active Antiretroviral Therapy
HCMV	Human Cytomegalovirus
HIV	Human Immunodeficieny Virus
HKD39	Heat-killed *Streptococcus pneumoniae* D39 strain
IgA	Immunoglobulin class A
IgD	Immunoglobulin class D
IgG	Immunoglobulin class G
IgM	Immunoglobulin class M
IFN-γ	Interferon gamma
IL	Interleukin
IPD	Invasive Pneumococcal Disease
JCVI	Joint Committee on Vaccination and Immunisation
KC	Keratinocyte-derived chemokine
MenC	Meningococcal C
MFI	Median fluorescence intensity
MGUS	Monoclonal Gammopathy of Undetermined Significance
MHC	Major histocompatibility complex proteins
MOI	Multiplicity of infection
MM	Mutliple Myeloma
M. tuberculosis	*Mycobacterium tuberculosis*
NHS	National Health Service
NOD	Nucleotide-binding oligomerisation domain-like receptors
N. meningitidis	*Neisseria meningitidis*
NF-κB	Nuclear factor kappa-light-chain-enhancer of activated B-cells
NVT	Non-vaccine-type pneumococci
PB	Plasmablasts
PBMC	Peripheral blood mononuclear cells
PBS	Phosphate buffered saline
PCV	Pneumococcal Conjugate Vaccine

PD-1	Programmed cell death protein 1
PPV	Pneumococcal Pneumococcal Vaccine
RHH	Royal Hallamshire Hospital
RM	Resting Memory Cells
RPMI	Roswell Park Memorial Institute medium
SSC-A	Side scatter area
S. pneumoniae	*Streptococcus pneumoniae*
STH	Sheffield Teaching Hospitals
TCR	T-cell receptor
TD	T-cell dependent
Tfh	T follicular helper cell
T_H	Helper T-cell
T_H1	Helper T-cell subset 1
T_H17	Helper T-cell subset 17
TI	T-cell independent
TLM	Tissue-like Memory Cells
TLR	Toll-like receptor
TNF	Tumour necrosis factor
µl	Microliter
µM	Micromolar
µg	Microgram
ViD	Amine Reactive Viability Dyes
WHO	World Health Organisation

CHAPTER ONE: LITERATURE OVERVIEW

The increased risk of pneumococcal disease in immunocompromised individuals has been described in the literature widely. In order to form a rationale for this present study, a literature review on the cause of pneumococcal disease (caused by *Streptococcus pneumoniae*), groups at risk of disease, normal and immunocompromised immunity, and current vaccine schemes as well as gaps in the literature are presented below.

1.1 *Streptococcus pneumoniae* and pneumococcal infections

1.1.1 *Streptococcus pneumoniae*

Streptococcus pneumoniae is a gram-positive bacterium that exists either as a single entity, a paired diplococcus, or in short chains. It is a facultative anaerobe, and can either be encapsulated or lack a capsule. The capsular polysaccharide elicits a type-specific antibody response in infected hosts which is protective, and should ordinarily clear the host of infection. This antibody response may also provide further protection against closely related serotypes. Currently, 97 serotypes of *S. pneumoniae* have been identified (CDC, 2012, Geno et al., 2015) with some serotypes being more predominant in particular geographical locations than others (Alonsodevelasco et al., 1995).

The identification of these pneumococcal serotypes was facilitated by the use of type-specific sera, and the serotypes were classified by the so-called 'Danish' and 'American' systems (Lund, 1960), the former being more widely used today. In the Danish nomenclature, serotype classification is based on structural differences in polysaccharide capsule, and antigenic characteristics. This polysaccharide capsule increases the virulence of the strain (Alonsodevelasco et al., 1995, Avery and Dubos, 1931), and virulence is caused by interfering with the hosts' phagocytic responses. In mice it has been shown that virulence is directly proportional to the amount of capsular polysaccharide produced by the pneumoccocci, *in vitro* (Macleod and Krauss, 1950). Some antigenic components of the *S. pneumoniae* polysaccharide capsules themselves are the virulence

factors and may be capable of eliciting antibody response (Jedrzejas, 2001).

S. pneumoniae also inhibits growth of *Haemophilus influenzae* and *N. meningitidis*, *in vitro*. This effect is most probably due to hydrogen peroxide produced by the pneumococci (Pericone et al., 2000). Indeed, in 1922 MacLeod and Gordon showed that pneumococci produce hydrogen peroxide which accumulates in culture and may interfere with the growth of other bacteria, including *Staphylococcus aureus* (McLeod and Gordon, 1922). Furthermore, *S. pneumoniae* growth was shown to increase upon co-culture with *N. meningitides*, while *N. meningitidis* growth decreased (Pericone et al., 2000), suggesting a positive relation between these two pathogens in favour of *S. pneumoniae* (Bogaert et al., 2004).

Pneumococcal carrier status is defined by the colonisation of the nasopharynx with pneumococci. These may occasionally invade the bloodstream or surrounding tissues in colonized individuals (Simell et al., 2012). Thus, disease onset is preceded by pneumococcal carriage, though only a small proportion of carriers will go on to develop invasive disease (Simell et al., 2012). However, reports imply that exposure results in an immunizing effect (Musher et al., 1997, Melegaro et al., 2006, Lipsitch et al., 2005), particularly with Th17-cells being shown to play a crucial role in clearing the nasopharynx of pneumococci in mouse models (Lu et al., 2008, Zhang et al., 2009, Trzcinski et al., 2008, Wang et al., 2014).

Transmission of pneumococci mostly occurs from children to adults with longer periods of carriage being associated with pneumococcal serotypes of lower immunogenicity (Mehr and Wood, 2012). Generally, a good immune response localized in the mucosa can clear initial pathogens (Harabuchi et al., 1994) with salivary IgA antibodies being locally produced to target pneumococcal capsular polysaccharides (Simell et al., 2002). Repeated exposure to the pneumococci should result in cumulative immunity over time. There is evidence for the development of serotype-independent antibody responses in children due to previous nasopharyngeal

carriage of pneumococci, which may likely confer cumulative immunity on these individuals into adulthood. Further, new colonisation in the children is reduced thereafter (Granat et al., 2009).

Concerns that have been raised regarding pneumococcal disease and treatment are vaccine coverage, treatment strategy (Bogaert et al., 2004) and multi-drug resistance (Whitney et al., 2000). The first concern highlights the limitations of current vaccine coverage which poses the future risk of non-vaccine serotypes causing disease. The second is related to the hypothesis that minimizing invasion whilst leaving nasopharyngeal colonies unharmed may be a better approach than eliminating these colonies altogether. This poses the risk of future colonisation by more virulent strains (Bogaert et al., 2004). These concerns are further confounded by the genetic capabilities of the bacteria themselves. *S. pneumoniae* has been shown to have extremely high rates of recombination in a single infection due to horizontal gene transfer (HGT) (Hiller et al., 2010). These high levels of homologous recombination in pneumococcal populations will likely result in the generation of vaccine escape strains, increasing the problem at hand (Donkor et al., 2011). Thus the need to understand mechanisms of susceptibility and infection for the improvement of treatment strategies cannot be over- emphasized. This is especially due to the current global burden of pneumococcal disease.

1.1.2 Burden of pneumococcal disease

As of 2013, the World Health Organisation (WHO) listed pneumonia as the worldwide leading cause of mortality in children, killing 1.1 million children below 5 years of age annually (WHO, 2013b). Bacterial meningitis also heavily affects children, and entire populations. A factor confounding prognosis is that clinical symptoms alone cannot distinguish whether meningitis cases are caused by pneumococcal or meningococcal

infections (WHO, 2013a). The former and latter being caused by *Streptococcus pneumoniae* and *Neisseria meningitidis*, respectively.

Older age and underlying disease have been linked to higher mortality rates due to invasive pneumococcal pneumonia. Pneumococcal disease is described as invasive when *S. pneumoniae* is isolated from sites that should ordinarily be sterile, such as pleural fluid, cerebrospinal fluid, or blood (Feikin et al., 2000) as well as the joints and bone tissue. Invasive Pneumococcal Disease (IPD) includes bacteraemia, septicaemia, pneumonia (which can also be non-invasive), meningitis, septic arthritis and osteomyelitis (NHS, 2012). The Centers for Disease Control and Prevention (CDC) estimates that in the post-PCV era, 62% of IPDs worldwide are caused by only 10 pneumococcal serotypes (CDC, 2012). Non-invasive pneumococcal infections are those occurring outside major organs, such as bronchitis, otitis media and sinusitis (NHS, 2012).

It has been estimated that *S. pneumoniae* is responsible for 11% of deaths in children below the age of 5, with a high proportion of these deaths occurring in Africa and Asia (O'Brien et al., 2009). It is thus obvious that the burden of pneumococcal disease while widespread, is especially pronounced in developing countries (Scott, 2007). This may be due to the inclusion of the 7-valent Protein-Conjugated Pneumococcal Vaccine (PCV7) on the vaccine scheme for children in developed countries, which is not the case in many developing countries (O'Brien et al., 2009, Mehr and Wood, 2012). However it is more likely due to the higher rates of pneumococcal carriage on the African continent, with the five most common serotypes in Sub-Saharan Africa being amongst the seven serotypes causing IPD in children on a global scale (Usuf et al., 2014).

In 2002 in England and Wales, there were close to 5800 pneumococcal hospitalisation cases (Melegaro et al., 2006). Statistics taken over the period of a decade (1996-2006) in England and Wales also revealed that cases of IPD for all age groups peaked seasonally over winter months.

This study also investigated the trends in IPD pre- and post- conjugate vaccine introduction. A significant observation was that not only incidence, but also serotype distribution changed over time, with highest burden of disease affecting the two extremes of age: children below one year, and the elderly. A decrease in disease due to serotype 14, and increase due to serotype 1 was also observed (Trotter et al., 2010).

The incidence of IPD in the UK over the period of 15 years is shown in fig. 1.1.
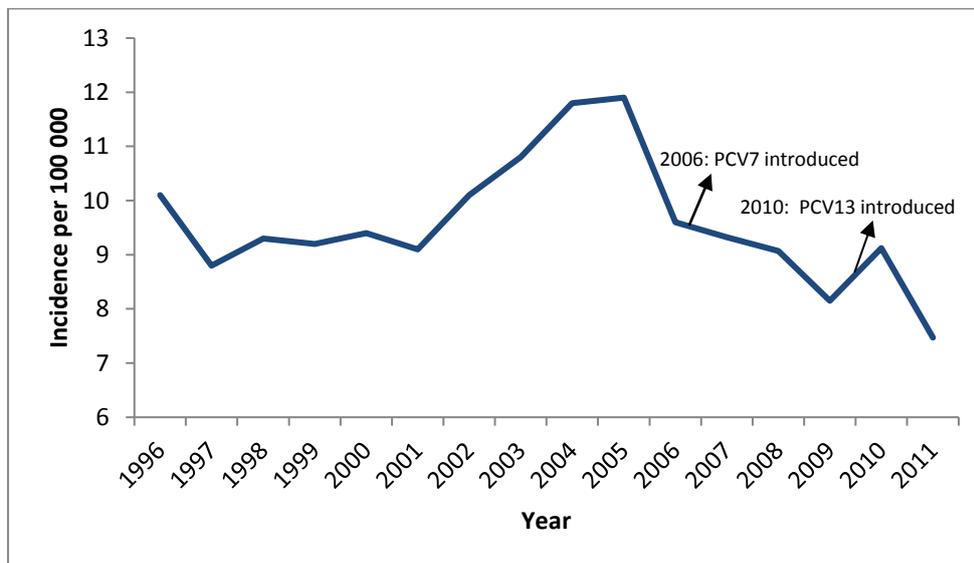
Figure 2.1: Trend line showing the incidence per 100 000 people, of IPD over a 15 year period for all age groups in the UK, highlighting the introduction of PCV into the UK vaccine scheme.

This trend line was constructed based on statistics obtained from Trotter et al. (2010) and the European Centre for Disease Prevention and Control (ECDC) annual epidemiological reports on communicable diseases (ECDC, 2007, ECDC, 2010, ECDC, 2013). The trendline shows a decrease in IPD incidence after the introduction of PCV into childhood vaccination schemes, boosting herd immunity (Millar et al., 2008).

An aspect in pneumococcal research which requires further investigation is why certain groups, particularly those with underlying disease, are at an increased risk of succumbing to pneumococcal infection.

1.1.3 Groups at risk of pneumococcal infection

1.1.3.1 Risk factors and genetics

About 50% of healthy people live with pneumococci colonies in their throats (Lund, 1960). While many individuals carry these colonies, they do not develop disease. This leads to the question, what risk factors cause disease onset? It is apparent that some individuals seem to be more susceptible to pneumococcal infections, and later disease, compared to others.   Risk factors associated with increased pneumococcal infections includes genetics,   socio-economic status (Greenwood, 1999),   HIV infection, especially with low CD4 counts, previous occurrence of pneumonia, cirrhosis, co-infection with hepatitis C, smoking, Injecting Drug Use (IDU), Pulmonary Tuberculosis (TB) and Chronic Obstructive Pulmonary Disease (COPD) (Pedersen et al., 2011).

In terms of genetics, polymorphisms in the human C reactive protein (which binds the C polysaccharide on the *S. pneumoniae* cell wall) have been associated with IPD in White individuals (Roy et al., 2002). Surfactant protein D (SFTPD) variants have also   been   associated   with   IPD (Lingappa et al., 2011) with   genetic polymorphisms also playing a role in meningococcal disease outcome (Brouwer and van de Beek, 2009). However, a meta-analysis integrating several genetic studies conducted across the world concluded that pneumococcal and meningococcal disease susceptibility has not been satisfactorily linked with any polymorphisms, beyond any reasonable doubt, mostly due to methodological flaws and small sample sizes (Brouwer et al., 2009).

In the US, pneumococcal infections from 1995-1998 were found to be highest in children below the age of 2, elderly people 65 years of age or older, and Black people (who had 2.6 times higher incidence rates than among White people)(Robinson et al., 2001). There is also a high mortality rate of the elderly due to pneumonia in England (Trotter et al., 2008). It is apparent that globally age is also a predisposing factor to severe

pneumococcal infection. However, of particular interest to us was the burden of pneumococcal disease in immunocompromised individuals.

1.1.3.2 Immunocompromised individuals

With regards to underlying disease, HIV increases risk of pneumococcal infection with pneumococcal-specific immune dysregulation shown in asymptomatic HIV-infected individuals (Glennie et al., 2011). Pneumococcal bacteraemia isolation rates were also higher in HIV-infected individuals in a population-based study in Kenya (Feikin et al., 2010). Therefore it is known that HIV-infection places affected individuals at an increased risk of succumbing to pneumococcal disease.

Immunity is also impaired in cancer patients. It has recently been shown that patients with advanced solid cancers have lower absolute numbers of B-cells, T-cells and some T-cell subsets, as well as natural killer (NK) cells, relative to healthy controls (Noguchi et al., 2014). Patients with haematological malignancies (across a spectrum from Monoclonal Gammopathy of Undetermined Significance; MGUS, to asymptomatic and symptomatic myeloma- discussed in chapter six) are also susceptible to community- and hospital-acquired *S. pneumoniae* infections when they go into hospital for treatments (Kumashi et al., 2005). Further, individuals with sickle cell disease (SCD), especially children below the age of 3, are at an increased risk of bacterial meningitis (mostly caused by *S. pneumoniae*) (Overturf, 2003, Barrettc.E, 1971). Since the introduction of the routine pneumococcal conjugate vaccine (PCV) however, rates of IPD have been shown to decrease in children with SCD who are less than 5 years old in Tennessee, USA (Halasa et al., 2007). This increases hope for better prognosis as IPD vaccine therapies keep improving.

After the licensing of PCV in the UK in 2001, a study carried out using Systems Biology modeling suggested that the 2004 vaccine prices would not be economically justified in the long run (Melegaro and

Edmunds, 2004). This sheds light on the financial aspect of disease treatment, further emphasizing the need not only to improve vaccine efficacy, but also cost.

1.2 Current pneumococcal vaccinations

1.2.1 Mechanism of function of pneumococcal vaccines

As of 2013, the pneumococcal vaccination scheme includes two vaccines: the Pneumococcal Polysaccharide Vaccine (PPV) and the Pneumococcal Conjugate Vaccine (PCV). The vaccines function by different biochemical mechanisms. The purified *S. pneumoniae* capsules contained in PPV, being a thymus-independent type 2 (TI-type 2) antigen, cross-links several B cell receptors (BCRs). This induces B-cell activation and proliferation thereafter, and the production of IgM by short-lived plasma cells. This response to invading bacteria is rapid. Due to the low immunogenicity of PPV in children, purified capsular polysaccharides were conjugated to diphtheria proteins (CRM_{197} mutant), thereby increasing the immunogenicity of the PCV vaccine as a whole and rendering memory (Goldblatt, 2000).

Not only does PCV elicit IgM production, but the diphtheria proteins which are T-cell-dependent antigens elicit T-cell help. These T-helper cells produce cytokines which induce the production of IgG by long-lived plasma cells (immunoglobulin switching). T-cell help induces the production of antibodies that are more functionally versatile, and have a higher affinity for the antigen (Murphy, 2012). Thus, this T-cell help in PCV elicits an immune response in children. The mechanism of function of PPV and PCV are depicted in fig. 1.2.

A: PPV: T-independent   **B:** PCV: T-dependent
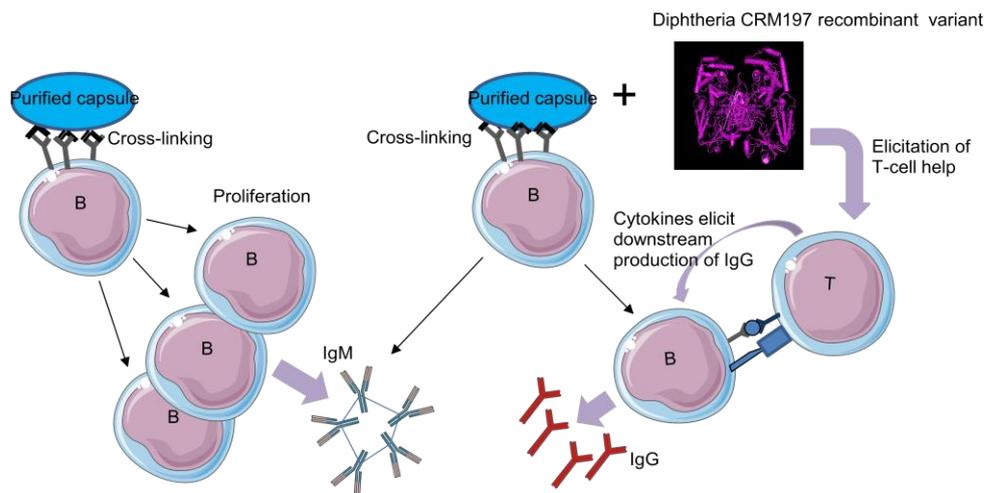
Figure 1.2: Cellular mechanisms by which PPV23 and PCV7/13 function. The T‑independent purified capsule crosslinks B‑cell receptors, eliciting proliferation of B-cells, and production of IgM (A). The T-dependent diphtheria proteins in the conjugate vaccine elicit T‑cell help, resulting in a more specific reaction due to the production of IgG (B). This occurs in addition to IgM produced as a result of capsular polysaccharide stimulation of B cells.

1.2.2 Vaccine composition and efficacy

The Joint Committee on Vaccination and Immunisation (JCVI) has several recommendations pertaining to dosage administration for these vaccinations dependent upon an individual's state of health, and age (JCVI, 2011, JCVI, 2013, PHE, 2013).

PPV was first licensed in the USA in 1977. The 23-valent PPV (PPV23) contains purified polysaccharide capsule from each serotype covered, and no adjuvant. Serotypes covered by this vaccine, which cause 85-90% of IPD in adults, are 1, 2, 3, 4, 5, 6B, 7F, 8, 9N, 9V, 10A, 11A, 12F, 14, 15B, 17F, 18C, 19A, 19F, 20, 22F, 23F and 33F. PPV23 is administered to adults 65 years of age and older and high-risk individuals younger than this (IAC, 2013). PPV23 should follow intramuscular administration rather than

inhalation, as inhaled vaccine does not elicit a significant antibody response (Gordon et al., 2008). PPV23 has been found to be effective and economical in a low risk elderly cohort in England and Wales, though protection was found to wane after 5 years (Andrews et al., 2012). A booster is thus required five years after the initial vaccination (IAC, 2013) as the antigens do not induce memory in the immune system (WHO, 2008).

The foundation for the modern conjugate vaccine was set in 1929, when Avery and Goebel showed that a purified polysaccharide from *S. pneumoniae* (on its own with low immunogenicity) conjugated to a protein carrier, had an enhanced immunogenicity (Avery and Goebel, 1929, Goldblatt, 2000). Nearly 60 years later in 1987, *Haemophilus influenzae* type b (Hib) conjugate vaccine would be the first glycoconjugate vaccine licensed for use in humans in the USA (Goldblatt, 2000). After introduction of this vaccine routinely, a sharp decline in Hib invasive disease was observed in children in different parts of the world (Peltola et al., 1992, Booy et al., 1994, Santosham et al., 1991). Thus, interest in the potential of reducing IPD incidence in children by the use of conjugate vaccines peaked.

PCV7 (containing serotypes 4, 6B, 9V, 14, 18C, 19F, and 23F) was the vaccine recommended for children 24-59 months of age (IAC, 2013) in the early 2000s. The routine use of this vaccine in children across Europe led to a decline in disease caused by vaccine serotypes. In the United States also, the vaccine was found to be effective against IPD in both healthy and chronically ill children (Whitney et al., 2006). However, the occurrence of serotypes 1, 3, 6A, 7F and 19A in isolates since the introduction of the vaccine stressed the importance for these serotypes to be included in future vaccines (Isaacman et al., 2010).

In 2010 Pfizer Inc. licensed a new Wyeth Pharmaceuticals-manufactured vaccine. Prevnar 13® pneumococcal 13-valent conjugate vaccine

(Diphtheria CRM$_{197}$ protein) (PCV13) covers serotypes 1, 3, 5, 6A, 7F, and 19A in addition to PCV7 serotypes and can also be administered to children 60-71 months who suffer from comorbidities. PCV13 is usually administered as a single dose, followed by a booster a few months later (IAC, 2013). Pfizer conducted clinical trials on a cohort of 7000 children, producing data supporting IPD prevention in young children who had received PCV13 (Pfizer, 2013a). A Prevnar 13® vaccine for use for adults 50 years of age and older has also been manufactured, and is delivered as a single dose (Pfizer, 2013b).

The elicitation of immunoglobulin G (IgG) anti-capsular antibody ≥ 0.35 µg/ml by PCV13 in a study cohort comprising infants (Bryant et al., 2010) showed compliance with recommendations made by the WHO in 2003, describing this antibody concentration as the IgG reference value conferring protection against IPD (Paradiso, 2009). Recent studies have also shown that PCV13 could potentially protect against serotypes 6C and 7A which are not covered by the vaccine, but closely related to vaccine-covered serotypes (Cooper et al., 2011). Thus the PCV vaccine scheme for children is highly advantageous for their own protection against IPD, and also the indirect protection of older children and adults by herd immunity (Whitney et al., 2003, Pilishvili et al., 2010).

In terms of nasopharyngeal carriage of pneumococci after vaccination, PCV7 has been shown to have a dose-dependent effect on vaccine-specific serotype carriage in a cohort of Fijian children. There was an inverse relationship between dose of PCV7 and vaccine type carriage. Additionally, despite eliciting an antibody response, boosting with PPV23 did not impact pneumococcal nasopharyngeal carriage (Russell et al., 2010).

Though use of the PCV7 vaccine in England and Wales led to a decrease in IPD in spite of serotype replacement, the biggest concern regarding the continued use of these vaccines covering limited serotypes still remains the potential surge in non-vaccine type (NVT) IPD (Miller et al., 2011). Table 1

summarises information regarding the vaccines currently used to prevent pneumococcal disease.

Table 1: Target groups of the current pneumococcal vaccines recommended by the Joint Committee on Vaccination and Immunisation*

Pneumococcal Vaccine	*Streptococcus pneumoniae* strains covered	Target group	Recommended dose
Pneumococcal Polysaccharide Vaccine (PPV23)	1, 2, 3, 4, 5, 6B, 7F, 8, 9N, 9V, 10A, 11A, 12F, 14, 15B, 17F, 18C, 19A, 19F, 20, 22F, 23F and 33F	1.Individuals ≥ 65 years of age. 2.Individuals with long-term health conditions who are at higher risk of developing pneumococcal disease. 3.Children > 2 years of age who have higher risk of developing pneumococcal disease.	1.One injection administered (which may be followed by a booster > 3 years later). 2.More than one dose: second dose administered > 3 years after first.
Pneumococcal Conjugate Vaccine (PCV13)	1, 3, 4, 5, 6A, 6B, 7F, 9V, 14, 18C, 19A,19F, and 23F	1.Children < 2 years of age. 2.Children ≥ 2 to 17 years of age. 3.Adults ≥ 18 years of age.	1.Three injections to be given: first at six weeks; subsequent two injections to be given at least one month apart. Booster to be given from 11 to 15 months of age. Infants from 7 to 11, and 12 to 23 months receive two injections which are spaced by one and two months respectively. 2.One injection administered. 3.One injection administered.

*Information gathered from (PHE, 2013, JCVI, 2011, JCVI, 2013, NHS, 2016a, NHS, 2016b, Pfizer, 2017, Pfizer, 2018)

In spite of the impact pneumococcal vaccines have had on disease, there still remain reported cases of vaccine failure.

1.2.3 Pneumococcal vaccine responses in HIV/other risk groups

Although Highly Active Anti-Retroviral Therapy (HAART) has decreased pneumonia in HIV-infected children, IPD still poses a significant health risk to the HIV-infected (Micheloud et al., 2012). The administration of PCV7 to HIV-infected Ugandan adults yielded significantly increased IgG

levels in the study cohort (Miiro et al., 2005). Further, PCV7 was found to be protective against serotype 6A in HIV-infected adolescents and adults who had previously had IPD (French et al., 2010).

As the efficacy of PPV23 to prevent IPD in HIV-infected adults is still suboptimal, PCV is now the preferred vaccine for administration to HIV-infected individuals. However, vaccine failures in PPV23 and PCV7 have still been reported. A PPV23 vaccine failure was reported in a 22 year old female due to serotype 9 (Willocks et al., 1995), a 44 year old male due to serotype 3 (Begemann and Policar, 2001) and a 13 year old boy (who had also received PCV7) due to serotype 18 C (Rives Ferreiro et al., 2008). These vaccine failures emphasize the need for vaccine optimisation in this high risk group.

In 2001, Kroon and colleagues found that PCV elicits an impaired antibody response in HIV-infected adults compared to controls. Further, both the HIV- infected cohort and normal healthy subjects were found to produce higher antibody concentrations after receiving sequential PCV and PPV, as opposed to PPV alone (Kroon et al., 2000). Another study found that pneumococcal vaccine protected against IPD in White, but not Black HIV-infected individuals (Breiman et al., 2000). Still, a more recent study did not find significant differences in antibody responses to both vaccines, between White and Black HIV-infected Americans who had equal health-care access (Crum-Cianflone et al., 2010). While in South Africa, PCV9 reduced IPD incidence in healthy and HIV-infected children. However, the efficacy of the vaccine to reduce IPD first-episode incidence was higher in the healthy compared with the HIV- infected children (Klugman et al., 2003). Though improvements have been made to both vaccines over the years since this study was published, it still stands to reason that HIV-infected individuals will still show an impaired response to the current vaccines due to their lowered immunity.

Effective pneumococcal vaccine schedules for HIV-infected individuals are thus, still highly debated. The Immunisation Action Coalition (IAC) advises

that HIV- infected individuals should be given PCV13, followed by PPV23 eight weeks later. Though the vaccine may not elicit an adequate antibody response in this high risk group, administration is still recommended nonetheless (IAC, 2013).

Taken together, these studies emphasize the need for constant improvement of pneumococcal vaccines, or the discovery of potential adjuvants which may facilitate antibody responses in high risk groups. Further, the reports of vaccine failures in high risk groups, and susceptibility to IPD due to impaired B-cell functioning in certain individuals emphasizes two points: first, more studies need to be undertaken in order to investigate how vaccines can be improved for the high risk groups. A nd second, to an extent B- cell defects in response to T-independent pneumococcal antigen mimics may be indicative of an increased susceptibility to IPD.

1.3 Immunity

1.3.1 Immune responses to *S. pneumoniae* infection

As reviewed by Koppe et al. (2012), upon infection by *S. pneumoniae*, the human host employs both innate and adaptive immune responses to combat infection. In terms of innate immunity, infecting *S. pneumoniae* is recognized by pattern recognition receptors (PRRs) including toll-like receptors (TLRs) and nucleotide-binding oligomerisation domain receptors (NOD-like receptors or NLRs) on phagocytic cells: in particular, TLR 2 and 4 and NOD2. These receptors induce the production of inflammatory mediators such as interleukins (IL-1β, IL6), tumour necrosis factor alpha (TNFα) and keratinocyte-derived chemokine (KC) (all NF-kB-dependent) while an as yet unidentified receptor induces the production of type I interferons (IFNs). Neutrophils and macrophages are also recruited for phagocytosis (Koppe et al., 2012). Lysozyme and β- defensin-2 (an anti-microbial peptide) have also been shown to act against *S. pneumoniae* in a synergistic manner (Lee et al., 2004). The innate immune defense against *S. pneumoniae* also involves the C3 component of the complement

system. It plays a protective role in the first hours of infection in the lungs, and is thus required systemically (Kerr et al., 2005).

Of particular interest to IPD prognosis and therapy is the adaptive immune response launched against the invading pathogen. This is because these immune responses are mimicked by the current vaccines used for disease prevention. Generally the adaptive immune system launches its attack making use of highly specialized T- and B-cell responses. The ultimate aim of this specific response is not only to clear the system of the invader, but also to induce immune memory which will be highly protective should future infection take place.

1.3.2 T- and B-cell responses in adaptive immunity

T- and B-cells originate from the common lymphoid progenitor in the bone marrow. They differentiate in the bone marrow and thymus respectively. A key feature of both these cells that set them apart from other blood cells is the expression of their respective antigen receptors, namely the T-cell receptor (TCR) and B-cell receptor (BCR). When a B-cell encounters an antigen (such as the *S. pneumoniae* polysaccharide capsule), it differentiates into a plasma cell, secreting antibodies for the clearance of that specific antigen (Murphy, 2012).

B- cells constitutively express major histocompatibility complex class II (MHC class II) cell surface glycoproteins, which present exogenous antigens which have been proteolytically processed within the cell. The B-cell is an Antigen Presenting Cell (APC) to T-helper (T_H) cells. The $\beta2$ domain on the MHC II molecule interacts with the phenotypic marker on T_H cells, CD4, enhancing interaction between the B- and T-cells. The MHC II molecule binds to the TCR, which itself comprises a CD3 complex consisting of transmembrane accessory chains. After binding the MHCII molecule, the TCR accessory chains on the T- cell transduce signals. T- and B- cells are fully activated when co-stimulatory molecules such as

CD28 on the T-cell and CD86 on the B-cell participate in cognate interactions (see review by (Chaplin, 2010) and figure 1.3).

The CD40 molecule expressed on B-cell surfaces binds to the CD40 ligand on T-cells, encouraging growth and differentiation of the T-cells, and proliferation of B-cells and antibody class switching. This binding elicits an increased production of co-stimulatory molecules by B-cells (such as those in the B7 family), and is key to the response of B-cells to thymus-dependent (T-cell dependent, TD) antigens. Follicular helper T-cells (Tfh) secrete cytokines to regulate antibody production by B-cells, and proliferation (Murphy, 2012). Further, Th17-cells play a crucial role in clearing the nasopharynx of pneumococci in mouse models (Lu et al., 2008, Zhang et al., 2009, Trzcinski et al., 2008, Wang et al., 2014). The development of T- and B-cells, and interaction between them thereafter is depicted in fig. 1. 3.
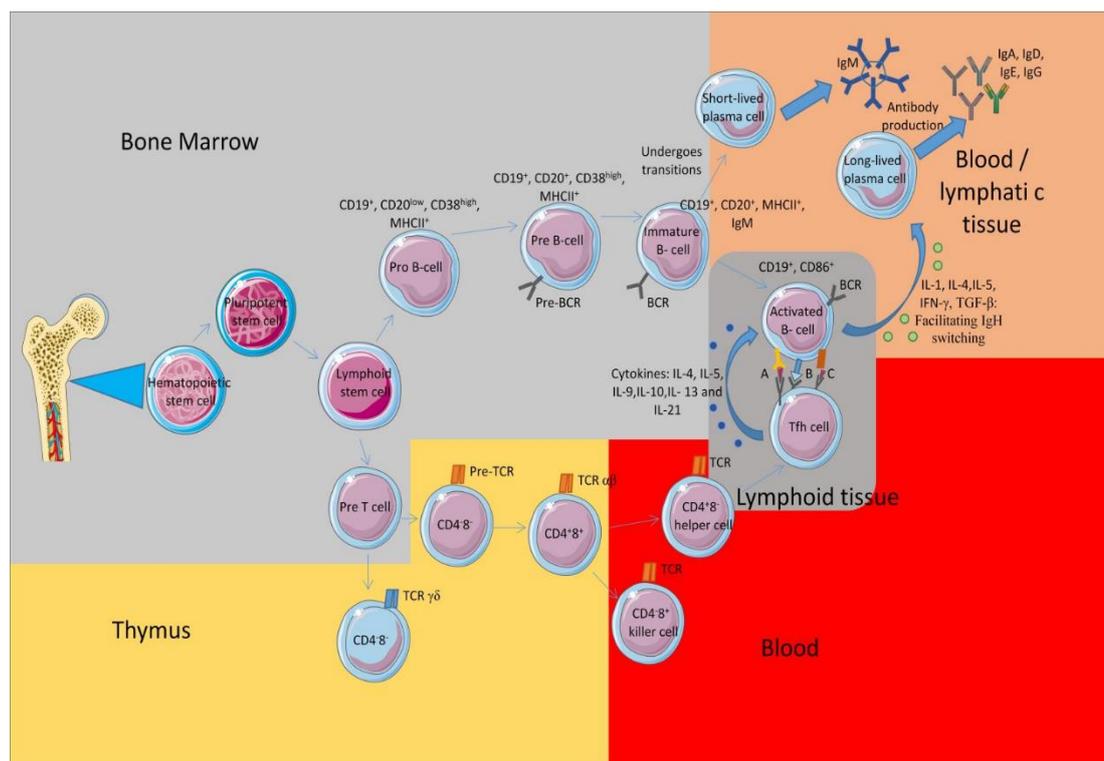
Figure 1.3: T- and B-cell development and interactions thereafter. The lymphoid stem cell progenitor for T- and B-cells originates in the bone marrow. The helper and cytotoxic T-cells are characterized by the expression of surface CD4 and CD8 respectively. The B-cell lineage goes through several stages characterized by the expression of certain cell

surface markers (cluster of differentiation (CD) and major histocompatibility complex (MHC) markers) as indicated in the diagram. Short-lived plasma cells produce IgM, while long-lived plasma cells produce IgA, IgD, IgE and IgG. Noteworthy interactions between mature T- and B-cells, which induce the production of antibodies by long-lived plasma cells include the presentation of antigen by the MHC class II molecule on the B-cell to the TCR on the Tfh-cell (A), the binding of CD40 on the B-cell to the CD40 ligand (CD40L) on the Tfh-cell (B) and the binding of co-stimulatory B7 on the B-cell to CD28 on the T-cell (C) which enhances the signal between MHCII and the TCR (Murphy, 2012).

1.4 Rationale for study

Taking the complex interplay between T- and B-cells in response to infecting *S. pneumoniae* into consideration, it becomes clear that an adequate immune response is dependent upon proper cell functioning. Defective B-cell responses relative to control subjects have been reported by our group in a cohort of individuals (with no pneumococcal vaccine history) who had previously suffered from IPD (Darton et al., 2011). Our group also uncovered a similar B- cell defect in previous sufferers of serogroup C meningococcal disease (Foster et al., 2009), and T-cell defect in meningococcal serogroup C vaccine (MCC) failures (Foster et al., 2010).

The Darton (2011) and Foster (2009; 2010) studies employed polyclonal stimulation of T- and B- cells using a validated immunologic assay. Of particular interest to the present study was the Darton study, in which all previous sufferers of IPD had no known susceptibility to the disease. Relative to controls the patient group showed significantly lower B-cell activation in response to the B-cell polyclonal mimic (which was not overcome with T cell help) (Darton et al., 2011). Results from the Darton and Foster studies indicate respectively that predisposition to pneumococcal and meningococcal disease may, to a certain extent, be observed at a cellular level. The present

study aimed to use the same immunologic assay to investigate potential defects in T- and/or B-cells in two patient groups as outlined below.

1.5 Hypothesis and aims of the research

Research question: Do HIV-infected patients and haematological malignancy patients have a defect in B- (and T-) cell activation and proliferation (relative to normal healthy controls) that could predispose them to pneumococcal infection?

The study aimed to:

1. Investigate the stringency required for matching controls to patients in terms of age, sex and ethnicity.

2. Compare the effectiveness of the *in vitro* T- and B-cell response in adults with immunosuppressive conditions : HIV and Monoclonal Gammopathy of Undetermined Significance (MGUS), with age-, sex- and ethnicity-matched controls, using a polyclonal TI-2 antigen ($\alpha\delta$dex) and polyclonal TD antigen (anti-CD3) as stimulants.

Specific objectives of the study were therefore to:

1. Optimise a flow cytometry panel comprising phenotypic, proliferation and activation markers for T- and B-cells.

2. Recruit a study group of sex- and ethnically diverse individuals to study the effects of age, sex and ethnicity on T- and B-cell responses.

3. Expand the immunologic assay (Darton et al. 2011; Foster et al. 2009; Foster et al. 2010) to include pneumococcal-stimulation by using the D39-strain of *Streptococcus pneumonia* and thereafter to compare apoptosis levels in B-cells of patients and controls.

4. Recruit a cohort of HIV-infected adults (with matched controls) to study their *in vitro* T- and B-cell responses to polyclonal and pneumococcal stimulation. And lastly,

5. Recruit a cohort of patients with Monoclonal Gammopathy of Undetermined Significance (MGUS) (with matched controls) to study their *in vitro* T- and B-cell responses to polyclonal and pneumococcal stimulation.

CHAPTER TWO: METHODOLOGY

2.1 Subject recruitment

2.1.1 HIV-infected patients

HIV-infected patients were recruited from cohorts followed up in outpatient HIV clinics based at the Department of Infection and Tropical Medicine and Department of Genitourinary Medicine at the Sheffield Teaching Hospitals (STH) NHS Foundation Trust. Inclusion criteria for the study was as follows: HIV-1-infected adults ($\geq$ 18 years), on antiretroviral therapy (ART), with undetectable blood HIV-1 viral load and CD4 count $\geq$ 350 cells/mm^3 within the last six months. Patients were approached by their clinical team to gauge interest in the study during routine outpatient clinic visits, prior to informed consent being obtained by a study team member. All subjects provided written informed consent prior to blood donation and participation in the study.

2.1.2 Patients with Monoclonal Gammopathy of Undetermined Significance (MGUS)

Patients with Monoclonal Gammopathy of Undetermined Significance (MGUS) were recruited from cohorts under outpatient follow up within the Department of Haematology, STH. Patients were approached by their clinical team to gauge interest in the study during routine outpatient clinic visits, prior to informed consent being obtained by a study team member. All subjects provided written informed consent prior to blood donation and participation in the study.

2.1.3 Healthy controls

Healthy controls were recruited from STH and the University of Sheffield employees. Blood samples from age-, sex- and ethnicity-matched controls were obtained and run in parallel with all cases (HIV-infected and MGUS

patients). Age matching was undertaken so controls were within a 10 year range (I.e. +/- 5 years) of the case. All subjects provided written informed consent prior to blood donation and participation in the study.

Ethical approval for this project was granted by the UK National Research Ethics Service Committee (14/YH/1118). The sequence of steps from patient recruitment to quantification of T- and B-cell responses is summarised in figure 2.1.
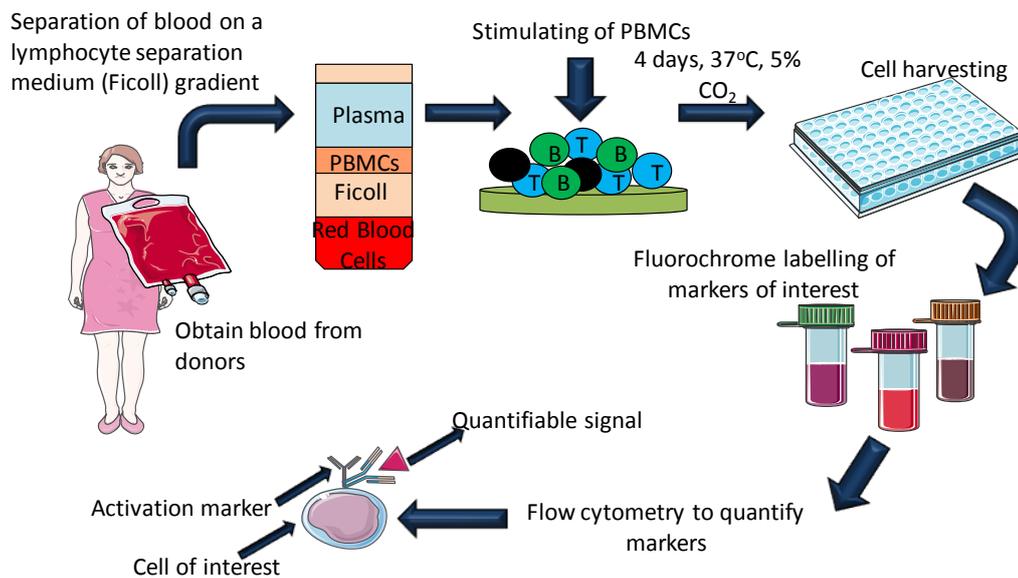
Figure 2.1: Flow diagram illustrating the sequential steps used in the methodology of this project.

Following the recruitment of informed and consenting patients and controls, blood was collected. Lymphocytes were enriched from these whole blood samples, and a validated immunologic assay optimised by our group (Foster et al., 2009) was performed to study *in vitro* T- and B-cell responses. These steps are detailed below.

2.2 Collection of blood samples

Peripheral blood samples were drawn by venepuncture in the Department of Infectious Diseases, Royal Hallamshire Hospital (RHH) and the Department

of Haematology, RHH. On average, 40 ml of blood was taken into a tube containing 80 µl heparin [Heparin (mucous) injection B.P. 5000 u/ml heparin sodium, Leo Labs, Ballerup].

2.3 Lymphocyte enrichment from whole blood

Work on blood samples was conducted in a Class II Microflow Biological safety cabinet, using aseptic technique (in a Containment Level 3 laboratory when processing HIV-infected samples). The blood was diluted with an equal volume of a 1 x working solution of phosphate buffered saline (PBS) (Dulbecco A; Oxoid Limited, Basingstoke Hampshire) at room temperature. Two parts of blood were carefully layered onto one part of lymphocyte separation medium (Density 1.077 g/ml, BioWhittaker® Lonza, Walkersville) at a slanted angle, ensuring the blood mixture did not break the density gradient. Formation of layers was achieved through centrifugation (settings: time; 35 min, RCF; 400 *xg*, temperature; 20°C, acceleration and deceleration; 0).

The interface between the top plasma layer and the bottom lymphocyte separation media contained the buffy coat layer (comprising the peripheral blood mononuclear cells-PBMCs). This layer was carefully removed using a plastic Pasteur pipette. Plasma was also taken out from the tubes and stored in sterile tubes on ice for later use.

The extracted PBMCs were washed with 20 ml sterile chilled PBS four times (centrifugation settings: 10 min, RCF; 600 *x g*, temperature; 4°C, acceleration and deceleration; 9). After the last wash, the cells were re-suspended in 1 ml cell culture media, which was made by adding 1 part of autologous plasma to 4 parts of RPMI 1640 [BioWhittaker®, Lonza, Verviers-supplemented with 200 µM L-glutamine (Lonza, Walkersville)].

Live PBMCs were counted using a 0.1 % Trypan blue solution (Sigma®, Sigma-Aldrich, St. Louis) and an improved Neubauer haemocytometer (Boeco, Hamburg) and made up to a final concentration of 1 x 10^7 cells/ml. For later use during the flow cytometry step, 2 x 10^6 unstained PBMCs were saved, while the rest were stained with the cell tracer dye-carboxyfluorescein diacetate succinimidyl ester (CFSE).

2.4 Cell proliferation assay

The well-established protocol using the CFSE reagent was used to track T- and B-cell proliferation, *in vitro*. This permeable dye diffuses into the cell cytoplasm, and the succinimidyl moiety forms a highly stable amide bond with intracellular amines. As cells divide, the dye splits equally between progeny (Lyons and Parish, 1994). It is used to track cell divisions in flow cytometry protocols by measuring the halving of fluorescent intensity after each subsequent division. CFSE is long-lived and can be tracked for up to eight T-cell divisions (Parish, 1999).

According to the manufacturers' instructions, a 10 mM CFSE (Vybrant® CFDA SE cell tracer kit, Invitrogen™, Molecular probes™, Oregon) stock solution was made by reconstituting the lyophilised CFSE reagent in 90 µl of sterile DMSO. Aliquots of CFSE were stored at -20°C. On the day when needed, 0.1 mM of CFSE was prepared from the frozen aliquots, using sterile PBS.

After PBMCs were enriched and re-suspended in media (section 2.3), 20 µl of CFSE was added per 1 x 10^7 cells, giving a final concentration of 2 µM CFSE-dyed PBMCs. The PBMCs were immediately incubated at 37°C (5 % CO_2) for 10 min (in the dark). The CFSE reaction was then quenched by the addition of equal volumes of cold autologous serum. The PBMCs were incubated at room temperature, in the dark, for another 10 min. After centrifugation (settings: time; 15 min, RCF; 600 *xg*, temperature; 4 °C), the PBMCs were washed three more times with prepared media (section 2.3).

After decantation of the supernatant, the PBMC pellet was re-suspended in 1 ml media, and counted using 0.1% trypan blue solution as previously described (section 2.3).

PBMCs were seeded at 1 x 10^6 cells per well, in a flat-bottomed tissue culture-treated, sterile 48-well plate (Costar, UK) in a final volume of 500 µl. The PBMCs were incubated at 37°C (5 % CO_2) until the commencement of the flow cytometry protocol.

Proliferation was detected using the 530/30 filter of the Blue 488 nm laser during the flow cytometry protocol (section 2.7.3). For the analysis of cell proliferation, the cell proliferation package on FlowJo version 7.6® was used: Each subsequent generation formed and emitting CFSE fluorescence is represented as a subsequent peak to the left of the parent generation (as seen in the representative histograms in figure 2.2).
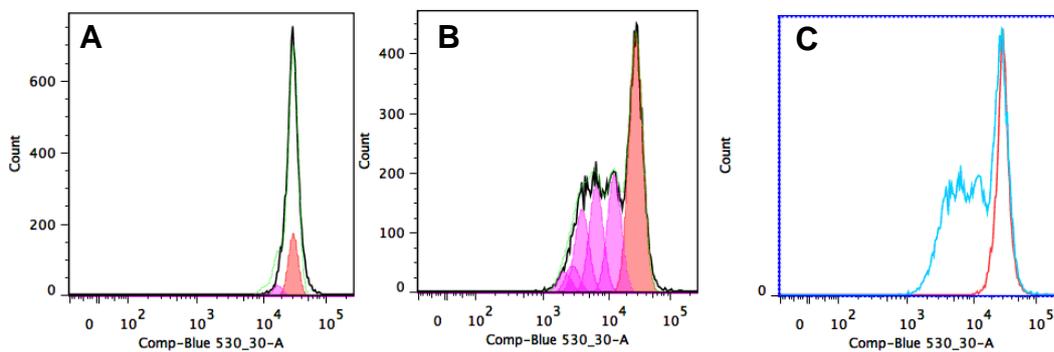
Figure 2.2: Proliferation of a stimulated lymphocyte sample (B) on the FlowJo Proliferation platform is indicated as subsequent peaks (in pink) formed to the left of generation 0- the parent generation (shown in coral). Each peak represents a new generation of cells. Generation 0 is also seen in the un-stimulated sample (A). An overlay of the un-stimulated and stimulated sample (C) gives a clearer indication of how many generations were induced upon stimulation. Image generated by the FlowJo 7.6® proliferation platform (section 2.7.4).

Proliferation results in this study are reported in proliferation index, which is the ratio of the total number of divisions to the number of cells that had undergone division. As such, proliferation index is always greater than 1. This parameter was chosen to study cell proliferation as it only takes those cells which have responded and divided into consideration.

Proliferation was studied using the proliferation platform provided within the FlowJo version 7.6® package (section 2.7.4). This platform superimposes adjustable gates onto the proliferation peaks detected. As a result the proliferation index is generated together with a root mean square (RMS) value. The process of assigning peaks influences the values, thus making the platform subjective to an extent. However, the 'best fit' peak was chosen based on the lowest RMS value generated (as prescribed in the FlowJo version 7.6® manual), thus rendering the proliferation values reliable.

Following staining of cells to track proliferation, cells were stimulated using the immunologic assay that our group optimized (Foster et al., 2009). This assay uses CD3-stimulation of T-cells and IgD-stimulation of B-cells (using a polyclonal antigen mimic) alone and in combination to study T- and B-cell responses, and T-cell help to B-cells.

2.5 T- and B-cell stimulation

2.5.1 Stimulation of T-cells

T-cell activation was achieved by using plate-bound purified anti-human anti-CD3 antibody (Geppert and Lipsky, 1987). Anti-CD3 has been widely reported as a T-cell stimulant, including in previous studies by our group (Darton et al., 2011, Foster et al., 2009, Foster et al., 2010, Preciado-Llanes et al., 2015) and is a polyclonal stimulant which engages the T-cell receptor (TCR). In addition, our group has also previously used a purified anti-human anti-CD28 antibody as an agonist to mimic further co-stimulatory interactions between the CD28 molecule and CD80/86 on B-cells (Foster et al., 2009).

At least 15 hr prior to seeding of cells, a 48-well sterile cell culture plate was pre-coated with 0.1 µg/ml anti-CD3 (Clone OKT3; Biolegend ®, San Diego) alone, or 0.5 µg/ml anti-CD3 in combination with 0.5 µg/ml anti-CD28 (Clone 10F3; Invitrogen™, Frederick). These concentrations used were enough to elicit sub-optimal T-cell activation and proliferation responses, thus enabling the detection of even minute differences between patient and control responses. Pre-coated plates were incubated at 4°C and the wells containing anti-CD3 were washed three times with sterile PBS prior to seeding. Seeded cells were stimulated for 96 hr.

2.5.2 Stimulation of B-cells

2.5.2.1 Anti-IgD-conjugated dextran (αδdex)

Anti-IgD-conjugated dextran (αδdex) is a B-cell receptor (BCR) cross-linking thymus-independent (TI-2) antigen mimic, which induces B-cell activation (Pecanha et al., 1991). This had been prepared as previously described (Pecanha et al., 1991, Rehe et al., 1990, Brunswick et al., 1988) and kindly provided by Dr. Andrew Lees, Biosynexus, Gaithersburg.

B-cell stimulation was achieved by direct addition of 1 µg/ml αδdex to 1 x 10^6 PBMCs as has been done by our group previously, for 96 hr (Foster et al., 2009, Darton et al., 2011, Preciado-Llanes et al., 2015).

2.5.2.2 *Streptococcus pneumoniae*

While our group had investigated T- and B-cell responses using the above described polyclonal antigen mimics, the present study sought to expand this immunologic assay to include pneumococcal-stimulation. The aim of this was to detect *Streptococcus pneumoniae*-specific responses in our study cohort, and investigate potential differences in responses between patients and

controls. Therefore, a pneumococcal strain was included amongst the stimulants in the immunologic assay.

The D39 virulent serotype 2 strain of *S. pneumoniae* has been used extensively for infection studies, and is widely accepted as a model strain for pneumococcal pathogenicity studies. While being isolated over a century ago, the strain's genomic sequence was only reported by Lanie and colleagues in 2007 (Lanie et al., 2007).

For D39 stimulation experiments, frozen bacterial stock was allowed to thaw then heat-killed by placing the vial into a heating block maintained at 37°C for one hour. The stock was then washed twice with sterile PBS (centrifuge settings: time; 3 min, RCF; 500 *xg*) and re-suspended in RPMI. PBMCs were infected with D39 at an MOI of 10 (optimized and presented in chapter four).

Our group had previously determined that a 96 hr time point (4 days) elicited maximal activation and proliferation before the cells begin to die (JB Wing and R Foster, unpublished data). Therefore, PBMCs were seeded at 1 x 10^6 in a final volume of 500 μl of media and incubated at 37°C with CO_2 levels at 5% for 96 hr in a humidified atmosphere after the stimulations were performed.

It was also critical to track the *in vitro* viability of all cell samples used in this study to ensure reliability and robustness of the final data set.

2.6 Viability assays

2.6.1 Cell death

Cell viability was monitored by the use of the Live/Dead® Fixable Blue Dead cell stain kit (Molecular Probes®, Life Technologies™, Oregon). This reagent is one of the amine reactive viability dyes (ViD) and penetration is possible

only through damaged cell membranes. The dye forms a fluorescent product after irreversibly binding with amine groups within the damaged cell cytoplasm, and with those on the extracellular surface. This product remains stable even after fixation of the cells. On the basis that live cells would exclude the dye and have a much lower fluorescence due to only their surface amines binding dye, discrimination of dead cells is made possible (Perfetto et al., 2006, Perfetto et al., 2010).

The Live/Dead® Fixable Blue Dead reagent was re-constituted according to the manufacturers' instructions by adding 50 μl high-grade DMSO to the vial of lyophilised reagent. Aliquots of the dye were stored at -20°C. On the day when needed, a 1:500 dilution of dye in sterile fluorescence activated cell sorting (FACS) buffer: PBS with 0.1 % BSA [Sterile 30 % w/v solution in PBS, First Link (UK) Ltd], was made. This blue fixable/FACS solution was used as the medium in which all fluorochromes in the flow cytometry panel (section 2.7.2) were incorporated.

2.6.2 Apoptosis

Detection of apoptosis in live cells can be achieved by the use of fluorochrome labeled-caspase inhibitors. These probes irreversibly bind to activated caspases, enabling *in situ* apoptosis detection, and are compatible with flow cytometry protocols (Amstad et al., 2001). Protocols for maintenance of cell viability require temperatures of 37°C, while those for the binding of antibody-fluorochrome to cell markers are carried out on ice. Therefore the probe can be used just prior to an already established flow cytometry protocol.

The violet live cell caspase probe (BD Biosciences, New Jersey) was used for the detection of apoptosis according to the manufacturers' instructions. This probe detects caspases-1, -2, -3, -6, -8, -9 and -10. Use of this pan-caspase probe would circumvent the risk of including only one marker of either the intrinsic or extrinsic apoptosis pathways (Elmore, 2007) within the flow cytometry panel.

The lyophilised probe was re-constituted with sterile DMSO at room temperature, and stored at -20ºC in aliquots. On the day of use at the 94 hr time point, the relevant wells in the 48-well plate received 1 µl of the probe, and were immediately incubated at 37ºC for one hour with CO_2 levels at 5%. The PBMCs were carefully aspirated and lifted, and washed once with pre-warmed RPMI supplemented with L-glutamine (settings: time; 5 min, RCF; 500 *xg*, temperature; 20ºC). Immediately after the wash, the PBMCs were re-seeded in a total volume of 500 µl with pre-warmed RPMI supplemented with L-glutamine. They were then incubated at 37ºC for one hour with CO_2 levels at 5%, allowing any unbound probe to diffuse out. At the 96 hr time point, PBMCs were harvested. Labeling of phenotypic and activation markers, and quantification of these using flow cytometry, was carried out thereafter.

2.7 Multicolour flow cytometry

2.7.1 LSRII flow cytometer

For this project the BD LSRII™ flow cytometer (BD Biosciences, New Jersey) at the University of Sheffield Medical School Flow Cytometry Core Facility was used. This machine has four lasers (blue, violet, UV and red) and numerous filters customised for the simultaneous detection of up to thirteen fluorochromes. Also, the LSRII in the core facility is maintained by running multicolour beads on it daily for calibration, thus minimizing inter-run variation (Herzenberg et al., 2006).

Spectral overlap is a normal occurrence in multicolour flow cytometry, hence compensation was necessary to correct for this. Compensation was carried out prior to sample runs using the BD FACSDiva™ software (BD Biosciences, New Jersey) operating in conjunction with cell-based single stains for the violet probe, UV live/dead blue fixable control, and CFSE; and anti-mouse compensation beads [BD™ CompBeads: anti-mouse Ig, k/

Negative control (FBS) compensation particle set, BD Biosciences, New Jersey] for the rest of the fluorochromes.

2.7.2 Staining extracellular markers of phenotype and activation

Expression markers determining cell phenotype and activation were labeled with specific antibody-fluorochrome conjugates outlined in table 2.1 (A & B- section 2.7.3). All these conjugates were titrated prior to use on clinical samples in order to determine the optimal concentrations for use. It was determined that 1 µl (approximately 0.025 µg) per reaction (of approximately 1 x 10^6 PBMCs) was sufficient for adequate labeling, for every antibody-fluorochrome conjugate used.

Cells were lifted off the 48-well plate by careful flushing with a pipette, and transferred to 1.1 ml Fluorescent Activated Cell Sorting (FACS) micro tubes (Elkay Laboratories, UK) for labeling. FACS buffer (PBS containing 1% Fetal Bovine Serum) was used to wash the samples three times (settings: time; 5 min, RCF; 500 *xg*, temperature; 4 °C).

Immunofluorescent staining was carried out by placing 80 µl of the staining master mix (containing all antibody-fluorochrome stains, and cell viability dye -section 2.6.1) directly into the micro tube. Therefore each antibody-fluorochrome conjugate was present in a 1 in 80 ratio (with FACS buffer) within the staining master mix. The samples were incubated at 4°C in the dark then washed three more times with FACS buffer under the same settings. Lastly, all samples were fixed with 300 µl of 2 % paraformaldehyde (Fisher Scientific, Waltham) and analysed with flow cytometry thereafter.

It was ensured that the phenotypic and activation markers used were compatible with the lasers in the LSRII, and also compatible with all other antibody-fluorochrome conjugates included per flow cytometry panel used in this study. Therefore at the commencement of the study, the markers and fluorochromes to be used were carefully selected.

2.7.3 Fluorochrome selection

Optimisation of the most appropriate antibody-fluorochrome combinations for detection of phenotypic and activation markers within a single assay has been done previously by our group (Table 2.1; A). Over the course of this study however, more markers were included to cover the aims of this project.

Table 2.1: Multicolour flow cytometry panels used in this project for the detection of T- and B-cell phenotypic and activation markers (A), and B-cell subsets (B); where 1 µl of each antibody was used per test in a final volume of 80 µl.

(A)

Laser (Excitation wavelength nm)	Filter	Molecule	Antigen location *	Fluorochrome	Clone	Supplier
Blue 488	530/30	Intracellular amines	IC	CFSE	N/A	Invitrogen™, Molecular probes™, Oregon
	575/26	CD25	EC	R-phycoerythrin (PE)	BC96	eBioscience Inc., San Diego
	780/60	CD19	EC	PECy®7	HIB19	Invitrogen™, Camarillo
Violet 405	450/40	CD8a	EC	Brilliant violet 421™	RPA-T8	BD Biosciences, New Jersey
	525/50	CD86	EC	Brilliant violet 510™	2331 (FUN-1)	BD Biosciences, New Jersey
UV 355 †	405/20	1. Free cytoplasmic amines ‡ and 2. CD14	1. IC and 2. EC	1. Live/Dead® Fixable Blue Dead cell stain kit and 2. BUV395	1. N/A and 2. MPhiP9	1. Molecular Probes®, Life Technologies ™, Oregon and 2. BD Biosciences, New Jersey
Red 633	660/20	CD4	EC	Allophycocyanin (APC)	S3.5	Invitrogen™, Frederick

(B)

Laser (Excitation wavelength nm)	Filter	Molecule	Antigen location*	Fluorochrome	Clone	Supplier
Blue 488	530/30	Intracellular amines	IC	CFSE	N/A	Invitrogen™, Molecular probes™, Oregon
	575/26	CD21	EC	R-phycoerythrin (PE)	LT21	ThermoFisher Scientific, Massachusetts
	610/20	CD10	EC	Qdot® 605	MEM-78	ThermoFisher Scientific, Massachusetts
	780/60	CD19	EC	PE-Cy®7	HIB19	Invitrogen™, Camarillo
Violet 405	450/40	Caspase-1, -2, -3, -6, -8, -9, -10	IC	Violet live cell caspase probe	N/A	BD Biosciences, New Jersey
	525/50	CD86	EC	Brilliant violet 510™	IT2.2	Biolegend, San Diego
UV 355 †	405/20	1. Free cytoplasmic amines ‡ and 2. CD14	1. IC and 2. EC	1. Live/Dead® Fixable Blue Dead cell stain kit and 2. BUV395	1. N/A and 2. MPhiP9	1. Molecular Probes®, Life Technologies™, Oregon and 2. BD Biosciences, New Jersey
Red 633	660/20	CD20	EC	Allophycocyanin (APC)	2H7	eBioscience Inc., San Diego
	730/45	HLA-DR	EC	Alexa Fluor® 700	L243	Biolegend, San Diego
	780/60	CD27	EC	APC-Alexa Fluor® 750	CLB-27/1	ThermoFisher Scientific, Massachusetts

*IC: Intracellular and EC: Extracellular

† The UV 405/20 filter was used as a 'dump' channel for the detection and elimination of all dead cells and CD14+ cells from the populations of interest. Hence, detection of these two unwanted populations was done together.

‡ Because all un-conjugated CFSE reagent passively diffuses out of the cell, CFSE is compatible with the Live/Dead® Fixable Blue Dead cell stain kit. Both reagents have been used successfully within the same flow cytometry panel in the literature (Perfetto et al., 2010) and by our group.

Once flow cytometry was completed per experiment, raw data was analysed. Several gating strategies had to be used to eliminate debris and unwanted cell populations, leaving only cell populations of interest, as detailed below.

2.7.4 Post-acquisition analysis

Raw data obtained after flow cytometry was analysed using FlowJo version 7.6® for MAC software (TreeStar Inc., Ashland).

Bioexponential transformation (logical implementation) was used in order to enable visualisation of populations with negative values. Sequential gating was then applied to each individual experiment to eliminate debris, cell clumps, dead cells and CD14+ cell populations from the T- and B-cell populations of interest (figure 2.3).

Proliferation values in this study are reported as proliferation indices (section 2.4) while activation values are reported in Median Fluorescence Intensity (MFI).
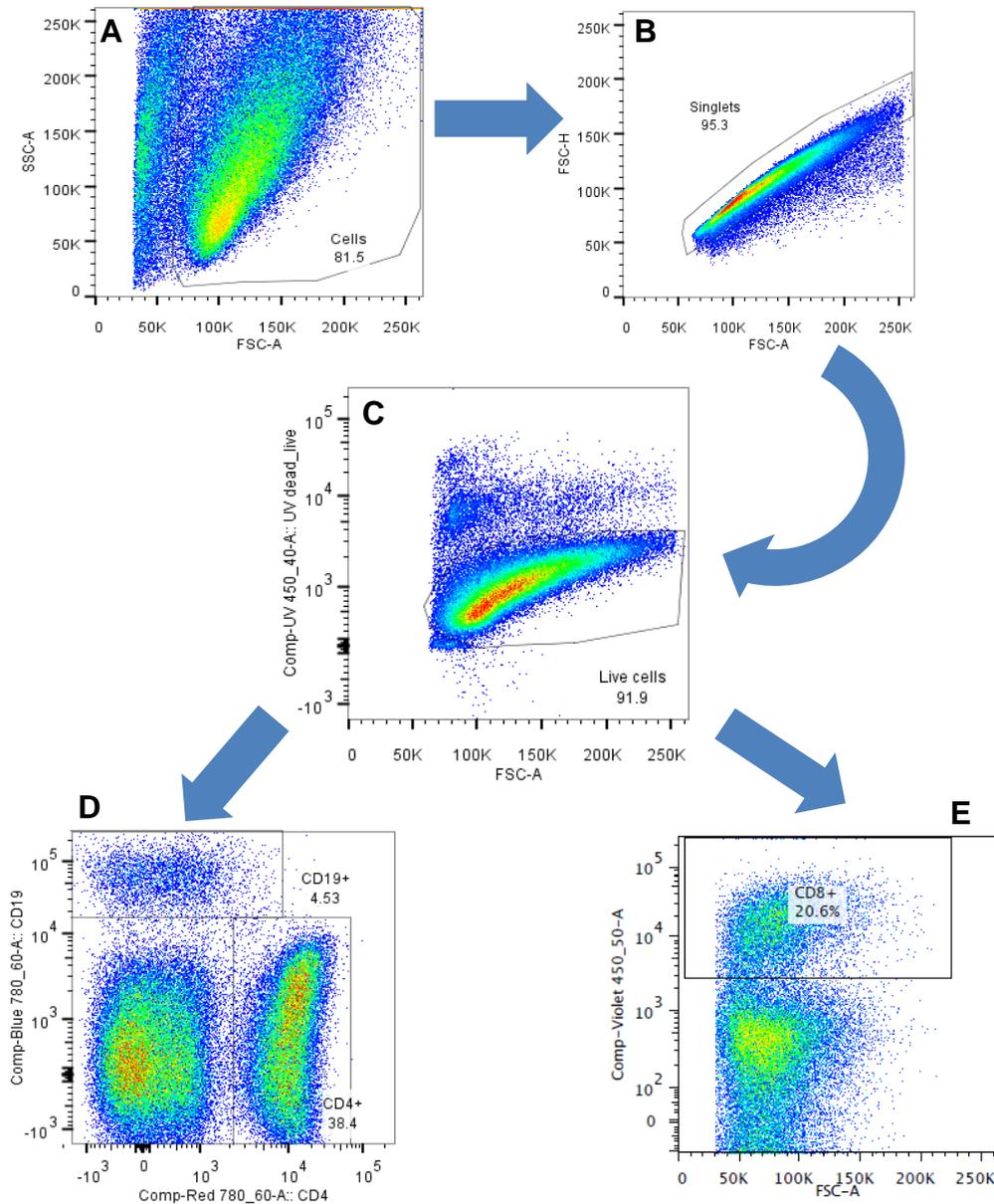
Figure 2.3: Flow cytometry gating strategy used to eliminate all unwanted cells/signals from the final data set. Gates were constructed around cells leaving out debris (FSC-Area versus SSC-Area; A), followed by the gating of singlets to exclude cell clumps (FSC-Height versus FSC-Area; B). Using the optimised panels presented in table 2.1, the UV 405/40 filter was used as a dump channel for dead cells (being identified through the use of the live/dead® fixable blue dye) and the entire CD14+ population. Therefore, gates were constructed around live cells (C). Fluorescence-Minus-One (FMO) controls (fig. 2.4) were used to construct gates around CD4+CD19- T-cells (D), CD8+ T-cells (E) and CD19+CD4- B-cells (D). The

percentage of events recorded in each gate is also shown. Additionally, in the case of the B-cell subsets, gating focused solely on CD19+ B-cells, and subsets defined by markers outlined in table 2.1 (B) thereafter.

FMO controls include every fluorochrome in a given flow cytometry panel, except one (Hulspas et al., 2009). Using FMO controls for gating ensures that gating thresholds set for the particular fluorochrome absent from the FMO are as precise as possible (Herzenberg et al., 2006).

The FMO controls used to select cell populations of interest are shown in fig. 2.4 to 2.6. Each experiment was performed with a full panel of FMO controls to ensure accurate gating per experiment. The FMO gating strategy for CD4+ and CD8+ T-cells, and CD19+ B-cells is presented in fig. 2.4.
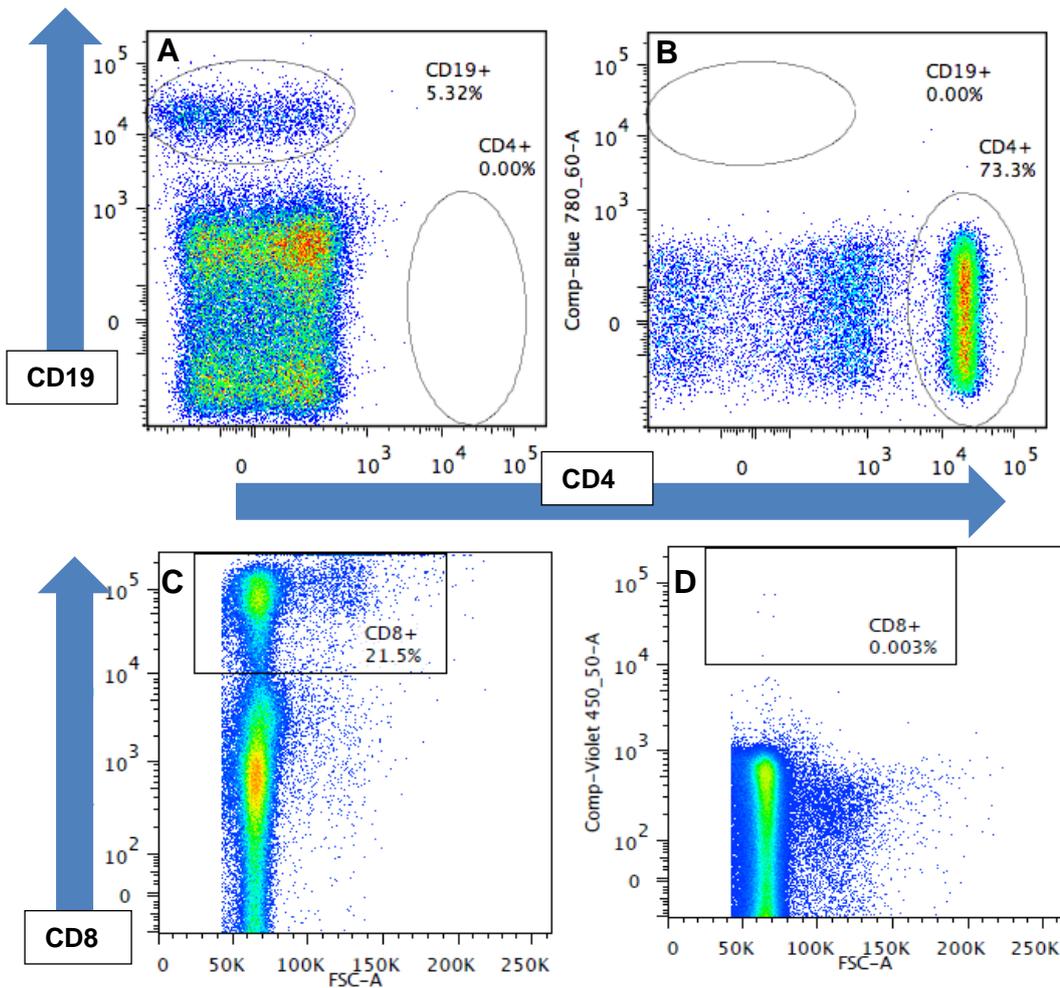
Figure 2.4: Representative dot plots of positively labelled CD19+ (A) B-cell, and CD4+ (B) and CD8+ T-cell populations (C) relative to their respective Fluorescence-Minus-One (FMO) gating controls (B for CD19+ B-cells, A for CD4+ T-cells, and D for CD8+ T-cells). The first three steps in the gating strategy presented in fig. 2.3 (A, B and C) were used prior to this FMO gating strategy. Also, this strategy was strictly used for the T- and B-cell panel presented in table 2.1 A.

The flow cytometry panel optimised to quantify CD19+ B-cell subsets was gated based on FMO controls presented in fig. 2.5.
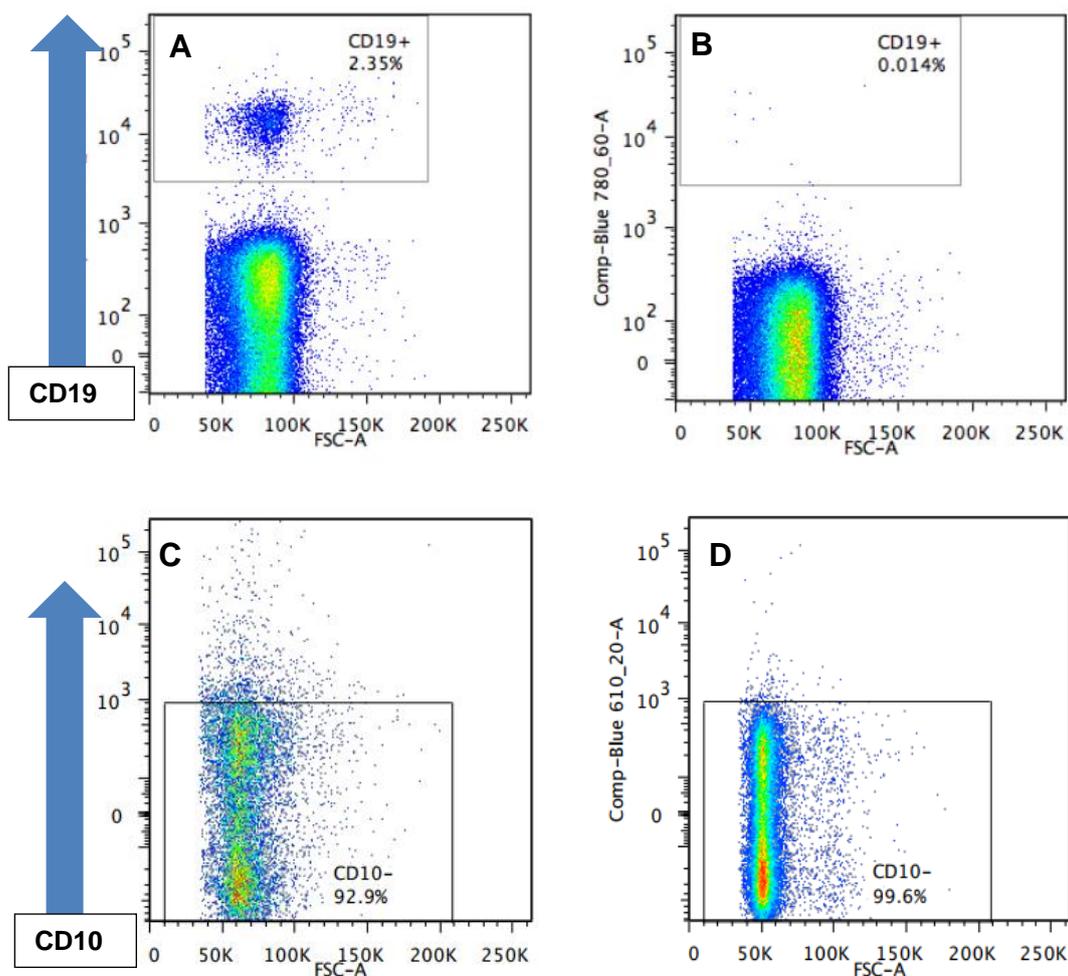
Figure 2.5: Representative dot plots of positively labelled CD19+ (A) and CD10+ B-cell populations (C) relative to their respective Fluorescence-Minus-One (FMO) gating controls (B for CD19+ B-cells and D for CD10+ B-cells). The first three steps in the gating strategy presented in fig. 2.3 (A, B and C) were used prior to this FMO gating strategy. Also, this strategy was strictly used for the B-cell subset panel presented in table 2.1 B.

Following the selection of the CD19+CD10- B-cell population, five B-cell subsets (fig. 2.6) were gated based on the CD27, CD21 and CD20 markers. Some of these subsets have been found to be perturbed in HIV-viraemic individuals (Moir and Fauci, 2013).
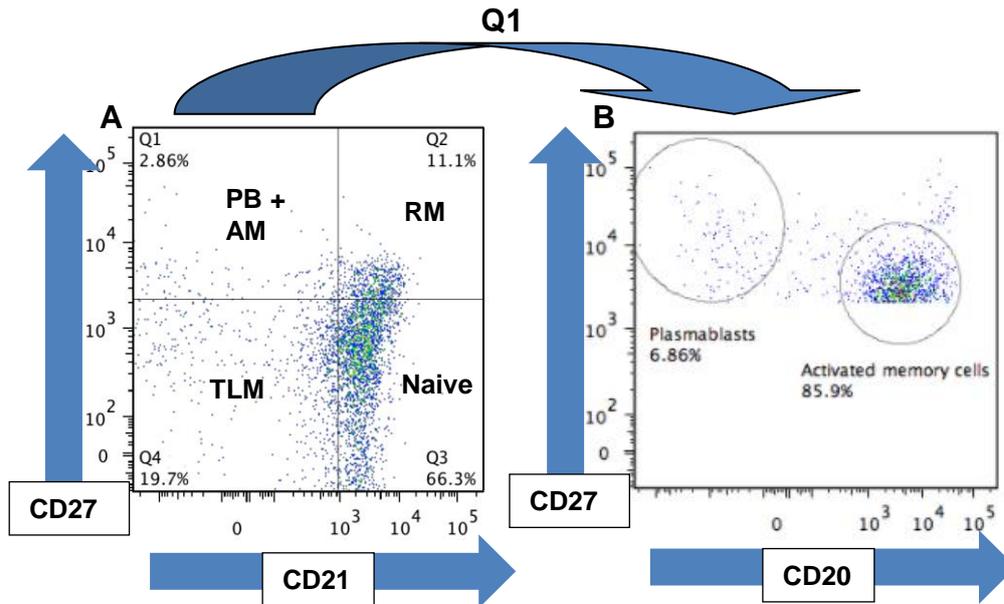
Figure 2.6: Representative dot plots showing B-cell subsets (A) and further separation of the Q1 quadrant into Plasmablasts and Activated Memory cells (B). Q1 comprises Plasmablasts (PB) and Activated Memory cells (AM), Q2; Resting Memory cells (RM), Q3; Naive B-cells, and Q4: Tissue-Like Memory cells (TLM) (Moir and Fauci, 2013). The Q1 compartment was separated into PB and AM subsets using the CD20 marker. As indicated by the gates, PBs are CD27^{hi}CD21^{lo}CD20^{lo} while AMs are CD27^{int}CD21^{lo}CD20^{hi} (Moir and Fauci, 2013, Wheatley et al., 2016).

All raw data was then statistically analysed to investigate differential T- and B-cell responses between patients and controls.

2.8 Statistical analysis

All statistical analyses and graphics were done using the IBM SPSS statistics 21 software (SPSS Inc., Illinois) and GraphPad Prism 7 (GraphPad Software, Inc., California).

The Kolmogorov-Smirnov test was used to test for data normality. Thereafter, appropriate statistical tests were used to investigate differential responses between patients and controls. Statistical tests used are presented in detail per results chapter.

CHAPTER THREE: THE EFFECT OF AGE, SEX AND ETHNICITY ON T- AND B-CELL RESPONSES

3.1 Introduction

The case-control study design is frequently used in public health research. While matching of cases to controls lends efficiency to a study, there has been a forty-year discussion surrounding the advantages and disadvantages of stringent matching (Rose and van der Laan, 2009). Kupper and colleagues described how there is no benefit in matching non-confounding variables between cases and controls (Kupper et al., 1981). Garey stated that only factors considered strongly confounding will largely affect the efficiency of the study (Garey, 2004). Furthermore, while a case-control study of quality of life of Irritable Bowel Syndrome (IBS) sufferers compared to controls found similar results irrespective of matching or non-matching (Faresjo and Faresjo, 2010), matching reduced the study's statistical power. Therefore, the use of case-control matching for research needs to be justified.

To investigate subtle defects in T- and B-cell responses in two immunocompromised patient groups in this study (HIV-infected individuals and MGUS patients), it was planned to individually match each case to a specific control based on four factors: age, sex, ethnicity and date of sample acquisition. Wherein, responses per patient would be compared to responses from a control subject whom to our knowledge did not have the same disease state. This matching should cover for any pre-existing differences caused by these inherent factors, especially as day-to-day variability in the immunologic assay itself could skew data to a certain extent. Thus assays were always run with cases and controls on the same day, as had always been previously done by our group (Foster et al., 2009, Foster et al., 2010, Wing et al., 2012, Darton et al., 2011, Preciado-Llanes et al., 2015). The next step was to ascertain how these factors affect immune responses, and if they were indeed potential confounders.

Jager et al (2008) have described variables to be 'potential confounders' if they fulfil three criteria: 1. The variable must be a known risk factor for the disease; 2. It should have unequal distribution between exposed and non-

exposed groups; and 3. It is not an effect of the exposure (Jager et al., 2008). It is well established that the burden of pneumococcal disease affects infants below the age of two, elderly people above the age of 65 (Robinson et al., 2001, Trotter et al., 2008), and the immunocompromised (Feikin et al., 2010, Kumashi et al., 2005, Overturf, 2003, Barrettc.E, 1971). Hence, it was decided that age-matching cases to controls in the present study would be appropriate. Indeed, Pearce (2016) stated that age-matching improves statistical precision in case-control studies (Pearce, 2016).

Additionally, cellular and humoral immune responses tend to be impaired in the elderly. The number of T-cells in PBMCs has been shown to be lower with age (Utsuyama et al., 1992). Specifically, these numbers begin to significantly decline from the third decade of life, hold relatively constant through to the seventh decade, then deplete thereafter (Utsuyama et al., 1992). Age-related immunosenescence is prominent in the T-cell population and can be accelerated by latent persistent human cytomegalovirus (HCMV) (Tu and Rao, 2016). The total number of CD19+ B-cells also decreases with age. These changes have vaccine-response implications (Frasca et al., 2011). Overall, the strong link between age and declining immunity further highlights the need for age-matching in case-control studies in immunological research.

Susceptibility to diseases and vaccine responses are also influenced by sex, with men often being more susceptible towards infectious disease and women mounting higher humoral responses (Giefing-Kroell et al., 2015). This sex difference is further confounded by the effect of age on the levels of sex hormones produced (Giefing-Kroell et al., 2015).

In 2012, Abdullah and colleagues found *in vitro* sex-specific differences in lymphocyte subsets of healthy adult humans. Males had higher levels of lymphocytes in whole blood. Regarding lymphocyte subsets enumeration from this whole blood, while males had higher levels of natural killer (NK) cells, females had higher levels of B-cells. Following culture, females showed a significant increase in B- and total T-cell percentages, whilst males showed

an increase in NK cells. However, upon stimulation with phytohaemagglutinin (PHA), males showed significantly higher total T-cell percentages whilst persisting with higher NK cells. On the other hand, females had higher total activated T-cells (CD69+). While the study cohort was small (n = 15), there are important implications from this study which can be extrapolated to sex-matching in case-control studies (Abdullah et al., 2012). Sex influences immune cell responses, indicating a potential to affect data interpretation should sex-matching be omitted.

Race of vaccinees following primary smallpox vaccination has been revealed to influence cell-mediated immune responses (Haralambieva et al., 2013). Caucasians had significantly higher total IFNγ ELISPOT responses (p=0.010), CD8+ IFNγ ELISPOT responses (p<0.001), secreted IL-2 (p=0.003), and IFNα (p<0.001) compared to African-Americans and Hispanics. Haralambieva and colleagues (2013) also reported significantly higher total IFNγ ELISPOT responses and higher IL-1β in men (both p<0.001) compared to women. Women had significantly higher secreted vaccinia-specific IL-2 (p<0.001) and IL-10 (p=0.017) compared to men. Whilst the clinical implications of these results remain unclear, a race and sex-based bias in immune responses to smallpox vaccination can be concluded. In a further study, racial/ethnic-influenced humoral immune responses were reported, following rubella vaccination (Haralambieva et al., 2014). In this study conducted by Haralambieva and colleagues, individuals of European descent and/or Hispanic ethnicity showed significantly lower levels of rubella-specific neutralizing antibody levels (p < 0.001) compared to individuals of African descent. However, sex showed no consistent association with immune response. These two studies conducted by the Haralambieva group suggest an influence of sex and ethnicity on cellular-mediated, and humoral immunity. This indicated the necessity for ethnicity-matching in the present study.

However, before embarking on studying how age, sex and ethnicity could affect *in vitro* T- and B-cell responses to the validated assay used widely in our laboratory (Foster et al., 2009, Foster et al., 2010, Darton et al., 2011,

Wing et al., 2012, Preciado-Llanes et al., 2015) it was essential to be able to reproduce our group results.

Thus data gathered and presented in this chapter had two aims: Firstly, to reproduce results showing that plate-bound anti-CD3 stimulates activation in CD4+ T-cells and to reproduce our laboratory group results showing that T-cell-independent Type 2 (TI-type 2) stimulation of B-cells using αδdex elicits significantly increased activation in these B-cells. Secondly, to ascertain if inherent factors- age, sex and ethnicity, would have any effect on T- and B-cell responses to anti-CD3 and αδdex separately, and in combination. This information would underpin the stringency of matching the cases to controls during recruitment for this study.

3.2 Methods

Blood donors were recruited from amongst the staff and students of the Medical School, Royal Hallamshire Hospital as described in chapter two (section 2.1). After informed consent was obtained, blood was drawn and PBMCs were cultured using aseptic technique. The immune assay was performed as described in chapter two (section 2.4 and 2.5). To increase the numbers in each study group in this chapter, data gathered by a member of our group, James Wing, was included in analysis with permission (as indicated in table 3.1). This data had not been previously analysed for age-based correlations or sex-based variations in immune response. The two cell populations of interest in this chapter, CD4+ T-cells and CD19+ B-cells, were gated according to the strategy detailed in fig. 2.3 (chapter two).

Table 3.1: Brief description of the workflow and outcome measures for results presented in chapter three

Aim	Work Flow	Outcome measures	Results presented in figure:	Study group number	Data collected by
Reproduce group results	CD4+ T-cell responses to TCR-stimulant; anti-CD3 alone, and in combination with αδdex, and αδdex + anti-CD28 respectively.	CD4+ T-cell frequency, proliferation (based on CFSE proliferation index), and activation (based on CD25 and HLA-DR expression).	3.1 – 3.2	12	Furaha Asani
	CD19+ B-cell responses to anti-IgD-stimulation using αδdex alone, and in combination with anti-CD3, and anti-CD3 + anti-CD28 respectively.	CD19+ B-cell frequency, proliferation (based on CFSE proliferation index), and activation (based on CD86, CD25 and HLA-DR expression).	3.3 – 3.5	12	Furaha Asani
Correlate age with immune responses	CD4+ T-cell responses to TCR-stimulant; anti-CD3 alone, and in combination with αδdex	CD4+ T-cell CD25 expression	3.6	106	Furaha Asani (n = 18); James Wing (n = 88)
	CD19+ B-cell responses to anti-IgD-stimulation using αδdex alone, and in combination with anti-CD3	CD19+ B-cell CD86 expression	3.7	106	Furaha Asani (n = 18); James Wing (n = 88)
Investigate sex-based variations in immune responses	CD4+ T-cell responses to TCR-stimulant; anti-CD3 alone, and in combination with αδdex	CD4+ T-cell CD25 expression	3.8	100	Furaha Asani (n = 12); James Wing (n = 88)
	CD19+ B-cell responses to anti-IgD-stimulation using αδdex alone, and in combination with anti-CD3	CD19+ B-cell CD86 expression	3.9	100	Furaha Asani (n = 12); James Wing (n = 88)
Investigate ethnicity-based variations in immune responses	CD4+ T-cell responses to TCR-stimulant; anti-CD3 alone, and in combination with αδdex, and αδdex + anti-CD28 respectively.	CD4+ T-cell frequency, proliferation (based on CFSE proliferation index), and activation (based on CD25 expression).	3.10 – 3.12	18	Furaha Asani
	CD19+ B-cell responses to anti-IgD-stimulation using αδdex alone, and in combination with anti-CD3, and anti-CD3 + anti-CD28 respectively.	CD19+ B-cell frequency, proliferation (based on CFSE proliferation index), and activation (based on CD86 and CD25 expression).	3.13 – 3.16	18	Furaha Asani

3.3 Results

A healthy population, with demographics shown in table 3.2, was recruited to reproduce the *in vitro* T- and B-cell assay results that have been published from our laboratory (Foster et al., 2009, Darton et al., 2011).

Table 3.2: Descriptive statistics showing the age, sex and ethnicity of 12 individuals used to investigate T- and B-cell responses to a validated stimulation assay

	Study group
Number	12
Mean age (Range)	27 (23 - 33)
Median age	25.50
Sex: Female	6
Male	6
Ethnicity : Black	6
White	6

3.3.1 CD3-stimulation of T-cells and IgD-stimulation of B-cells results in activation

The initial phase of this project sought to validate an immunologic assay used by our laboratory showing significant up-regulation of CD25 expression in CD4+ T-cells following TCR-stimulation (Foster et al., 2009, Foster et al., 2010, Preciado-Llanes et al., 2015) (fig. 3.2 A). Also, to validate B-cell activation as measured by CD86 and CD25 expression after polyclonal stimulation with αδdex, with and without T-cell help (Darton et al., 2011).

It was essential to first determine what effect the stimulus had, if any, on the frequency distribution of the cells. While CD4+ T-cell frequencies remained unchanged upon stimulation (fig. 3.1) CD19+ B-cell frequencies significantly reduced upon αδdex-stimulation, relative to the un-stimulated control (fig.

3.3). As demonstrated by Darton et al. (2011) up-regulation of CD86 expression in CD19+ B-cells was seen upon stimulation with a combination of αδdex, anti-CD3 and anti-CD28 (fig.3.4 A). A similar trend was seen for HLA-DR (fig. 3.5).

Using the one-sample Kolmogorov-Smirnov test, data in figures 3.1 to 3.5 were ascertained to be non-parametric. Thus the Kruskal-Wallis H test (which is the non-parametric equivalent of the Analysis of variance test) was used to study pair-wise variances between the un-stimulated and stimulated conditions. The *p* values shown were adjusted by Bonferroni correction, to correct for type I errors introduced by multiple comparisons. Data are presented as median values within confidence intervals. Stimulation concentrations used were as described in chapter 2 (section 2.4 and 2.5), and previously determined by our group (Foster et al., 2009, Foster et al., 2010, Darton et al., 2011, Wing et al., 2012, Preciado-Llanes et al., 2015): 1µg/ml of αδdex, 0.1µg/ml anti-CD3 alone, and 0.5µg/ml anti-CD3 in combination with 0.5µg/ml anti-CD28 for 96 hr.
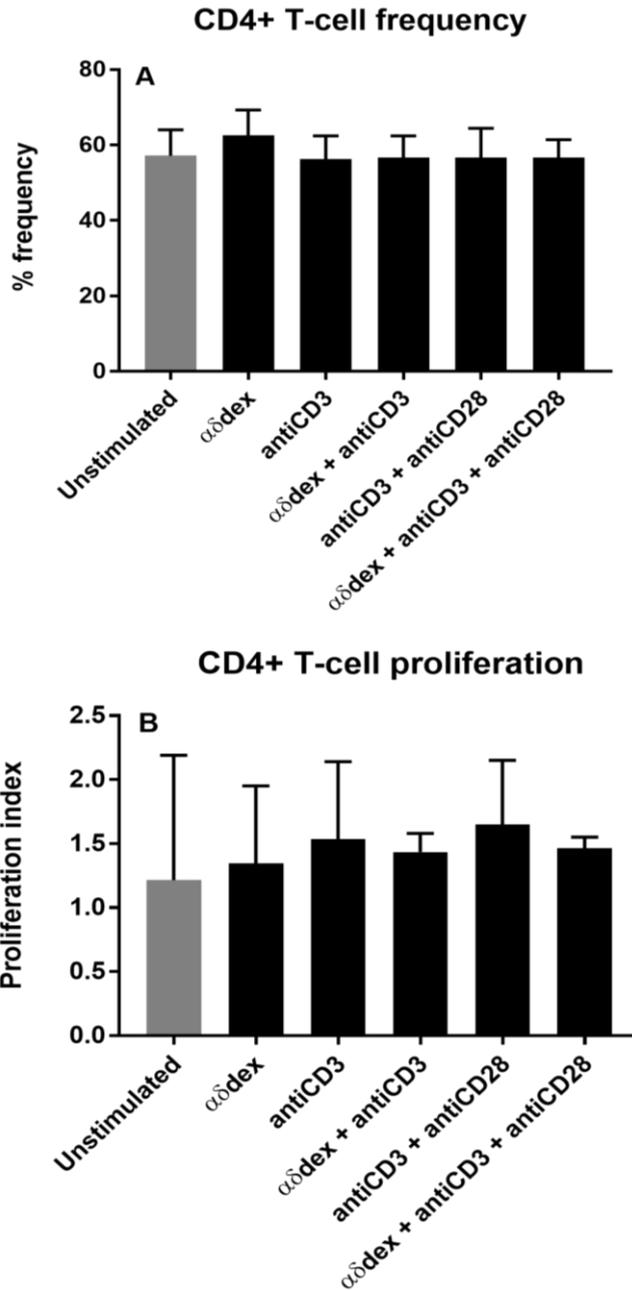
Figure 3.1: Frequency (A) and proliferation (B) of CD4+ T-cells following
in vitro **CD3-stimulation alone, in combination with CD28-costimulation,**
and αδdex. Up-regulation in stimulated conditions was analysed relative to
the un-stimulated control. Kruskal-Wallis H test with Bonferroni correction
was used to study pair-wise variances (n = 12). Concentrations of stimulants
used: 1μg/ml of αδdex, 0.1μg/ml anti-CD3 alone, and 0.5μg/ml anti-CD3 in
combination with 0.5μg/ml anti-CD28.
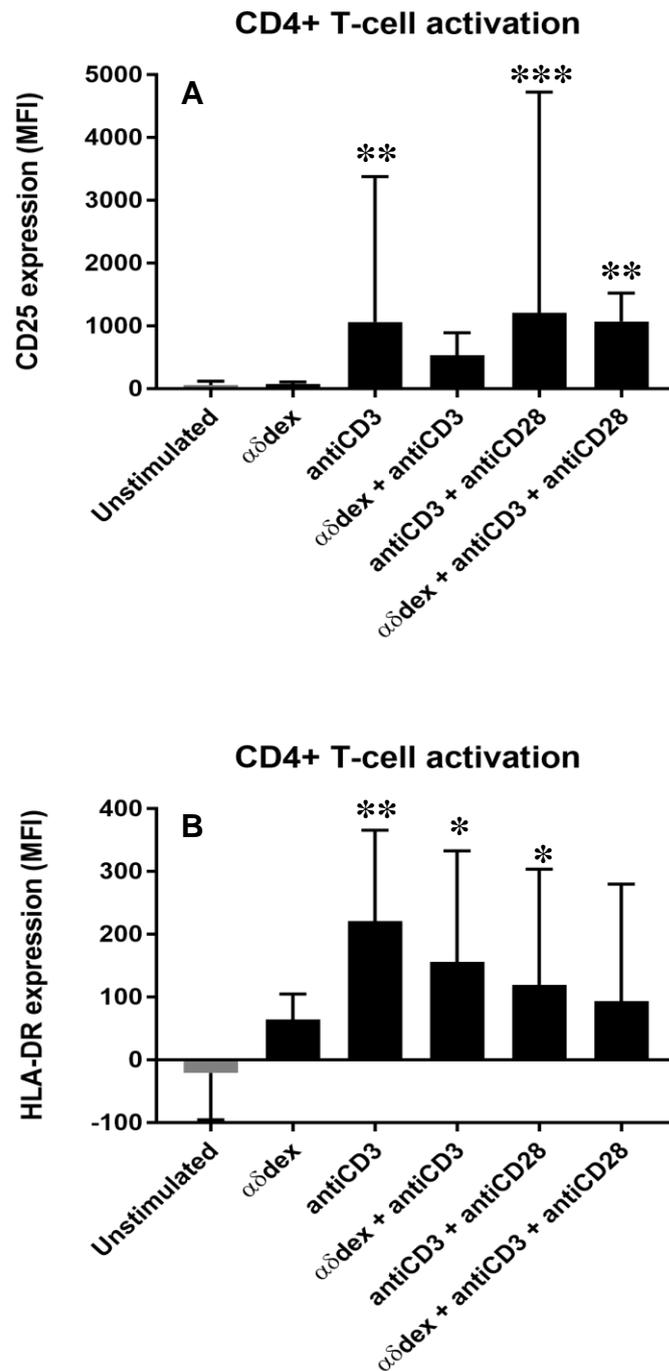
Figure 3.2: Activation of CD4+ T-cells in terms of CD25 (A) and HLA-DR expression (B) following *in vitro* CD3-stimulation alone, in combination with CD28-costimulation, and αδdex. Up-regulation in stimulated conditions was analysed relative to the un-stimulated control. Kruskal-Wallis H test with Bonferroni correction was used to study pair-wise variances (n = 12). Concentrations of stimulants used: 1µg/ml of αδdex, 0.1µg/ml anti-CD3

alone, and 0.5µg/ml anti-CD3 in combination with 0.5µg/ml anti-CD28. (Where * $p \leq 0.050$, ** $p \leq 0.010$, *** $p \leq 0.001$).
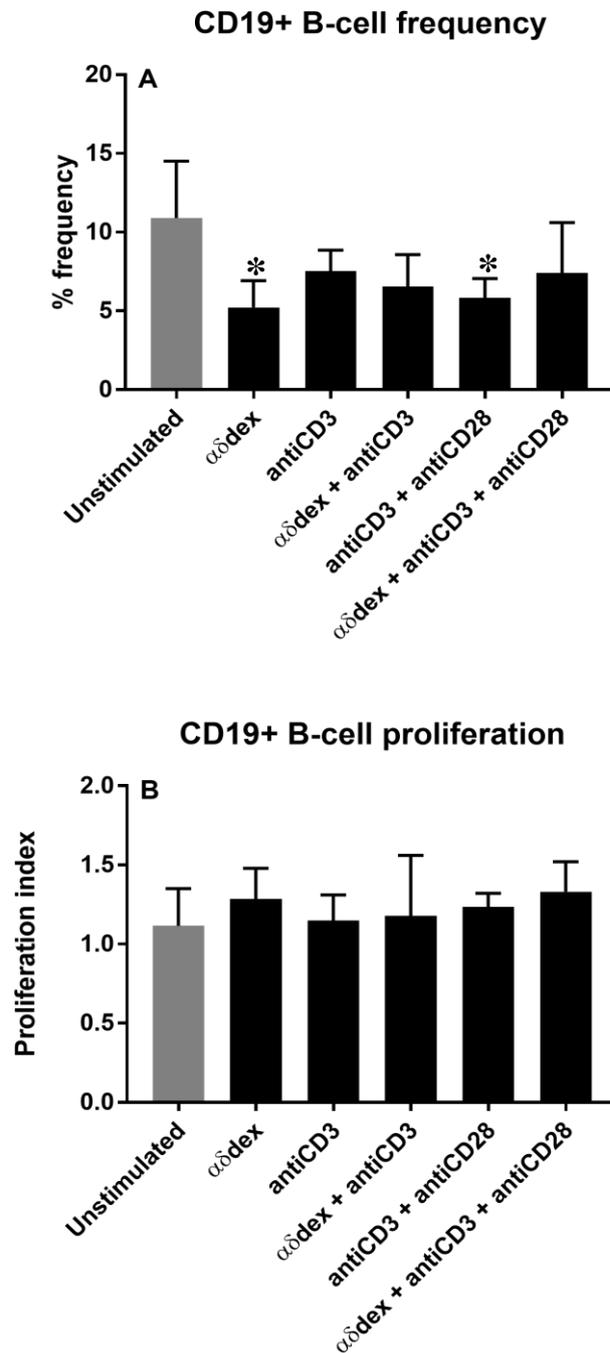
Figure 3.3: Frequency (A) and proliferation (B) of CD19+ B-cells following *in vitro* IgD-stimulation with αδdex alone, and in the presence of T-cell help. Up-regulation in stimulated conditions was analysed relative to the un-stimulated control. Kruskal-Wallis H test with Bonferroni correction was used to study pair-wise variances (n = 12). Concentrations of stimulants

used: 1µg/ml of αδdex, 0.1µg/ml anti-CD3 alone, and 0.5µg/ml anti-CD3 in combination with 0.5µg/ml anti-CD28. (Where * $p \leq 0.050$).
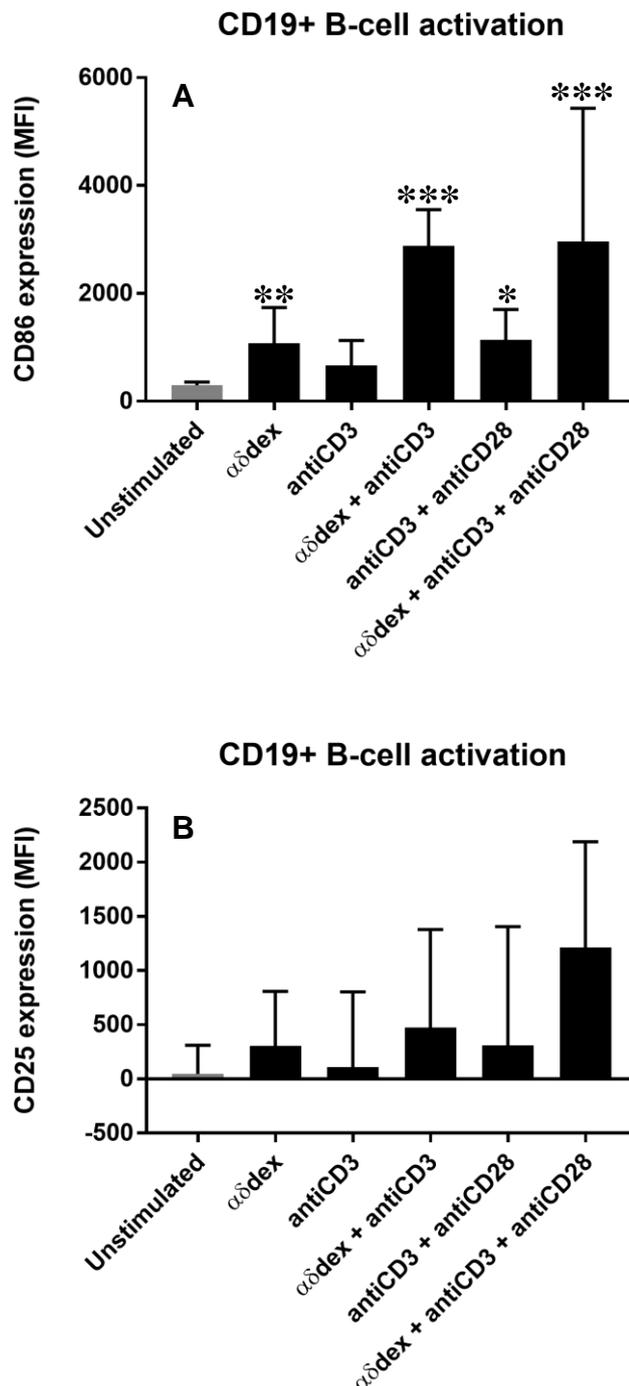
Figure 3.4: Activation of CD19+ B-cells in terms of CD86 (A) and CD25 expression (B) following *in vitro* IgD-stimulation with αδdex alone, and in the presence of T-cell help. Up-regulation in stimulated conditions was analysed relative to the un-stimulated control. Kruskal-Wallis H test with

Bonferroni correction was used to study pair-wise variances (n = 12). Concentrations of stimulants used: 1µg/ml of αδdex, 0.1µg/ml anti-CD3 alone, and 0.5µg/ml anti-CD3 in combination with 0.5µg/ml anti-CD28. (Where * *p* ≤ 0.050, ** *p* ≤ 0.010, *** *p* ≤ 0.001).
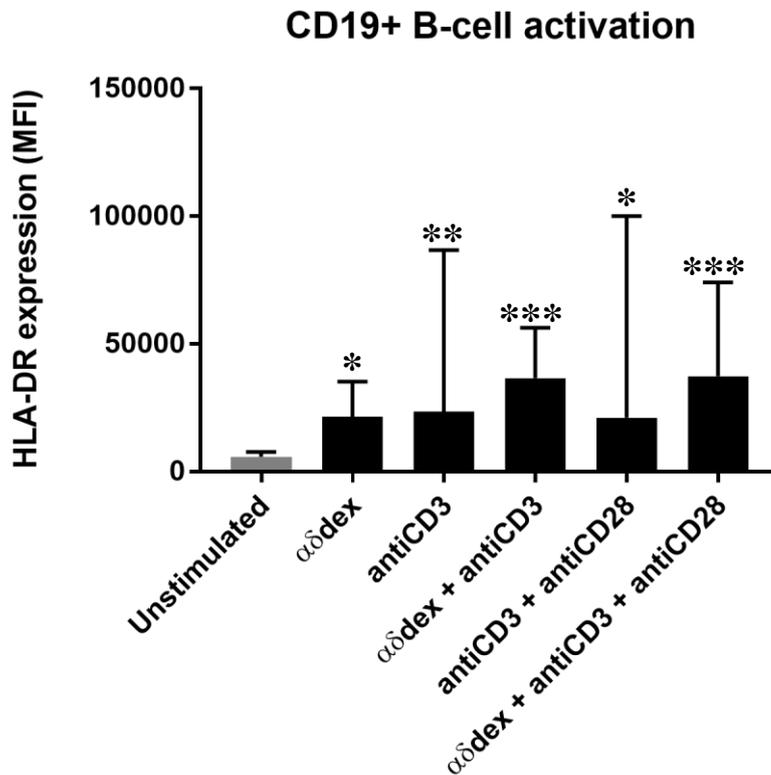
Figure 3.5: Activation of CD19+ B-cells in terms of HLA-DR expression, following *in vitro* IgD-stimulation with αδdex alone, and in the presence of T-cell help. Up-regulation in stimulated conditions was analysed relative to the un-stimulated control. Kruskal-Wallis H test with Bonferroni correction was used to study pair-wise variances (n = 12). Concentrations of stimulants used: 1µg/ml of αδdex, 0.1µg/ml anti-CD3 alone, and 0.5µg/ml anti-CD3 in combination with 0.5µg/ml anti-CD28. (Where * *p* ≤ 0.050, ** *p* ≤ 0.010, *** *p* ≤ 0.001).

3.3.2 Age significantly affects stimulated CD4+ T-cell, and un-stimulated CD19+ B-cell activation

To investigate the effects of age on T- and B-cell responses, a group comprising 106 healthy individuals (table 3.3) was recruited for study.

Table 3.3: Age range of 106 individuals used to investigate the correlative effects of age on T- and B-cell responses to CD3- and αδdex-stimulation respectively. The sex categorisation of a large portion of this study group were unknown, hence were unrecorded in the table.

	Study group
Number	106
Mean age (Range)	32.02 (23 - 57)
Median age	30.00

Using the one-sample Kolmogorov-Smirnov test, data obtained from this study group yielded some sets that were parametric, and others which were non-parametric. As a result both parametric and non-parametric correlative tests: Pearson's correlation and Spearman's rho respectively, were used.

Data are presented as scatter plots, with age on the x-axis and activation markers (in MFI) on the y-axis. Stimulation concentrations used were as described in chapter 2 (section 2.4 and 2.5): 1µg/ml of αδdex, 0.1µg/ml anti-CD3 alone, and 0.5µg/ml anti-CD3 in combination with 0.5µg/ml anti-CD28. R^2 values are shown on fig. 3.6 and 3.7 to indicate the percentage of activation values that can be predicted from the age data. Older individuals showed an increase in CD25 expression in CD4+ T-cells upon *in vitro* stimulation with anti-CD3 and αδdex ($p \leq 0.050$; fig. 3.6C) compared to younger individuals. This occurred in spite of comparable CD4+ T-cell activation across all ages under un-stimulated conditions (fig. 3.6A).
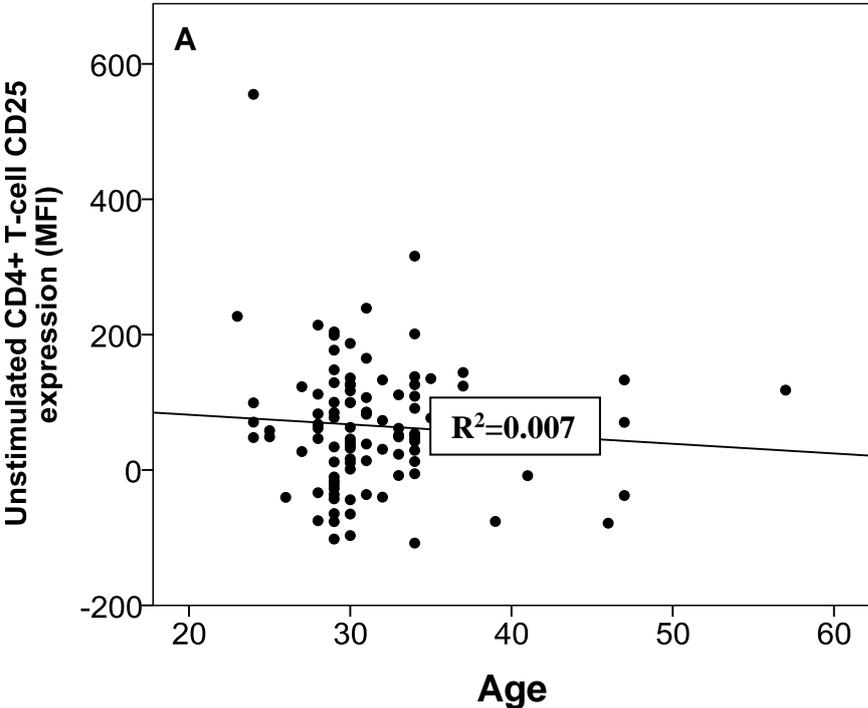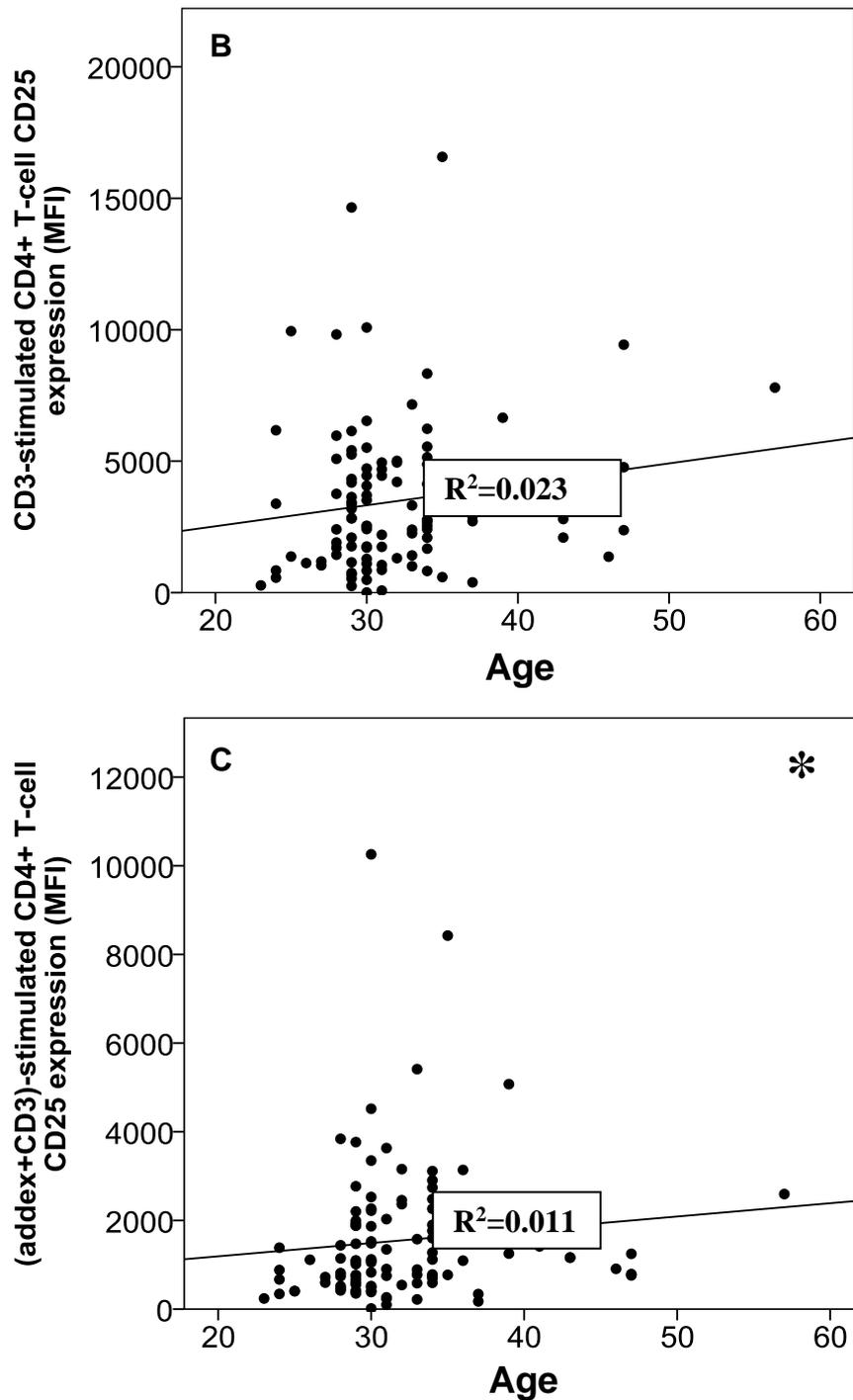
Figure 3.6: Correlation of age with *in vitro* CD4+ T-cell activation, in terms of CD25 expression, under unstimulated conditions (A), with CD3-stimulation alone (B) and combined with αδdex (C). Spearman's rho bivariate correlation for non-parametric data was used to determine this significance (n = 106). Concentrations of stimulants used: 1µg/ml of αδdex,

0.1µg/ml anti-CD3 alone, and 0.5µg/ml anti-CD3 in combination with 0.5µg/ml anti-CD28. (Where * $p \leq 0.050$).

Under un-stimulated conditions, older individuals showed lower CD19+ CD86 expression ($p \leq 0.050$; fig. 3.7A) compared to younger individuals. Stimulation eliminated the significance of this activation response (fig. 3.7B and C).
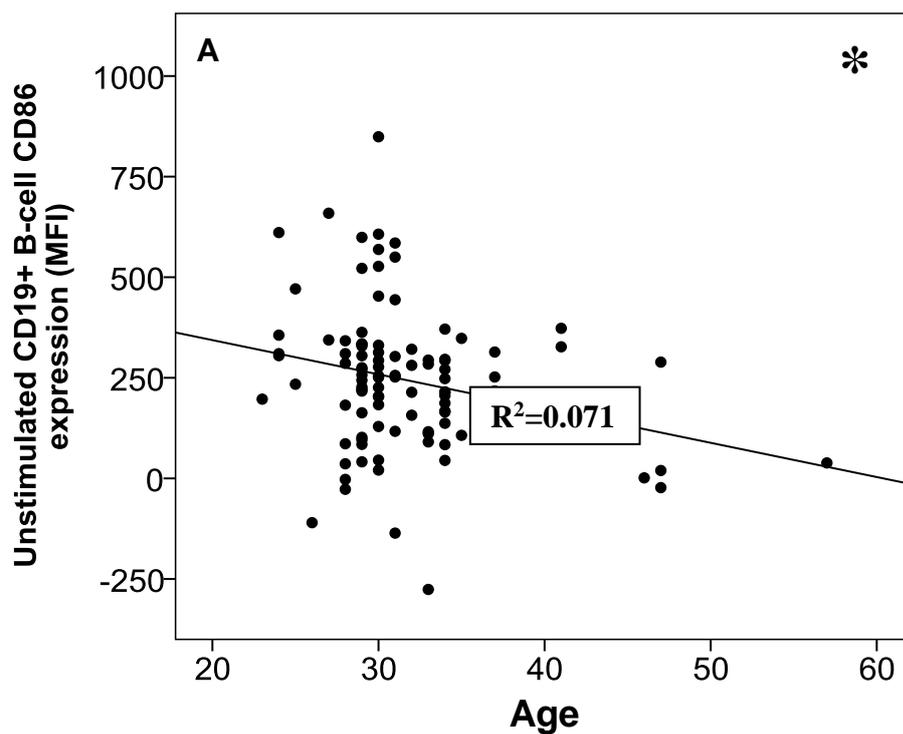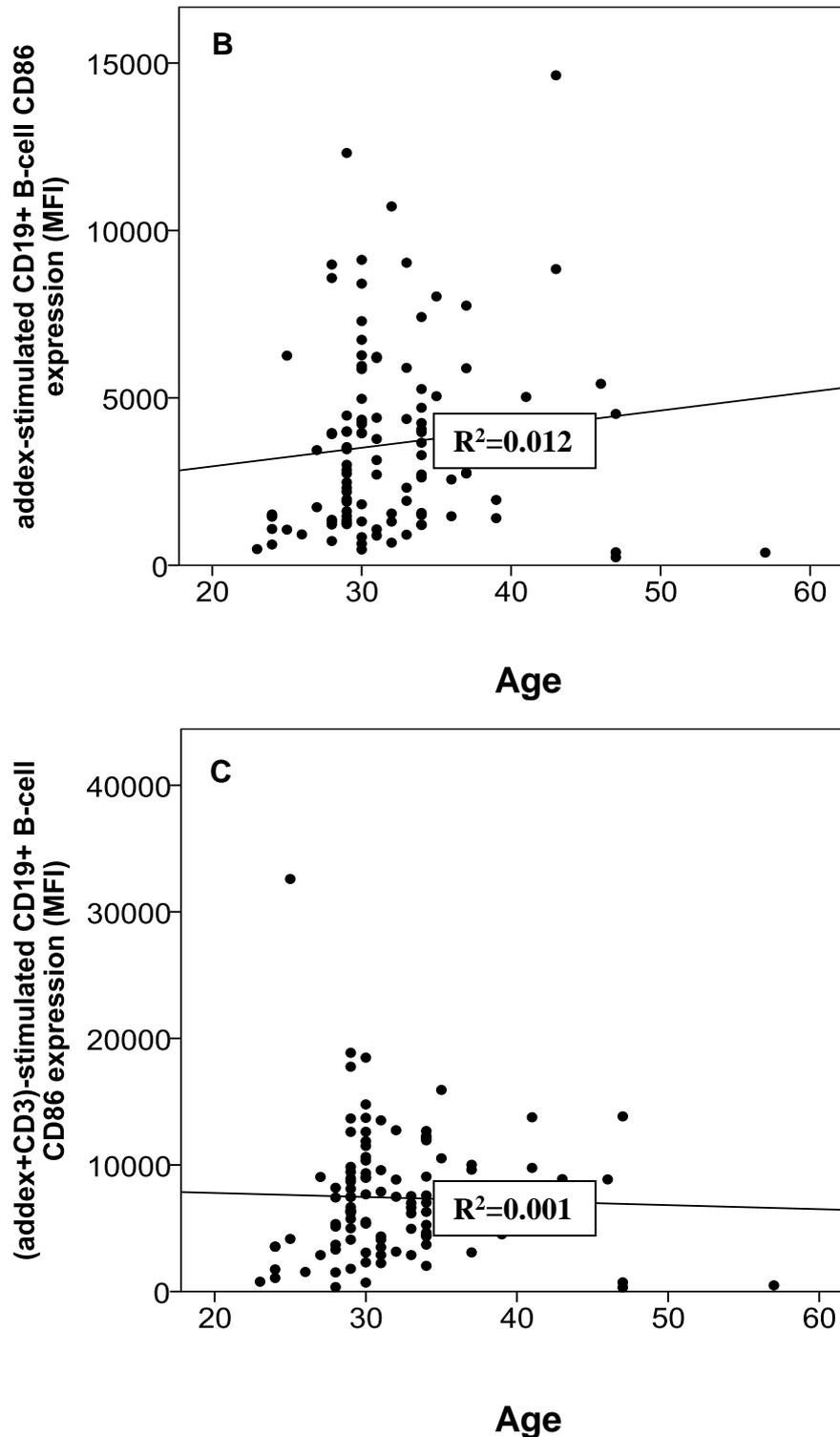
Figure 3.7: Correlation of age with *in vitro* CD19+ B-cell activation, in terms of CD86 expression, under unstimulated conditions (A), with αδdex-stimulation alone (B) and T-cell help (C). This un-stimulated CD86 expression on B-cells shown in A drops off around age 30. Spearman's rho bivariate correlation for non-parametric data was used for A and B; Pearson

correlation for parametric data was used for C (n = 106). Concentrations of stimulants used: 1µg/ml of αδdex, 0.1µg/ml anti-CD3 alone, and 0.5µg/ml anti-CD3 in combination with 0.5µg/ml anti-CD28. (Where * $p \leq 0.050$).

3.3.3 Sex and ethnicity influence CD4+ T- and CD19+ B-cell proliferation and activation

Towards appropriately matching cases to controls in this study, a group of healthy individuals (table 3.4) was first studied to ascertain sex-based influences on *in vitro* T- and B-cell responses. Data are presented as median values within confidence intervals, with each data point corresponding to one individual. Stimulation concentrations used were as described in chapter 2 (section 2.4 and 2.5): 1µg/ml of αδdex, 0.1µg/ml anti-CD3 alone, and 0.5µg/ml anti-CD3 in combination with 0.5µg/ml anti-CD28.

3.3.3.1 The effects of sex on CD4+ T- and CD19+ B-cell responses

Table 3.4: Age range of 100 individuals used to investigate the *in vitro* effects of sex on T- and B-cell responses to CD3- and IgD-stimulation respectively. Ethnicities of a large portion of this study group were unknown, hence were unrecorded in the table. Age did not significantly differ between females and males.

	Study group
Number	100
Mean age (Range)	31.63 (23 - 47)
Median age	30.00
Female	48
Mean age (Range)	31.31 (24 – 43)
Median age	30.00
Male	52
Mean age (Range)	31.92 (23 – 47)
Median age	30.00

Females and males had comparable CD4+ T-cell activation under un-stimulated and stimulated conditions (fig. 3.8). Males however did show higher CD19+ B-cell activation upon stimulation ($p \leq 0.050$; fig. 3.9B and C).
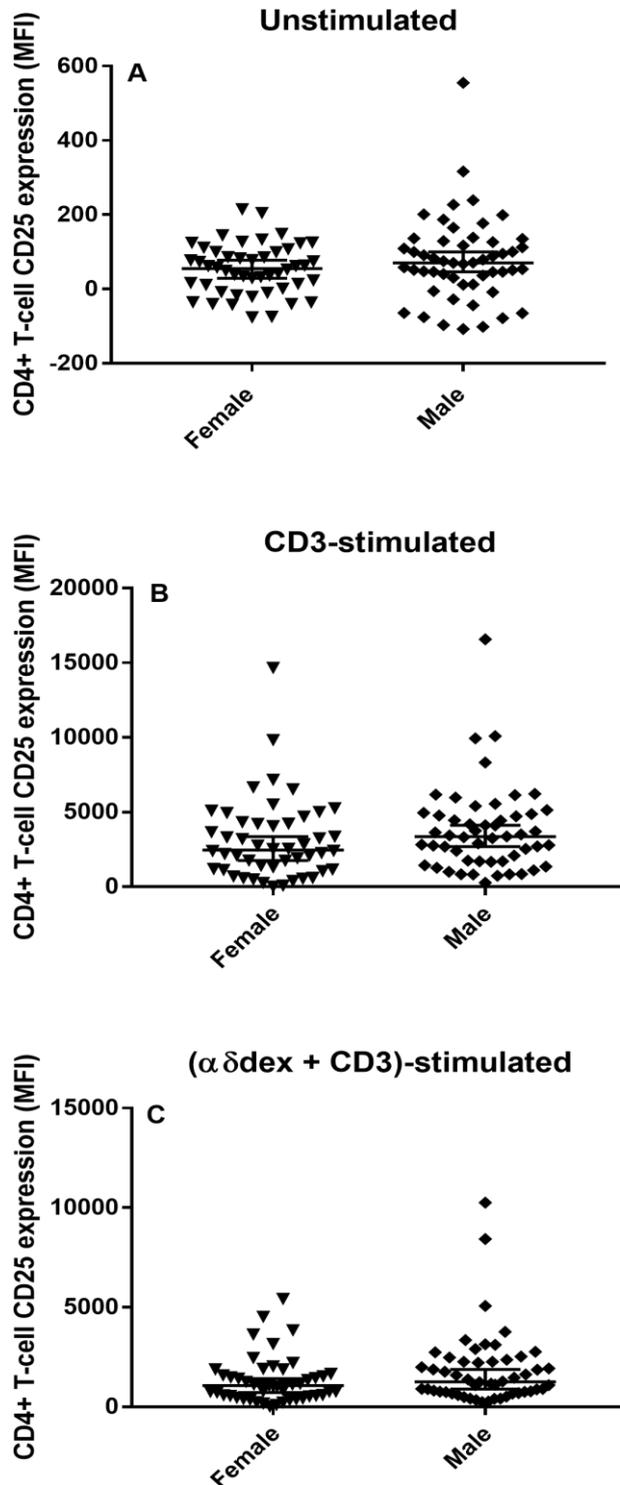
Figure 3.8: The effect of sex on CD4+ T-cell activation under unstimulated conditions (A), with CD3-stimulation alone (B) and combined with αδdex (C). The Mann Whitney U test for non-parametric data was used to investigate differences between males and females in A, B and C (n = 100). Each data point corresponds to one individual. Data points are superimposed over median values in 95% confidence intervals.

Concentrations of stimulants used: 1μg/ml of αδdex, 0.1μg/ml anti-CD3 alone, and 0.5μg/ml anti-CD3 in combination with 0.5μg/ml anti-CD28.
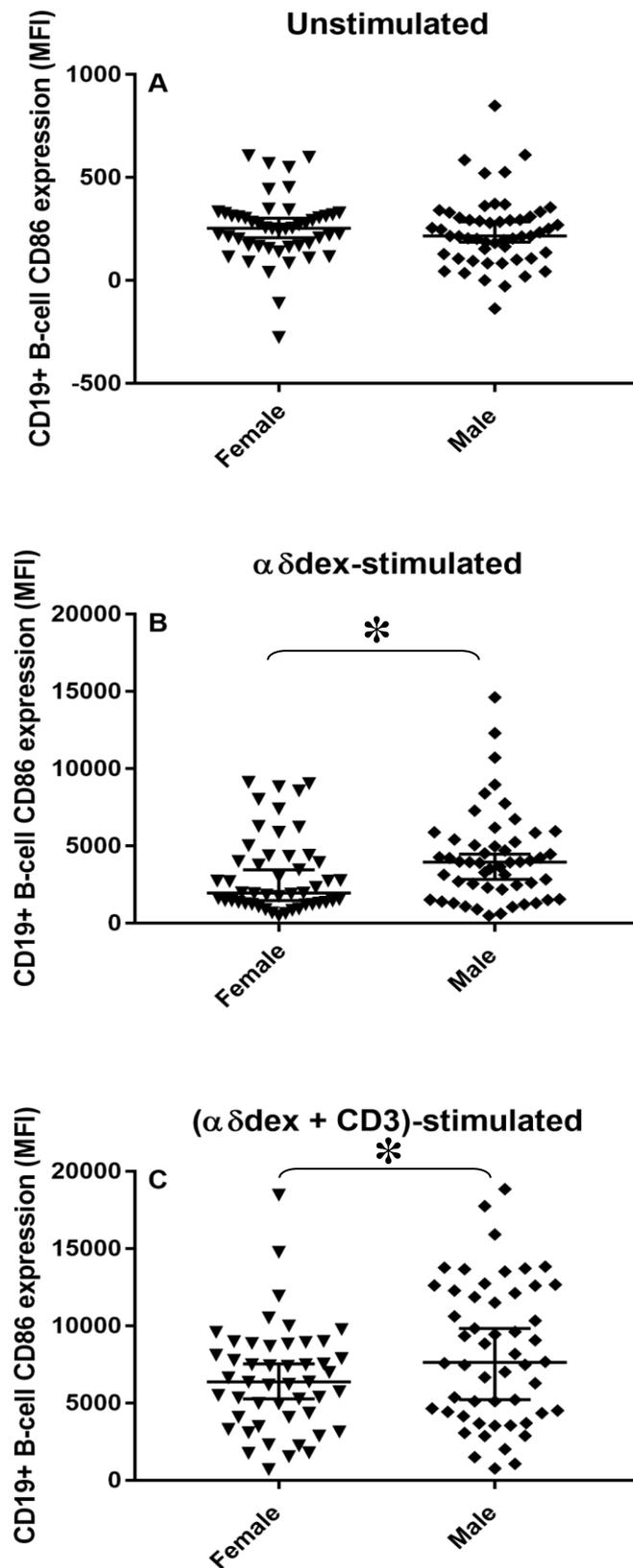
Figure 3.9: The effect of sex on CD19+ B-cell activation under unstimulated conditions (A), with αδdex-stimulation alone (B) and T-cell help (C). The Mann Whitney U test for non-parametric data was used to investigate differences between males and females in A and B, whilst the Independent samples t-test for parametric data was used to determine differences in C (n = 100). Each data point corresponds to one individual. Data points are superimposed over median values in 95% confidence intervals. Concentrations of stimulants used: 1µg/ml of αδdex, 0.1µg/ml anti-CD3 alone, and 0.5µg/ml anti-CD3 in combination with 0.5µg/ml anti-CD28. (Where * $p \leq 0.050$).

Having found sex-based differences in B-cell responses, the influence of ethnicity on T- and B-cell responses was investigated to further inform case-control matching.

3.3.3.2 The effects of ethnicity on CD4+ T- and CD19+ B-cell responses

A group of healthy individuals (table 3.5) was recruited based on ethnicity to investigate T- and B-cell variable responses.

Table 3.5: Age range of 18 individuals used to investigate the *in vitro* effects of ethnicity on T- and B-cell responses to CD3- and αδdex-stimulation respectively. Age did not significantly differ between sexes or ethnicities.

	Study cohort
Number	18
Mean age (Range)	34.39 (23 - 65)
Median age	30.50
Female	8
Mean age (Range)	31.63 (24 – 46)
Median age	30.50
Male	10
Mean age (Range)	36.60 (23 – 65)
Median age	29
Black	8
Mean age (Range)	31.13 (23 – 46)
Median age	30.50
White	10
Mean age (Range)	37.00 (24 – 65)
Median age	30.00

Data are presented as median values within confidence intervals, with each data point corresponding to one individual. Stimulation concentrations used were as described in chapter 2 (section 2.4 and 2.5): 1µg/ml of αδdex, 0.1µg/ml anti-CD3 alone, and 0.5µg/ml anti-CD3 in combination with 0.5µg/ml anti-CD28.

While Black and White individuals had comparable CD4+ T-cell frequencies across un-stimulated and stimulated conditions (fig. 3.10), proliferation (fig. 3.11) and activation (fig. 3.12) of CD4+ T-cells revealed ethnicity-based differences.
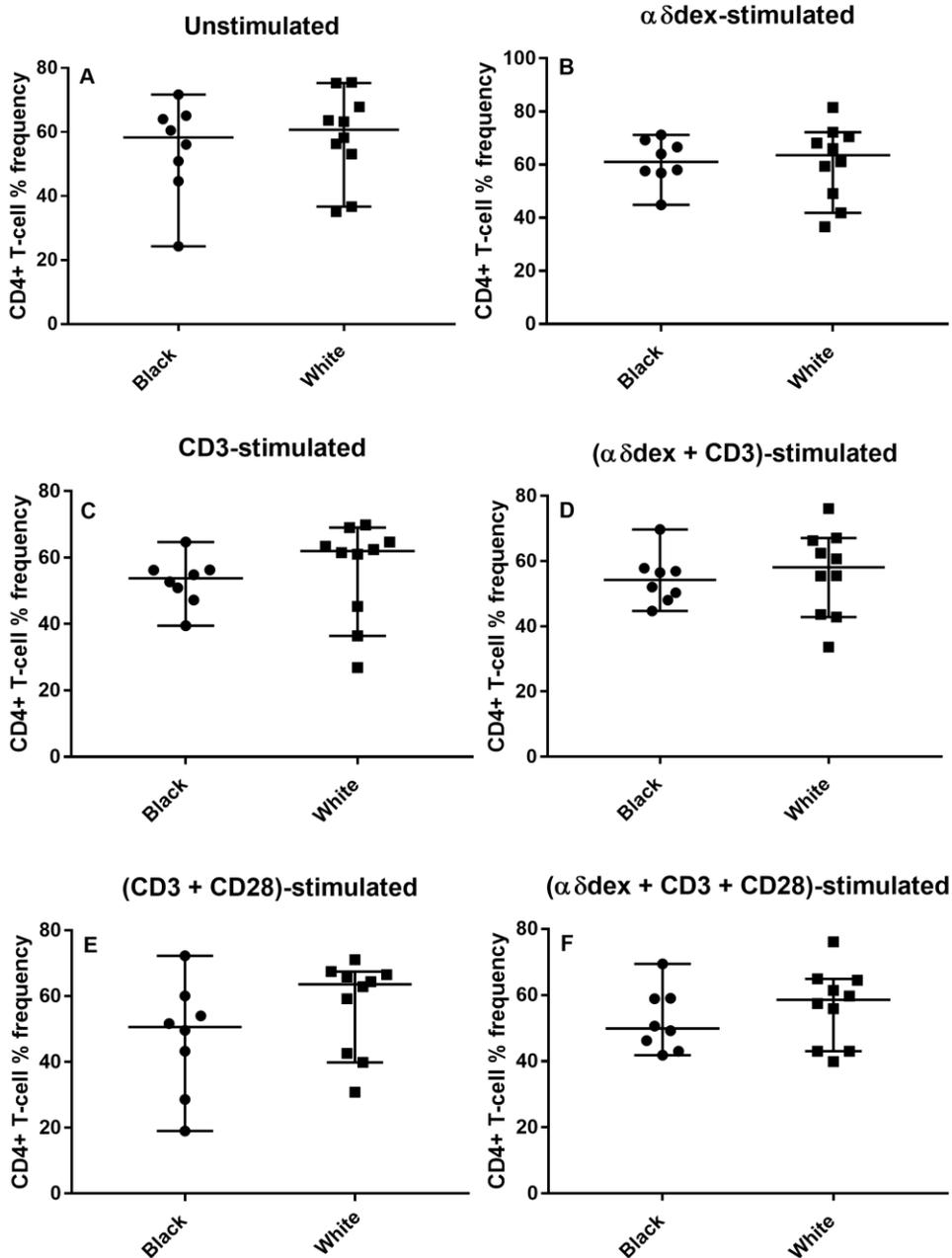
Figure 3.10: The effect of ethnicity on *in vitro* CD4+ T-cell frequencies under un-stimulated and stimulated conditions. The Mann Whitney U test was used to investigate ethnicity-based differences. (Black, n = 8; White, n = 10). Concentrations of stimulants used: 1µg/ml of αδdex, 0.1µg/ml anti-CD3 alone, and 0.5µg/ml anti-CD3 in combination with 0.5µg/ml anti-CD28.
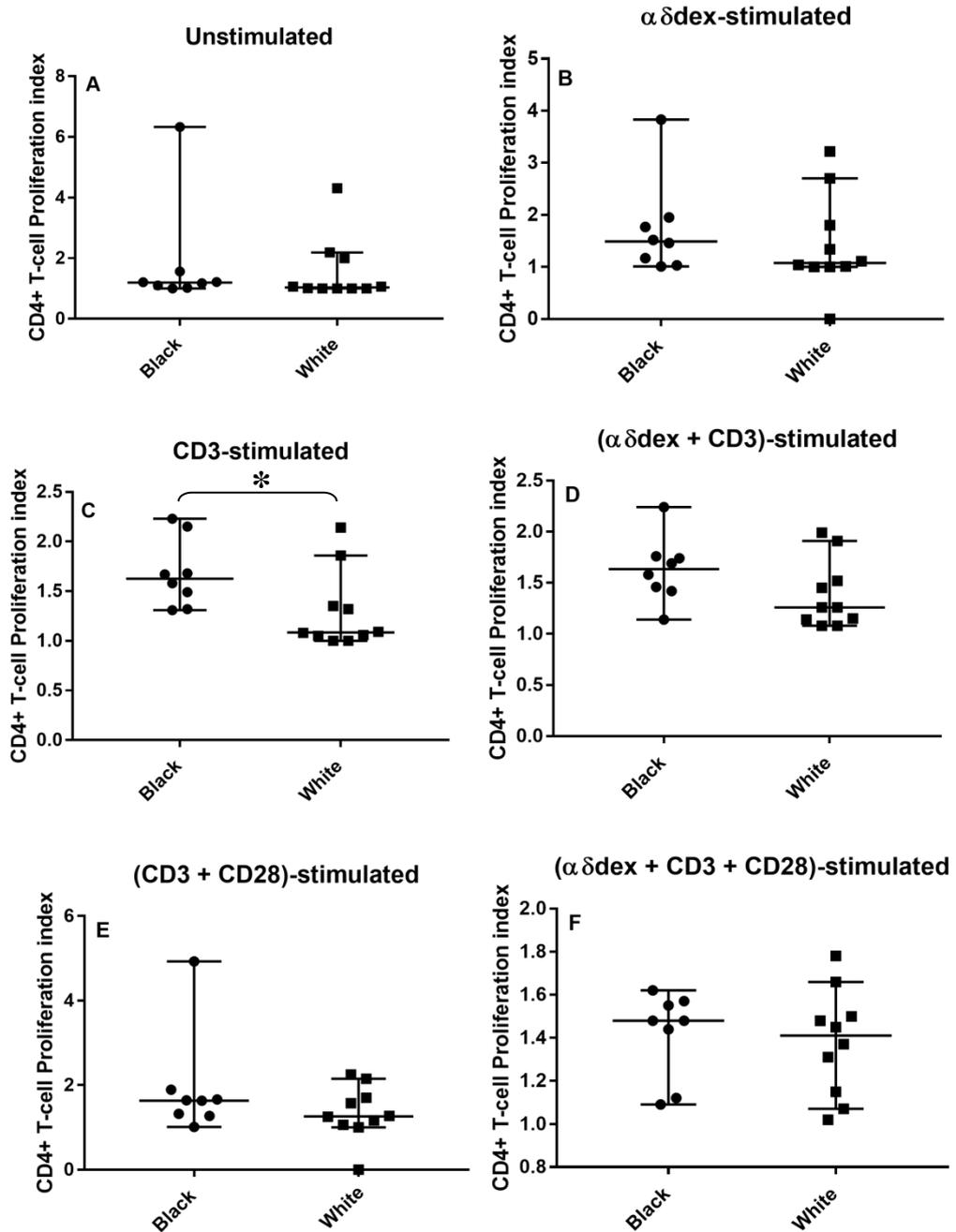
Figure 3.11: The effect of ethnicity on *in vitro* CD4+ T-cell proliferation under un-stimulated and stimulated conditions. The Mann Whitney U test was used to investigate ethnicity-based differences. (Black, n = 8; White, n = 10); (Where * *p* ≤ 0.050). Concentrations of stimulants used: 1µg/ml of αδdex, 0.1µg/ml anti-CD3 alone, and 0.5µg/ml anti-CD3 in combination with 0.5µg/ml anti-CD28.
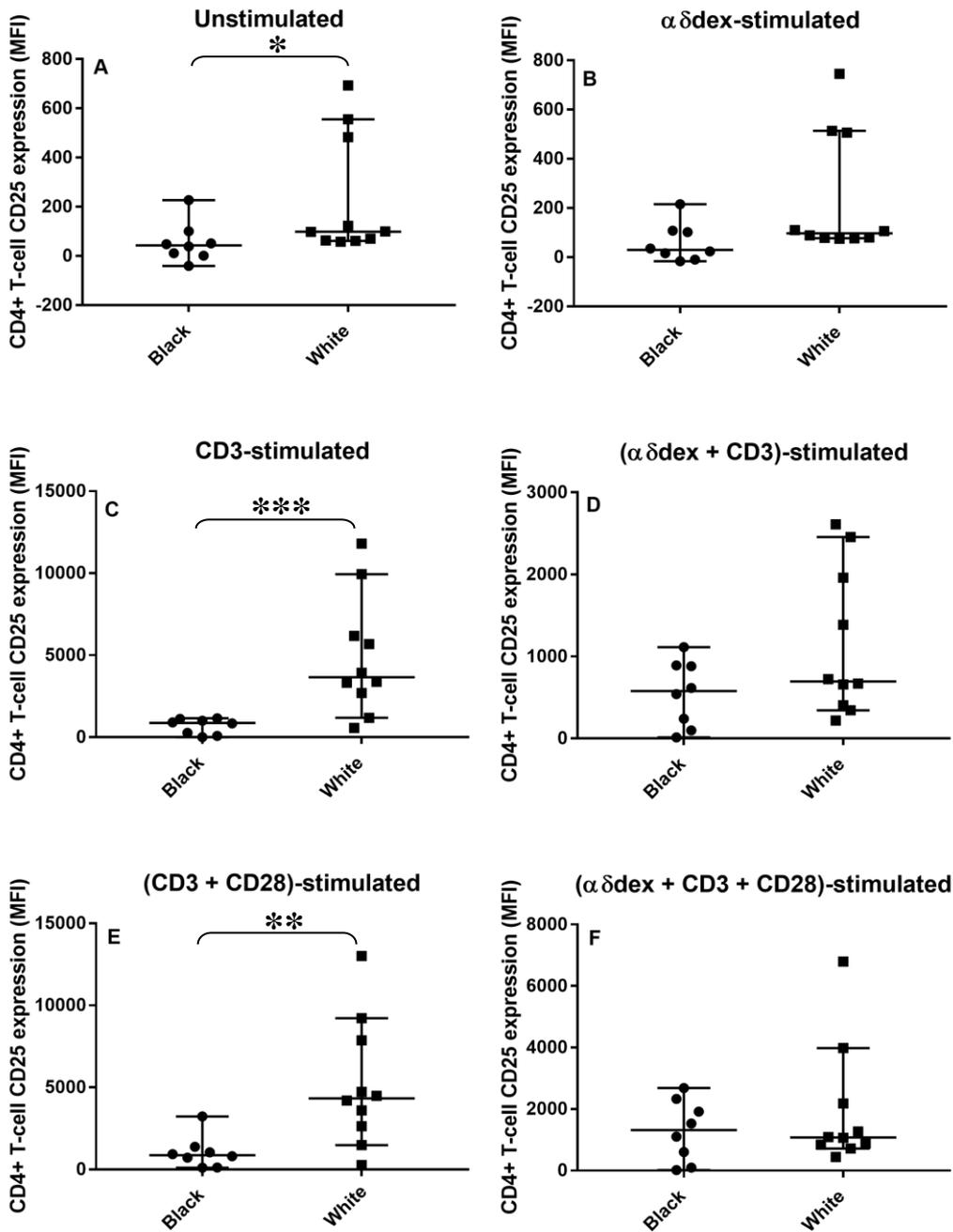
Figure 3.12: The effect of ethnicity on *in vitro* CD4+ T-cell activation, in terms of CD25 expression, under un-stimulated and stimulated conditions. The Mann Whitney U test was used to investigate ethnicity-based differences. (Black, n = 8; White, n = 10); (Where * $p \leq 0.050$, ** $p \leq 0.010$, *** $p \leq 0.001$). Concentrations of stimulants used: 1µg/ml of αδdex, 0.1µg/ml anti-CD3 alone, and 0.5µg/ml anti-CD3 in combination with 0.5µg/ml anti-CD28.

Similarly for CD19+ B-cells, there was no ethnicity-based variation for frequencies (fig. 3.13). However, proliferation (fig. 3.14) and activation (fig. 3.15) revealed ethnicity-based variations.
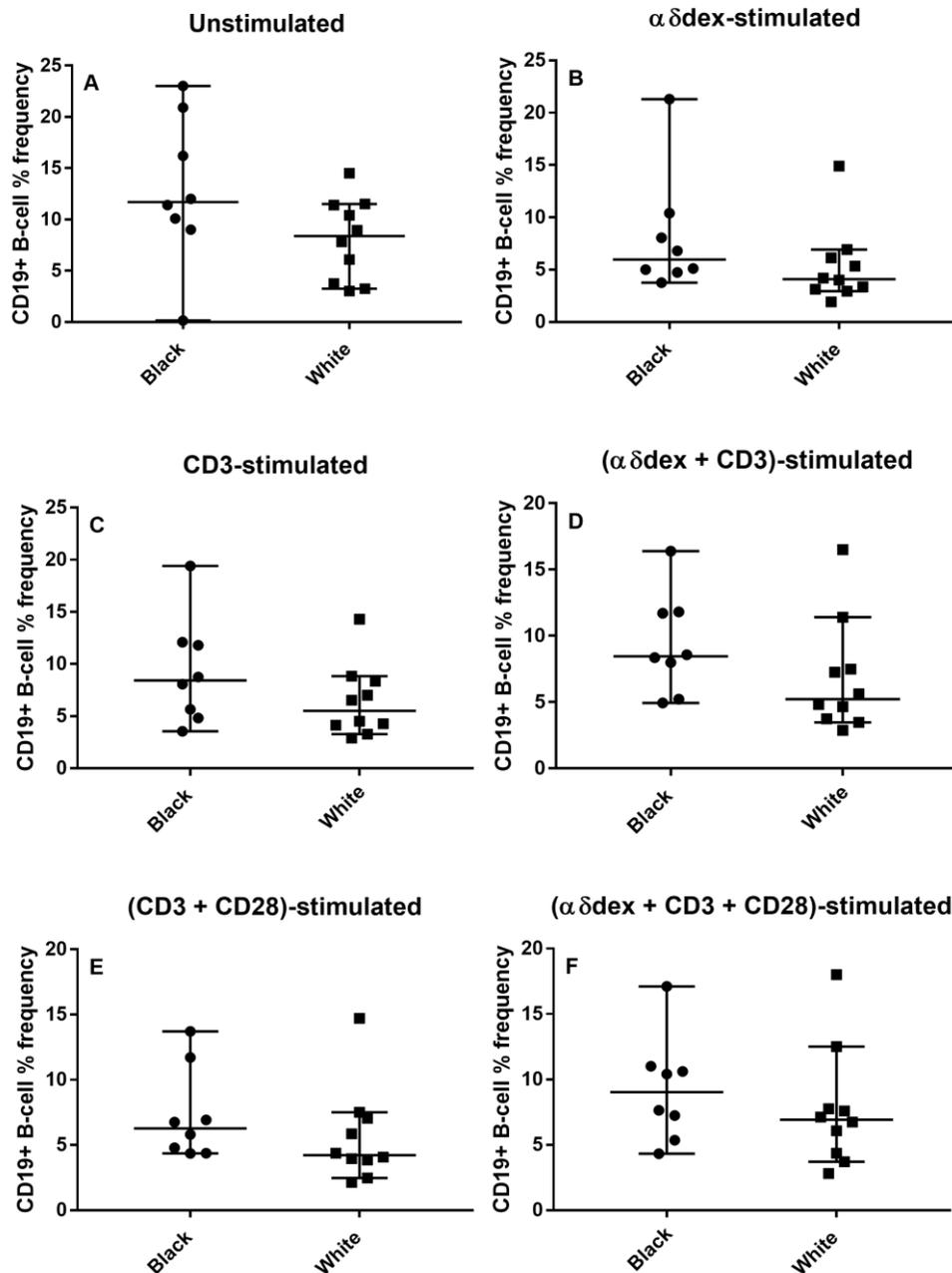
Figure 3.13: The effect of ethnicity on *in vitro* CD19+ B-cell frequencies under un-stimulated and stimulated conditions. The Mann Whitney U test was used to investigate ethnicity-based differences. (Black, n = 8; White, n = 10). Concentrations of stimulants used: 1µg/ml of αδdex, 0.1µg/ml anti-CD3 alone, and 0.5µg/ml anti-CD3 in combination with 0.5µg/ml anti-CD28.
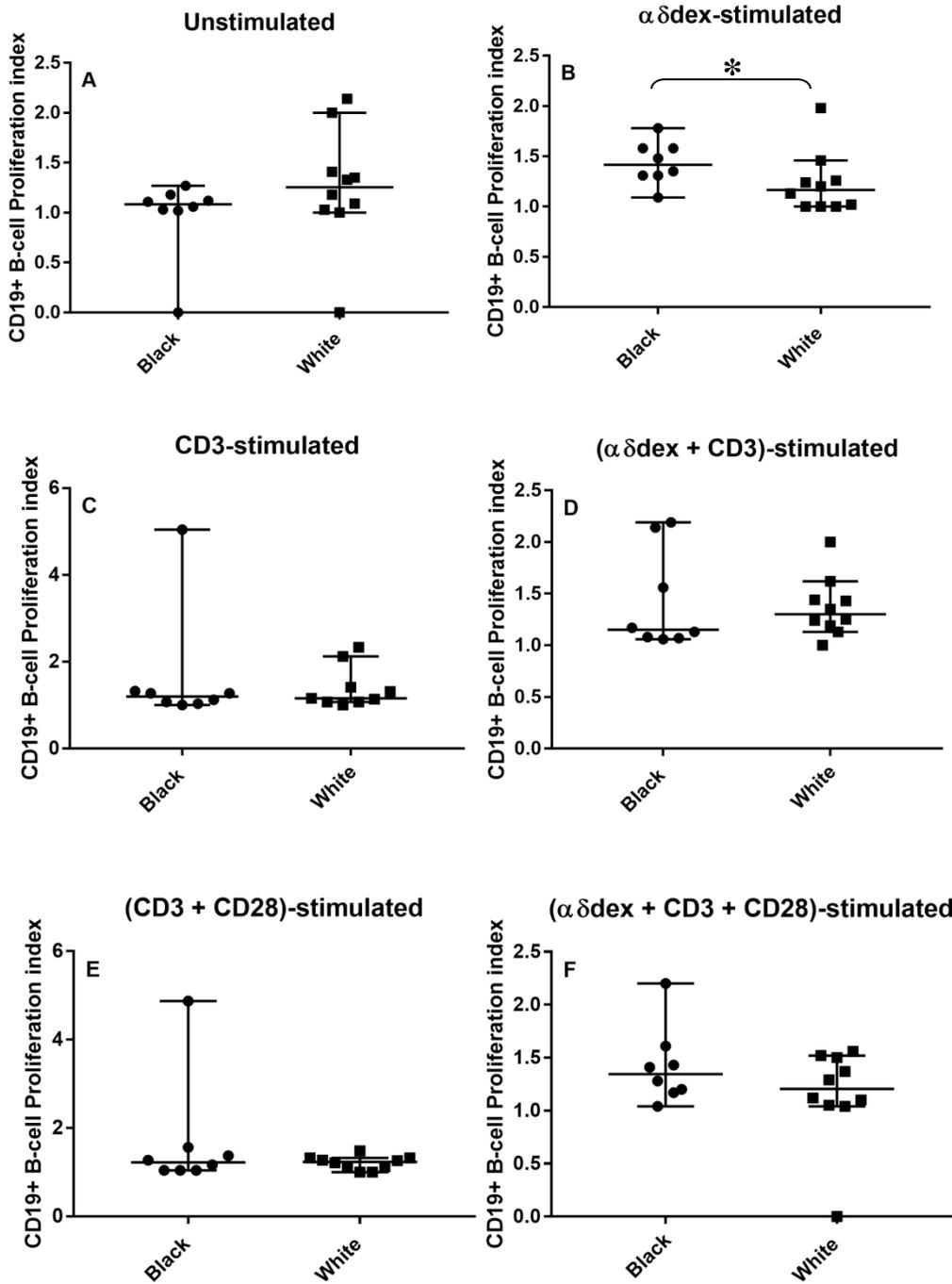
Figure 3.14: The effect of ethnicity on *in vitro* CD19+ B-cell proliferation under un-stimulated and stimulated conditions. The Mann Whitney U test was used to investigate ethnicity-based differences. (Black, n = 8; White, n = 10); (Where * *p* ≤ 0.050). Concentrations of stimulants used: 1µg/ml of αδdex, 0.1µg/ml anti-CD3 alone, and 0.5µg/ml anti-CD3 in combination with 0.5µg/ml anti-CD28.

In terms of CD86 expression levels, both ethnicities were comparable in un-stimulated conditions (fig 3.15 A). However, stimulation led to higher *in vitro* CD19+ B-cell activation in White individuals (fig. 3.15C, D and E).
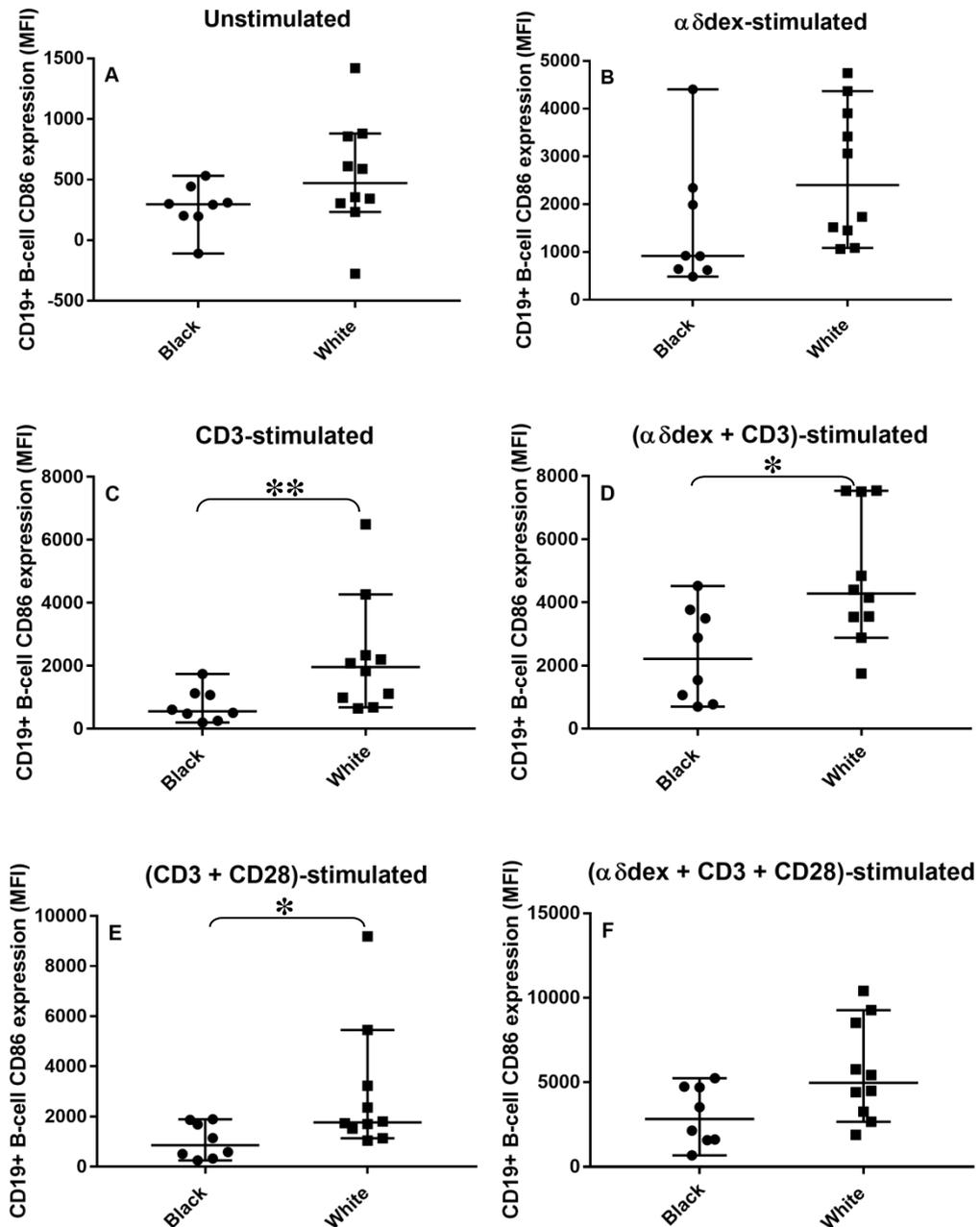
Figure 3.15: The effect of ethnicity on *in vitro* CD19+ B-cell activation, in terms of CD86 expression, under un-stimulated and stimulated conditions. The Mann Whitney U test was used to investigate ethnicity-based differences. (Black, n = 8; White, n = 10); (Where * $p \leq 0.050$, ** $p \leq 0.010$). Concentrations of stimulants used: 1µg/ml of αδdex, 0.1µg/ml anti-CD3 alone, and 0.5µg/ml anti-CD3 in combination with 0.5µg/ml anti-CD28.

CD25 expression levels between Black and White individuals were comparable under *in vitro* un-stimulated and stimulated conditions (fig 3.16).
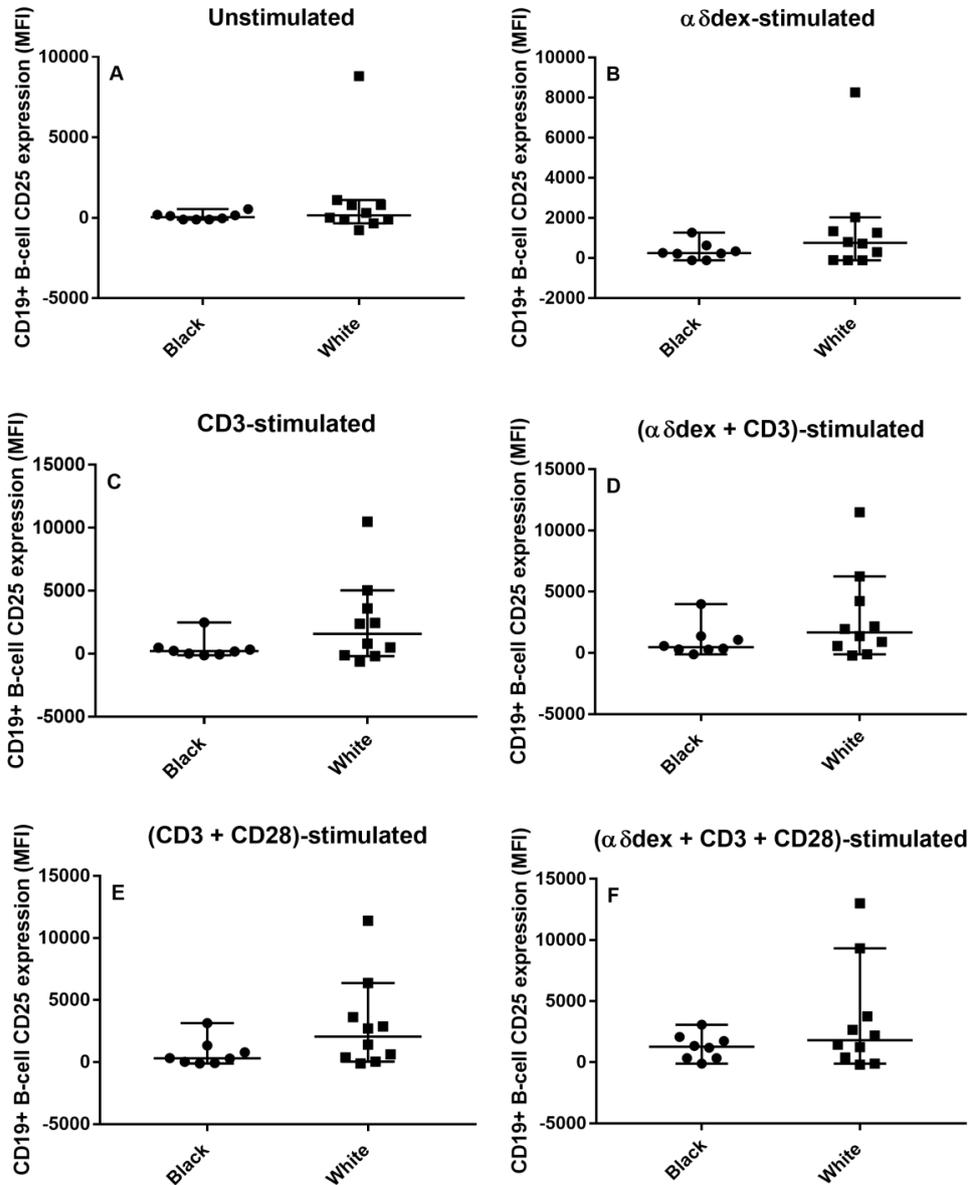
Figure 3.16: The effect of ethnicity on *in vitro* CD19+ B-cell activation, in terms of CD25 expression, under un-stimulated and stimulated conditions. The Mann Whitney U test was used to investigate ethnicity-based differences. (Black, n = 8; White, n = 10). Concentrations of stimulants used: 1µg/ml of αδdex, 0.1µg/ml anti-CD3 alone, and 0.5µg/ml anti-CD3 in combination with 0.5µg/ml anti-CD28.

3.4 Discussion of Findings

Using the anti-CD3- and αδdex-stimulation assay, a sample size of 10 individuals at minimum is needed for statistical power (Darton et al., 2011). This consideration was at the forefront of recruitment during each stage of data collection presented in this chapter.

3.4.1 T- and B-cell responses to the validated immunologic assay

In a group of 12 healthy adults with an equal spread of females and males, stimulation had no effect on the *in vitro* frequency distribution (fig. 3.1 A) or proliferation (fig. 3.1 B) of CD4+ T-cells. In terms of activation, CD4+ T-cell responses showed up-regulation of CD25 expression to sub-optimal concentrations of plate-bound anti-CD3 (0.1μg/ml), relative to an un-stimulated control ($p \leq 0.010$; fig. 3.2 A). This sub-optimal concentration elicits minimal T-cell activation (Foster et al., 2009) and facilitates the detection of small differences between patient and control responses (Foster et al., 2009, Foster et al., 2010, Darton et al., 2011, Wing et al., 2012, Preciado-Llanes et al., 2015). This up-regulated CD25 expression was also seen when CD3-stimulation was boosted by costimulation of CD28 ($p \leq 0.001$; fig. 3.2 A). Further while αδdex dampened this CD4+ T-cell response, a significant increase in CD25 expression was still seen nonetheless relative to the un-stimulated ($p \leq 0.010$; fig. 3.2 A). This immunosuppressive effect of αδdex-stimulated B-cells on T-cell activation has been reported previously by our group (Preciado-Llanes et al., 2015). Our group showed that while T-cell activation is up-regulated by anti-CD3 stimulation (alone, and with anti-CD28 costimulation), the presence of αδdex-stimulated B-cells significantly reduces this T-cell activation (Preciado-Llanes et al., 2015).

Our group had established an immunologic assay that has been used to study B-cell responses to αδdex, a TI- type 2 antigen mimic that elicits polyclonal B-cell responses. By using this mimic to activate B-cells alone, and in the presence of TCR-activated T-cells, cognate interactions between

B- and T-cells have been studied. This validated stimulation assay has enabled the elucidation of subtle immune defects in several patient groups including adult MenC sufferers (Foster et al., 2009), adolescent Meningitis C vaccine failures (Foster et al., 2010) and adult IPD survivors (Darton et al., 2011) compared to healthy controls.

The decision was made to include HLA-DR as an additional activation marker in this study. This is because along with the traditionally used CD25, HLA-DR is an indicator of late T-cell activation (Reddy et al., 2004, Starska et al., 2011). Furthermore, HLA-DR expression on T-cells has been shown to increase HIV-1 transcription (Saifuddin et al., 2000). In a cohort of HAART-treated aviraemic HIV-infected patients, baseline percentage levels of CD4+ HLA-DR+ were significantly higher ($p \leq 0.050$) than in HIV-negative controls. Moreover, though not significant, the levels of CD8+ HLA-DR+ cells were also increased in the patient group (Tincati et al., 2012). With the aim of studying differences in T-cell responses between HIV-infected individuals and controls later on in the study, HLA-DR would serve as a validated second marker of immune activation.

CD4+ T-cells showed significant up-regulation of HLA-DR in the presence of sub-optimal anti-CD3 levels, and anti-CD3 combined with anti-CD28 (fig. 3.2 B). Interestingly, this up-regulation of HLA-DR persisted even in the presence of αδdex combined with anti-CD3. Because αδdex on its own did not elicit up-regulation of CD25 (fig 3.2 A) or HLA-DR (fig 3.2 B) it can be concluded that αδdex itself has no effect on CD4+ T-cell activation, at least not with respect to these particular activation markers. This conclusion was also drawn previously in our group (Preciado-Llanes et al., 2015).

Receptor-mediated endocytosis occurs to an extent when using antibody labelling protocols (Liao-Chan et al., 2015, Ingle et al., 2008), especially when cell populations are stimulated and activated. Therefore it cannot be concluded whether stimulations actually reduced the frequency of CD19+ B-cells relative to the un-stimulated control ($p \leq 0.050$; fig 3.3 A), or if receptor internalisation had occurred. If indeed αδdex suppressed CD19+ B-cell

frequency ($p \leq 0.050$; fig 3.3 A), it is noteworthy that αδdex-stimulation still elicited significant up-regulation of CD86 expression ($p \leq 0.010$; fig 3.4 A). These αδdex-stimulated CD19+ B-cells also showed further up-regulation of CD86 expression in the presence of CD3 stimulation alone and in combination with CD28-costimulation (both $p \leq 0.001$; fig 3.4 A). These results mimic those found by Darton et al. (2011) in their healthy control group. However one difference is that while Darton's work showed significant up-regulation in CD25 expression upon stimulation with αδdex plus anti-CD3 and anti-CD28, the same was not the case in the present study (fig 3.4 B). Lastly, the additional HLA-DR activation marker showed significant up-regulation across all stimulations relative to the un-stimulated control ($p \leq 0.050$; fig 3.5).

These results indicated that the immune stimulation assay used in our group was reproducible. Also, that HLA-DR would be a relevant marker to include that could potentially provide interesting results from the HIV cohort. The next step was to determine how stringent matching of control subjects to patients needed to be.

3.4.2 Age as an inherent influencer of T- and B-cell responses

In a group of 106 individuals ranging in age from 23 – 57, results indicated that age did not significantly impact CD4+ T-cell activation responses under un-stimulated conditions, and upon CD3-stimulation (fig. 3.6 A and B). However, younger individuals showed significantly lower ($p \leq 0.050$) CD3-stimulated CD4+ T-cell activation in the presence of αδdex-stimulated CD19+ B-cells compared to older individuals (fig. 3.6 C). Our group had previously demonstrated that in the presence of *in vitro* αδdex-stimulated B-cells, CD3-stimulated CD4+ T-cell CD25 expression is significantly suppressed (Preciado-Llanes et al., 2015). Considering the phenomenon of age-related immunosenescence being prominent in the T-cell population (Tu and Rao, 2016), rather than an increased activation of T-cells in the older individuals, it is likely that the B-cell immunosuppressive effect diminishes with age.

Further, un-stimulated CD19+ B-cells of older individuals showed significantly lower B-cell activation ($p \leq 0.050$; fig. 3.7 A) compared to younger individuals. However, upon stimulation (fig. 3.7 B and C) responses in older and younger individuals were comparable.

Due to the lack of ethnicity data for these 106 individuals, there was no way of knowing if there was an equal spread of ethnicities across the age spectrum. This limits conclusions that can be drawn. Another limitation to this portion of the study is that out of 106 individuals, only seven were beyond 40 years of age, with one of these being 57. This would have excluded the age range ($\geq$ 65 years) who are known to be predisposed to pneumococcal disease more so than younger individuals. The conclusion drawn from the *in vitro* responses in this group of 106 healthy individuals was that age did have an affect on T- and B-cell responses, though not dramatically. It was decided that a margin of 10 years at most between cases and controls would be used during the recruitment phase of this study. The choice of this 10 year margin would enable us to account for an age-effect on T- and B-cell responses, whilst facilitating feasibility of matching.

3.4.3 Sex-based variation in T- and B-cell responses

Firstly, because there was no significant difference between the ages of females and males (table 3.4), it was concluded that there would be no confounding effect of age on sex-based results.

Sex had no effect on *in vitro* CD4+ T-cell activation. Thus, females and males had comparable CD25 expression under un-stimulated conditions (fig 3.8 A), and upon CD3-stimulation alone (fig 3.8 B) and with αδdex (fig 3.8 C). While sex had no effect on *in vitro* un-stimulated CD19+ B-cell CD86 expression (fig. 3.9 A), stimulation elicited sex-based differences. Males had significantly higher CD19+ B-cell CD86 expression upon αδdex-stimulation alone ($p \leq 0.050$; fig. 3.9 B), and in combination with anti-CD3 ($p \leq 0.050$; fig. 3.9 C). Because αδdex combined with anti-CD3 did not elicit sex-based differences in CD4+ T-cell activation, the higher activation in males seen in

fig 3.9 C may likely be confined to CD19+ B-cells as opposed to cognate interactions between T- and B-cells.

A limitation to this portion of the study is the absence of data for investigating sex-based differences in proliferation responses of T- and B-cells. This is because the parameter for reporting proliferation data in the present study (which accounts for only 12 individuals out of 100; table 3.4) which is proliferation index, differs from that used in the Wing study (2012) which was divisional index. Proliferation data could have strengthened a conclusive message from these results.

Despite the lack of proliferation data, the activation data for CD19+ B-cells led to the conclusion that sex-matching for the case-control study further on would be appropriate. A mismatch could likely introduce sex-based variable CD19+ B-cell responses.

3.4.4 Variations in T- and B-cell responses based on ethnicity

Age did not significantly differ between the sexes or ethnicities amongst the cohort used to study ethnicity-based variations in T- and B-cell responses (table 3.5). Thus, age was not considered to be a confounding factor on the interpretation of results.

A striking result uncovered was less T-cell activation in Black, as opposed to White, individuals under un-stimulated conditions ($p \leq 0.050$; fig. 3.12 A), following CD3-stimulation alone ($p \leq 0.001$; fig. 3.12 C) and combined with CD28-costimulation ($p \leq 0.010$; fig. 3.12 E). This result was paralleled in B-cell activation when relying upon T-cell help ($p \leq 0.050$; fig. 3.15 C and E). It is likely that this poor T-cell activation in the Black individuals is reflected in the poor T-cell help to B-cells that was detected. Noteworthy also is that even while not significant, White individuals also had higher CD19+ B-cell activation under un-stimulated, αδdex-stimulated and αδdex with anti-CD3 and anti-CD28-stimulation (fig. 3.15 A, B and F respectively).

However, while both ethnicities had comparable un-stimulated CD4+ T-cell proliferation (fig. 3.11 A), CD3-stimulation induced a significantly higher *in vitro* proliferation response in Black individuals compared to White individuals ($p \leq 0.050$; fig. 3.11 C). Further, though White individuals had higher *in vitro* CD19+ B-cell proliferation under un-stimulated conditions compared to Black individuals (fig. 3.15 A), proliferation in Black individuals significantly surpassed that in White individuals upon αδdex-stimulation ($p \leq 0.050$; fig. 3.14 B).

A study from the USA reported higher total IFNγ ELISPOT and CD8+ IFNγ ELISPOT responses in White compared to Black Americans, upon receipt of the Dryvax® smallpox vaccination (Haralambieva et al., 2013). Yet, another study found higher levels of rubella-specific neutralising antibody in Black compared to White Americans in response to rubella vaccination (Haralambieva et al., 2014). Ethnicity-based variations in BCR signalling pathways have also been found between healthy White and Black Americans. The Black individuals had lower *in vitro* anti-IgD-induced phosphorylation of multiple components of the BCR pathway, compared to White individuals (Longo et al., 2012). Taken together, these three studies highlight the existence of ethnicity-based differences in immune cell signalling and vaccine responses. And in the context of the findings of the present study, further emphasize ethnicity-based variations in adaptive immune responses.

In the healthy cohort, Black individuals showed higher TCR-induced CD4+ T-cell, and αδdex-induced CD19+ B-cell proliferation, compared to White individuals. In terms of activation however, it was White individuals who had higher responses. These results may indicate higher CD4+ T- and CD19+ B-cell cognate interactions in White individuals, specifically upon TCR-stimulation and CD28-costimulation.

Presently, and to our knowledge, the literature does not have studies which have investigated differences between Black and White individuals specifically based on *in vitro* T- and B-cell counts, proliferation and activation

upon stimulation with a combination of anti-CD3 and αδdex. However, there is indication that ethnicity-based differences in cell count and function are an important consideration for research. Benign ethnic neutropenia, the phenomenon in which low leukocyte and neutrophil counts are found in 25 – 50% of individuals of African descent, is well-established however (Haddy et al., 1999). Results from the present study also suggest that ethnicity-based variations at a cellular level could be crucial to immunological responses. This, especially in light of the 2016 work showing that genetic ancestry of African and European populations drives the differences in their immune responses to pathogens which may explain the differing incidence of specific diseases often found in these two populations (Nedelec et al., 2016).

The limited number of study participants in the present study (Black, n = 8 and White, n =10; table 3.5) restricted firm conclusions that can be drawn from these results. However, regardless of numbers the findings showing higher T-cell activation in White compared to Black individuals (fig. 3.12) are very clear and strong. These warrant further investigation. These results highlighted the necessity of ethnicity-matching between cases and controls during patient recruitment. A mismatch could potentially introduce an ethnicity-based variation in responses to the stimulation assay.

Still, one drawback to ethnicity-matching was the fact that unlike age which was absolute, and sex which was either male or female in the context of the study, ethnic identities are varied, even within one race. Thus, the conclusion made was to match-based on outward-presenting race together with self-declared racial identity.

3.5 Conclusion

After reproducing our group results showing αδdex-induced up-regulation of CD86 expression in CD19+ B-cells, age-, sex- and ethnicity-based variations in response to the immune stimulation assay were investigated. Results indicated a need for matching between cases and controls in terms of these three inherent factors. It was concluded that a margin of 10 years at most between cases and controls would be used, whilst sex- and ethnicity-matching would be strict.

CHAPTER FOUR: T- AND B-CELL RESPONSES IN HIV-INFECTED INDIVIDUALS FOLLOWING POLYCLONAL AND PNEUMOCOCCAL STIMULATION

4.1 Introduction

A 2016 report published by Public Health England (PHE, 2016) shows that HIV prevalence in the UK is currently at 1.6 per 1000 in the population. This equates to 101,200 people in total, of which over 13,000 are living undiagnosed. Antiretroviral therapy (ART) has currently been available for two decades within the UK, making HIV a chronic and manageable health condition and rendering infected individuals aviraemic (Cohen et al., 2011, Rodger et al., 2016). The increased susceptibility of HIV-infected individuals to Invasive pneumococcal disease (IPD) despite Antiretroviral therapy (ART) (Glennie et al., 2011, Micheloud et al., 2012) and with reported vaccine failures (Willocks et al., 1995, Begemann and Policar, 2001, Rives Ferreiro et al., 2008) warrants an investigation into the cellular mechanisms that put HIV-infected individuals at increased risk of disease compared to the general uninfected population.

Cellular targets of HIV include CD4+ T cells, dendritic cells, monocytes and macrophages, astrocytes and renal epithelial cells. Viral proteins interact with cellular membrane proteins: viral envelope protein gp120 recognizes and binds the CD4 receptor and chemokine co-receptors (CCR5 or CXCR4), facilitating exposure of gp41 on the viral envelope and its fusion to the cell membrane. The viral RNA genome and enzymes are then released into the host cell. Once inside, the RNA reverse transcribes and integrates into the host genome, as a proviral region. After transcription, cleavage and assembly of new viral polypeptides, a new virus is released from the cell as a mature viral particle (Wilen et al., 2012, Maartens et al., 2014).

The CD4+ and CD8+ T-cells, and B-cells of HIV-infected individuals undergo polyclonal hyperactivation and increased apoptosis (activation-induced cell death) (Meyaard et al., 1992, Appay and Sauce, 2008, Day et al., 2006, Nicholas et al., 2013) likely stimulated by HIV proteins (Moir and Fauci, 2009). Interestingly this hyperactivation of CD4+ T-cells is unaccompanied by increased proliferation (Gougeon and Montagnier, 1993). Polyclonal activators induce apoptosis in CD4+ and CD8+ T-cells even in asymptomatic

HIV-infected individuals (Gougeon and Montagnier, 1993, Groux et al., 1992). Hyperactivation induces increased expression of the Apoptosis antigen-1 (APO-1) death receptor (CD95) on CD4+ T-cells (Bohler et al., 1997) and the inhibitory receptor PD-1 on B-cells (Nicholas et al., 2013) leading to B-cell exhaustion (Moir and Fauci, 2009). HIV-induced B-cell polyclonal activation also leads to hypergammaglobulinemia, elevated levels of immunoglobulins in serum (Lane et al., 1983, Mizuma et al., 1988, Shirai et al., 1992). A landmark in disease progression is the rapid decline in both CD4+ and CD8+ T-cell populations, which is an indication of homeostasis failure, (Margolick et al., 1995) together with persistent hyperactivation and apoptosis (Hazenberg et al., 2000, Hazenberg et al., 2003, Appay and Sauce, 2008, Samuelsson et al., 1997a). This immune activation persists even with the use of Combination Antiretroviral Therapy (cART) and is likely due to microbial translocation across the gastrointestinal tract (Klatt et al., 2013).

Thus, HIV-infection causes impairment of both cellular (Okoye and Picker, 2013) and humoral immunity (Samuelsson et al., 1997a, Samuelsson et al., 1997b). HIV-1 infection further induces terminal differentiation of B-cells (in blood and Gut-Associated Lymphoid Tissue- GALT) (Levesque et al., 2009). Levesque and colleagues found that even in patients as early as 17 days post-HIV-1 infection, GALT memory B-cells produced HIV-1 specific antibodies in addition to autoreactive and influenza-specific antibodies. These results indicate polyclonal activation even in acute HIV-1 infection.

Additionally in acute HIV-1 infection a cytokine storm occurs with elevated levels of IL-15 and IFNα, then TNF, IL-18 and IL-10 (McMichael et al., 2010). HIV-1 is also characterized by depletion of the CD4+ and CD8+ T-cell naive subsets (Roederer et al., 1995, Connors et al., 1997). While mature CD4+ T-cells also get depleted and lead to disease progression (Hazenberg et al., 2000, Cloyd et al., 2001, Fauci, 1993), there is an expansion of CD8+ T-cells compared to uninfected populations (Sachsenberg et al., 1998, Margolick et al., 1993). This decline in CD4+ T-cells is followed by replacement with newly

generated CD4+ T-cells, and eventually net replacement by CD8+ T-cells (Margolick et al., 1993).

HIV-1 affects pulmonary innate immunity by impairing the phagocytic function and proteolytic activity of alveolar macrophages (Jambo et al., 2014). This together with T- and B-cell immunity in HIV, has implications in pneumococcal disease susceptibility particularly as pneumococcal carriage significantly increases IL-17A-secreting CD4$^+$ memory T-cells in the lung, which can enhance the killing of pneumococci by alveolar macrophages (Wright et al., 2013). Indeed, HIV-infected individuals show impaired bronchoalveolar lavage (BAL) CD4+ T-cell responses to Influenza virus- and *M. tuberculosis.* These *in vitro* results presented as lower total antigen-specific CD4$^+$ T cells and of poly-functional IFN-γ and TNF-α-secreting cells in HIV-infected individuals (Jambo et al., 2011).

Some of these immune impairments are controlled by the use of ART, which also slows and reverses disease progression (Moir et al., 2008b). ART has been reported to resolve hypergammaglobulinemia, and reduce circulating immunoglobulin (Ig)G antibody-secreting cell (ASC) frequencies in both acute and chronic infections, whilst suppressing HIV-1 replication (Morris et al., 1998). ART initiation also reconstitutes absolute lymphocyte and CD4+ T-cell counts, with reduced apoptosis in CD4+ and CD8+ T-cells even in viraemic patients (Bohler et al., 1997, Autran et al., 1997). Further, Art also dampens T-cell hyperactivation (Autran et al., 1997). Moreover, the ART-mediated decrease of HIV viraemia has also been shown to elicit normalisation of certain B-cell activation markers (Moir and Fauci, 2009) particularly CD80 and CD86 (Malaspina et al., 2003) and increases B-cell counts (Moir et al., 2008b). ART also effectively inhibits viral replication to a large extent (Martinez-Picado and Deeks, 2016).

However, even in the Highly Active Antiretroviral Therapy (HAART) era, HIV-infected individuals are still at risk of lower respiratory tract infections. Patients are up to 35-fold more likely to develop IPD than their uninfected

counterparts (Heffernan et al., 2005, Westerink et al., 2012). Therefore improving pneumococcal vaccine efficacy in the context of HIV is imperative.

Firstly, AIDS patients show reduced antibody levels to pneumococcal polysaccharide antigens before and after immunisation, compared to controls (Ammann et al., 1984). However in the context of HIV, HIV-specific IgA responses at mucosal sites are low (Moir and Fauci, 2009). There are also reported defects in IgM memory B-cells in HIV-1 infection (D'Orsogna et al., 2007, Hart et al., 2007, Titanji et al., 2005) with the percentage of marginal zone B-cells remaining unrestored by ART. IgM memory B-cell depletion in untreated HIV patients may increase their risk of pneumococcal infection (D'Orsogna et al., 2007). Furthermore, PPV23 responses (both IgM and IgG levels) in HIV-1 patients are impaired (Hart et al., 2007) with one study even showing that most vaccine non-responders were those on HAART (Tsachouridou et al., 2015). Moreover, in a cohort of HAART-naive HIV-infected patients who had no history of pneumococcal disease or having received pneumococcal vaccination, no defective mucosal responses to pneumococcal antigens were found in BAL fluid or serum samples. In fact, the pneumolysin- and PspA-specific IgG levels were significantly higher in patients compared to matched controls ($p < 0.0001$), with comparable levels for pneumolysin- and PspA-specific IgA in BAL (Collins et al., 2013). As a result, Collins and colleagues concluded that an increase in anti-pneumococcal IgG levels induced by vaccination would likely not be sufficient to prevent disease development in HIV patients. Indeed, a meta-analysis of 19 studies found that seroprotection conferred by vaccine-induced antibodies wanes more quickly in HIV patients (Kerneis et al., 2014). Specifically with pneumococcal vaccines, low CD4 counts at time of vaccination and failure to suppress virus were two factors contributing to poor response (Hung et al., 2010).

PCV7 was however found to protect HIV-infected individuals who have recovered from a past episode of IPD, from vaccine serotypes or serotype 6A (French et al., 2010). While one or two doses of PCV7 can elicit protective responses in HIV-treated individuals, two doses will likely be more

robust in areas with less cART coverage (Cheng et al., 2016). Another study showed that post-PCV7, HAART-naive HIV-infected Malawian adults showed serum and lung pneumococcal capsule-specific IgG responses (based on serum and BAL measurements). Further, this study concluded that circulating IgG had been transferred to the fluid lining the lung. Additionally, IgG did not correlate with CD4 counts (Gordon et al., 2007). These studies imply greater protection conferred by the conjugate vaccine.

There is still much to be understood regarding the host-pathogen interactions and immune responses thereafter which render patients at risk to opportunistic infections and in the context of the present study particularly, pneumococcal disease. It is therefore imperative that while current research investigates mechanisms by which HIV reservoirs can be depleted, concurrent studies also investigate how HIV influences disease susceptibility at the level of T- and B-cell responses and cognate interactions.

In light of our group uncovering subtle immune defects in previous sufferers of IPD with no known vaccination history (Darton et al., 2011), in adult MenC sufferers (Foster et al., 2009) and adolescent MenC vaccine failures (Foster et al., 2010), data presented in this chapter sought to uncover a defect in an HIV cohort with known predisposition to IPD (Glennie et al., 2011).

Therefore, data gathered and presented in this chapter had two aims: The first was to investigate any *in vitro* differences in the proliferation and activation responses of HIV-infected CD4+ and CD8+ T-cells upon CD3-stimulation; next, the responses of these T-cell populations in the presence of TI-type 2 stimulated B-cells. Thus, *in vitro* T-cell function alone, and cognate interactions with B-cells, in an HIV-infected cohort compared to matched HIV-negative controls. And as outlined in chapter three, the matching of HIV-infected individuals to HIV-negative controls was stringently regulated to minimize age-, sex- and ethnicity-based variations.

The second aim was to uncover *in vitro* differences in the proliferation and activation of the overall CD19+ B-cell population alone and with T-cell help, between the HIV-infected cohort and matched controls. Even subtle differences observed could contribute to an explanation for the higher predisposition to pneumococcal disease observed in this immunocompromised patient group and reported in the literature.

CHAPTER FOUR

4.2 Methods

4.2.1 Expansion of the stimulation assay

The stimulation assay using αδdex mimics capsular polysaccharides by cross-linking B-cell receptors on all B-cells which express surface IgD (Pecanha et al., 1991). This polyclonal stimulation has been used extensively by our group as a model for total B-cell stimulation. The inclusion of *S. pneumoniae* would target only a small population of cells that have already experienced class-switching due to previous exposure to capsular polysaccharide. The assay was expanded to include *S. pneumoniae*-stimulation in order to investigate differences in antigen-specific responses between patients and controls, bearing in mind that differences in *in vivo* exposure to *S. pneumoniae* would have to be considered when interpreting results. Also, that the effect of pneumococcal-specific stimulation was likely to be minimal compared to polyclonal stimulation.

In optimisation experiments, using live bacteria (MOI of 5 and 10) killed the entire culture of lymphocytes even as little as 24 hr after incubation. Thus using live bacteria for the 96 hr time point required for the assay would have been impractical. Following replication of the T- and B-cell immunologic assay using the same concentration of anti-CD3, anti-CD28 and αδdex as previously described (Foster et al., 2009, Darton et al., 2011), heat-killed *S. pneumoniae* D39 strain (HKD39) at an optimized multiplicity of infection (MOI; fig. 4.1) was included as a stimulant. In theory, heat-killing the bacteria should have no effect on the recognition of the bacterial capsular polysaccharide by the B-cells. Further, antigen presentation of the bacteria to T-cells should proceed as normal.
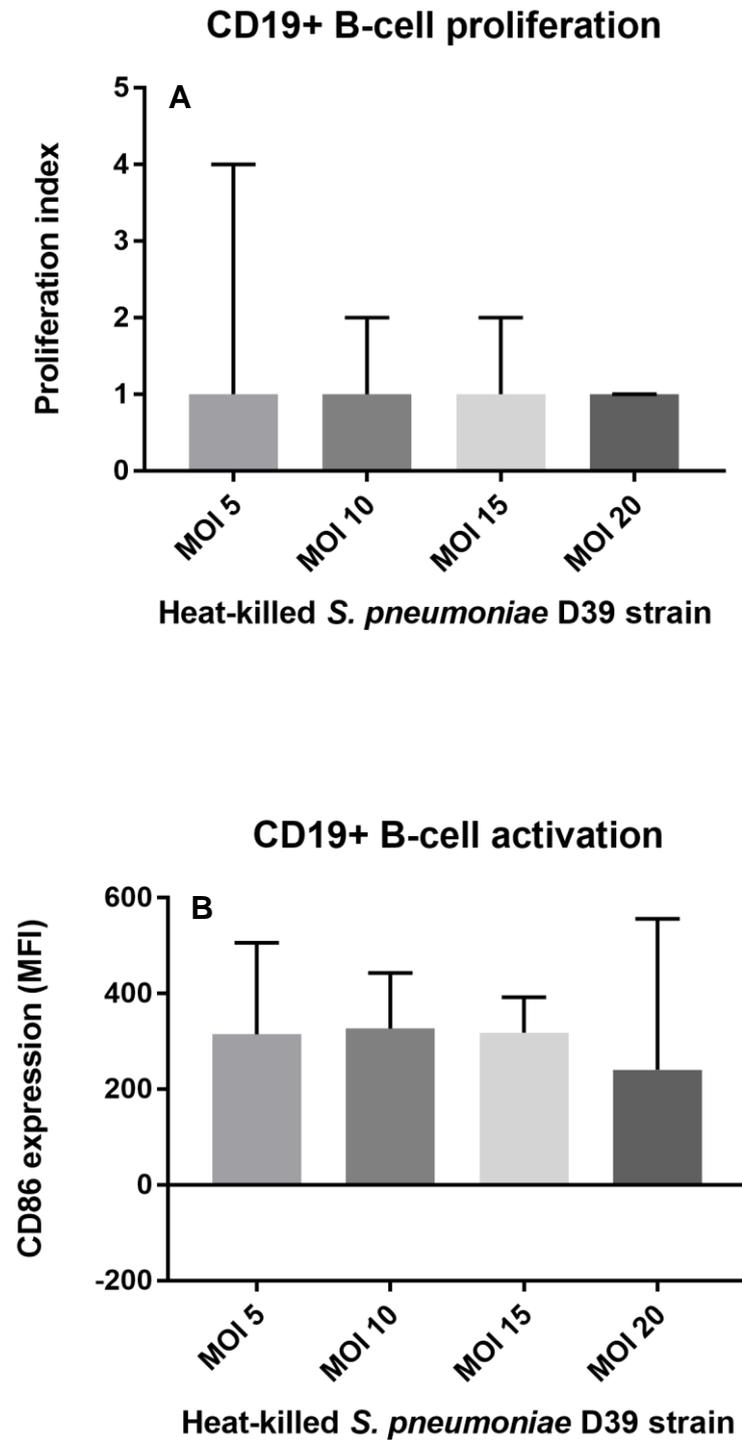
Figure 4.1: Proliferation (A) and activation (B) of CD19+ B-cells after *in vitro* stimulation using four different concentrations of heat-killed *S. pneumoniae* D39 strain (HKD39). The Kruskal-Wallis H test was used to study variances, with post-hoc Bonferroni correction for multiple comparisons. (n = 5).

A multiplicity of infection (MOI) of 10 (Gordon et al., 2000) was chosen for use in further stimulation assays. It is noteworthy that the Gordon study used live bacteria, whilst the present study proceeded with heat-killed bacteria. Thus, it was expected that stimulations in the present study would occur to a different extent than if live bacteria was used.

Once the MOI of 10 was chosen, statistical analysis was performed to study differences in responses of B-cells following αδdex and HKD39 stimulations (fig 4.2).

CD19+ B-cell activation
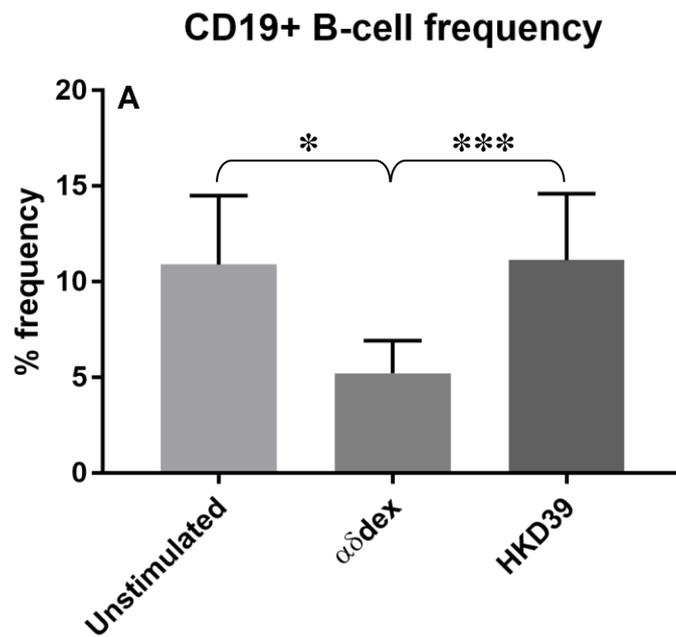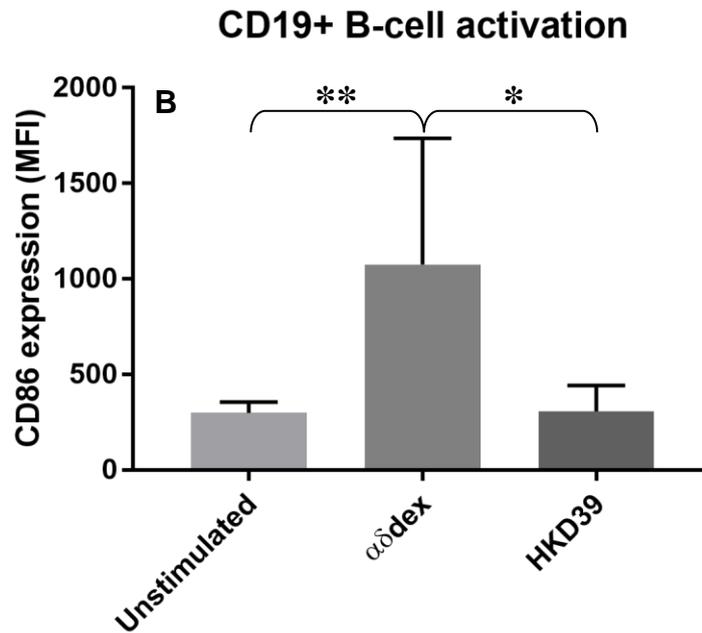
Figure 4.2: Frequency (A) and activation (B) of CD19+ B-cells after *in vitro* stimulation using 1µg/ml of αδdex and MOI 10 of HKD39. The Kruskal-Wallis H test was used to study variances with *p* values adjusted by Bonferroni correction (n = 12; study group described in table 3.2); (Where * *p* ≤ 0.050, ** *p* ≤ 0.010, *** *p* ≤ 0.001).

As expected, the αδdex activation response elicited by cross-linking of multiple B-cell receptors was significantly higher than the response to HKD39-stimulation from the small antigen-specific population ($p \leq 0.050$; (Pecanha et al., 1991)).

4.2.2 Recruitment of patients and controls

HIV-infected individuals were recruited from HIV clinics based at the Department of Infection and Tropical Medicine and Department of Genitourinary Medicine at the STH NHS Foundation Trust as described in chapter two (section 2.1). Age-, sex- and ethnicity-matched controls were recruited from amongst the staff of the Sheffield Medical School and the Royal Hallamshire Hospital (RHH). After informed consent was obtained, blood was drawn and PBMCs were cultured using aseptic technique. The stimulation assay was performed as described in chapter two (section 2.4 and 2.5). The three cell populations of interest in this chapter, CD4+ T-cells and CD19+ B-cells, are shown in representative dot plots in fig. 2.3 (chapter two).

Fig. 4.3 and table 4.1 outline the workflow used during patient recruitment and *in vitro* work, respectively, for this portion of the study.
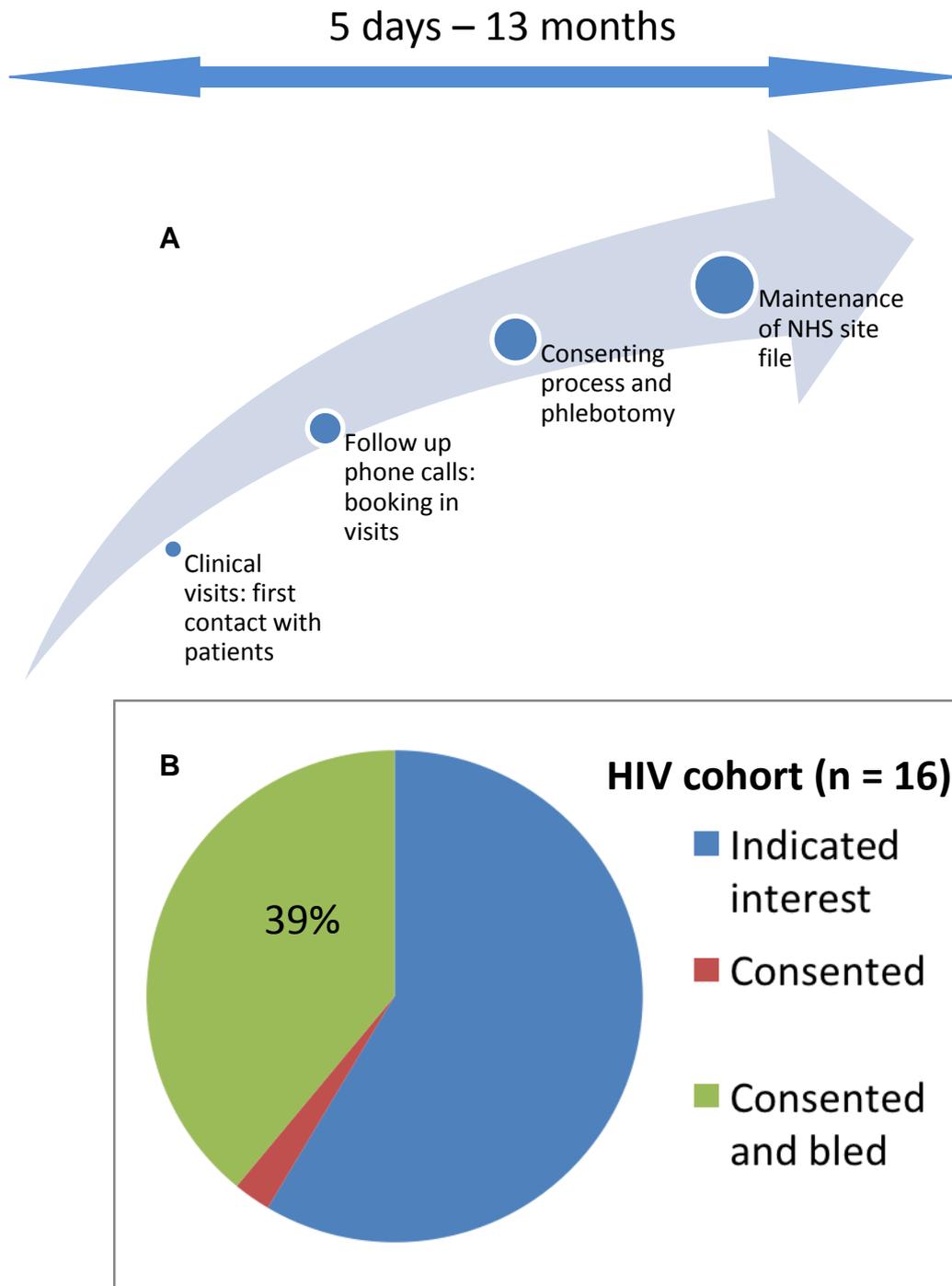
Figure 4.3: Workflow for patient recruitment during this project (A). Of 41 patients who initially indicated interest in participating in this project, 17 were consented, and 16 were bled (B). All these patients were on Highly Active Antiretroviral Therapy (HAART), described in table 4.1.

Table 4.1: Antiretroviral therapy (ART) drug classifications from the US Department of Health and Human Services (2017)(AIDSInfo, 2017)

Table 4.3 classification	Drug classification	ART drug	Mechanism of function
A	Combination HIV medicine	Kivexa: Abacavir (Nucleoside Reverse Transcriptase Inhibitor; NRTI) and Lamivudine (NRTI)	Combined functions of component classes. Pharmacokinetic enhancers increase HIV medicine effectiveness by interfering with drug breakdown.
		Rezolsta: Darunavir (Protease Inhibitor; PI) and Cobicistat (Pharmacokinetic enhancer)	
		Atripla: Efavirenz (Non-Nucleoside Reverse Transcriptase Inhibitor; NNRTI), Emtricitabine (NRTI) and Tonofovir disoproxil fumarate (NRTI)	
		Descovy: Emtricitabine (NRTI) and Tenofovir alafenamide (NRTI)	
		Truvada: Emtricitabine (NRTI) and Tenofovir disoproxil fumarate (NRTI)	
		Triumeq: Abacavir (NRTI), Dolutegravir (Integrase Inhibitor; II), and Lamuvidine (NRTI)	
B	Non-Nucleoside Reverse Transcriptase Inhibitor (NNRTI)	Efavirenz, Etravirine	Alters viral reverse transcriptase enzyme after binding to it.
C	Protease Inhibitor (PI)	Darunavir, Ritonavir, Atazanavir	Prevents HIV replication by blocking HIV protease enzyme.
D	Integrase Inhibitor (II)	Dolutegravir, Raltegravir	Prevents HIV replication by blocking HIV integrase enzyme.
E	Nucleoside Reverse Transcriptase Inhibitor (NRTI)	Zidovudine	Prevents HIV replication by blocking HIV reverse transcriptase enzyme.
F	Entry Inhibitor	Maraviroc	Inhibits viral entry by binding to CD4+ T-cell CCR5 coreceptor.

Table 4.2: Brief description of the workflow and outcome measures for results presented in chapter four

Aim	Work Flow	Outcome measures	Results presented in figure*:	HIV+ cohort number
Investigate differences in T- and B-cell responses between HIV-infected individuals and matched controls, based on our group immunologic assay	CD4+ T-cell responses to TCR-stimulant; anti-CD3 alone, and in combination with αδdex, and αδdex + anti-CD28 respectively.	CD4+ T-cell frequency, proliferation (based on CFSE proliferation index), and activation (based on CD25 and HLA-DR expression).	4.4 – 4.7	16 (except for HLA-DR, where n = 8)
	CD8+ T-cell responses to TCR-stimulant; anti-CD3 alone, and in combination with αδdex, and αδdex + anti-CD28 respectively.	CD8+ T-cell frequency, proliferation (based on CFSE proliferation index), and activation (based on CD25 and HLA-DR expression).	4.8 – 4.11	16 (except for HLA-DR, where n = 8)
	CD19+ B-cell responses to anti-IgD-stimulation using αδdex alone, and in combination with anti-CD3, and anti-CD3 + anti-CD28 respectively.	CD19+ B-cell frequency, proliferation (based on CFSE proliferation index), and activation (based on CD86, CD25 and HLA-DR expression).	4.12 – 4.16	16 (except for HLA-DR, where n = 8)
Investigate differences in T- and B-cell responses between HIV-infected individuals and matched controls, based on the expanded immunologic assay including *S. pneumoniae*-stimulation	CD4+ T-cell responses to D39 strain of *S. pneumoniae* alone, and in combination with anti-CD3, and anti-CD3 + anti-CD28 respectively.	CD4+ T-cell frequency, proliferation (based on CFSE proliferation index), and activation (based on CD25 and HLA-DR expression).	4.4 – 4.7	8
	CD8+ T-cell responses to D39 strain of *S. pneumoniae* alone, and in combination with anti-CD3, and anti-CD3 + anti-CD28 respectively.	CD8+ T-cell frequency, proliferation (based on CFSE proliferation index), and activation (based on CD25 and HLA-DR expression).	4.8 – 4.11	8
	CD19+ B-cell responses to D39 strain of *S. pneumoniae* alone, and in combination with anti-CD3, and anti-CD3 + anti-CD28 respectively.	CD19+ B-cell frequency, proliferation (based on CFSE proliferation index), and activation (based on CD86, CD25 and HLA-DR expression).	4.12 – 4.16	8

* All data was collected by Furaha Asani.

4.3 Results

4.3.1 Characteristics of patient recruits and matched controls

Table 4.2 outlines the patient and control characteristics, while table 4.3 shows the current ART regimes used by each patient.

Table 4.3: Characteristics of the HIV-infected cohort recruited for this study, with matched controls

	HIV+	HIV- controls
Number	16	16
Mean age (Range)	50.45 (40 – 61)	50.65 (35 – 65)
Sex: Female	2	2
Male	14	14
Ethnicity: Black	2	2
White	14	14
Mean CD4 count (/mm^3) (Range)	677.63 (359 – 921)	N/A
Mean total globulin levels (g/L) (Range) *	27.38 (23 – 37)	N/A

*The normal range of total globulin in HIV-uninfected individuals visiting the Royal Hallamshire Hospital (RHH) is 18 – 36 g/L, indicating that this cohort of HIV-infected individuals fell within the normal range of total globulin levels expected at RHH.

Table 4.4: Clinical characteristics of the HIV-infected individuals who participated in this study. Information for some individuals was unavailable from records due to transferring from other hospitals or countries onto the Sheffield Teaching Hospitals (STH) database.

Patient	Age at bleed	Sex *	Ethnicity°	CD4 Count (/mm³)	Total globulin count (g/L)	Time post starting ART (years)	Pre-ART viral load (cp/ml) †	Current ART regime [a]	Time post last viral detection (years)
1	55	M	W	706	29	14	D	Kivexa (A), Efavirenz (B)	6
2	50	M	W	869	23	13	69,700	Etravirine (B), Darunavir (C), Ritonavir (C), Dolutegravir (D)	N/A
3	53	M	W	359	29	20	D	Zidovudine (E), Truvada (A)	3
4	43	M	W	895	31	18	D	Triumeq (A)	8
5	40	F	B	529	37	6	N/A	Dolutegravir (D), Maraviroc (F)	4
6	42	M	W	695	24	17	D	Kivexa (A), Maraviroc (F)	8
7	50	F	B	494	28	11	6630	Triumeq (A)	9
8	61	M	W	361	27	19	D	Truvada (A), Dolutegravir (D)	N/A
9	42	M	W	655	24	N/A	10,600	Rezolsta (A)	N/A
10	40	M	W	793	26	7	38,071	Atripla (A)	N/A
11	52	M	W	458	26	6	59,406	Descovy (A), Efavirenz (B)	N/A
12	59	M	W	787	29	5	34,666	Truvada (A), Atazanavir (C), Ritonavir (C)	5
13	54	M	W	631	28	8	N/A	Triumeq (A)	1
14	52	M	W	921	28	6	43,318	Etravirine (B)	4
15	58	M	W	691	26	11	30,100	Truvada (A), Raltegravir (D)	N/A
16	53	M	W	827	26	8	122,431	Ritonavir (C), Atazanavir (C), Truvada (A)	< 6 months

*Classification of sex by female (F) or male (M).
°Classification of ethnicity by Black (B) or White (W).
† Records for some individuals merely stated 'Detected' regarding pre-ART viral load. This is represented as 'D' in the table. Notably, these five individuals had been diagnosed in the late nineties, or early two-thousands.
[a] ART classifications were expatiated upon in table 4.1.

Using the one-sample Kolmogorov-Smirnov test, some datasets presented in figures 4.4 to 4.16 were ascertained to contain both parametric and non-parametric datasets. Thus the paired-samples *t*-test and the Wilcoxon signed ranks test were respectively used for statistical analyses of these data. Pair-wise comparisons between HIV-infected individuals and age-, sex- and ethnicity-matched HIV-negative controls were conducted. The *p* values shown are two-tailed, testing for differences in both directions. Paired data are presented as spot-line graphs not only to show differences between HIV-infected individuals and matched controls, but inter-pair variations. Shaded circles represent one individual, with a line connecting matched patient-control pairs. The graph grid is organised to facilitate comparisons across rows, and down columns. (Patient n = 16 except for HKD39-stimulations, where patient n = 8). Each graph grid is accompanied by line graphs tracking patient cohort and control cohort responses separately, to facilitate visualisation of how individuals responded to the different stimulation conditions.

Stimulation concentrations used were as described in chapter 2: 1µg/ml of αδdex, 0.1µg/ml anti-CD3 alone, and 0.5µg/ml anti-CD3 in combination with 0.5µg/ml anti-CD28 for 96 hr. HKD39 MOI used was 10, for 96 hr. Stimulation conditions are indicated per graph.

4.3.2 Variations in CD4+ T-cell responses to the stimulation assay, between HIV-infected individuals and matched controls

CD4+ T-cell frequency percentages were higher in HIV-uninfected controls compared to patients (fig. 4.4i) but were comparable after all stimulations except for anti-CD3 combined with anti-CD28 (fig. 4.4i C) and αδdex (fig. 4.4i D).
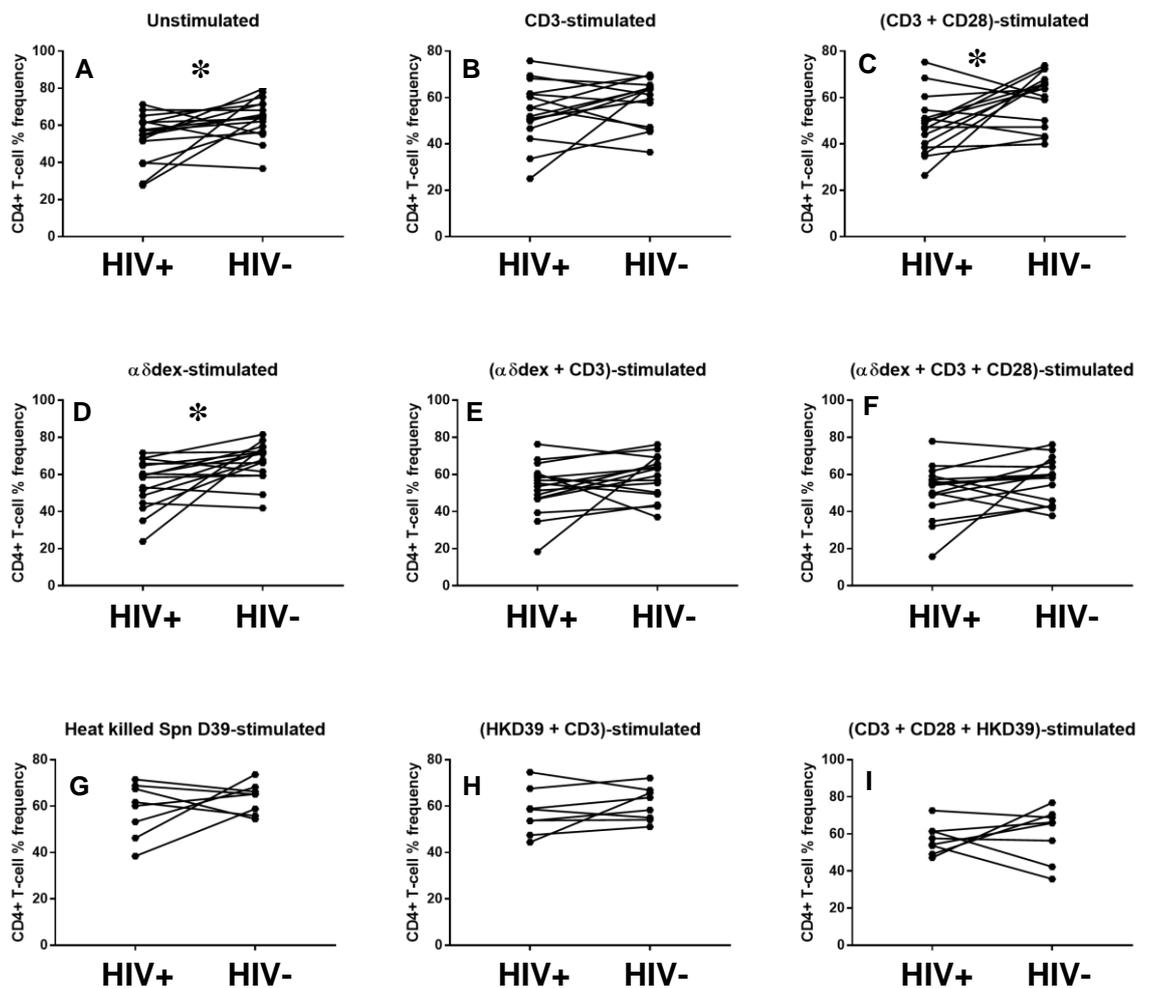
Figure 4.4i: Percentage frequencies of *in vitro* CD4+ T-cells in HIV-infected individuals and matched controls under un-stimulated and stimulated conditions. Dots and lines match each patient-control pair. The paired-samples *t*-test and Wilcoxon signed ranks test were used for parametric and non-parametric datasets respectively. (Patient n = 16 except for HKD39-stimulations, where patient n = 8; Where * $p \leq 0.050$).

Concentrations of stimulants used: 1µg/ml of αδdex, 0.1µg/ml anti-CD3 alone, and 0.5µg/ml anti-CD3 in combination with 0.5µg/ml anti-CD28. Patient cohort and control cohort tracking data for this graph grid is presented in fig. 4.4ii.

Figure 4.4ii: Tracking data showing the changes in *in vitro* CD4+ T-cell frequencies in HIV-infected individuals (A) and matched controls (B) upon stimulation. Matched patient-control pairs are represented using the same colour across A and B. Conditions: 1; Un-stimulated, 2; CD3-stimulated, 3; (CD3+CD28)-stimulated, 4; αδdex-stimulated, 5; (αδdex +CD3)-stimulated, 6; (αδdex +CD3+CD28)-stimulated, 7; HKD39-stimulated, 8; (HKD39+CD3)-stimulated, 9; (CD3+CD28+HKD39)-stimulated.

The HIV-uninfected controls also had higher *in vitro* CD4+ T-cell proliferation under un-stimulated conditions (fig. 4.5i).

Figure 4.5i: Proliferation of *in vitro* CD4+ T-cells in HIV-infected individuals and matched controls under un-stimulated and stimulated conditions. Dots and lines match each patient-control pair. The paired-samples *t*-test and Wilcoxon signed ranks test were used for parametric and non-parametric datasets respectively. (Patient n = 16 except for HKD39-stimulations, where patient n = 8; Where * $p \leq 0.050$). Concentrations of stimulants used: 1µg/ml of αδdex, 0.1µg/ml anti-CD3 alone, and 0.5µg/ml anti-CD3 in combination with 0.5µg/ml anti-CD28. Patient cohort and control cohort tracking data for this graph grid is presented in fig. 4.5ii.

Figure 4.5ii: Tracking data showing the changes in *in vitro* CD4+ T-cell proliferation in HIV-infected individuals (A) and matched controls (B) upon stimulation. Matched patient-control pairs are represented using the same colour across A and B. Conditions: 1; Un-stimulated, 2; CD3-stimulated, 3; (CD3+CD28)-stimulated, 4; αδdex-stimulated, 5; (αδdex +CD3)-stimulated, 6; (αδdex +CD3+CD28)-stimulated, 7; HKD39-stimulated, 8; (HKD39+CD3)-stimulated, 9; (CD3+CD28+HKD39)-stimulated.

Differences in activation of CD4+ T-cells between patients and controls were determined by quantifying *in vitro* expression of CD25 (fig. 4.6i) and HLA-DR (fig. 4.7i).

Figure 4.6i: CD25 expression on *in vitro* CD4+ T-cells in HIV-infected individuals and matched controls under un-stimulated and stimulated conditions. Dots and lines match each patient-control pair. The paired-samples *t*-test and Wilcoxon signed ranks test were used for parametric and non-parametric datasets respectively. (Patient n = 16 except for HKD39-stimulations, where patient n = 8; Where * $p \le 0.050$). Concentrations of stimulants used: 1µg/ml of αδdex, 0.1µg/ml anti-CD3 alone, and 0.5µg/ml anti-CD3 in combination with 0.5µg/ml anti-CD28. Patient cohort and control cohort tracking data for this graph grid is presented in fig. 4.6ii.

Figure 4.6ii: Tracking data showing the changes in *in vitro* CD4+ T-cell CD25 expression in HIV-infected individuals (A) and matched controls (B) upon stimulation. Matched patient-control pairs are represented using the same colour across A and B. Conditions: 1; Un-stimulated, 2; CD3-stimulated, 3; (CD3+CD28)-stimulated, 4; αδdex-stimulated, 5; (αδdex +CD3)-stimulated, 6; (αδdex +CD3+CD28)-stimulated, 7; HKD39-stimulated, 8; (HKD39+CD3)-stimulated, 9; (CD3+CD28+HKD39)-stimulated.
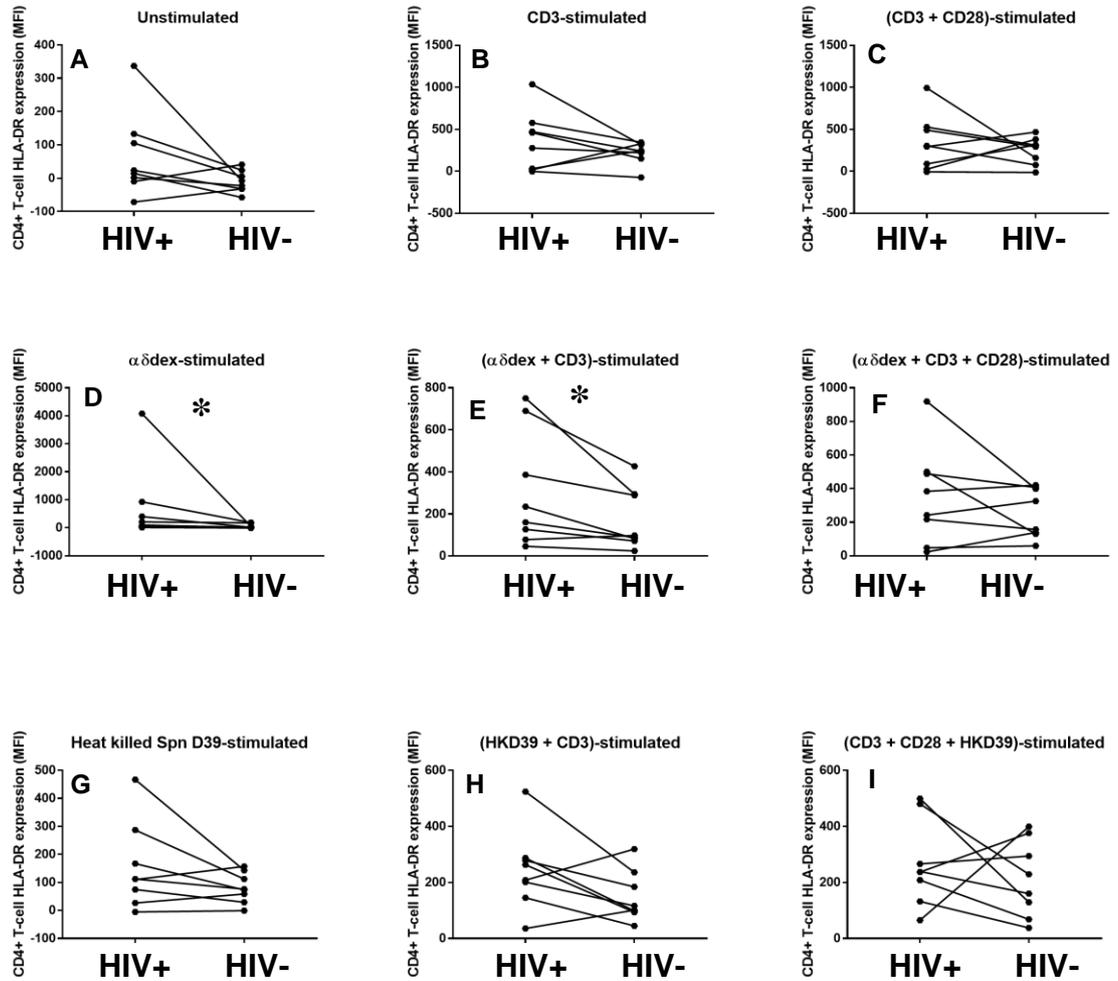
Figure 4.7i: HLA-DR expression on *in vitro* CD4+ T-cells in HIV-infected individuals and matched controls under un-stimulated and stimulated conditions. Dots and lines match each patient-control pair. The paired-samples *t*-test and Wilcoxon signed ranks test were used for parametric and non-parametric datasets respectively. (Patient n = 16 except for HKD39-stimulations, where patient n = 8; Where * $p \leq 0.050$). Concentrations of stimulants used: 1µg/ml of αδdex, 0.1µg/ml anti-CD3 alone, and 0.5µg/ml anti-CD3 in combination with 0.5µg/ml anti-CD28. Patient cohort and control cohort tracking data for this graph grid is presented in fig. 4.7ii.

Figure 4.7ii: Tracking data showing the changes in *in vitro* CD4+ T-cell HLA-DR expression in HIV-infected individuals (A) and matched controls (B) upon stimulation. Matched patient-control pairs are represented using the same colour across A and B. Conditions: 1; Un-stimulated, 2; CD3-stimulated, 3; (CD3+CD28)-stimulated, 4; αδdex-stimulated, 5; (αδdex +CD3)-stimulated, 6; (αδdex +CD3+CD28)-stimulated, 7; HKD39-stimulated, 8; (HKD39+CD3)-stimulated, 9; (CD3+CD28+HKD39)-stimulated.

4.3.3 CD3-stimulated hyperactivation in the CD8+ T-cells of HIV-infected individuals compared to matched controls

Differences in CD8+ T-cell responses between patients and controls were investigated next. Percentage frequencies were analysed (fig. 4.8i), before proliferation (fig. 4.9i) and activation responses (fig. 4.10i and 4.11i).

Figure 4.8i: Percentage frequencies of *in vitro* CD8+ T-cells in HIV-infected individuals and matched controls under un-stimulated and stimulated conditions. Dots and lines match each patient-control pair. The paired-samples *t*-test and Wilcoxon signed ranks test were used for parametric and non-parametric datasets respectively. (Patient n = 16 except for HKD39-stimulations, where patient n = 8; Where * $p \leq 0.050$; ** $p \leq 0.010$). Concentrations of stimulants used: 1µg/ml of αδdex, 0.1µg/ml anti-

CD3 alone, and 0.5μg/ml anti-CD3 in combination with 0.5μg/ml anti-CD28. Patient cohort and control cohort tracking data for this graph grid is presented in fig. 4.8ii.

Figure 4.8ii: Tracking data showing the changes in *in vitro* CD8+ T-cell frequencies in HIV-infected individuals (A) and matched controls (B) upon stimulation. Matched patient-control pairs are represented using the same colour across A and B. Conditions: 1; Un-stimulated, 2; CD3-stimulated, 3; (CD3+CD28)-stimulated, 4; αδdex-stimulated, 5; (αδdex

+CD3)-stimulated, 6; (αδdex +CD3+CD28)-stimulated, 7; HKD39-stimulated, 8; (HKD39+CD3)-stimulated, 9; (CD3+CD28+HKD39)-stimulated.

CD8+ T-cell yielded mostly comparable responses between patients and controls (fig. 4.9i).
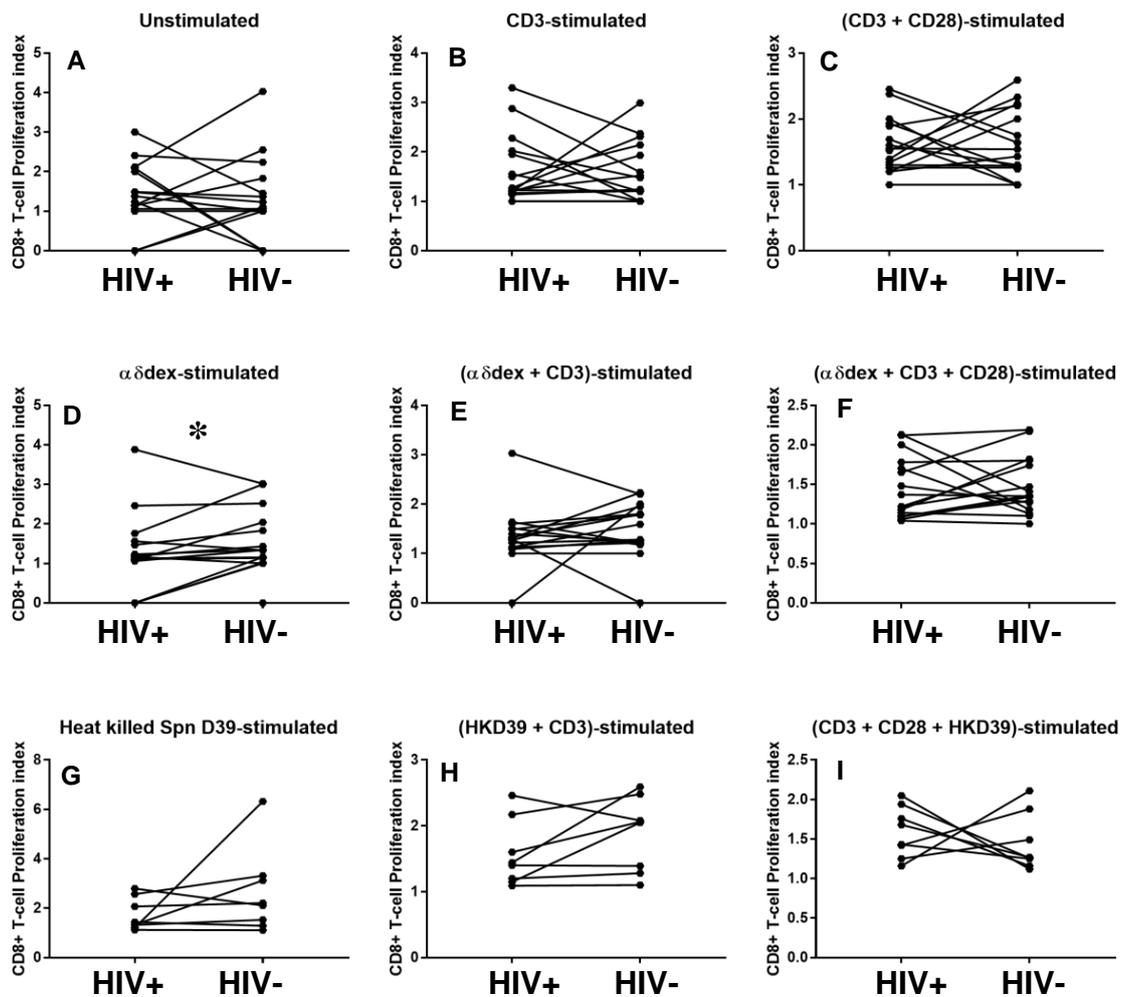
Figure 4.9i: Proliferation of *in vitro* CD8+ T-cells in HIV-infected individuals and matched controls under un-stimulated and stimulated conditions. Dots and lines match each patient-control pair. The paired-samples *t*-test and Wilcoxon signed ranks test were used for parametric and non-parametric datasets respectively. (Patient n = 16 except for HKD39-stimulations, where patient n = 8; Where * $p \leq 0.050$). Concentrations of stimulants used: 1µg/ml of αδdex, 0.1µg/ml anti-CD3 alone, and 0.5µg/ml anti-CD3 in combination with 0.5µg/ml anti-CD28. Patient cohort and control cohort tracking data for this graph grid is presented in fig. 4.9ii.

Figure 4.9ii: Tracking data showing the changes in *in vitro* CD8+ T-cell proliferation in HIV-infected individuals (A) and matched controls (B) upon stimulation. Matched patient-control pairs are represented using the same colour across A and B. Conditions: 1; Un-stimulated, 2; CD3-stimulated, 3; (CD3+CD28)-stimulated, 4; αδdex-stimulated, 5; (αδdex +CD3)-stimulated, 6; (αδdex +CD3+CD28)-stimulated, 7; HKD39-stimulated, 8; (HKD39+CD3)-stimulated, 9; (CD3+CD28+HKD39)-stimulated.

Activation responses in CD8+ T-cells were determined by quantifying CD25 (fig. 4.10i) and HLA-DR (fig. 4.11i) expression.
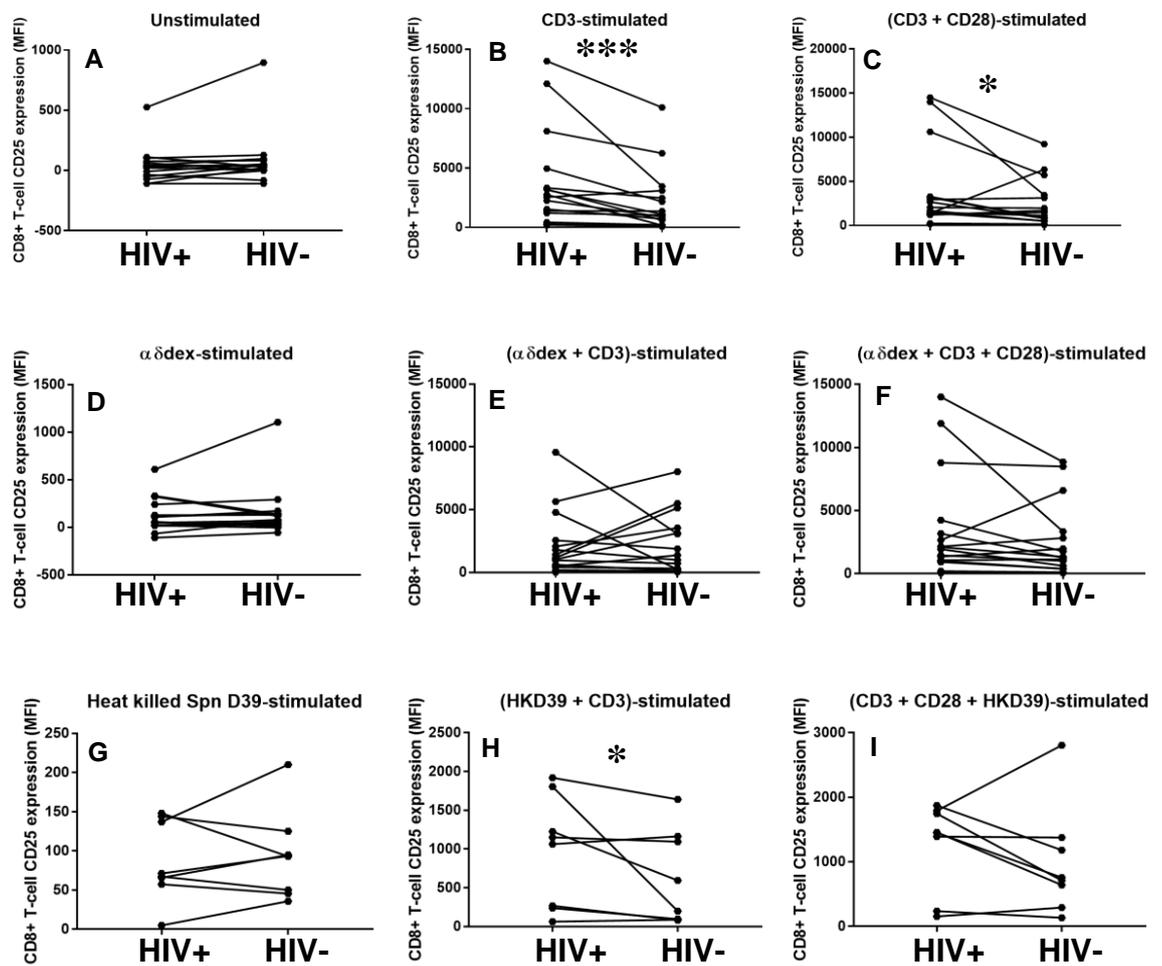
Figure 4.10i: CD25 expression on *in vitro* CD8+ T-cells in HIV-infected individuals and matched controls under un-stimulated and stimulated conditions. Dots and lines match each patient-control pair. The paired-samples *t*-test and Wilcoxon signed ranks test were used for parametric and non-parametric datasets respectively. (Patient n = 16 except for HKD39-stimulations, where patient n = 8; Where * $p \leq 0.050$; *** $p \leq 0.001$). Concentrations of stimulants used: 1µg/ml of αδdex, 0.1µg/ml anti-CD3 alone, and 0.5µg/ml anti-CD3 in combination with 0.5µg/ml anti-CD28. Patient cohort and control cohort tracking data for this graph grid is presented in fig. 4.10ii.
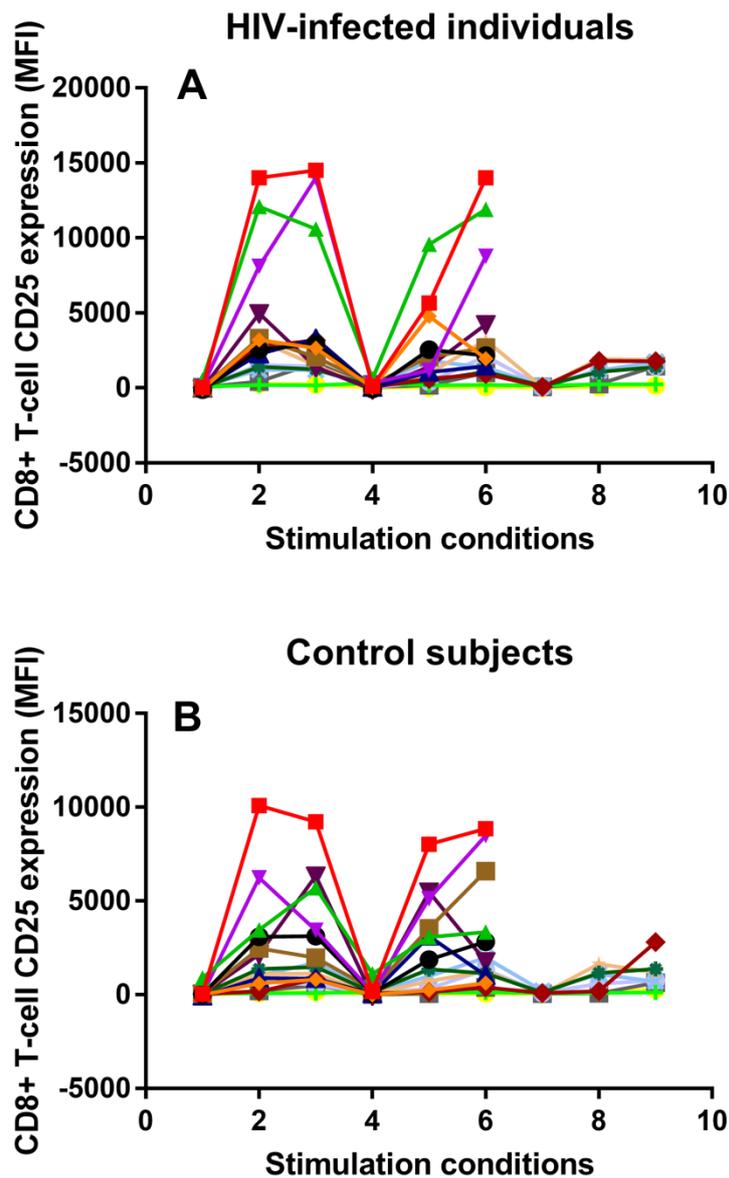
Figure 4.10ii: Tracking data showing the changes in *in vitro* CD8+ T-cell CD25 expression in HIV-infected individuals (A) and matched controls (B) upon stimulation. Matched patient-control pairs are represented using the same colour across A and B. Conditions: 1; Un-stimulated, 2; CD3-stimulated, 3; (CD3+CD28)-stimulated, 4; αδdex-stimulated, 5; (αδdex +CD3)-stimulated, 6; (αδdex +CD3+CD28)-stimulated, 7; HKD39-stimulated, 8; (HKD39+CD3)-stimulated, 9; (CD3+CD28+HKD39)-stimulated.
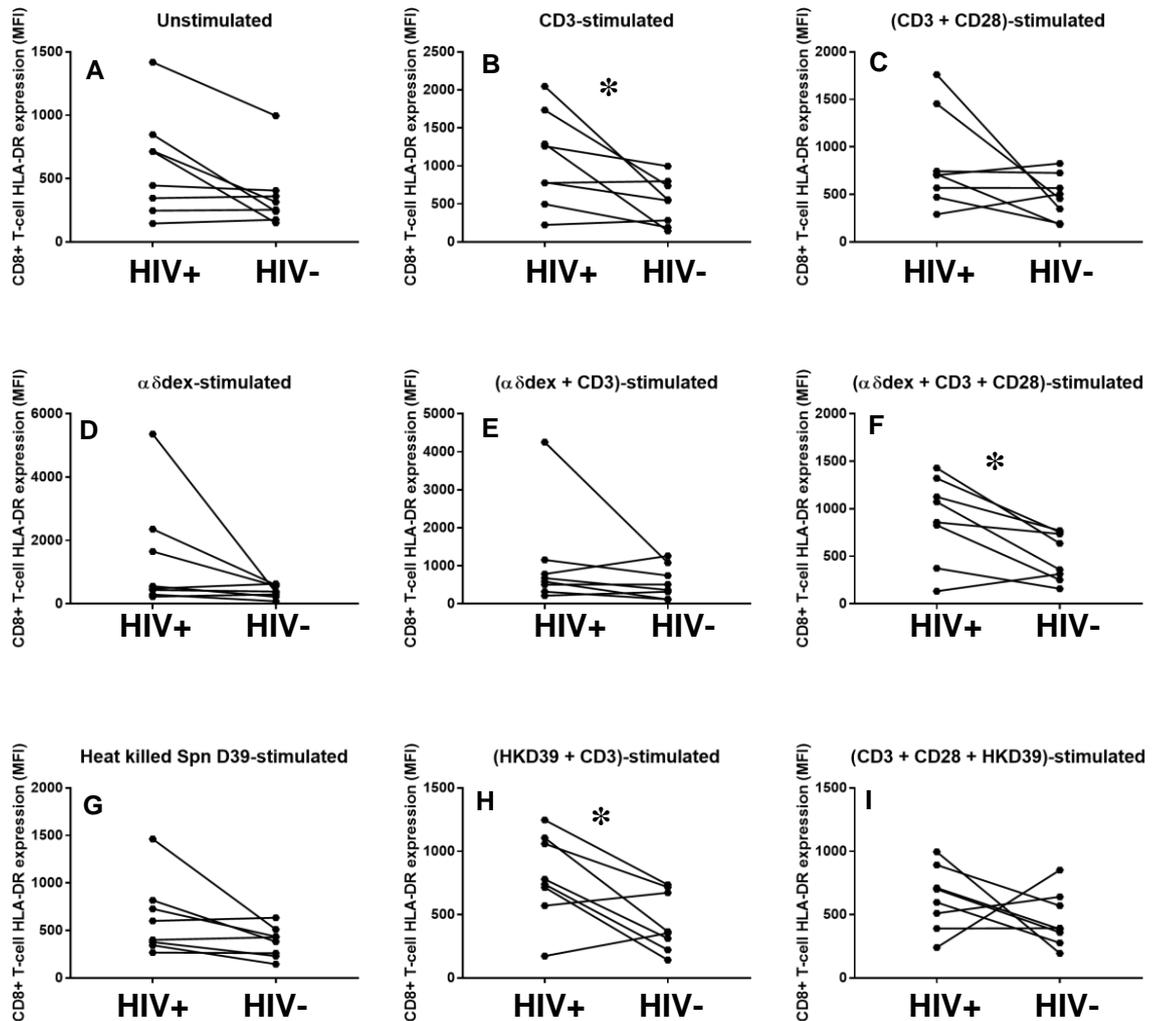
Figure 4.11i: HLA-DR expression on *in vitro* CD8+ T-cells in HIV-infected individuals and matched controls under un-stimulated and stimulated conditions. Dots and lines match each patient-control pair. The paired-samples *t*-test and Wilcoxon signed ranks test were used for parametric and non-parametric datasets respectively. (Patient n = 16 except for HKD39-stimulations, where patient n = 8; Where * $p \leq 0.050$). Concentrations of stimulants used: 1µg/ml of αδdex, 0.1µg/ml anti-CD3 alone, and 0.5µg/ml anti-CD3 in combination with 0.5µg/ml anti-CD28. Patient cohort and control cohort tracking data for this graph grid is presented in fig. 4.11ii.

Figure 4.11ii: Tracking data showing the changes in *in vitro* CD8+ T-cell HLA-DR expression in HIV-infected individuals (A) and matched controls (B) upon stimulation. Matched patient-control pairs are represented using the same colour across A and B. Conditions: 1; Un-stimulated, 2; CD3-stimulated, 3; (CD3+CD28)-stimulated, 4; αδdex-stimulated, 5; (αδdex +CD3)-stimulated, 6; (αδdex +CD3+CD28)-stimulated, 7; HKD39-stimulated, 8; (HKD39+CD3)-stimulated, 9; (CD3+CD28+HKD39)-stimulated.

4.3.4 Increased proliferation in the CD19+ B-cells of HIV-infected individuals compared to matched controls after T-cell-helped pneumococcal-stimulation

The percentage frequency of *in vitro* CD19+ B-cells, and differences between patients and controls was analysed (fig. 4.12i). Thereafter, differences in CD19+ B-cell proliferation (fig. 4.13i).
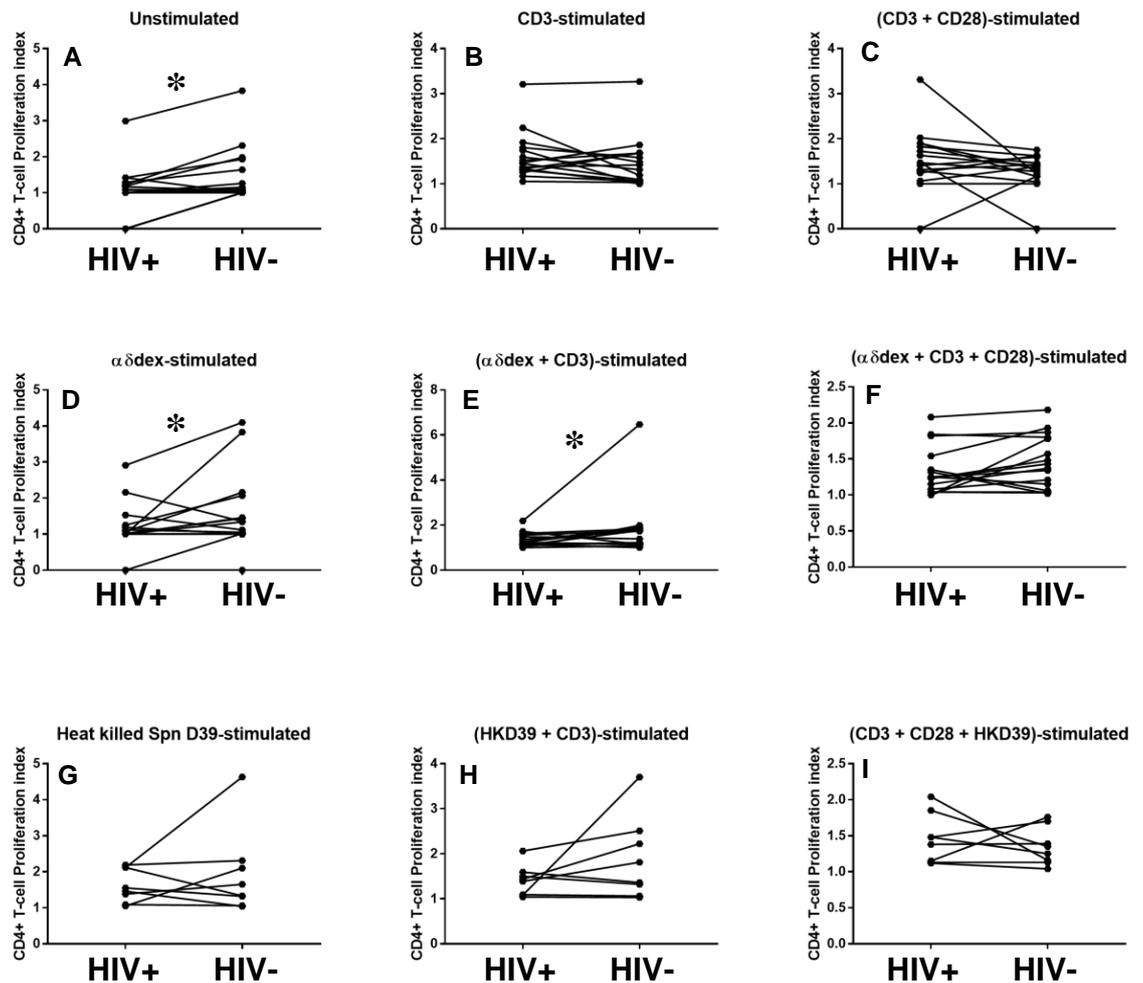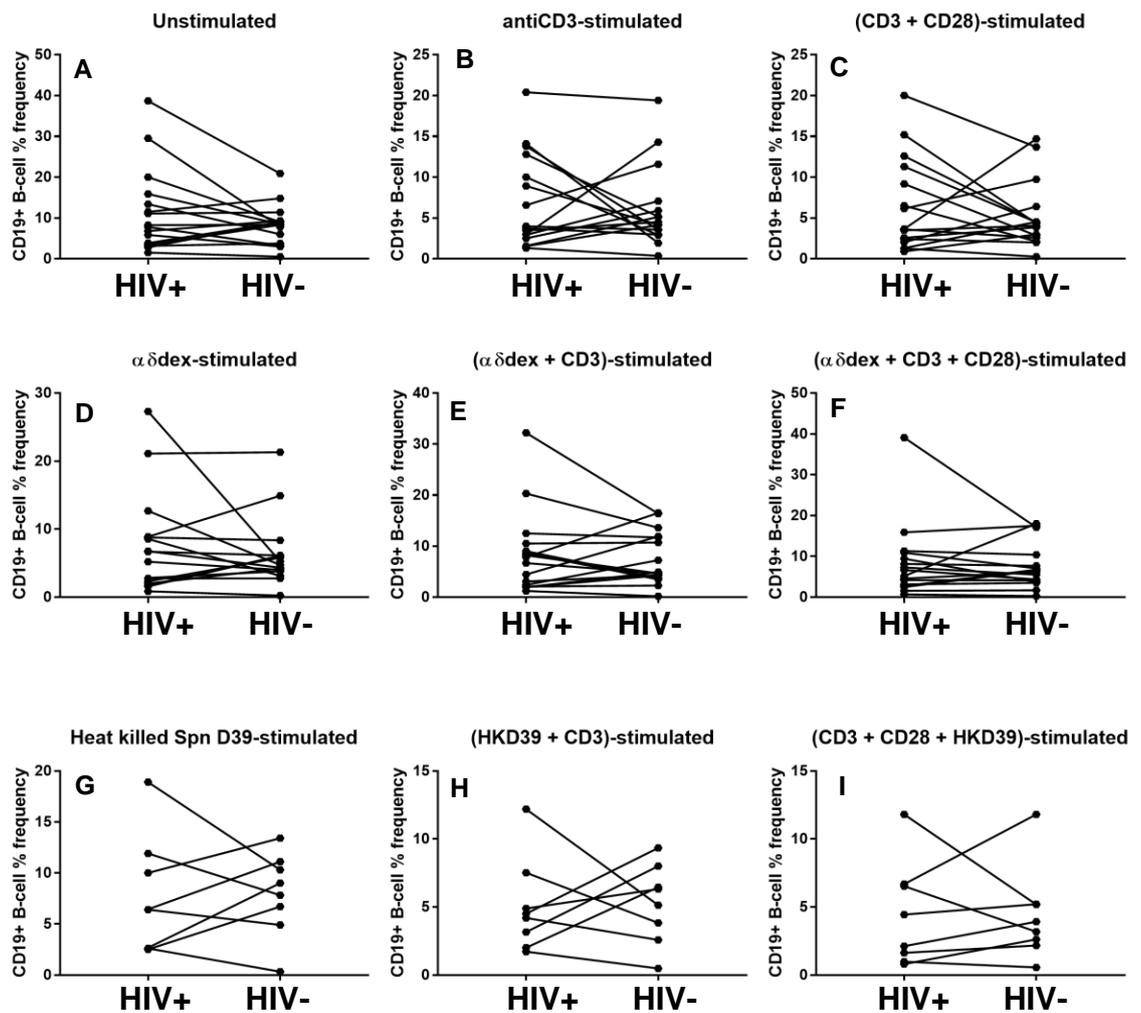

Figure 4.12i: Percentage frequencies of *in vitro* CD19+ B-cells in HIV-infected individuals and matched controls under un-stimulated and stimulated conditions. Dots and lines match each patient-control pair. The paired-samples *t*-test and Wilcoxon signed ranks test were used for parametric and non-parametric datasets respectively. (Patient n = 16 except for HKD39-stimulations, where patient n = 8). Concentrations of stimulants

used: 1μg/ml of αδdex, 0.1μg/ml anti-CD3 alone, and 0.5μg/ml anti-CD3 in combination with 0.5μg/ml anti-CD28. Patient cohort and control cohort tracking data for this graph grid is presented in fig. 4.12ii.

HIV-infected individuals
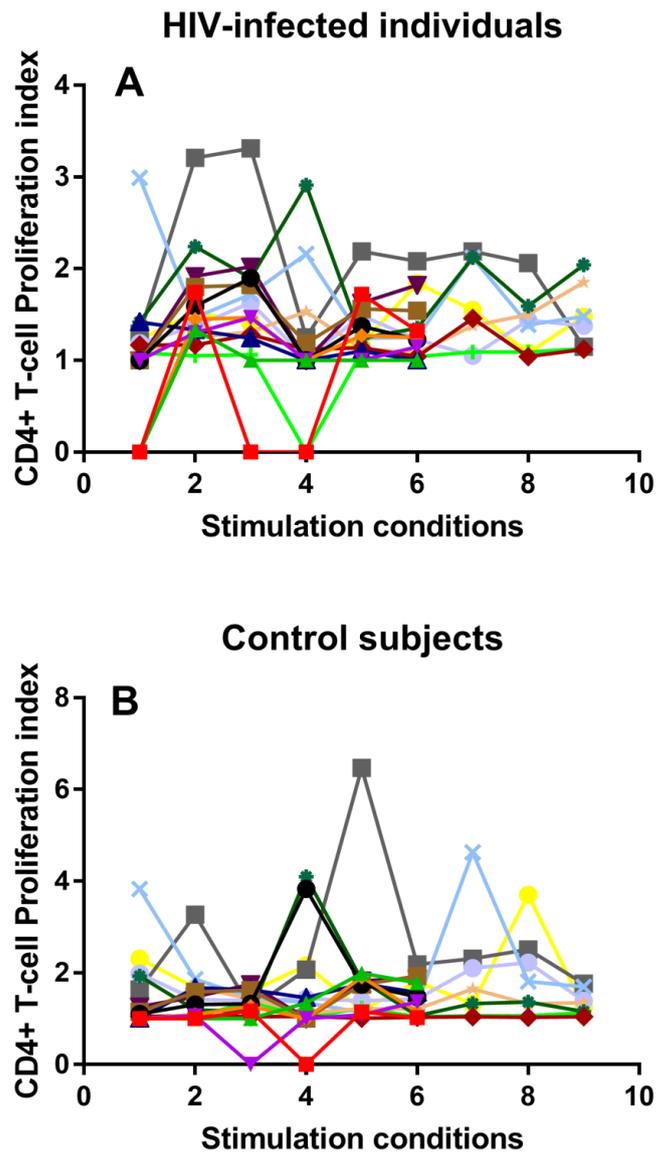

Control subjects
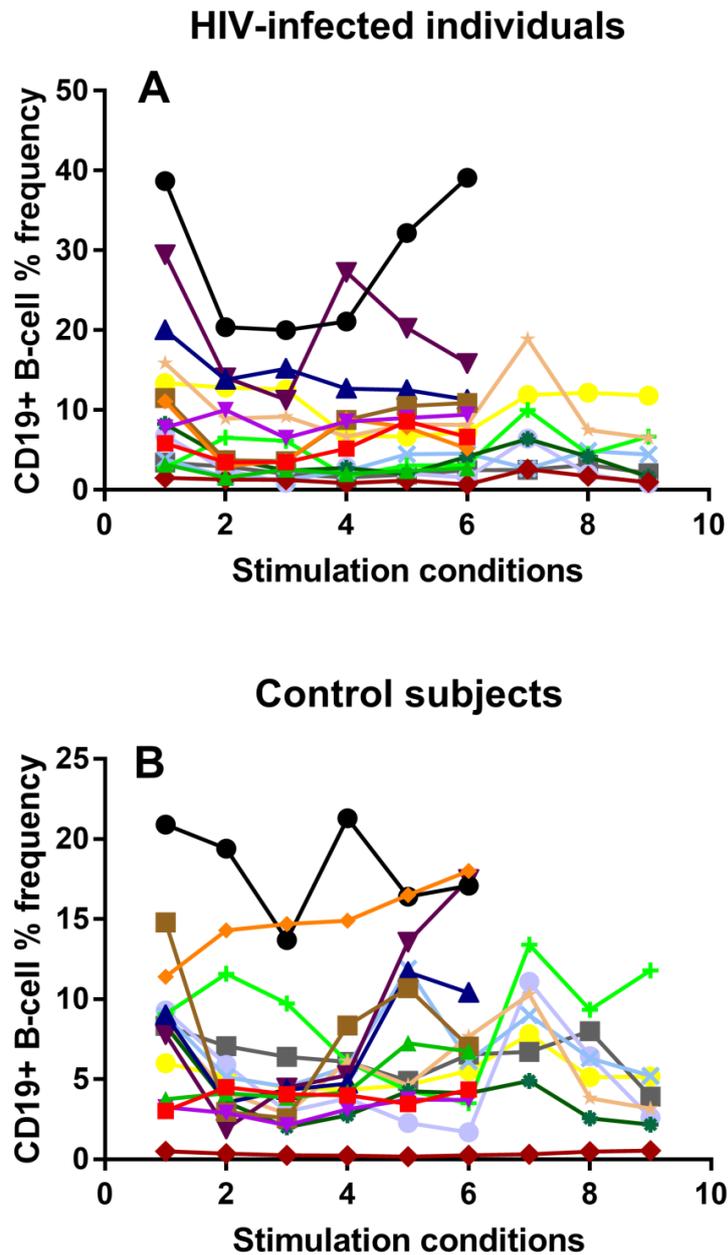
Figure 4.12ii: Tracking data showing the changes in *in vitro* CD19+ B-cell frequencies in HIV-infected individuals (A) and matched controls (B) upon stimulation. Matched patient-control pairs are represented using the same colour across A and B. Conditions: 1; Un-stimulated, 2; CD3-stimulated, 3; (CD3+CD28)-stimulated, 4; αδdex-stimulated, 5; (αδdex

+CD3)-stimulated, 6; (αδdex +CD3+CD28)-stimulated, 7; HKD39-stimulated,
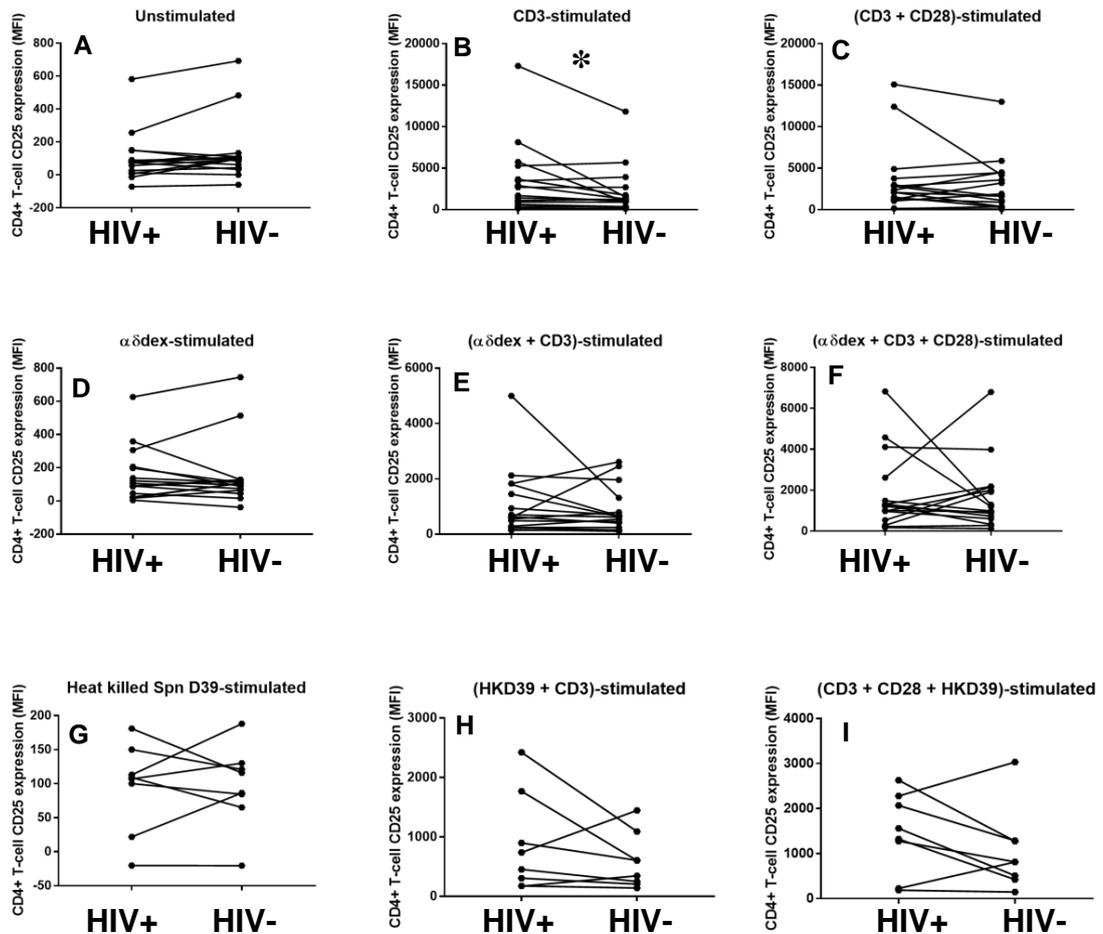8; (HKD39+CD3)-stimulated, 9; (CD3+CD28+HKD39)-stimulated.
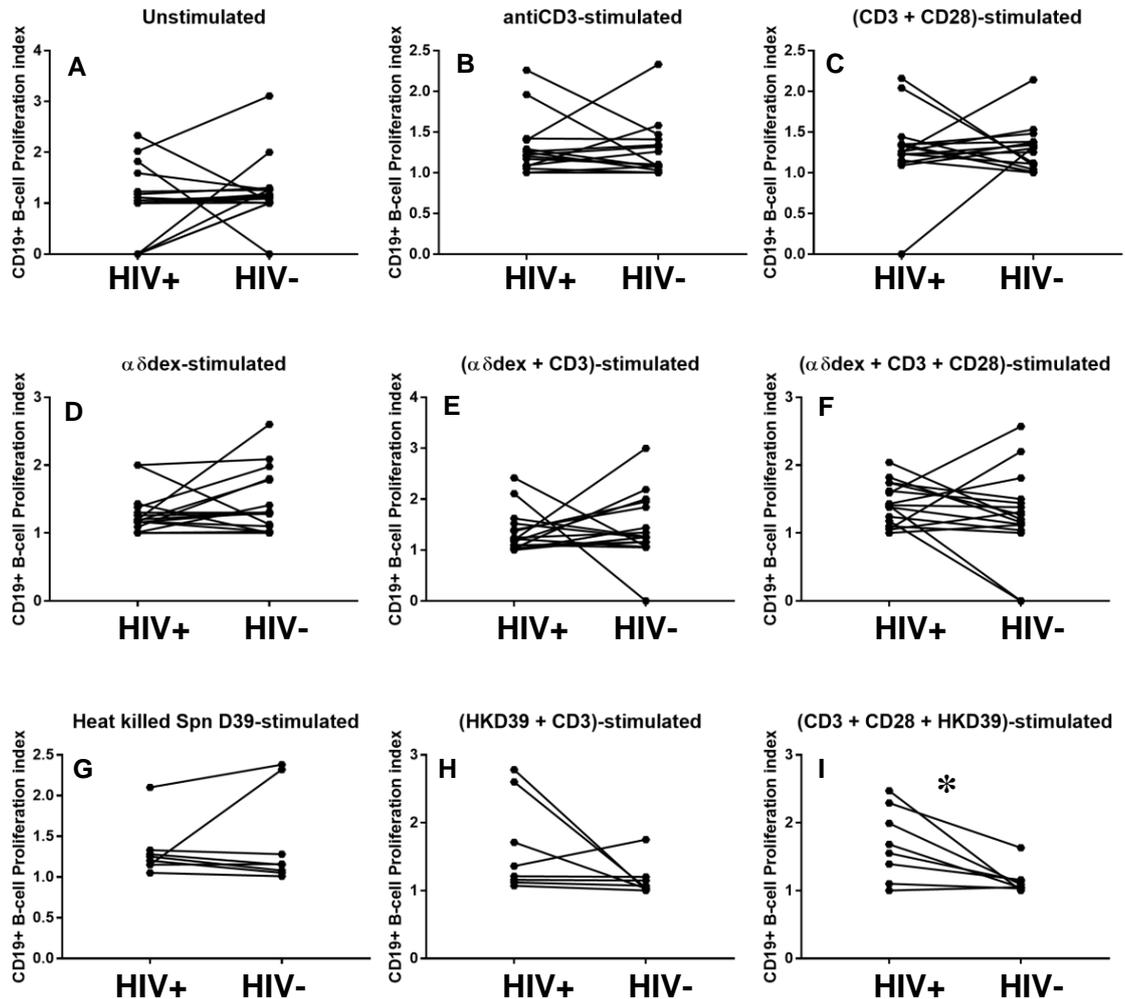
Figure 4.13i: Proliferation of *in vitro* CD19+ B-cells in HIV-infected individuals and matched controls under un-stimulated and stimulated conditions. Dots and lines match each patient-control pair. The paired-samples *t*-test and Wilcoxon signed ranks test were used for parametric and non-parametric datasets respectively. (Patient n = 16 except for HKD39-stimulations, where patient n = 8; Where * $p \leq 0.050$). Concentrations of stimulants used: 1µg/ml of αδdex, 0.1µg/ml anti-CD3 alone, and 0.5µg/ml anti-CD3 in combination with 0.5µg/ml anti-CD28. Patient cohort and control cohort tracking data for this graph grid is presented in fig. 4.13ii.
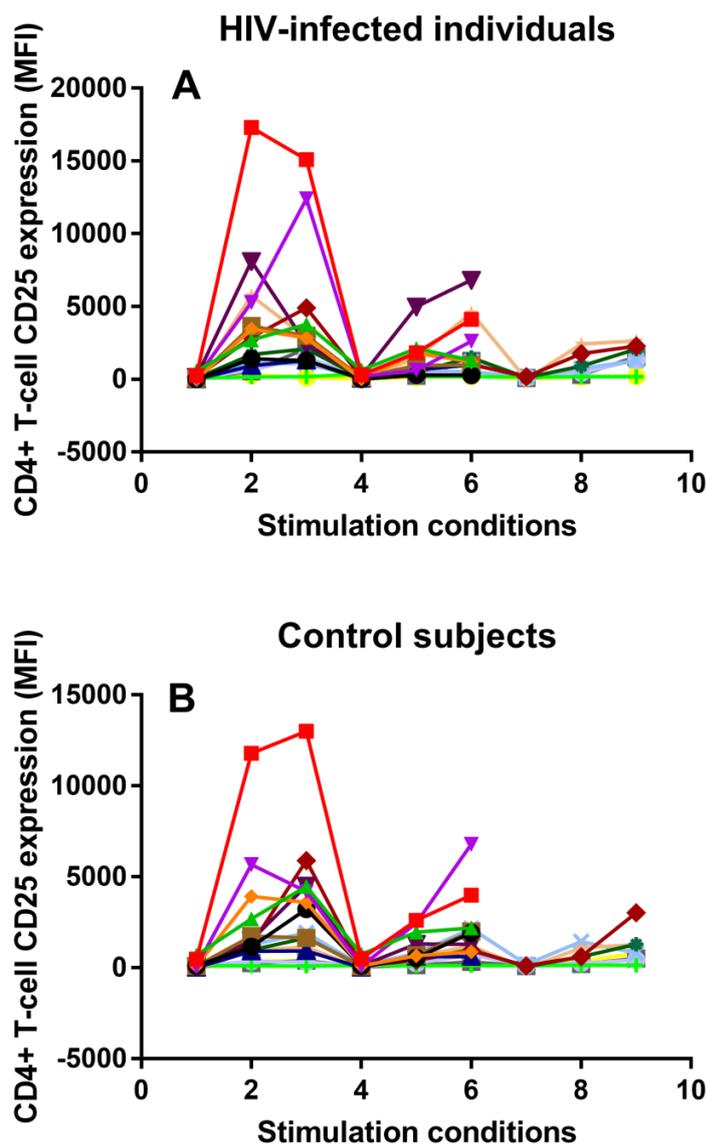
Figure 4.13ii: Tracking data showing the changes in *in vitro* CD19+ B-cell proliferation in HIV-infected individuals (A) and matched controls (B) upon stimulation. Matched patient-control pairs are represented using the same colour across A and B. Conditions: 1; Un-stimulated, 2; CD3-stimulated, 3; (CD3+CD28)-stimulated, 4; αδdex-stimulated, 5; (αδdex +CD3)-stimulated, 6; (αδdex +CD3+CD28)-stimulated, 7; HKD39-stimulated, 8; (HKD39+CD3)-stimulated, 9; (CD3+CD28+HKD39)-stimulated.

Activation of CD19+ B-cells was determined by quantifying CD86 (fig. 4.14i), CD25 (fig. 4.15i), and HLA-DR (fig. 4.16i) expression.
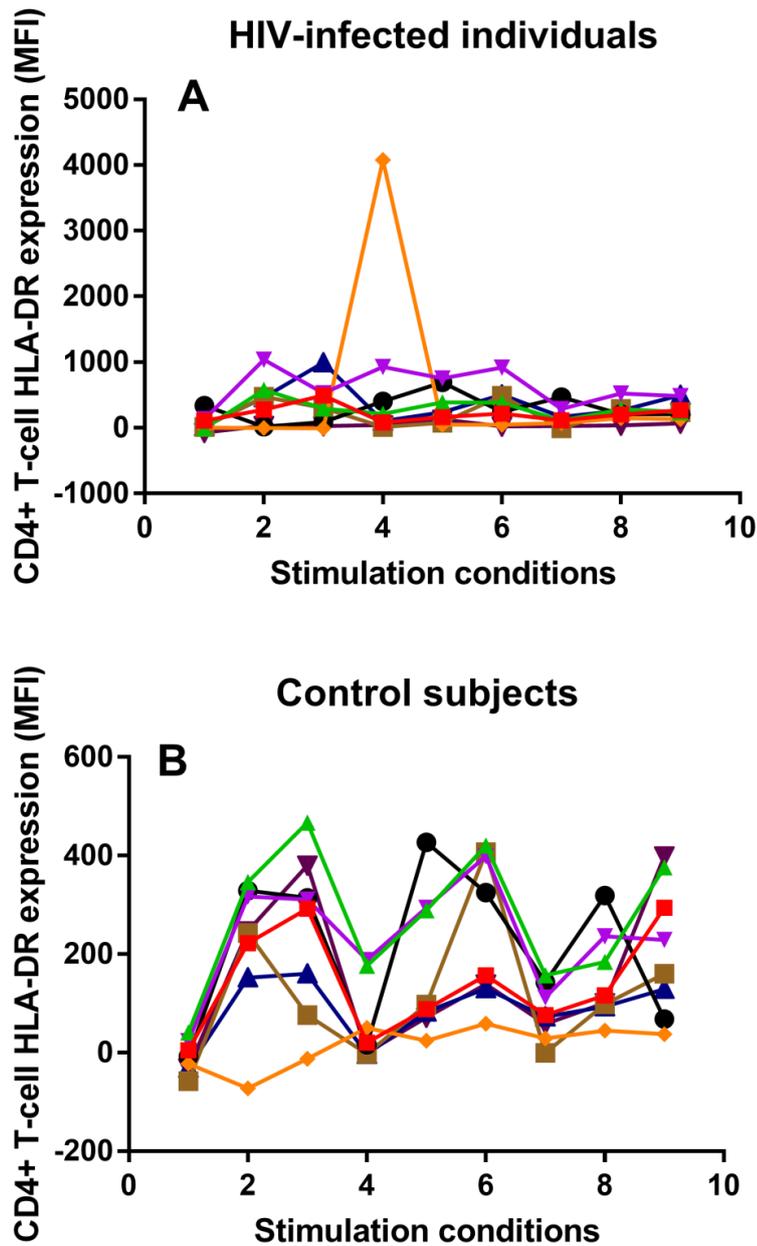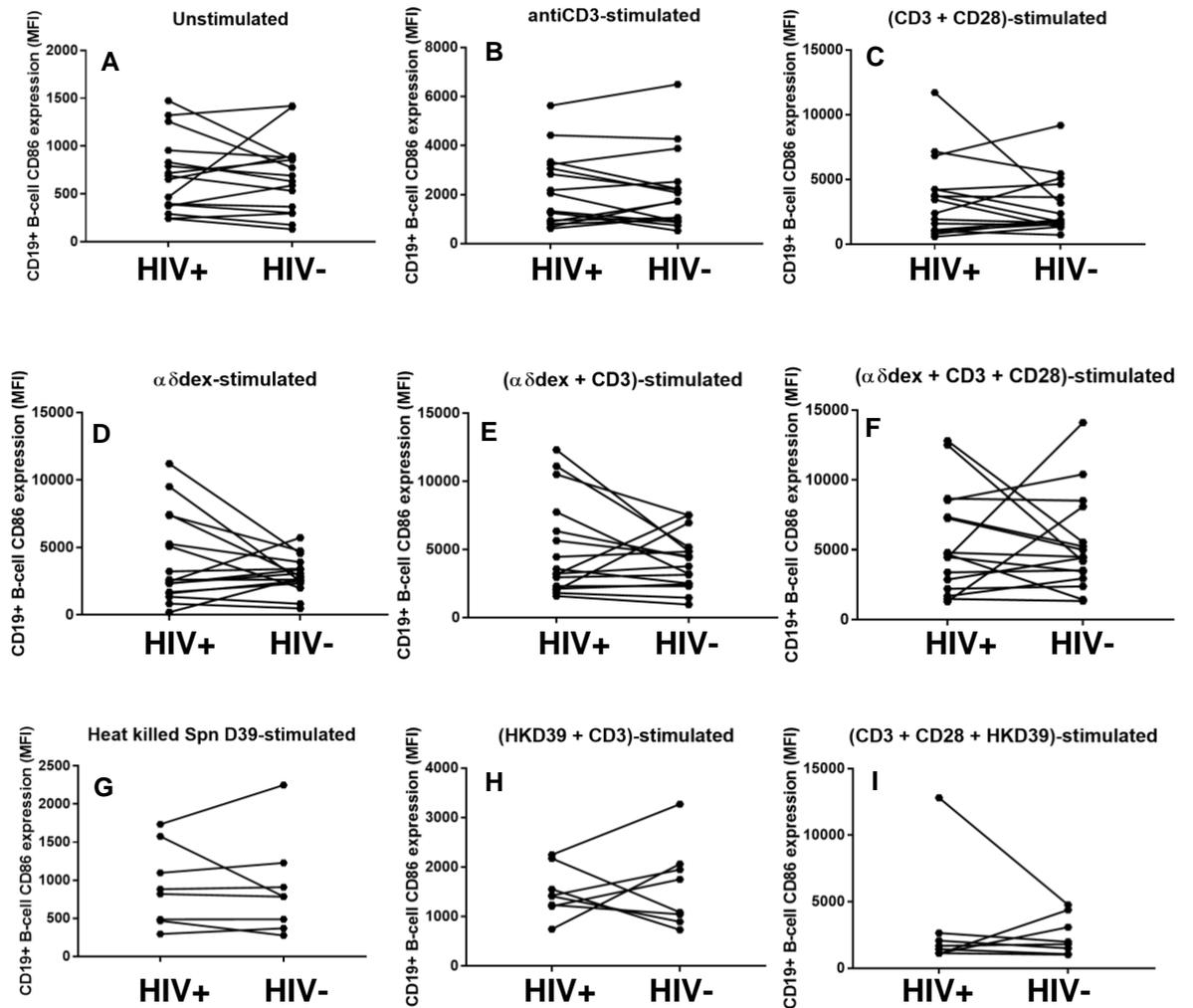
Figure 4.14i: CD86 expression on *in vitro* CD19+ B-cells in HIV-infected individuals and matched controls under un-stimulated and stimulated conditions. Dots and lines match each patient-control pair. The paired-samples *t*-test and Wilcoxon signed ranks test were used for parametric and non-parametric datasets respectively. (Patient n = 16 except for HKD39-stimulations, where patient n = 8). Concentrations of stimulants used: 1µg/ml of αδdex, 0.1µg/ml anti-CD3 alone, and 0.5µg/ml anti-CD3 in combination with 0.5µg/ml anti-CD28. Patient cohort and control cohort tracking data for this graph grid is presented in fig. 4.14ii.

Figure 4.14ii: Tracking data showing the changes in *in vitro* CD19+ B-cell CD86 expression in HIV-infected individuals (A) and matched controls (B) upon stimulation. Matched patient-control pairs are represented using the same colour across A and B. Conditions: 1; Un-stimulated, 2; CD3-stimulated, 3; (CD3+CD28)-stimulated, 4; αδdex-stimulated, 5; (αδdex +CD3)-stimulated, 6; (αδdex +CD3+CD28)-stimulated, 7; HKD39-stimulated, 8; (HKD39+CD3)-stimulated, 9; (CD3+CD28+HKD39)-stimulated.
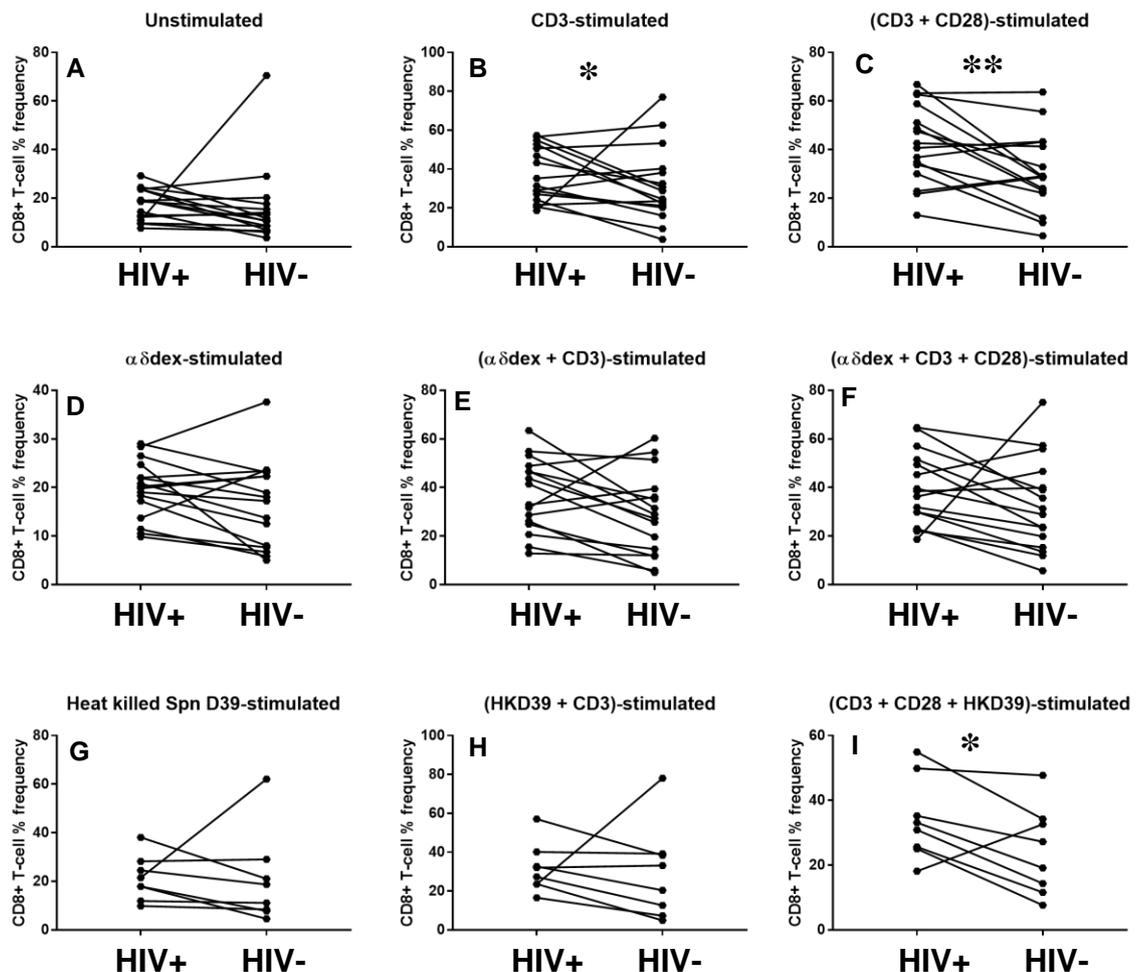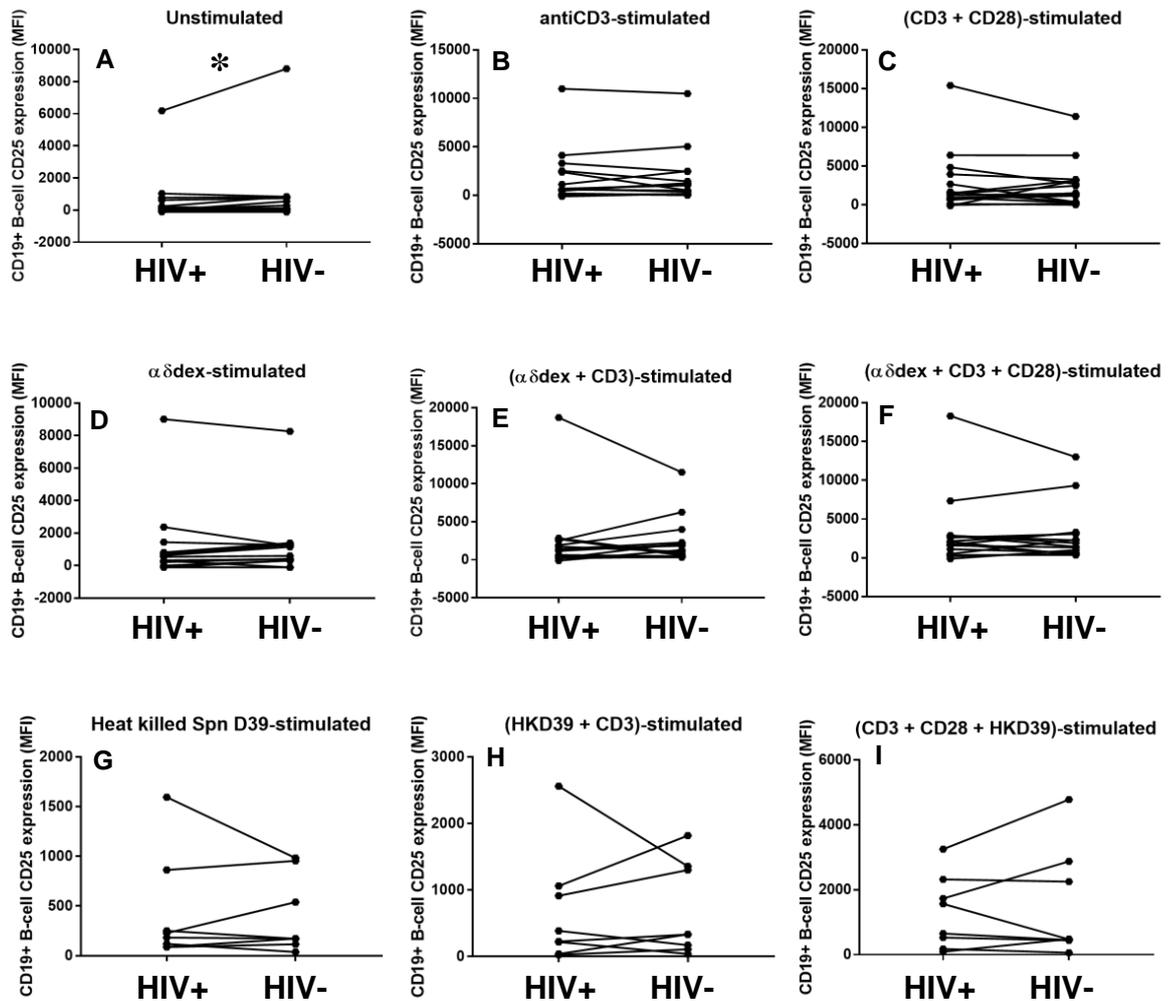
Figure 4.15i: CD25 expression on *in vitro* CD19+ B-cells in HIV-infected individuals and matched controls under un-stimulated and stimulated conditions. Dots and lines match each patient-control pair. The paired-samples *t*-test and Wilcoxon signed ranks test were used for parametric and non-parametric datasets respectively. (Patient n = 16 except for HKD39-stimulations, where patient n = 8; Where * $p \leq 0.050$). The significance seen in the un-stimulated control conditions (A) was likely due to the single outlier in the control group. Concentrations of stimulants used: 1µg/ml of αδdex, 0.1µg/ml anti-CD3 alone, and 0.5µg/ml anti-CD3 in combination with 0.5µg/ml anti-CD28. Patient cohort and control cohort tracking data for this graph grid is presented in fig. 4.15ii.
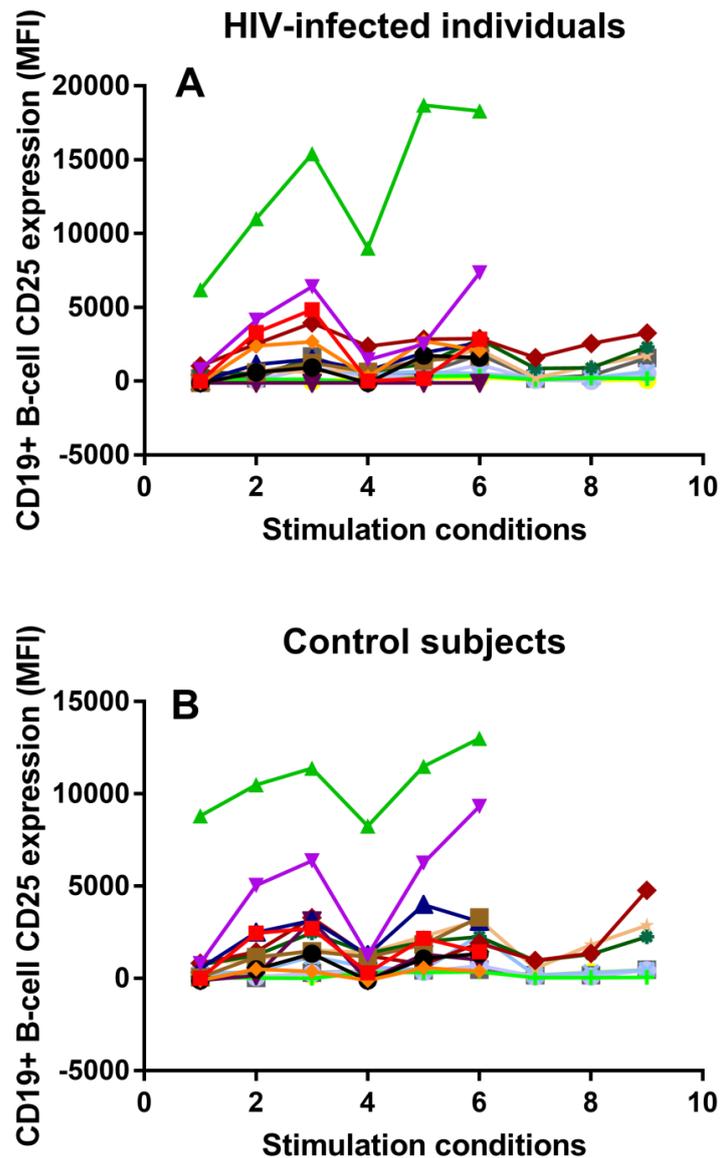
Figure 4.15ii: Tracking data showing the changes in *in vitro* CD19+ B-cell CD25 expression in HIV-infected individuals (A) and matched controls (B) upon stimulation. Matched patient-control pairs are represented using the same colour across A and B. Conditions: 1; Un-stimulated, 2; CD3-stimulated, 3; (CD3+CD28)-stimulated, 4; αδdex-stimulated, 5; (αδdex +CD3)-stimulated, 6; (αδdex +CD3+CD28)-stimulated, 7; HKD39-stimulated, 8; (HKD39+CD3)-stimulated, 9; (CD3+CD28+HKD39)-stimulated.

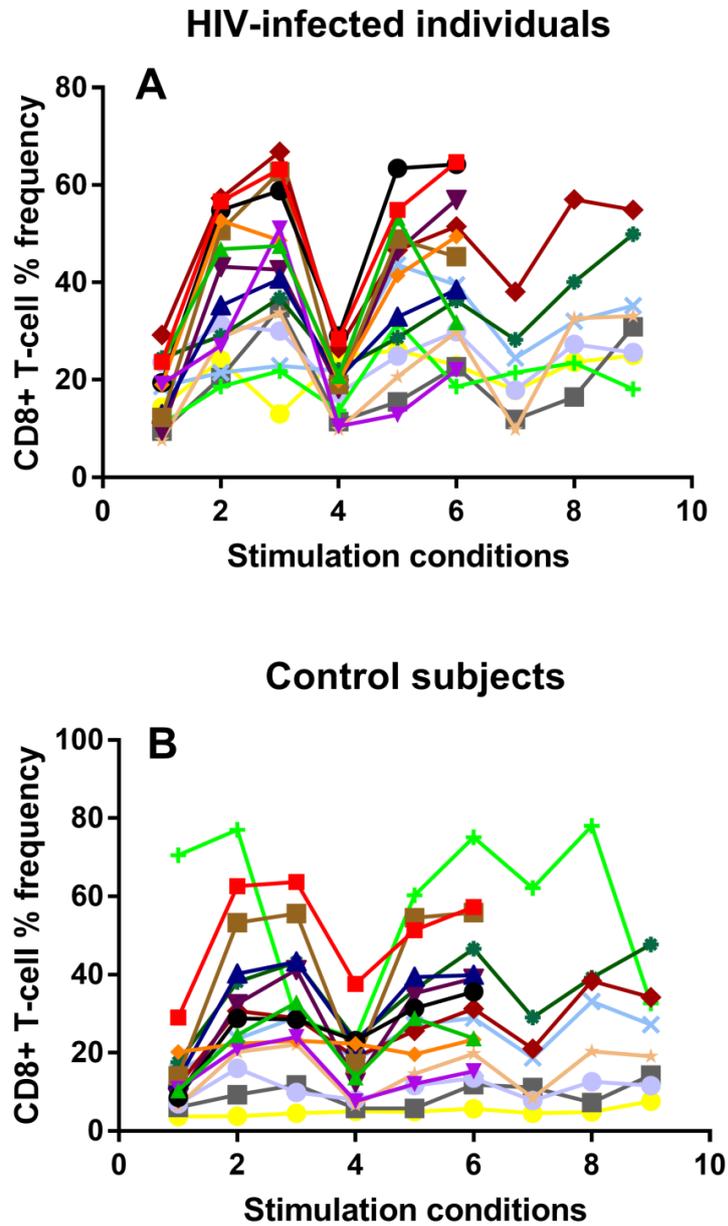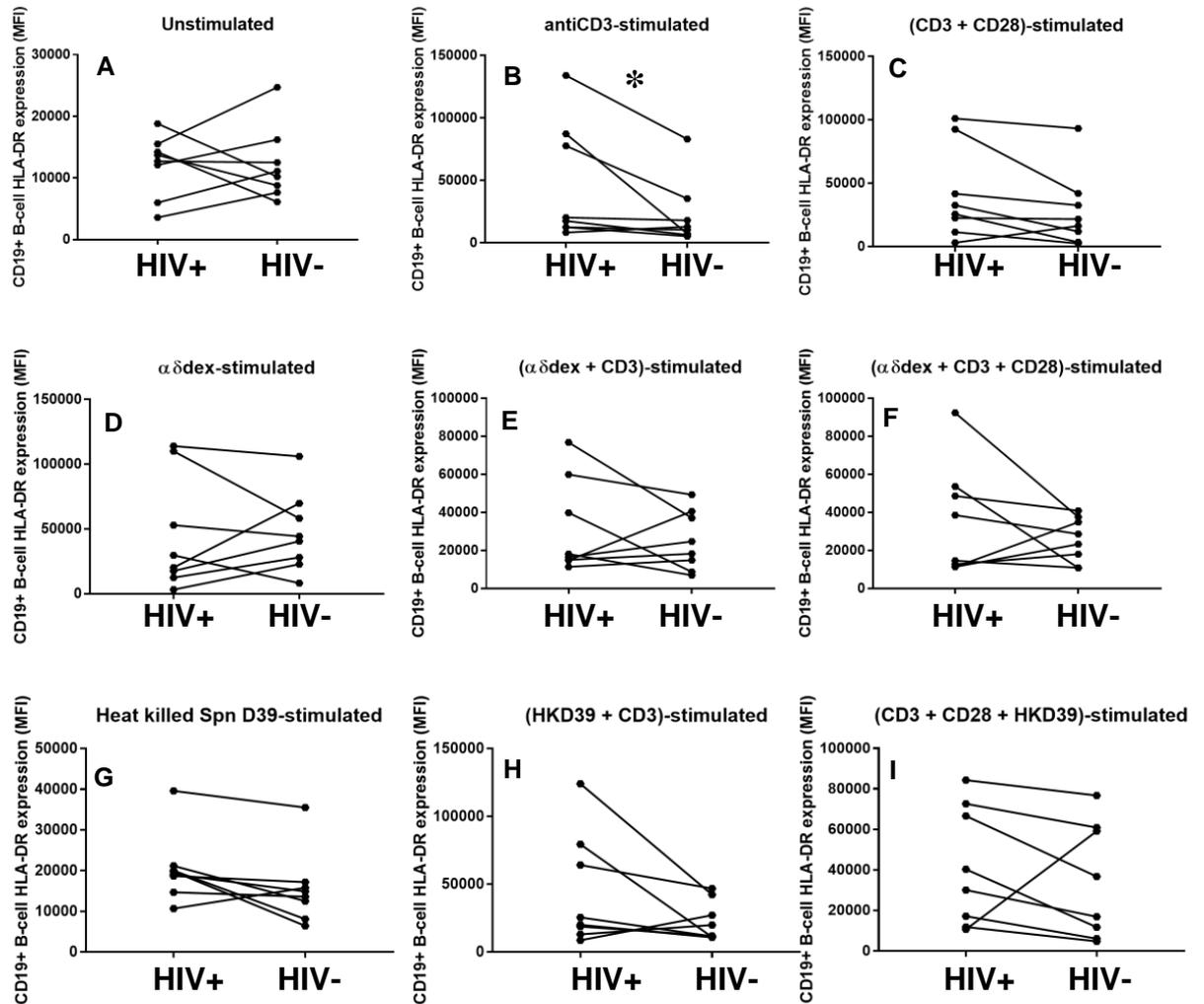**Fig 4.16i: HLA-DR expression on *in vitro* CD19+ B-cells in HIV-infected individuals and matched controls under un-stimulated and stimulated conditions.** Dots and lines match each patient-control pair. The paired-samples *t*-test and Wilcoxon signed ranks test were used for parametric and non-parametric datasets respectively. (Patient n = 16 except for HKD39-stimulations, where patient n = 8; Where * $p \leq 0.050$). Concentrations of stimulants used: 1μg/ml of αδdex, 0.1μg/ml anti-CD3 alone, and 0.5μg/ml anti-CD3 in combination with 0.5μg/ml anti-CD28. Patient cohort and control cohort tracking data for this graph grid is presented in fig. 4.16ii.

Figure 4.16ii: Tracking data showing the changes in *in vitro* CD19+ B-cell HLA-DR expression in HIV-infected individuals (A) and matched controls (B) upon stimulation. Matched patient-control pairs are represented using the same colour across A and B. Conditions: 1; Un-stimulated, 2; CD3-stimulated, 3; (CD3+CD28)-stimulated, 4; αδdex-stimulated, 5; (αδdex +CD3)-stimulated, 6; (αδdex +CD3+CD28)-stimulated, 7; HKD39-stimulated, 8; (HKD39+CD3)-stimulated, 9; (CD3+CD28+HKD39)-stimulated.

4.4 Discussion of Findings

4.4.1 Clinical characteristics of patient recruits

T- and B-cell *in vitro* responses to polyclonal and pneumococcal stimulation were studied in a cohort of 16 HIV-infected individuals with a mean age, CD4 count and total globulin count of 50.45, 677.63 /mm^3 and 27.38 g/L respectively (table 4.2). Responses investigated were confined to CD4+ and CD8+ T-cell, and CD19+ B-cell populations. Furthermore, these responses were compared to age-, sex- and ethnicity-matched HIV-uninfected controls, who were also matched to the patients in terms of date of bleed.

Except for one individual who had a viral detection blip within six months of participating in the study (patient 16; table 4.3), most of the patients had been virally-suppressed for a number of years. Thus, these individuals fell within the study inclusion criteria and had given consent prior to and on the day of bleeding. Most of the patient cohort comprised White males, while there were two Black females.

4.4.2 CD4+ T-cell responses in HIV-infected individuals compared to matched controls

CD4+ T-cells are known to be suppressed in HIV patients and CD8+ to be expanded (Margolick et al., 1993), and CD19+ B-cells to be hyperactivated (Moir and Fauci, 2009) with perturbations of B-cell subsets (Moir and Fauci, 2013). This knowledge necessitated a study into any differences in the percentage frequencies at which these cell populations occurred between the patients and controls. Only after this could the proliferation and activation responses of the T- and B-cells be analysed.

The percentage frequency of un-stimulated CD4+ T-cells in patients was significantly lower compared to controls ($p \leq 0.050$; fig. 4.4i A). Interestingly, while CD3-stimulation did not yield different responses between patients and controls (fig. 4.4i B), the addition of costimulatory anti-CD28 induced a higher

CD4+ T-cell percentage frequency in controls ($p \leq 0.050$; fig. 4.4i C). Another finding was that while αδdex-stimulation itself has no effect on CD4+ T-cell frequency, proliferation, or activation (chapter three: fig. 3.2 and 3.3), the controls had significantly higher CD4+ T-cell percentage frequency in the presence of αδdex, compared to patients ($p \leq 0.050$; fig. 4.4i D). Stimulation with HKD39 alone, and further with CD3 and CD28 (fig. 4.4i G, H, I) yielded comparable responses within the cohort. These results suggested that interpretation of any differences in CD4+ T-cell proliferation and activation responses for the un-stimulated, CD3- and CD28-costimulated and αδdex-stimulated conditions between patients and controls would have to be carried out with caution.

Indeed, un-stimulated and αδdex-stimulated CD4+ T-cell proliferation was significantly higher in controls compared to patients (both $p \leq 0.050$; fig. 4.5i D). As such a clear conclusion cannot be drawn as to whether this higher response was due to stimulation or merely due to the higher percentage of CD4+ T-cells present in controls *in vitro*. Further, the significantly higher CD4+ T-cell proliferation seen upon αδdex and CD3-stimulation ($p \leq 0.050$; fig. 4.4i E) was likely due to the single outlier control response.

CD3-stimulated hyperactivation (in terms of CD25 expression) has been shown *in vitro* in CD4+ T-cells of viraemic HIV-infected individuals off ART, with a weak negative correlation of CD25 expression to viral load ($p = 0.056$; Nicholas et al., 2013). While the patients in this study were virally-suppressed and on ART, they showed *in vitro* hyperactivation in CD4+ T-cells upon CD3-stimulation, in terms of up-regulated CD25 expression compared to controls ($p \leq 0.050$; fig. 4.6i B). Further, patients also had increased HLA-DR expression upon stimulation with αδdex alone ($p \leq 0.050$; fig. 4.7i D) and in combination with anti-CD3 ($p \leq 0.050$; fig. 4.6i E). These results suggest that in line with what is known about HIV patients having increased T-cell hyperactivation and exhaustion phenotypes (Haas et al., 2011, Okoye and Picker, 2013, Mauricio Rueda et al., 2012, Ott et al., 1997), *in vitro* hyperactivation still occurs in patients on HAART. Haas and colleagues (2011) already concluded that viral replication cannot be the sole

controller of T-cell hyperactivation in HIV patients. Indeed, results from this cohort of virally-suppressed individuals echo this conclusion.

4.4.3 CD8+ T-cell responses in HIV-infected individuals compared to matched controls

Patients had higher frequencies of CD8+ T-cells elicited by CD3-stimulation alone ($p \leq 0.050$; fig. 4.8i B), combined with CD28-costimulation ($p \leq 0.010$; fig. 4.8i C), and further with HKD39 ($p \leq 0.050$; fig. 4.8i I). Similar to the case with CD4+ T-cells (fig. 4.5i D), proliferation in CD8+ T-cells following αδdex-stimulation was significantly lower in patients compared to controls ($p \leq 0.050$; fig. 4.9i D). Proliferation following all other stimulations elicited comparable responses within the cohort (fig. 4.9i). The patients showed a strong hyperactivation response in CD8+ T-cells following stimulation with anti-CD3 alone ($p \leq 0.001$; fig. 4.10i B), combined with anti-CD28 ($p \leq 0.050$; fig. 4.10i C), and combined with HKD39 ($p \leq 0.050$; fig. 4.10i H). This hyperactivation also extended to CD8+ T-cell expression of HLA-DR in the patients compared to controls. Patients had higher levels of CD8+ HLA-DR expression upon stimulation with anti-CD3 alone ($p \leq 0.050$; fig. 4.11i B), combined with αδdex and CD28-costimulation ($p \leq 0.050$; fig. 4.11i F), and combined with HKD39 ($p \leq 0.050$; fig. 4.11i H).

The *in vitro* hyperactivation response in the patient CD8+ T-cells upon stimulation with anti-CD3 and HKD39 is noteworthy especially in light of the lack of a similar response to αδdex alone or combined with anti-CD3 for CD25 expression (fig. 4.10i D and E). Both αδdex and HKD39 are antigens recognised by the B-cell receptor (BCR). In the case of the former, polyclonal recognition ensures that the entire population of B-cells should be activated in a TI-type 2 manner by the polysaccharide antigen mimic. With the latter, only a specific population of class-switched B-cells with prior exposure to the *S. pneumoniae* capsular proteins would mount a response. Consequently, the stimulation conditions comprising both anti-CD3 and HKD39 showcase cognate interactions between the MHC class II molecule on the antigen-

presenting B-cell (Obukhanych and Nussenzweig, 2006), and the T-cell receptor (TCR) on the CD8+ T-cell thus, T-dependent antigen recognition. A limitation to the interpretation of these results is the absence of data detailing Streptococcal colonisation in the study cohort. Such data could have illuminated whether this HKD39-dependent *in vitro* hyperactivation in patient CD8+ T-cells was a true response, or merely as a coincidental result of the controls not being previously exposed to *S. pneumoniae*. Especially in light of adults having *S. pneumoniae* carriage rates of 3 – 4% (Mehr and Wood, 2012). Another factor confounding result interpretation is that the HKD39 stimulations in this study may not have been optimal. However, HKD39 on its own did not induce upregulation of either CD8+ T-cell CD25 or HLA-DR expression in a healthy study group (data not shown). It is thus likely that the HKD39-dependent results obtained from the patient group are indeed indicative of a true hyperactivation response.

The *in vitro* infection of human peripheral blood lymphocytes and stimulation of T-cell CD3 and CD28 receptors has been shown to lead to increased production of IL-2, of which the CD25 molecule is a receptor (Ott et al., 1997). Therefore, uncovering hyperactivation in CD4+ and CD8+ T-cell populations of HIV-infected individuals upon *in vitro* stimulation of CD3 and CD28 echo what has already been shown. The significance of these results is that hyperactivation persists *in vitro*, even with ART usage. Of greater interest in the present study were any differences within the *in vitro* CD19+ B-cell population in the patient cohort.

4.4.4 CD19+ B-cell responses in HIV-infected individuals compared to matched controls

The initial hypothesis of this study sought to uncover a defect primarily in the CD19+ B-cell responses in patients, compared to controls. Specifically, a hyperactivation response in B-cells of patients following IgD-stimulation using the polyclonal antigen mimic, αδdex, was expected. Finding such a defect may, in part, provide some explanation as to why even in the era of HAART

HIV-infected individuals still have a 35-fold increased relative risk of succumbing to IPD compared to their healthy counterparts (Heffernan et al., 2005).

Studying CD19+ B-cells after *in vitro* stimulation revealed comparable frequencies between patients and controls (fig. 4.12i). In terms of proliferation, only after stimulation with a combination of anti-CD3, anti-CD28 and HKD39 did patients show a significantly higher response compared to controls ($p \leq 0.050$; fig. 4.13i I). Activation in terms of CD86 (fig. 4.14i) and CD25 expression (fig. 4.15i) expression was also comparable within the cohort except for a seemingly higher CD25 expression response in controls under un-stimulated conditions (fig. 4.15i A). This was however likely due to a single control outlier response. Results in fig. 3.6 show that anti-CD3 significantly upregulates HLA-DR expression in CD19+ B cells of healthy individuals ($p \leq 0.010$; fig. 3.6). The present study also revealed a CD3-induced increase in *in vitro* HLA-DR expression in patients compared to controls ($p \leq 0.050$; fig. 4.16i B).

Because B-cell perturbations occur in HIV patients (Moir and Fauci, 2013), and αδdex-stimulation did not induce any hyper- or hypo-responsiveness in the overall CD19+ B-cell population in the patient group, we sought to determine if such polyclonal defects could be uncovered within B-cell subsets.

4.5 Conclusion

CD3-stimulated *in vitro* hyperactivation was shown in the CD4+ and CD8+ T-cells in HIV-infected individuals, indicating persistent *in vitro* hyperactivation even with ART usage. HKD39, in the presence of anti-CD3, also induced a hyperactivation response in the CD8+ T-cells of patients most likely due to increased cognate interactions with CD19+ B-cells. This was concluded because CD8+ T-cells themselves remain unaffected by HKD39 and further, the HKD39 did not stimulate hyperactivation in the CD19+ B-cells of patients. However, an increased proliferation response in patient CD19+ B-cells was uncovered upon stimulation with HKD39 in the presence of CD3-stimulation and CD28-costimulation of T-cells. In conclusion, hyperactivation responses to TCR and pneumococcal stimulation were uncovered in the T- and B-cells of a virally-suppressed cohort of 16 HIV-infected individuals with at least few years of ART-usage.

Because preliminary findings at the start of this project suggested αδdex-induced variation in B-cell responses between the HIV-infected individuals and the controls, CD19+ B-cell subsets which could potentially be responsible for these variations were investigated.

CHAPTER FIVE: B-CELL SUBSET RESPONSES IN HIV-INFECTED INDIVIDUALS FOLLOWING POLYCLONAL AND PNEUMOCOCCAL STIMULATION

5.1 Introduction

Ongoing HIV replication induces immune activation which, early on in the disease, drives perturbations of all major lymphocyte cell populations. Most of the knowledge gained about these dysregulations has been from peripheral blood. A focus on B-cell subsets could inform the development of an antibody-based HIV vaccine (Moir and Fauci, 2013). In the context of the present study, investigating B-cell subsets could provide some clues as to how the HIV-infected humoral immune response can be boosted specifically against pneumococcal disease.

B-cell subset perturbations in HIV are likely the cause for the ineffective antibody response to the virus and other antigens (Moir and Fauci, 2009). Additionally, these perturbations are not the result of new or different B-cell subsets in HIV, but rather an imbalance in B-cell subsets that would be present in healthy individuals of all ages to varying degrees (Moir and Fauci, 2013). These B-cell subsets are classed according to their encounters with antigen. Consequently, of all CD19+ B-cells, those that are CD10+ are immature/transitional. Furthermore, within the CD19+CD10- population, five subsets can be identified: Plasmablasts (PB), Activated-Memory (AM), Resting Memory (RM), naive, and Tissue-Like Memory (TLM) B-cells based on expression of CD20, CD21 and CD27 (Moir and Fauci, 2013).

The PB population is increased in HIV-viraemic patients (Moir and Fauci, 2013). HIV-viraemic patients also show premature exhaustion in the TLM subset (CD27^{neg}CD20^{hi}CD21^{lo}) compared to aviraemic patients and HIV-uninfected controls (Moir et al., 2008a). These TLMs from the peripheral blood of viraemic individuals expressed increased levels of Fc-receptor-like-4 (FCRL4). The FCRL4 protein is a putative inhibitory receptor with an unknown ligand, whose over-expression on tissue-like and classical memory B-cells in blood uniquely features in HIV infection. Moir et al (2008) further showed this FCRL4 to be increased on TLMs, compared to classical memory (CD27+) and naive B-cells (CD27^{neg}CD21^{hi}). In spite of specific B-cell

stimulus, the TLMs of viraemic individuals proliferated poorly *in vitro* (Moir et al., 2008).

The frequency distribution of these B-cell subsets has also been studied in the context of the HIV timeline: early and chronic infection, pre- and post-ART. Uninfected controls had higher baseline peripheral B-cell counts compared to early and chronic HIV-infected patients. ART usage increased B-cell counts in both patient groups (as is the case with CD4+ but not CD8+ T-cells (Moir et al., 2010)). With regards to the B-cell subset compartments present in each stage, early stage patients had higher baseline plasmablasts and resting memory B-cells compared to chronically-infected patients. Additionally, the chronic patients had higher levels of exhausted and immature/transitional B-cells. One year post-ART, the 'early' patients still had higher resting memory percentages compared to the chronic patients, indicating the necessity for an early ART initiation (Moir et al., 2010). Another study found a normalisation of B-cell subsets in 43 asymptomatic HAART-treated HIV patients (Fogli et al., 2012). Both these studies highlight that even within a cohort of HIV-infected individuals, B-cell subset compartments differ based on ART-usage.

An aberrant response due to B-cell perturbations in HIV patients is hyperactivation (Nicholas et al., 2013), resulting in over-expression of activation markers and hypergammaglobulinemia (De Milito, 2004). B-cells from HIV-infected samples are also primed for apoptosis (De Milito, 2004). Increased apoptosis in samples from HIV patients has also been reported when compared to controls (Samuelsson et al., 1997a, Samuelsson et al., 1997b), with memory B-cells of patients expressing increased Fas/Fas ligand (De Milito et al., 2001), Samuelsson et al., 1997b) and PD-1 (Nicholas et al., 2013). This study aimed not only to investigate potential hyperactivation in the B-cell subsets of the HIV-infected patient cohort, but also increased expression of apoptosis markers.

At the start of this project a flow cytometry panel was optimised to investigate the five CD19+CD10- B-cell subsets described by Moir and Fauci (2013) to

uncover which of the B-cell subsets in the HIV-infected cohort may be associated with aberrant responses to a polyclonal stimulus and/or pneumococci. Using CD10, CD20, CD21 and CD27 (Moir and Fauci, 2013, Wheatley et al., 2016) and a caspase probe, in addition to the optimised flow cytometry panel presented in chapter 2, B-cell subsets in the cohort were studied.

Therefore, data gathered and presented in this chapter had three aims: The first was to investigate any *in vitro* effects of culture on the frequency distribution and activation of B-cell subsets. Secondly, to quantify any *in vitro* differences in the proliferation and activation responses of HIV-infected B-cell subsets to the αδdex TI-type 2 antigen mimic and pneumococcal stimulation (with and without T-cell help), compared to age-, sex- and ethnicity-matched controls. Finally, to investigate differences in apoptosis levels between the patients and controls. Subsequently the decision was made to utilize a pan-caspase probe capable of detecting caspases-1, -2, -3, -6, -8, -9, and -10.

5.2 Methods

The HIV-infected cohort described in chapter four (sections 4.2.2 and 4.3) were used to study CD19+ B-cell subset responses to polyclonal and pneumococcal stimulation, compared to age-, sex- and ethnicity-matched controls. Clinical characteristics of this cohort were described in table 4.2. Table 5.1 outlines the workflow used for this portion of the study.

Table 5.1: Brief description of the workflow and outcome measures for results presented in chapter five.

Aim	Cell populations of interest and stimulations	Outcome measures	Results presented in †:	Study group number
Investigate the effects of culture and stimulation on the frequency distribution and activation of B-cell subsets in a healthy group.	Baseline and un-stimulated CD19+ B-cell subset responses, compared to responses after anti-IgD-stimulation using αδdex alone, and in combination with anti-CD3.	CD19+ B-cell frequency, and activation based on CD86 expression.	Tables 5.2 – 5.3	4
Investigate differences in HIV-infected and HIV-uninfected B-cell subset responses to polyclonal and pneumococcal stimulationl using αδdex- and *S. pneumoniae*-stimulation respectively.	CD19+ B-cell responses to αδdex and heat-killed D39 strain of *S. pneumoniae* (HKD39) both alone, and in combination with anti-CD3, and anti-CD3 + anti-CD28 respectively.	CD19+CD10- B-cell subset frequency, proliferation (based on CFSE median fluorescence intensity; MFI*), and activation (based on CD86 expression).	Fig. 5.3 – 5.10	Patient n = 12 (except for HKD39-stimulation, 2here n = 8)
Investigate differential apoptosis levels between patients and controls after polyclonal stimulation.	CD19+ B-cell responses to αδdex, compared to the un-stimulated control.	CD19+CD10- B-cell subset caspase+ frequency.	Fig. 5.11	Patient n = 5

*Due to a lower number of events per B-cell subset quadrant, the decision was made to quantify CFSE MFI rather than use proliferation index. Our group had previously ascertained that using CFSE MFI to describe the proliferation within a population of low cell count provided more accurate data than using proliferation index (data not shown). CFSE intensity is inversely proportional to proliferation (Evrard et al., 2010) due to undivided cell populations retaining the dye, and dye splitting evenly between proliferating cells (Lyons and Parish, 1994).
† All data was collected by Furaha Asani.

The cell populations of interest in this chapter were CD19+CD10- B-cell subsets namely: Plasmablasts (PB), Activated memory cells (AM), Resting memory cells (RM), Naive cells, and Tissue-like memory cells (TLM) described in fig. 5.1.
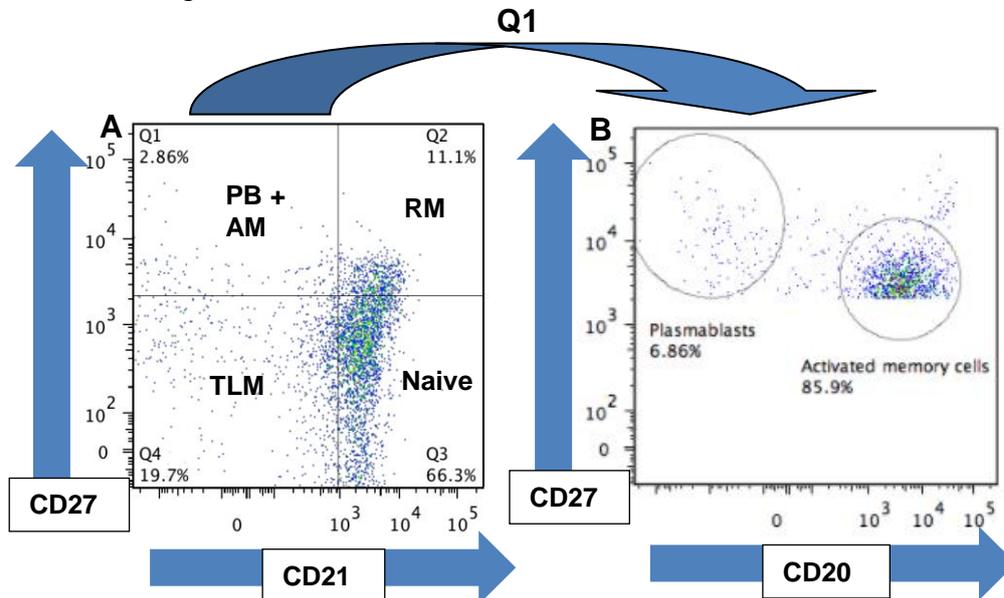
Figure 5.1: Gating strategy to separate B-cell subsets. Q1 comprises Plasmablasts (PB) and Activated Memory cells (AM), Q2; Resting Memory cells (RM), Q3; Naive B-cells, and Q4: Tissue-Like Memory cells (TLM) (A) (Moir and Fauci, 2013). The Q1 compartment was separated into PB and AM subsets using the CD20 marker (B). Thus, the Q1 compartment was always analysed prior to separating it into PB and AM populations. As indicated by the gates, PBs are CD27^{hi}CD21^{lo}CD20^{lo} while AMs are CD27^{int}CD21^{lo}CD20^{hi} (Moir and Fauci, 2013; Wheatley et al, 2016). Technical support in selecting PB and AM gates was provided by the Flow Cytometry Core Facility within the Sheffield Medical School.
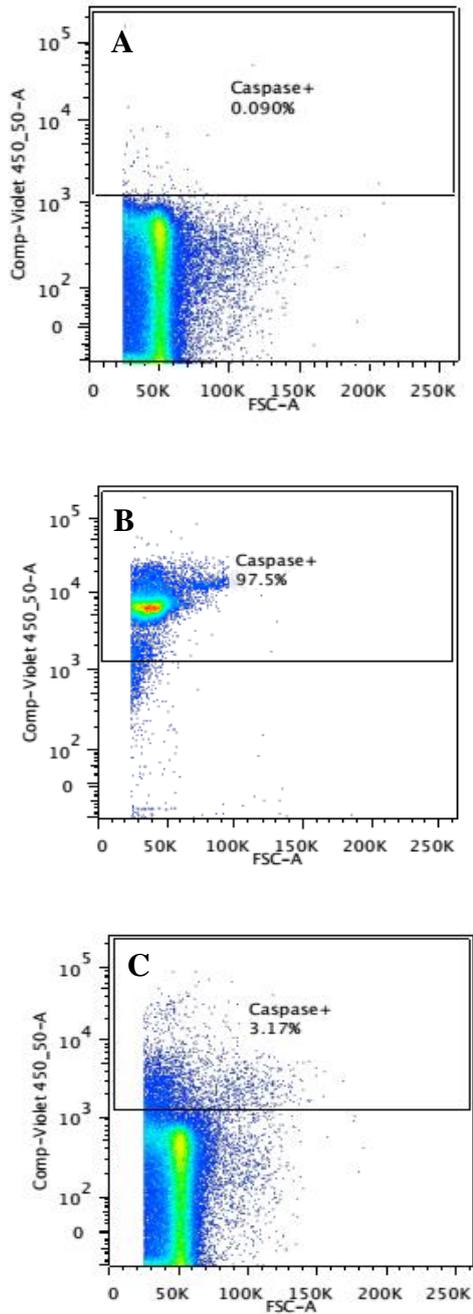
After gating on the populations of interest and quantifying proliferation and activation levels based on CFSE MFI and CD86 expression (chapter two; sections 2.4 and 2.7.3 respectively), Caspase detection was conducted by gating on Caspase-positive cells (fig. 5.2).

Figure 5.2: Gating strategy showing a CD19+CD10-Caspase+ population in a 20% ethonal-treated apoptosis positive control (B) and an un-stimulated control (C), relative to an unstained control (A).

5.3 Results

5.3.1 The effect of culture and stimulation on CD19+CD10- B-cell subset compartments

Prior to investigating differential B-cell subset responses between patients and controls, the effect culture and stimulation had on B-cell subsets from healthy controls was investigated. The inclusion of anti-CD3 and anti-CD28 to αδdex in one condition served the purpose of quantifying T-cell help to B-cell subsets (in addition to T-cell and B-cell proliferation/activation separately) (Foster et al., 2009, Foster et al., 2010, Darton et al., 2011, Wing et al., 2012, Preciado-Llanes et al., 2014).

The frequency distribution and CD86 expression levels were compared across four healthy individuals, for baseline (cells extracted from whole blood then processed through the flow cytometry protocol *ex vivo*; chapter two, on the same day), un-stimulated and stimulated conditions (both at 96 hr).

Stimulation concentrations used were as described in chapter 2: 1µg/ml of αδdex, 0.1µg/ml anti-CD3 alone, and 0.5µg/ml anti-CD3 in combination with 0.5µg/ml anti-CD28 for 96 hr. HKD39 MOI used was 10, for 96 hr. Stimulation conditions are indicated per figure on top of each graph.

Using the one-sample Kolmogorov-Smirnov test, some datasets presented in tables 5.2 and 5.3 were ascertained to contain both parametric and non-parametric datasets. Thus the paired-samples *t*-test and the Wilcoxon signed ranks test were respectively used for statistical analyses of these data. Comparisons were made between the *ex vivo* baseline and the 96 hr un-stimulated condition per individual (table 5.2), as well as the un-stimulated versus stimulated conditions (αδdex alone and with CD3-stimulated T-cell help) (table 5.3) per individual. The Q1 quadrant was analysed as a single population (fig. 5.1) before being analysed as its constituent B-cell subsets: plasmablasts (PB) and activated memory cells (AM).

Table 5.2: The effect of culture on the frequency distribution of B-cell subsets (n = 4). A 96 hr period of culture significantly reduced the frequency distribution of resting memory B-cells (p = 0.008). The frequency distribution of the rest of the B-cell subsets were unaffected by culture. Baseline and 96 hr un-stimulated conditions were paired per individual.

	B-cell subsets	Baseline Mean (Range)	96 hr un-stimulated Mean (Range)	p value
Frequency distribution (%)	Q1 compartment (Plasmablasts + Activated Memory cells)	9.35 (2.53 – 18.8)	21.7 (1.27 – 47)	0.465
	Plasmablasts	0.093 (0 – 0.37)	0.82 (0.05 – 2.13)	0.273
	Activated Memory	84.93 (67.1 – 98.7)	40.52 (6.96 – 73.8)	0.068
	Resting Memory	56.93 (46.2 – 72.3)	19.44 (2.58 – 37.7)	**0.008***
	Naive	27.83 (12.8 – 43.4)	30.5 (0.5 – 63)	0.923
	Tissue-like Memory	5.9 (3.04 – 10.2)	28.4 (2.88 – 56.6)	0.465

Table 5.3: The effect of stimulation on the frequency distribution of, and CD86 expression on, B-cell subsets (n = 4). Stimulation with αδdex significantly up-regulated CD86 expression in resting memory B-cells only. The 96 hr un-stimulated and stimulated conditions were paired per individual.

	B-cell subsets	Un-stimulated Mean (Range)	αδdex-stimulated Mean (Range)	*p* value	(αδdex + anti-CD3)-stimulated Mean (Range)	*p* value
Frequency distribution (%)	Q1 compartment (Plasmablasts + Activated Memory cells)	21.7 (1.27 – 47)	29.1 (1.85 – 56.5)	0.068	25.71 (1.33 – 51.7)	0.068
	Plasmablasts	0.82 (0.05 – 2.13)	0.1 (0.05 – 2.13)	0.715	1.23 (0 – 4.05)	0.465
	Activated Memory	40.52 (6.96 – 73.8)	34.65 (29.2 – 37)	0.465	29.2 (18.2 – 37.6)	0.465
	Resting Memory	19.44 (2.58 – 37.7)	39.2 (9.09 – 71.1)	0.074	36.5 (11.2 – 69.2)	0.081
	Naive	30.5 (0.5 – 63)	14.67 (2.47 – 32.2)	0.212	19.5 (3.76 – 41.8)	0.309
	Tissue-like Memory	28.4 (2.88 – 56.6)	17.02 (1.78 – 34.7)	0.068	18.31 (1.37 – 38.3)	0.068
CD86 expression (MFI)	Q1 compartment (Plasmablasts + Activated Memory cells)	75.83 (-109 – 274)	2269 (1250 – 4265)	0.067	1981 (851 – 3700)	0.062
	Plasmablasts	140.15 (90.6 – 196)	225.6 (0 – 877)	0.715	412.33 (0 – 1407)	1
	Activated Memory	208 (19.3 – 399)	2693.25 (873 – 6192)	0.068	2186.25 (841 – 3605)	0.068
	Resting Memory	653 (471 – 784)	1713.5 (1130 – 2267)	**0.022***	2995.5 (1558 – 5133)	0.064
	Naive	316.5 (111 – 580)	1857.5 (1298 – 2568)	0.068	4634.5 (2245 – 8949)	0.068
	Tissue-like Memory	-62.4 (-110 – 20)	2893.25 (1029 – 6706)	0.068	5112.75 (2439 – 11700)	0.068

Frequency distribution of the B-cell subsets remained unaffected by stimulation, compared to the 96 hr un-stimulated condition (table 5.3). This indicates that the frequency of most of the B-cell subsets remain constant across the stimulation conditions used in this portion of the project. Additionally, neither frequency distribution nor CD86 expression significantly

differed for any B-cell subsets between αδdex-stimulation alone, and with T-cell help.

Furthermore, the frequency distribution trend of B-cell subsets in the study group comprising HIV-infected individuals and matched controls (table 4.2) were compared to those in representative HIV-viraemic and HIV-negative individuals studied *ex vivo* by Moir and Fauci (2013). These comparisons are presented in table 5.4.

Table 5.4: Comparison of B-cell subset frequency distribution trends between the present study and Moir and Fauci's study (2013)

Increasing frequency	One HIV-viraemic individual (Moir and Fauci, 2013)	% frequency (Moir and Fauci, 2013)*	Mean from 12 ART-controlled HIV-infected individuals (Present study)	% frequency in present study°
↑	TLM	34	TLM	62.45
	Naive	34	Naive	27
	PB + AM	21	PB + AM	5.6
	RM	11	RM	5
Increasing frequency	One HIV-negative individual (Moir and Fauci, 2013)	% frequency (Moir and Fauci, 2013)*	Mean from 12 HIV-uninfected individuals (Present study)	% frequency in present study°
↑	Naive	66	TLM	62
	RM	28	Naive	24.9
	PB + AM	3.4	PB + AM	6.7
	TLM	2.6	RM	6.3

*Studies carried out *ex vivo*.

°Studies carried out 96 hr post-culture.

Differences in the frequency distribution seen between the Moir and Fauci study and the present study (table 5.4) are likely due to: 1. The different timeline at which cells were harvested (baseline versus 96 hr post-culture); 2. Only one individual per patient and control group being investigated in the Moir and Fauci study, versus 12 per group in the present study, and; 3. The patient being viraemic in the Moir and Fauci study, versus the cohort in the present study being ART-controlled and virally suppressed.

5.3.2 Differences in B-cell subsets between HIV-infected individuals and matched controls after polyclonal and pneumococcal stimulation

Using the one-sample Kolmogorov-Smirnov test, some datasets presented in figures 5.3 to 5.11 were ascertained to contain both parametric and non-parametric datasets. Thus the paired-samples *t*-test and the Wilcoxon signed ranks test were respectively used for statistical analyses of these data. Pair-wise comparisons between HIV-infected individuals and age-, sex- and ethnicity-matched HIV-negative controls were conducted. The *p* values shown are two-tailed, testing for differences in both directions. Paired data are presented as spot-line graphs not only to show differences between HIV-infected individuals and matched controls, but inter-pair variations. Shaded circles represent one individual, with a line connecting matched patient-control pairs. The graph grid is organised to facilitate comparisons across rows and down columns, with the un-stimulated condition presented first. (Patient n = 12 except for HKD39-stimulations, where patient n = 8 and Caspase detection, where patient n = 5). Each graph grid is accompanied by line graphs tracking patient cohort and control cohort responses separately, to facilitate visualisation of how individuals responded to the different stimulation conditions.

The proliferation (CFSE MFI) of the Q1 compartment comprising plasmablasts (PB) and activated memory cells (AM) was investigated (fig. 5.3i).
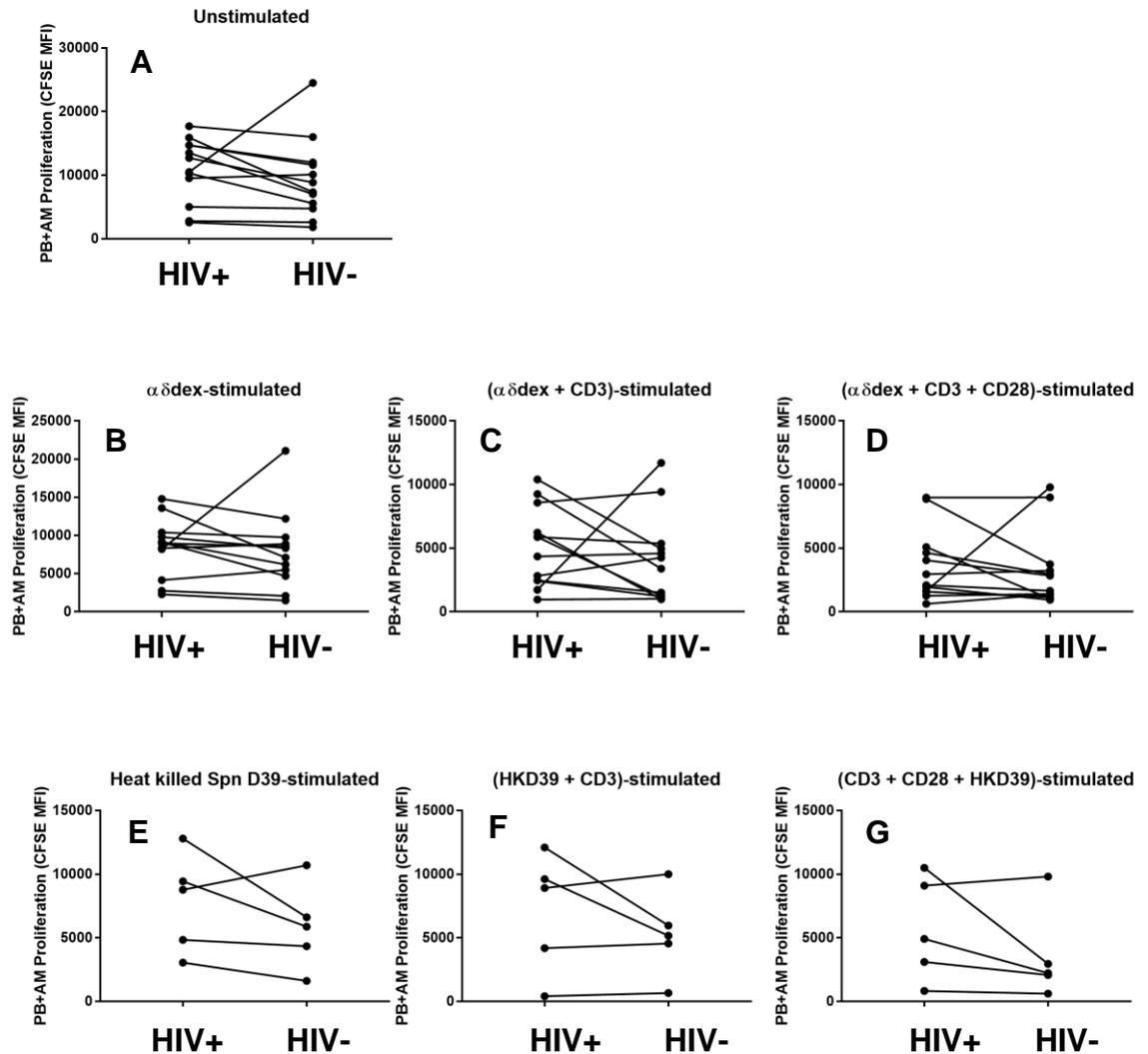
Figure 5.3i: Proliferation of *in vitro* Plasmablasts and Activated Memory B-cells in HIV-infected individuals and matched controls under un-stimulated and stimulated conditions. Dots and lines match each patient-control pair. The paired-samples *t*-test and Wilcoxon signed ranks test were used for parametric and non-parametric datasets respectively. (Patient n = 12 except for HKD39-stimulations, where patient n = 5). Concentrations of stimulants used: 1µg/ml of αδdex, 0.1µg/ml anti-CD3 alone, and 0.5µg/ml anti-CD3 in combination with 0.5µg/ml anti-CD28. Patient cohort and control cohort tracking data for this graph grid is presented in fig. 5.3ii.

Figure 5.3ii: Tracking data showing the changes in *in vitro* Plasmablast and Activated Memory B-cell proliferation in HIV-infected individuals (A) and matched controls (B) upon stimulation. Matched patient-control pairs are represented using the same colour across A and B. Conditions: 1; Un-stimulated, 2; CD3-stimulated, 3; (CD3+CD28)-stimulated, 4; αδdex-stimulated, 5; (αδdex +CD3)-stimulated, 6; (αδdex +CD3+CD28)-stimulated, 7; HKD39-stimulated, 8; (HKD39+CD3)-stimulated, 9; (CD3+CD28+HKD39)-stimulated.

CD86 expression on the B-cell subsets within the Q1 compartment was investigated next, revealing differences between the patients and controls (fig. 5.4i).
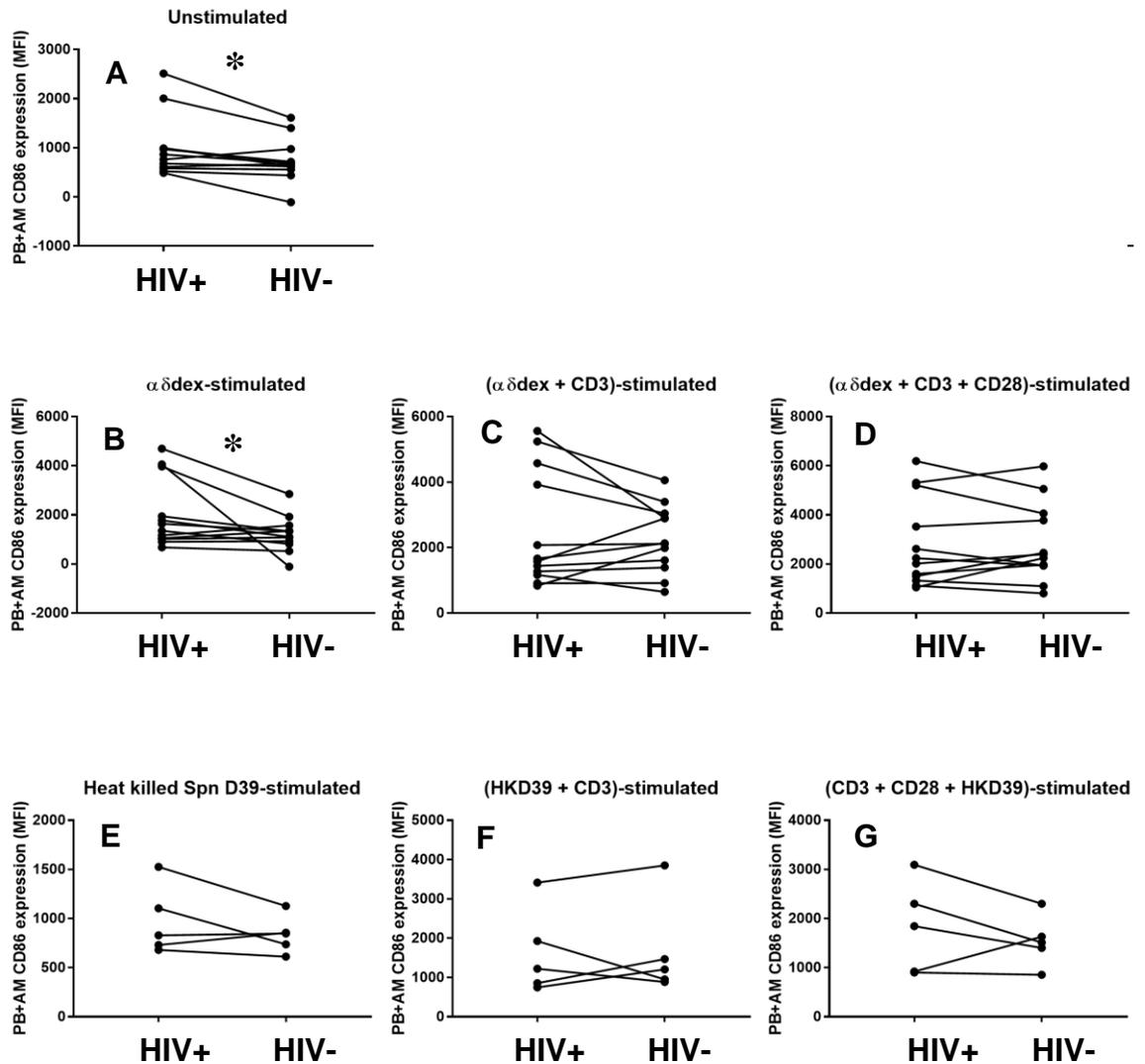
Figure 5.4i: CD86 expression on *in vitro* Plasmablasts and Activated Memory B-cells in HIV-infected individuals and matched controls under un-stimulated and stimulated conditions. Dots and lines match each patient-control pair. The paired-samples *t*-test and Wilcoxon signed ranks test were used for parametric and non-parametric datasets respectively. (Patient n = 12 except for HKD39-stimulations, where patient n = 5; Where * $p \leq 0.050$). Concentrations of stimulants used: 1µg/ml of αδdex, 0.1µg/ml anti-CD3 alone, and 0.5µg/ml anti-CD3 in combination with 0.5µg/ml anti-

CD28. Patient cohort and control cohort tracking data for this graph grid is presented in fig. 5.4ii.

Figure 5.4ii: Tracking data showing the changes in *in vitro* Plasmablast and Activated Memory B-cell CD86 expression in HIV-infected individuals (A) and matched controls (B) upon stimulation. Matched patient-control pairs are represented using the same colour across A and B. Conditions: 1; Un-stimulated, 2; CD3-stimulated, 3; (CD3+CD28)-stimulated, 4; αδdex-stimulated, 5; (αδdex +CD3)-stimulated, 6; (αδdex +CD3+CD28)-stimulated, 7; HKD39-stimulated, 8; (HKD39+CD3)-stimulated, 9; (CD3+CD28+HKD39)-stimulated.

In order to ascertain which of the two populations (PB or AM) was responsible for the higher *in vitro* activation responses uncovered in patients in the Q1 compartment, PBs and AMs were separated based on the CD20 marker (fig. 5.1 B). PBs were analysed first for proliferation (fig. 5.5i).
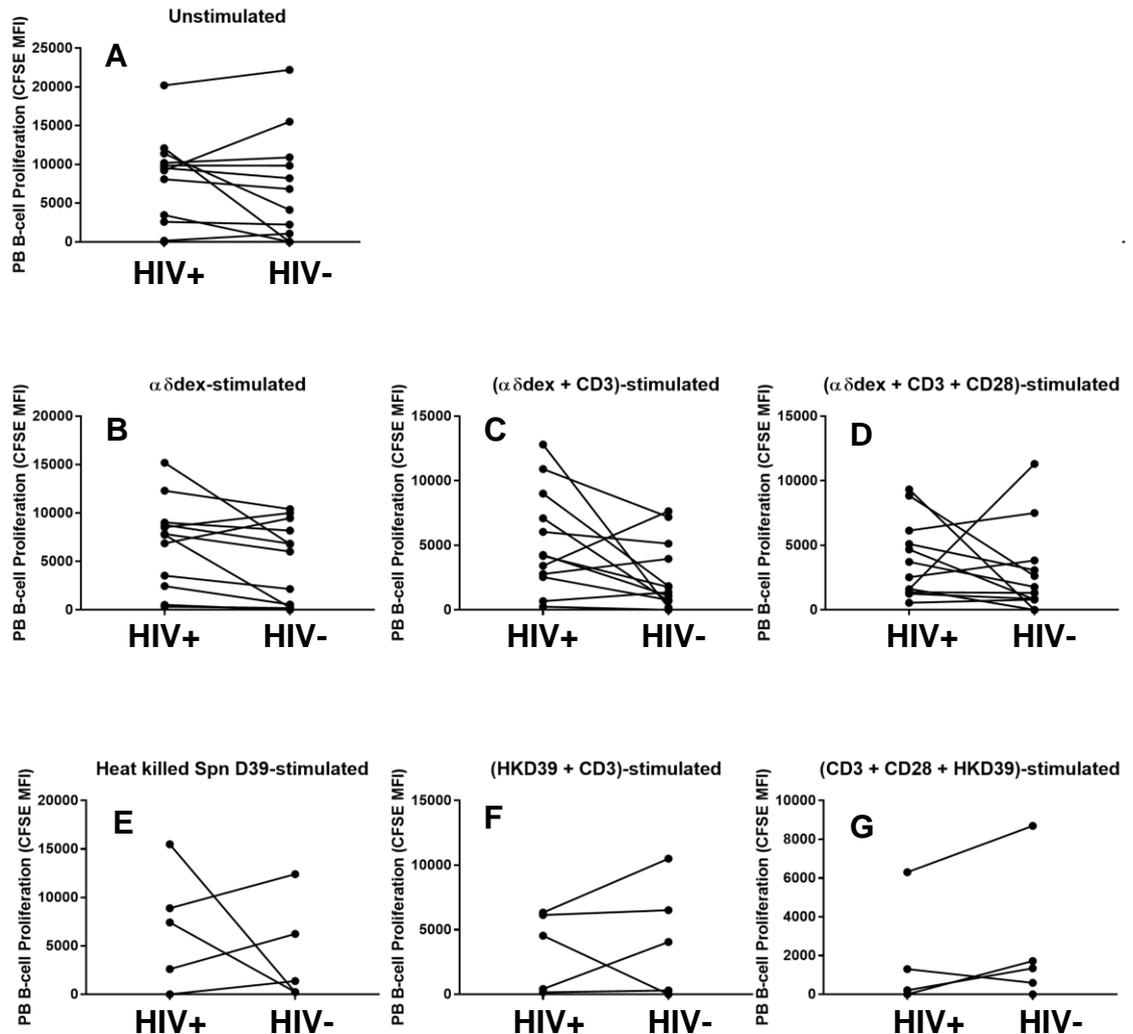
Figure 5.5i: Proliferation of *in vitro* Plasmablasts in HIV-infected individuals and matched controls under un-stimulated and stimulated conditions. Dots and lines match each patient-control pair. The paired-samples *t*-test and Wilcoxon signed ranks test were used for parametric and non-parametric datasets respectively. (Patient n = 12 except for HKD39-stimulations, where patient n = 5). Concentrations of stimulants used: 1μg/ml of αδdex, 0.1μg/ml anti-CD3 alone, and 0.5μg/ml anti-CD3 in combination with 0.5μg/ml anti-CD28. Patient cohort and control cohort tracking data for this graph grid is presented in fig. 5.5ii.

Figure 5.5ii: Tracking data showing the changes in *in vitro* Plasmablast proliferation in HIV-infected individuals (A) and matched controls (B) upon stimulation. Matched patient-control pairs are represented using the same colour across A and B. Conditions: 1; Un-stimulated, 2; CD3-stimulated, 3; (CD3+CD28)-stimulated, 4; αδdex-stimulated, 5; (αδdex +CD3)-stimulated, 6; (αδdex +CD3+CD28)-stimulated, 7; HKD39-stimulated, 8; (HKD39+CD3)-stimulated, 9; (CD3+CD28+HKD39)-stimulated.

However, αδdex-stimulation of the PB B-cell subset uncovered greater activation in PB B-cells from HIV-infected patients (fig. 5.6i).
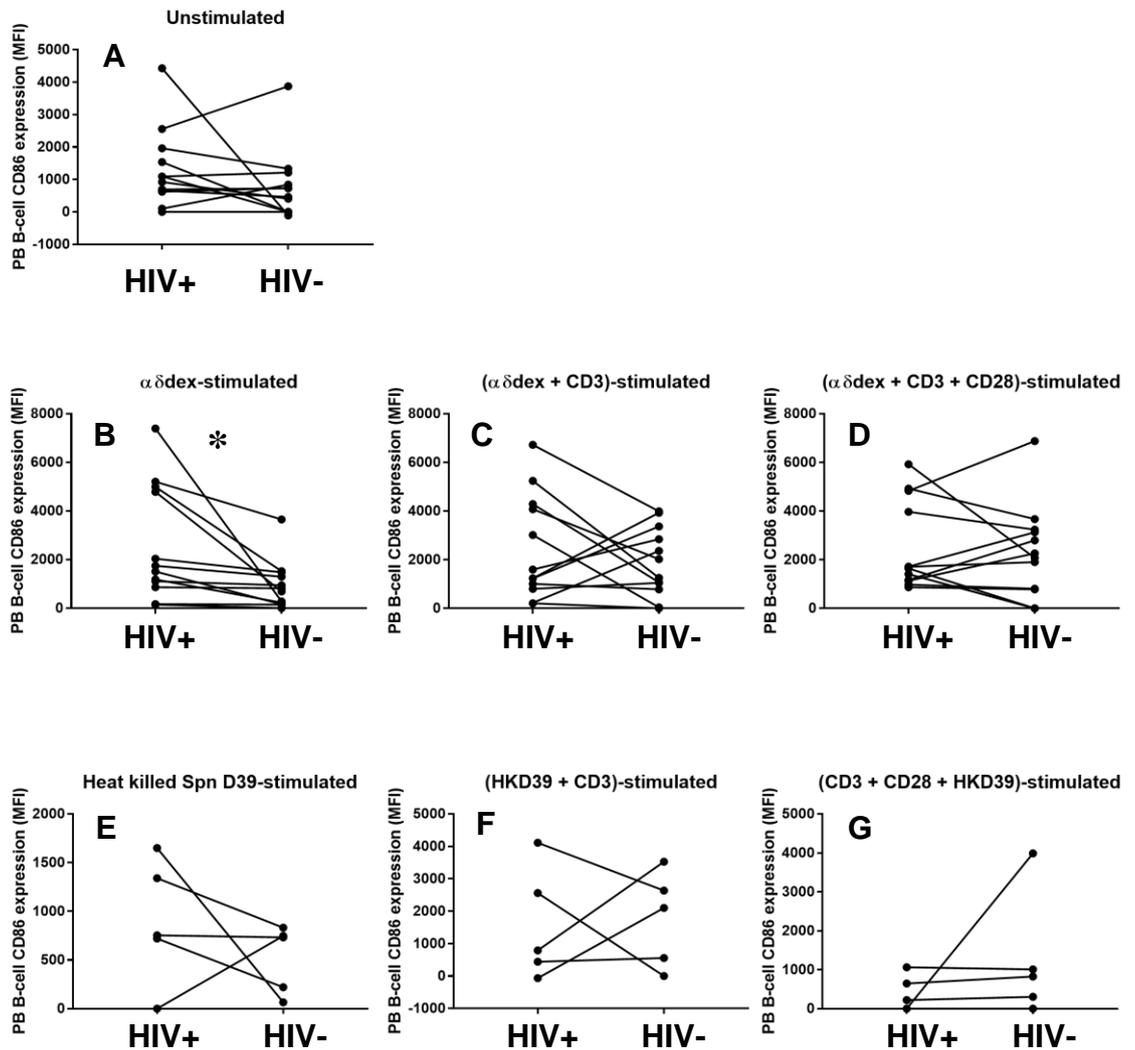
Figure 5.6i: CD86 expression on *in vitro* in HIV-infected individuals and matched controls under un-stimulated and stimulated conditions. Thus the PB subset was most likely responsible for the hyperactivation signal seen in the Q1 compartment comprising PBs and AMs, in fig. 5.9i D. Dots and lines match each patient-control pair. The paired-samples *t*-test and Wilcoxon signed ranks test were used for parametric and non-parametric datasets respectively. (Patient n = 12 except for HKD39-stimulations, where patient n = 5; Where * $p \leq 0.050$). Concentrations of stimulants used: 1µg/ml of αδdex, 0.1µg/ml anti-CD3 alone, and 0.5µg/ml anti-CD3 in combination

with 0.5µg/ml anti-CD28. Patient cohort and control cohort tracking data for this graph grid is presented in fig. 5.6ii.
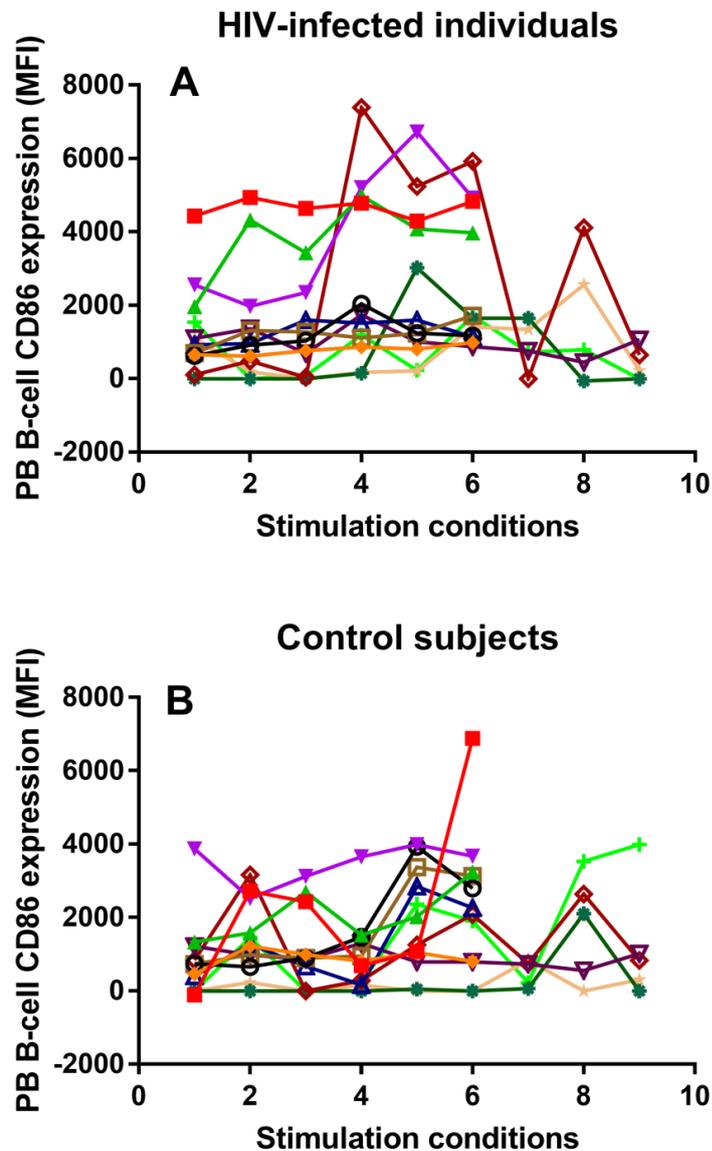
Figure 5.6ii: Tracking data showing the changes in *in vitro* Plasmablast CD86 expression in HIV-infected individuals (A) and matched controls (B) upon stimulation. Matched patient-control pairs are represented using the same colour across A and B. Conditions: 1; Un-stimulated, 2; CD3-stimulated, 3; (CD3+CD28)-stimulated, 4; αδdex-stimulated, 5; (αδdex +CD3)-stimulated, 6; (αδdex +CD3+CD28)-stimulated, 7; HKD39-stimulated, 8; (HKD39+CD3)-stimulated, 9; (CD3+CD28+HKD39)-stimulated.

The AM subset was investigated next, and no significant differences were found between patients and controls in terms of proliferation (fig. 5.7i).
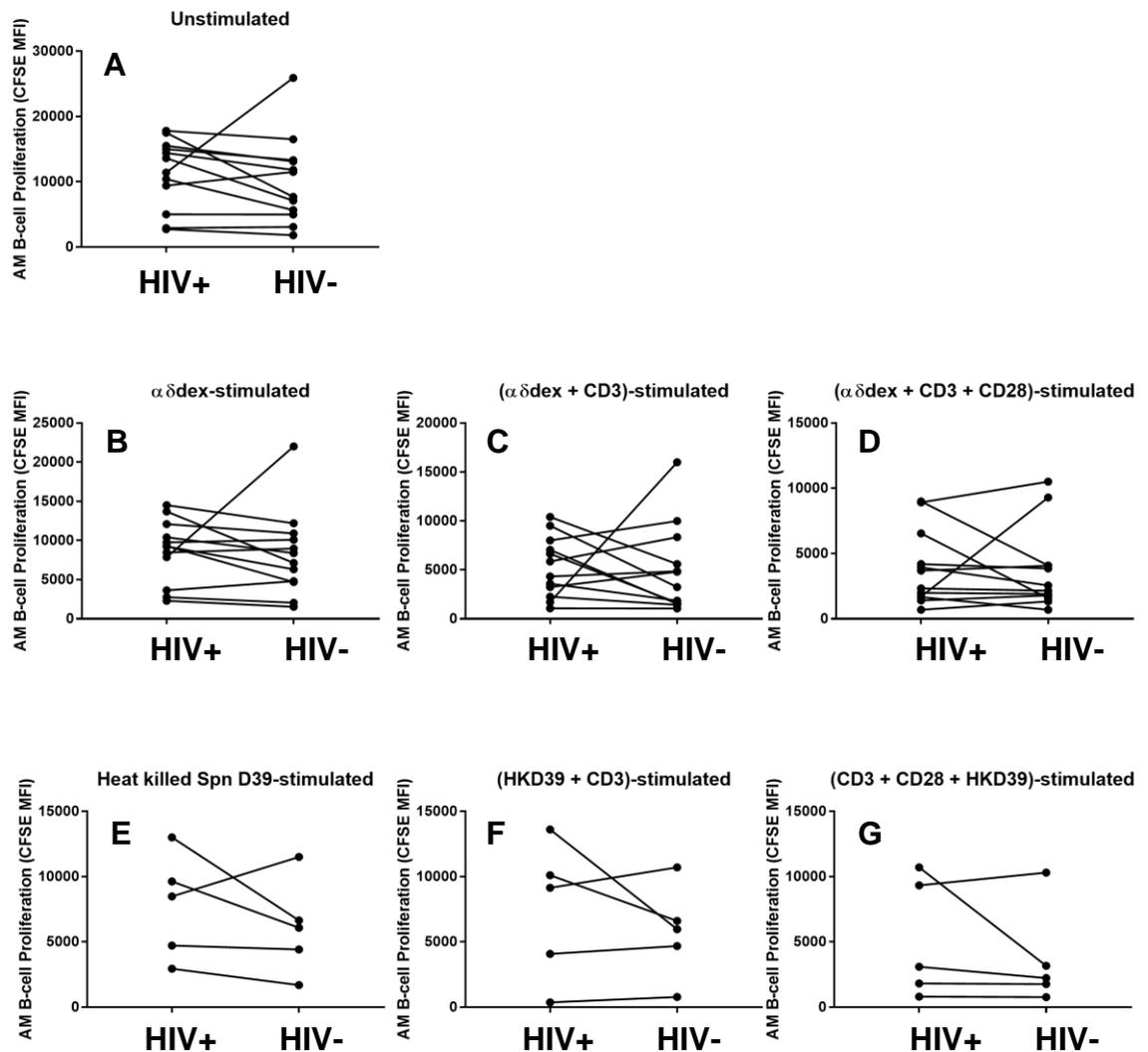
Figure 5.7i: Proliferation of *in vitro* **Activated Memory B-cells in HIV-infected individuals and matched controls under un-stimulated and stimulated conditions.** Dots and lines match each patient-control pair. The paired-samples *t*-test and Wilcoxon signed ranks test were used for parametric and non-parametric datasets respectively. (Patient n = 12 except for HKD39-stimulations, where patient n = 5). Concentrations of stimulants used: 1µg/ml of αδdex, 0.1µg/ml anti-CD3 alone, and 0.5µg/ml anti-CD3 in combination with 0.5µg/ml anti-CD28. Patient cohort and control cohort tracking data for this graph grid is presented in fig. 5.7ii.
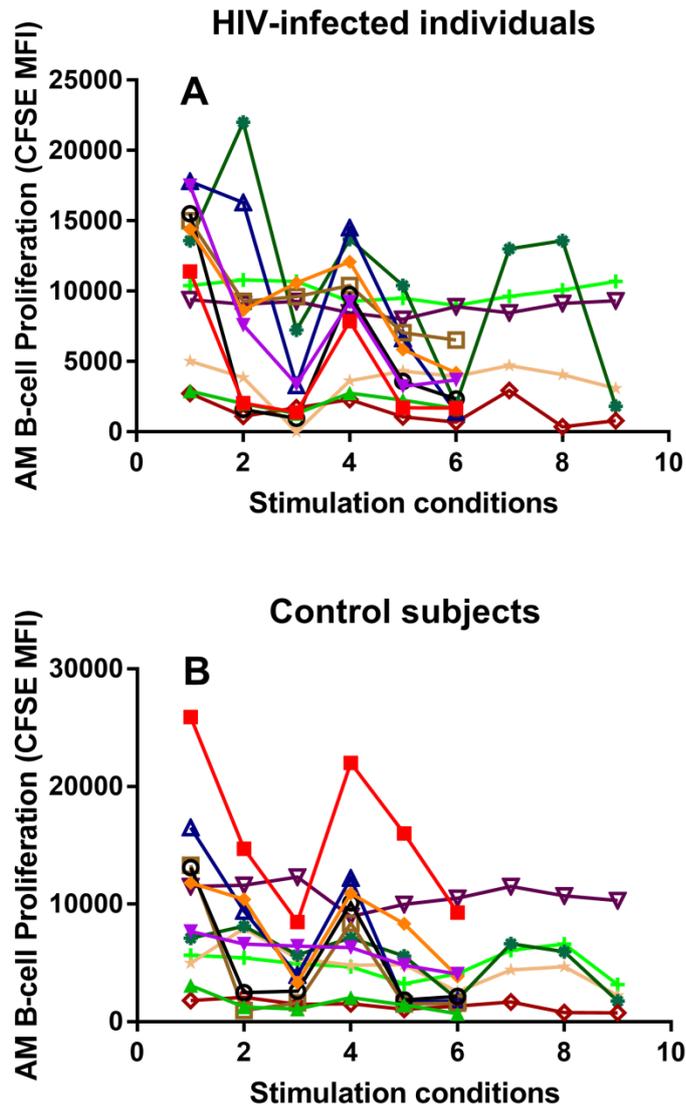
Figure 5.7ii: Tracking data showing the changes in *in vitro* Activated Memory B-cell proliferation in HIV-infected individuals (A) and matched controls (B) upon stimulation. Matched patient-control pairs are represented using the same colour across A and B. Conditions: 1; Un-stimulated, 2; CD3-stimulated, 3; (CD3+CD28)-stimulated, 4; αδdex-stimulated, 5; (αδdex +CD3)-stimulated, 6; (αδdex +CD3+CD28)-stimulated, 7; HKD39-stimulated, 8; (HKD39+CD3)-stimulated, 9; (CD3+CD28+HKD39)-stimulated.

172

Investigating CD86 expression revealed that the AM subset in patients (fig. 5.8i) was responsible for the un-stimulated hyperactivation response seen in the Q1 compartment (fig. 5.4i).
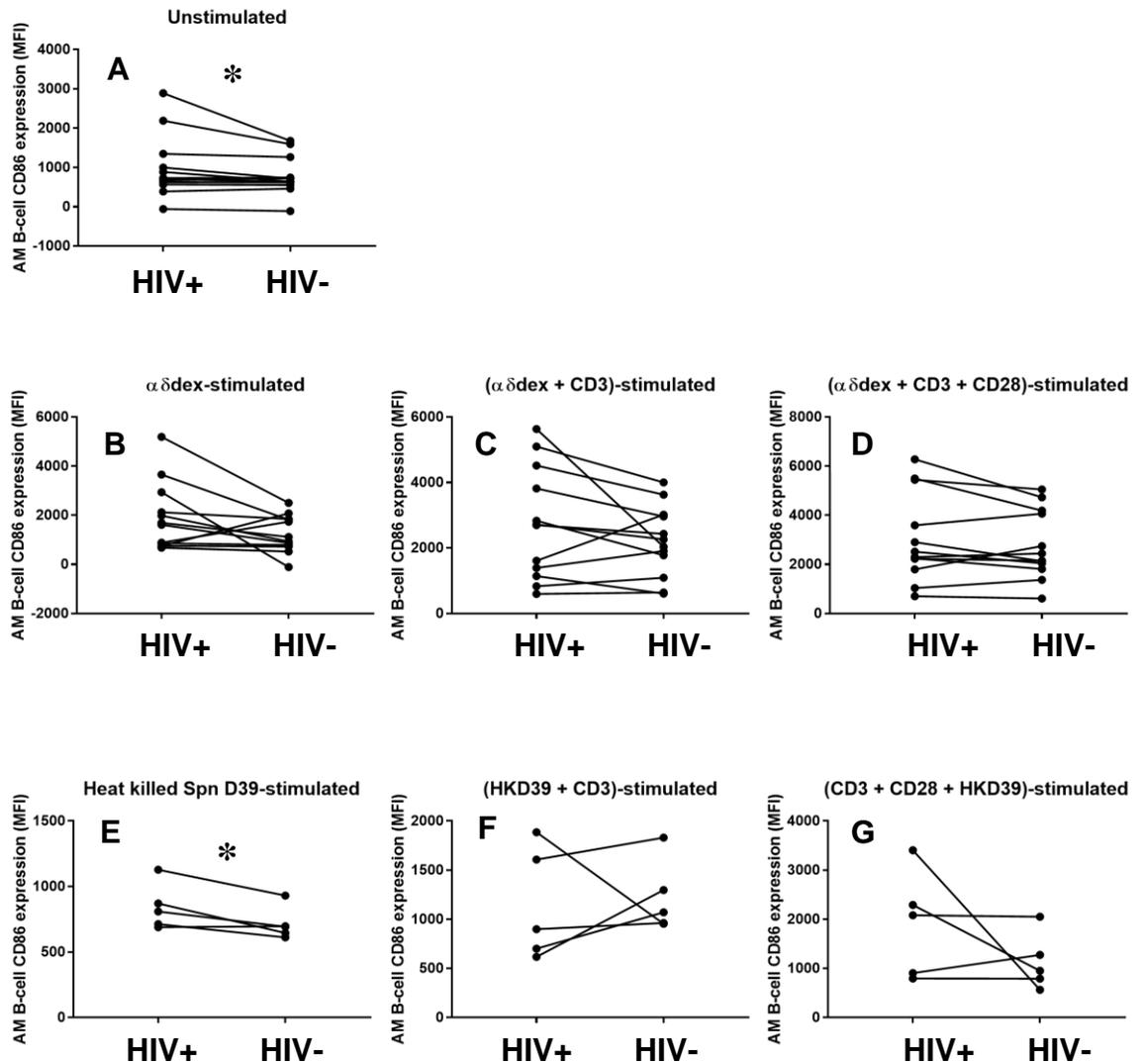
Figure 5.8i: CD86 expression on *in vitro* Activated Memory B-cells in HIV-infected individuals and matched controls under un-stimulated and stimulated conditions. Further, activated memory cells were determined to be the subset giving off the higher activation signal in the un-stimulated condition (A) seen in patients in the Q1 compartment (fig. 5.9i). Dots and lines match each patient-control pair. The paired-samples *t*-test and Wilcoxon signed ranks test were used for parametric and non-parametric datasets respectively. (Patient n = 12 except for HKD39-stimulations, where patient n = 5; Where * $p \leq 0.050$). Concentrations of stimulants used: 1µg/ml

of αδdex, 0.1μg/ml anti-CD3 alone, and 0.5μg/ml anti-CD3 in combination with 0.5μg/ml anti-CD28. Patient cohort and control cohort tracking data for this graph grid is presented in fig. 5.8ii.
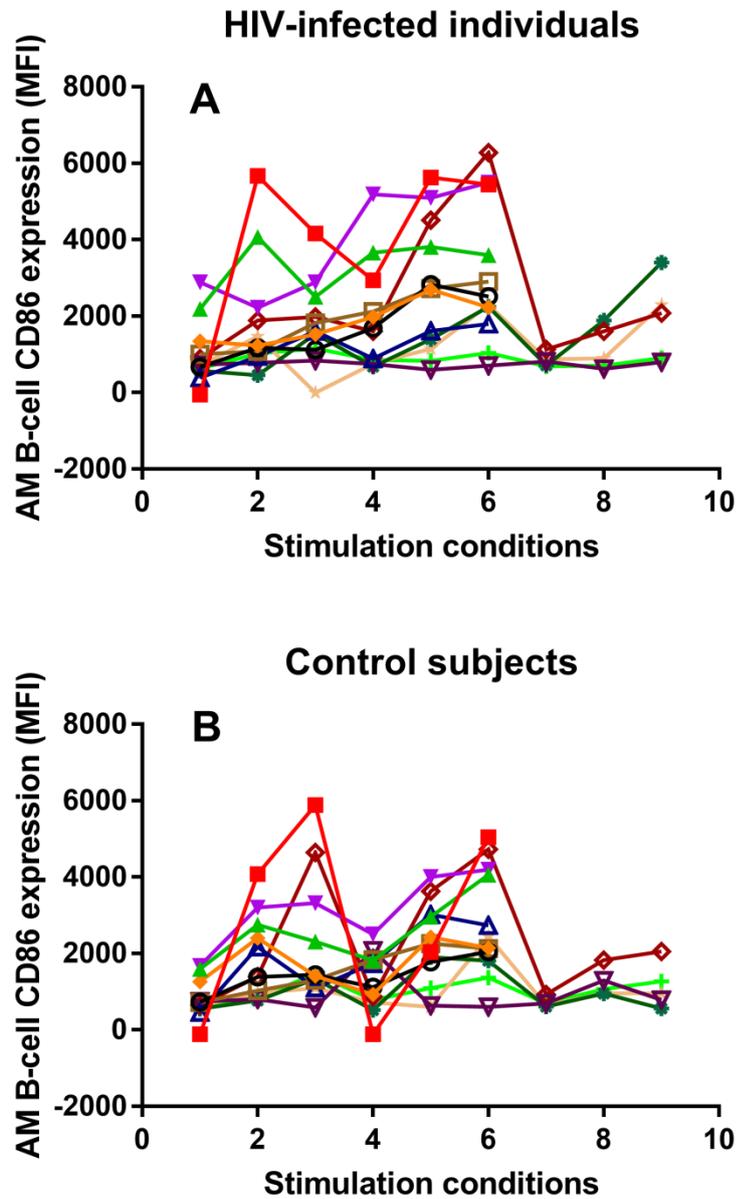
Figure 5.8ii: Tracking data showing the changes in *in vitro* Activated Memory B-cell CD86 expression in HIV-infected individuals (A) and matched controls (B) upon stimulation. Matched patient-control pairs are represented using the same colour across A and B. Conditions: 1; Un-stimulated, 2; CD3-stimulated, 3; (CD3+CD28)-stimulated, 4; αδdex-stimulated, 5; (αδdex +CD3)-stimulated, 6; (αδdex +CD3+CD28)-stimulated,

7; HKD39-stimulated, 8; (HKD39+CD3)-stimulated, 9; (CD3+CD28+HKD39)-stimulated.

No difference was found between patients and controls for proliferation or activation of resting memory or tissue-like memory cells (data not shown). Further, patients and controls did not significantly differ in the proliferation of their naive B-cells (fig. 5.9i).
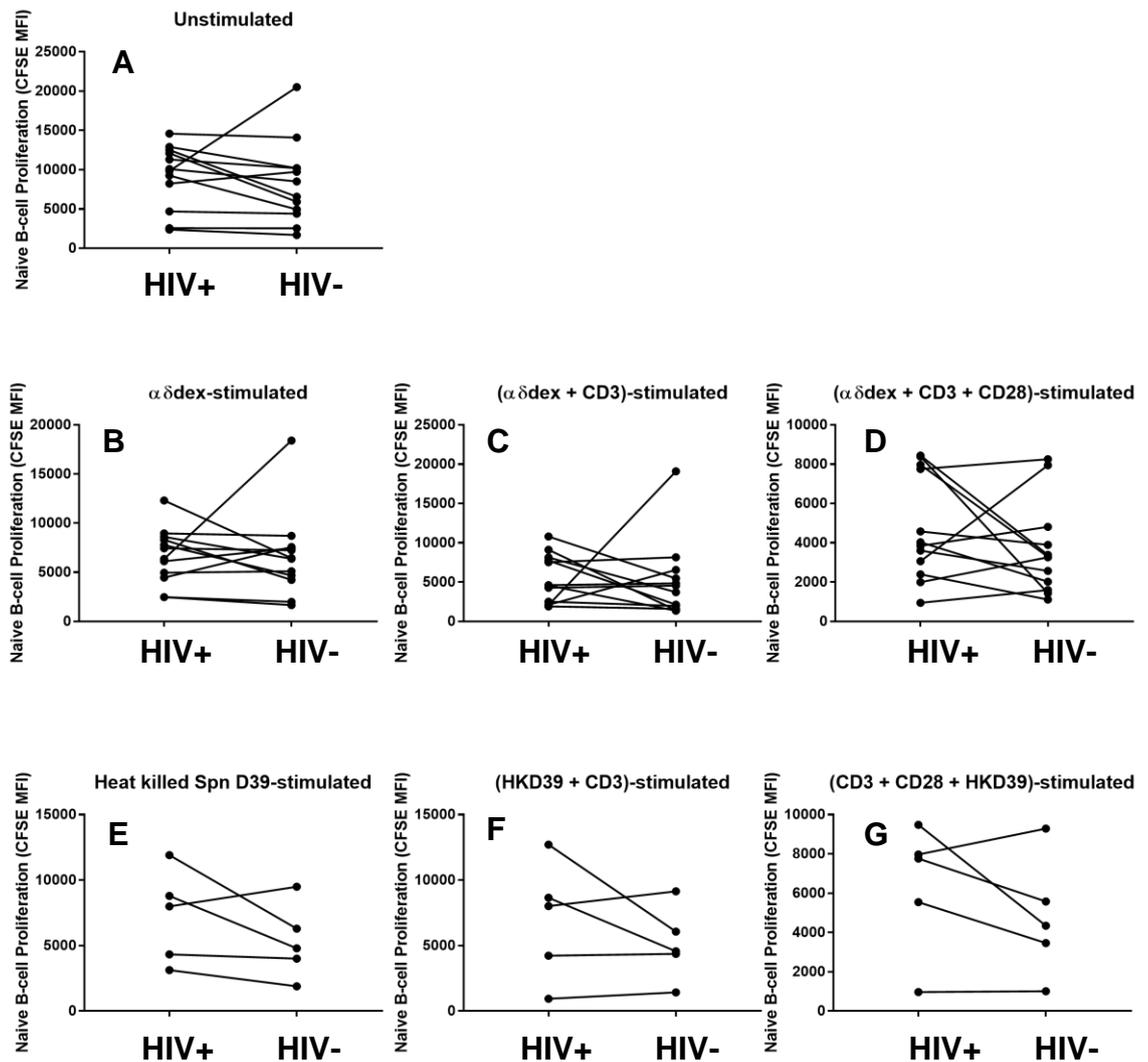
Figure 5.9i: Proliferation of *in vitro* Naive B-cells in HIV-infected individuals and matched controls under un-stimulated and stimulated conditions. Dots and lines match each patient-control pair. The paired-samples *t*-test and Wilcoxon signed ranks test were used for parametric and non-parametric datasets respectively. (Patient n = 12 except for HKD39-stimulations, where patient n = 5). Concentrations of stimulants used: 1µg/ml

of αδdex, 0.1µg/ml anti-CD3 alone, and 0.5µg/ml anti-CD3 in combination with 0.5µg/ml anti-CD28. Patient cohort and control cohort tracking data for this graph grid is presented in fig. 5.9ii.
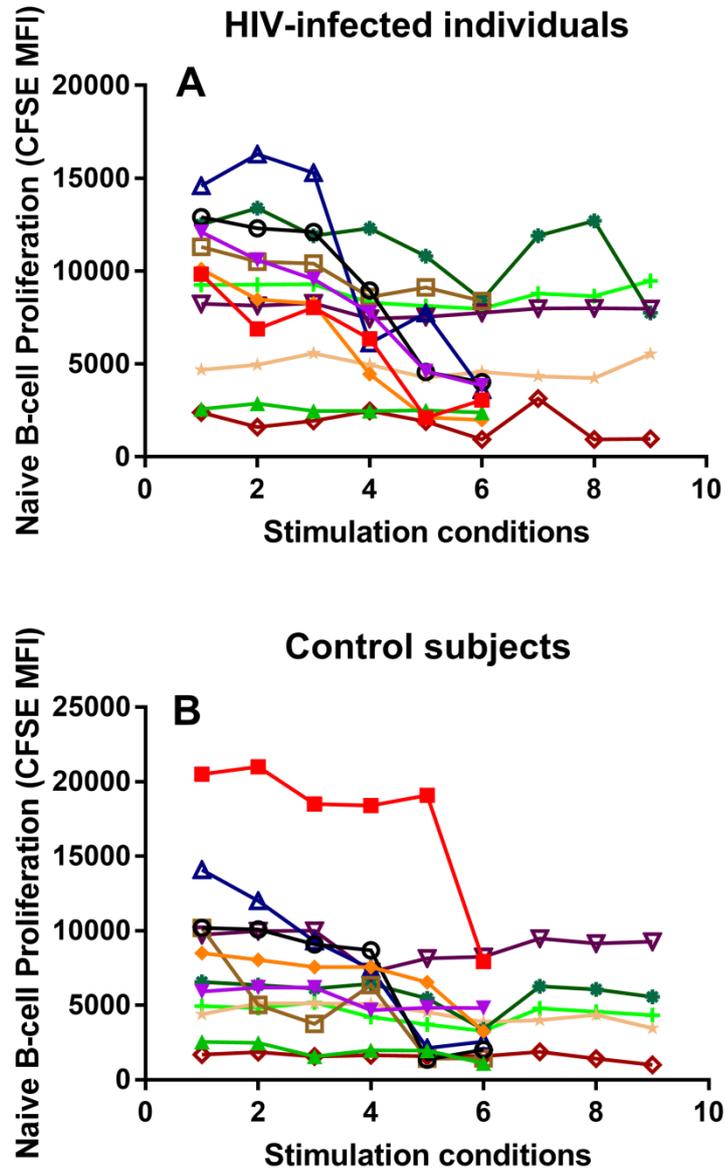
Figure 5.9ii: Tracking data showing the changes in *in vitro* Naive B-cell proliferation in HIV-infected individuals (A) and matched controls (B) upon stimulation. Matched patient-control pairs are represented using the same colour across A and B. Conditions: 1; Un-stimulated, 2; CD3-stimulated, 3; (CD3+CD28)-stimulated, 4; αδdex-stimulated, 5; (αδdex +CD3)-stimulated, 6; (αδdex +CD3+CD28)-stimulated, 7; HKD39-stimulated, 8; (HKD39+CD3)-stimulated, 9; (CD3+CD28+HKD39)-stimulated.

CD86 expression on naive B-cells yielded a difference between patients and controls upon pneumococcal-stimulation (fig. 5.10i).
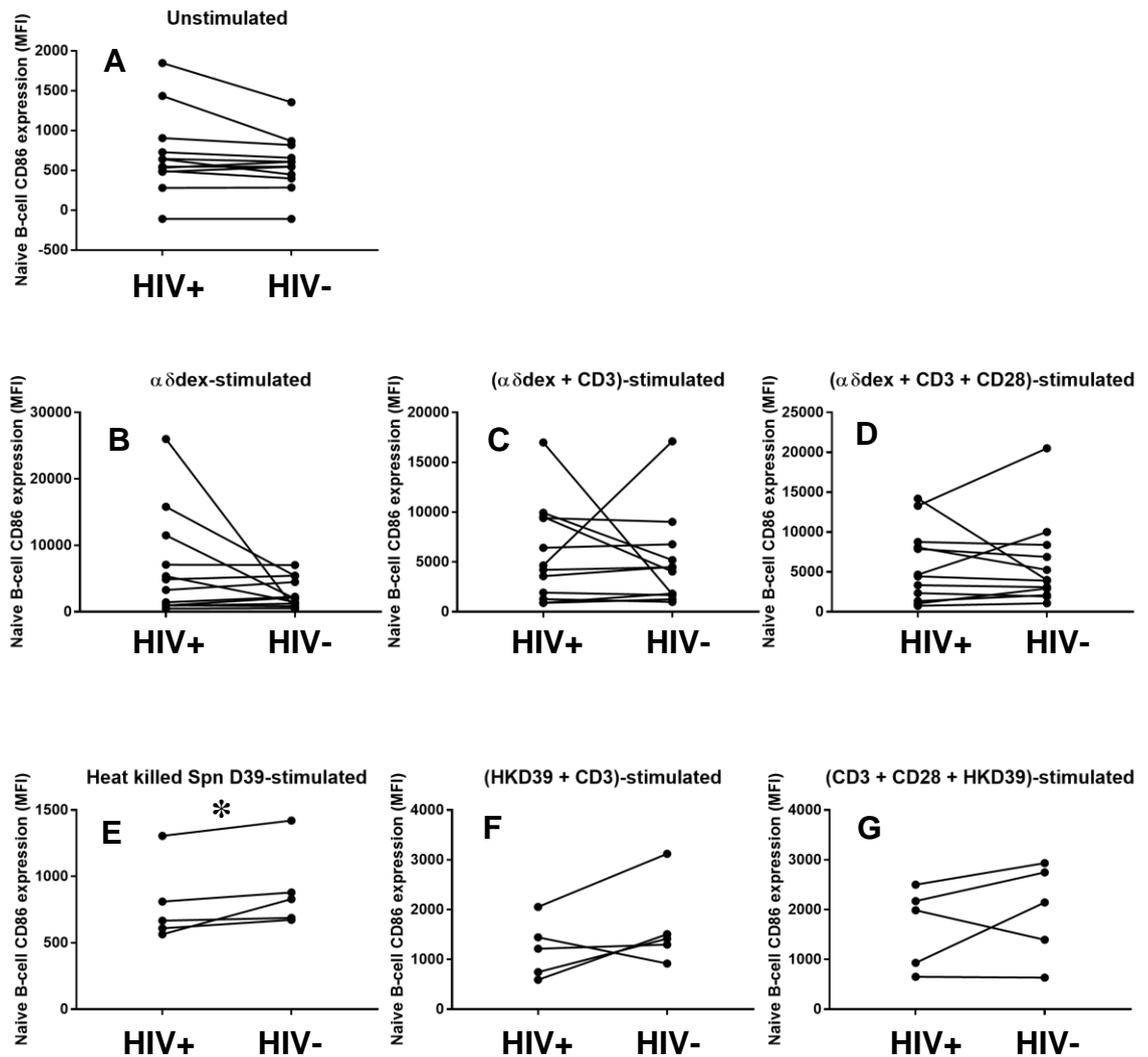
Figure 5.10i: CD86 expression on *in vitro* Naive B-cells in HIV-infected individuals and matched controls under un-stimulated and stimulated conditions. Dots and lines match each patient-control pair. The paired-samples *t*-test and Wilcoxon signed ranks test were used for parametric and non-parametric datasets respectively. (Patient n = 12 except for HKD39-stimulations, where patient n = 5; Where * $p \leq 0.050$). Concentrations of stimulants used: 1µg/ml of αδdex, 0.1µg/ml anti-CD3 alone, and 0.5µg/ml anti-CD3 in combination with 0.5µg/ml anti-CD28. Patient cohort and control cohort tracking data for this graph grid is presented in fig. 5.10ii.

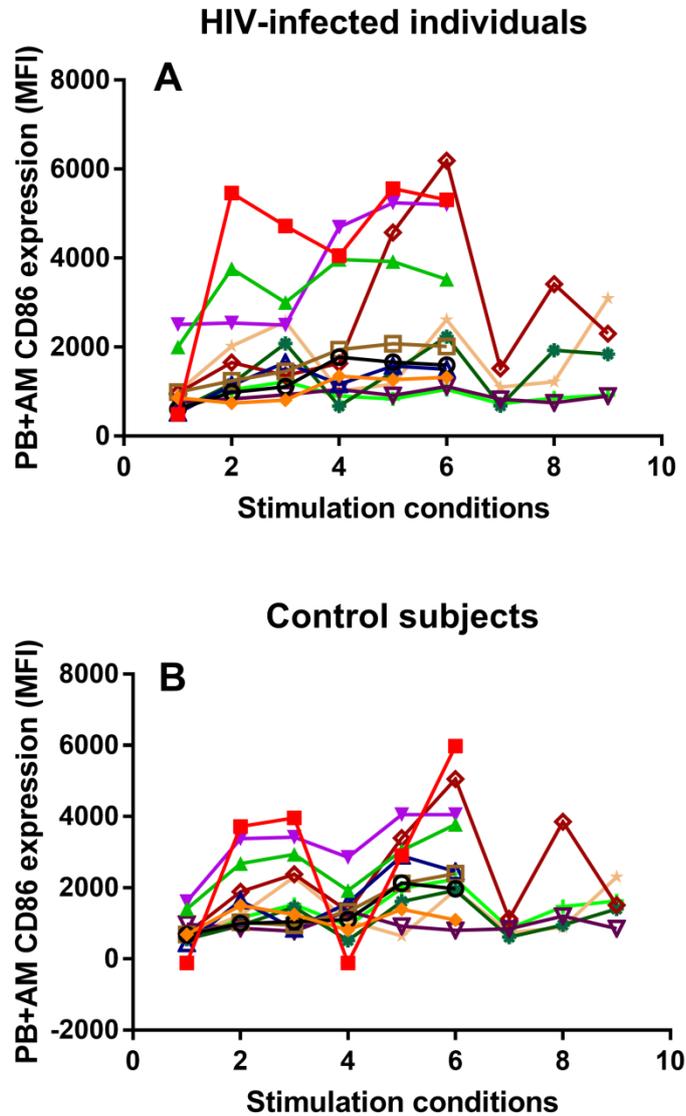**Figure 5.10ii: Tracking data showing the changes in *in vitro* Naive B-cell CD86 expression in HIV-infected individuals (A) and matched controls (B) upon stimulation.** Matched patient-control pairs are represented using the same colour across A and B. Conditions: 1; Un-stimulated, 2; CD3-stimulated, 3; (CD3+CD28)-stimulated, 4; αδdex-stimulated, 5; (αδdex +CD3)-stimulated, 6; (αδdex +CD3+CD28)-stimulated, 7; HKD39-stimulated, 8; (HKD39+CD3)-stimulated, 9; (CD3+CD28+HKD39)-stimulated.

The last phase of B-cell subset analysis involved investigating differences in caspase levels between patients and controls (fig. 5.11i).
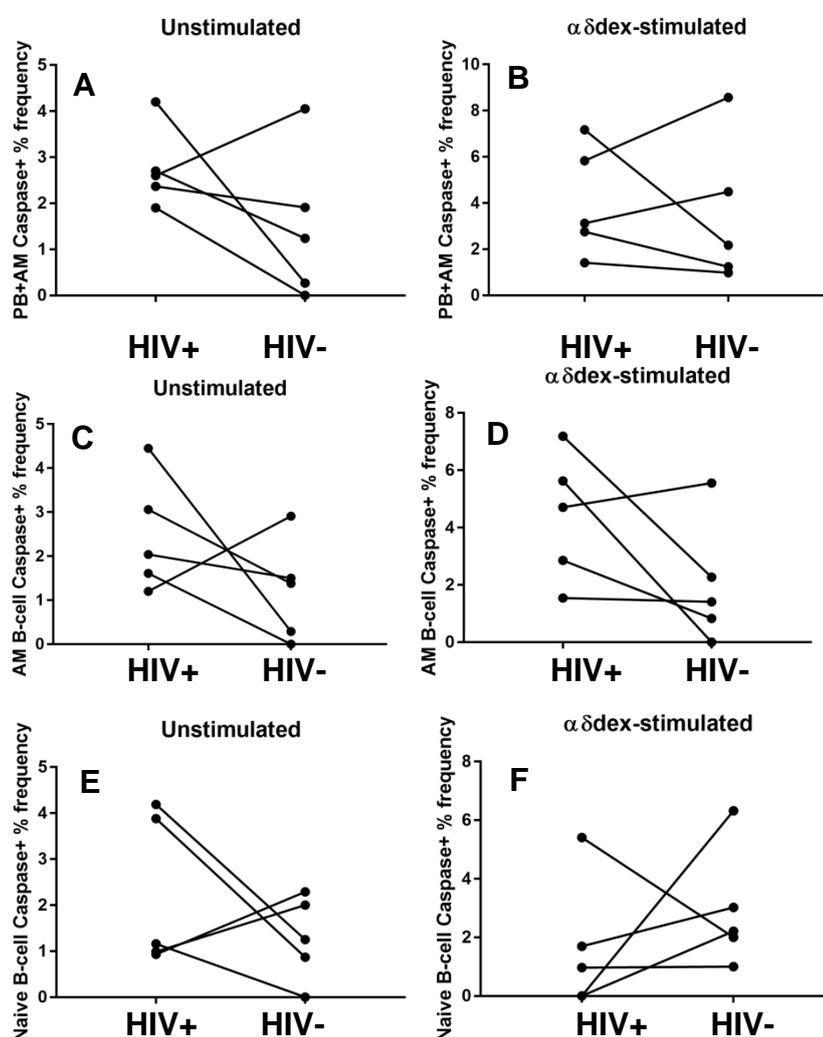
Figure 5.11i: Percentage frequencies of caspase positive Plasmablasts (PB) and Activated Memory (AM) B-cells, AMs alone, and Naïve B-cells under un-stimulated and αδdex-stimulated conditions. Neither PBs alone, RMs nor TLMs showed any differences in percentage of caspase positive cells between patients and controls (data not shown). Dots and lines match each patient-control pair. The paired-samples *t*-test and Wilcoxon signed ranks test were used for parametric and non-parametric datasets respectively. (Patient n = 5). Concentrations of stimulants used: 1µg/ml of αδdex, 0.1µg/ml anti-CD3 alone, and 0.5µg/ml anti-CD3 in combination with 0.5µg/ml anti-CD28. Patient cohort and control cohort tracking data for this graph grid is presented in fig. 5.11ii, 5.11iii and 5.11iv.
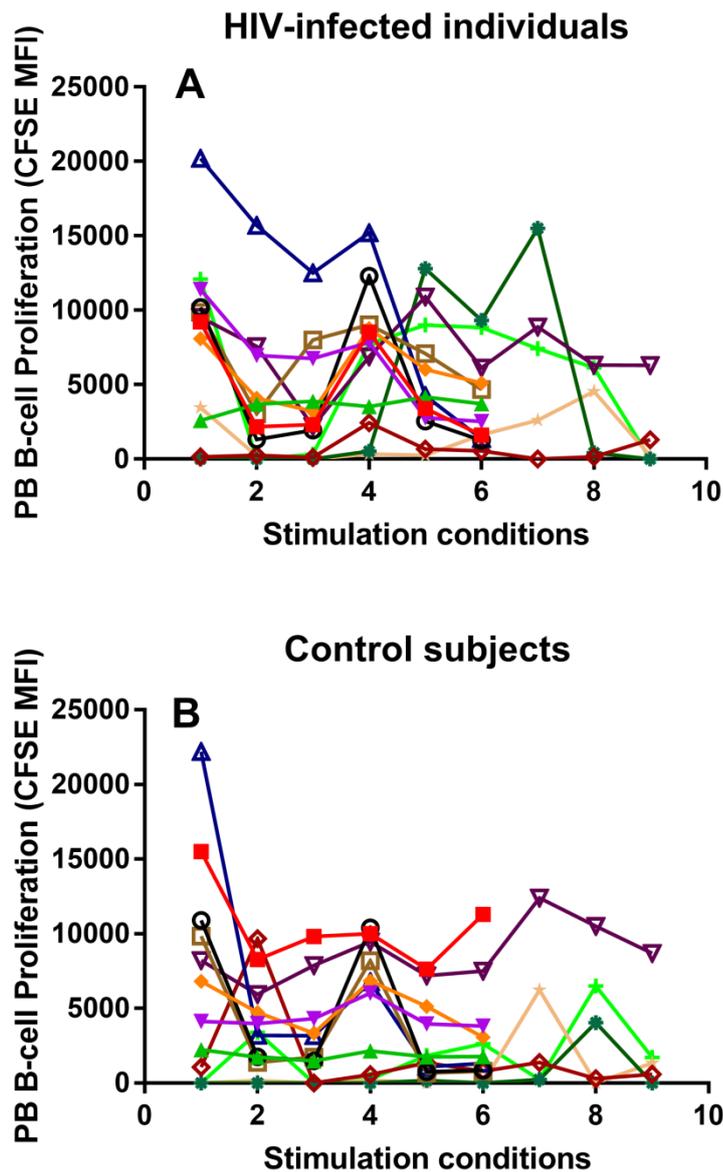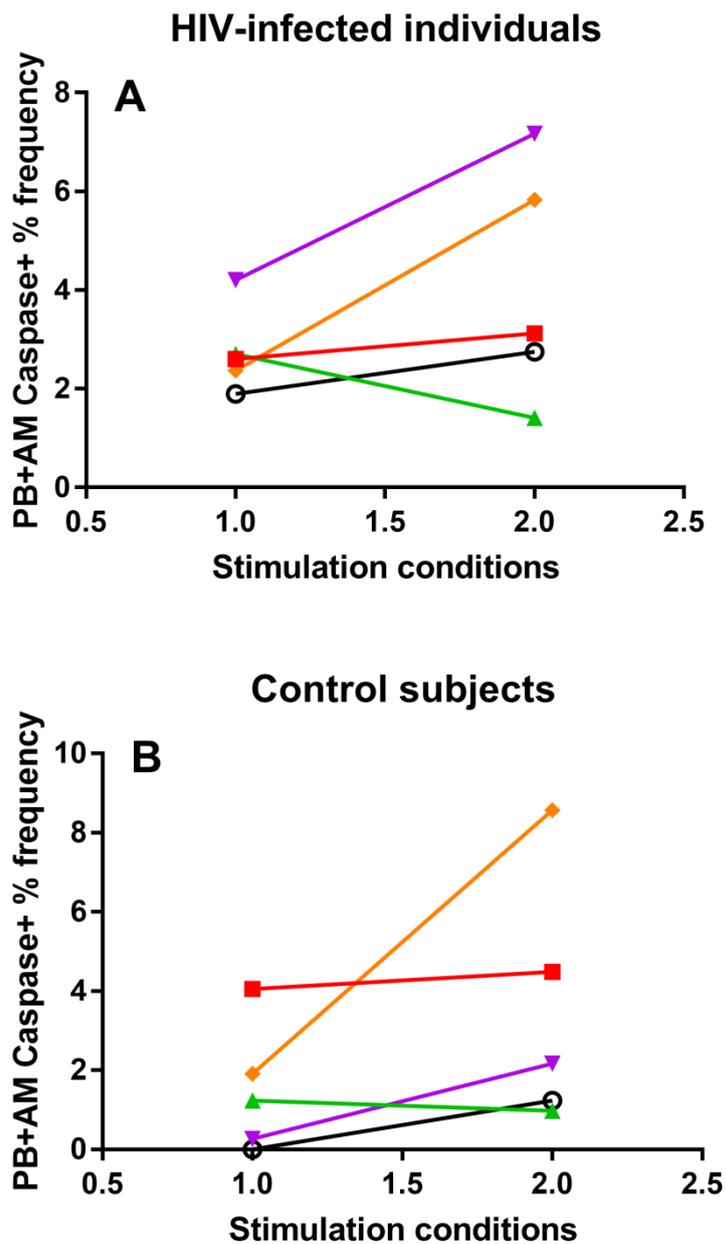
Figure 5.11ii: Tracking data showing the changes in percentage frequencies of *in vitro* caspase positive Plasmablast and Activated Memory B-cells in HIV-infected individuals (A) and matched controls (B) upon stimulation. Matched patient-control pairs are represented using the same colour across A and B. Conditions: 1; Un-stimulated, 2; CD3-stimulated.
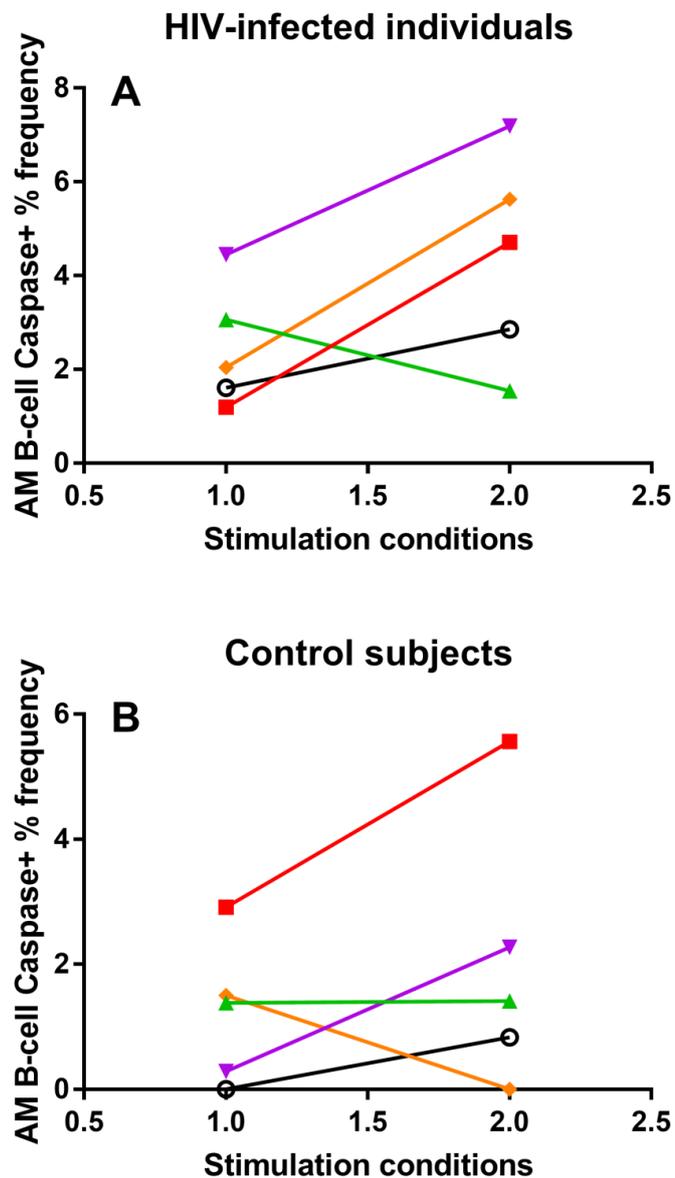
Figure 5.11iii: Tracking data showing the changes in percentage frequencies of *in vitro* caspase positive Activated Memory B-cells in HIV-infected individuals (A) and matched controls (B) upon stimulation. Matched patient-control pairs are represented using the same colour across A and B. Conditions: 1; Un-stimulated, 2; CD3-stimulated.
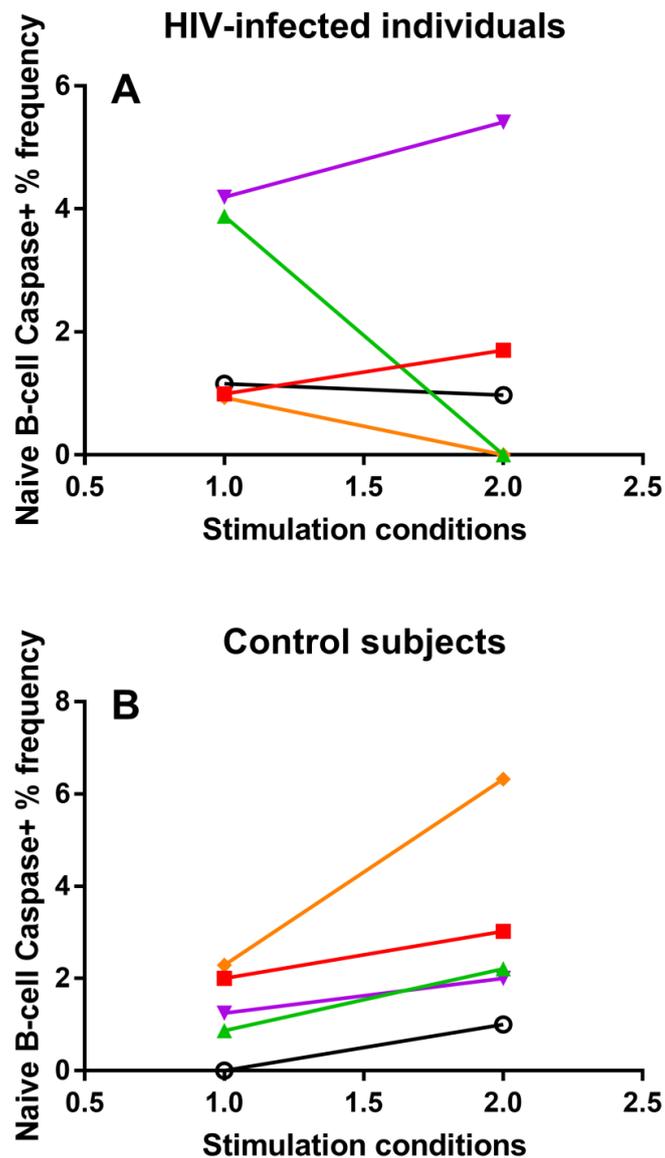
Figure 5.11iv: Tracking data showing the changes in percentage frequencies of *in vitro* caspase positive Naive B-cells in HIV-infected individuals (A) and matched controls (B) upon stimulation. Matched patient-control pairs are represented using the same colour across A and B. Conditions: 1; Un-stimulated, 2; CD3-stimulated.

5.4 Discussion of Findings

Significantly higher *in vitro* T-cell-helped pneumococcal-induced proliferation was uncovered in the CD19+ B-cell population of eight HIV-infected individuals compared to controls ($p \leq 0.050$; fig. 4.14i). With no paralleled hyperactivation in this overall CD19+ B-cell population after polyclonal and pneumococcal stimulation, in terms of CD86 or HLA-DR expression, patient responses at the level of B-cell subsets were investigated next.

5.4.1 Culture does not affect B-cell subset distribution

The first aim of this portion of the study was to investigate what effects culture and stimulation had on CD19+CD10- B-cell subsets. To achieve this, frequency distribution and CD86 expression were quantified in baseline, un-stimulated and stimulated healthy samples from four individuals (section 3.3.1). For the five B-cell subsets investigated: plasmablasts (PB), activated memory (AM), resting memory (RM), naive, and tissue-like memory (TLM) cells, culture only significantly affected the frequency distribution of RM B-cells (table 5.2); RM B-cell frequency distribution was reduced upon 96 hr culture. Stimulation induced up-regulated CD86 expression only in RM B-cells (table 5.3) as well. These results suggest that most of the B-cell subsets remain constant in culture, and post-stimulation.

5.4.2 Subtle defects uncovered in the B-cell subsets of HIV-infected individuals

Once the effect of culture and stimulation on healthy B-cell subsets was ascertained, differences in subset responses between HIV-infected individuals and age-, sex- and ethnicity-matched controls were investigated. Results presented show subsets in which differences between patient and control responses were uncovered. Therefore, the Q1 quadrant (PBs and AMs), PBs and AMs alone, and naive B-cells were presented in section 3.3.2.

Within the Q1 compartment, the patients expressed significantly higher levels of CD86 under un-stimulated conditions ($p \leq 0.050$; fig. 5.4i A) and further, αδdex-induced hyperactivation ($p \leq 0.050$; fig. 5.4i B) compared to controls. Another noteworthy finding is the lack of hyperactivation in patients following pneumococcal-stimulation (fig. 5.4i E) even though αδdex induced hyperactivation. This may however be due to the low study numbers for the pneumococcal-stimulation (patient n = 5) or due to suboptimal HKD39 stimulation. Further, T-cell-helped activation did not differ between patients and controls (fig. 5.4i C, D, F and G).

Using the CD20 marker, the Q1 compartment was split into PBs and AMs (fig. 5.1 B) to investigate which of these B-cell subsets was producing differential responses between patients and controls. PBs and AMs are increased in HIV-viraemic patients (Moir et al., 2001, Moir et al., 2004, Moir and Fauci, 2009, Moir and Fauci, 2013). However, evidence suggests that irreversible damage of the immune system can be prevented by early initiation of ART (Moir et al., 2010). While data on the time difference between diagnosis and ART-initiation in the HIV-infected cohort was not accessed, except for one individual with a viral blip less than six months before partaking in the study, the cohort comprised aviraemic individuals (table 4.3). Supporting ART-control of B-cell subset responses to an extent was the proliferation in the patient Q1 compartment (fig. 5.3i) which did not significantly differ to that of controls. In addition, whilst PBs (fig. 5.5i) and AMs (fig. 5.7i) of patients in this study showed higher proliferation compared to controls, this was not statistically significant. Whereas, highly viraemic patients show defective B-cell proliferation capabilities (Moir et al., 2001).

While un-stimulated CD86 expression on PBs was also comparable between patients and controls (fig. 5.6i), it was the AM subset that expressed higher levels of the CD86 activation marker under un-stimulated conditions ($p \leq 0.050$; fig. 5.8i A) seen in the Q1 compartment (fig. 5.4i A). Further, αδdex-stimulation induced significant hyperactivation in patient PBs compared to controls ($p \leq 0.050$; fig. 5.6i B) that was seen in the Q1 compartment (fig. 5.4i

B). Patient AMs also showed increased CD86 expression upon pneumococcal stimulation ($p ≤ 0.050$; fig. 5.8i E) compared to controls. While αδdex-stimulation did not induce significant hyperactivation in the patient AMs compared to controls (fig. 5.8i B), the p value obtained (0.094) is suggestive of a trend. Further, adding T-cell help to both PBs (fig. 5.6i C and D) and AMs (fig. 5.8i F and G) resulted in the disappearance of hyperactivation responses in the patients. AMs in viraemic patients express increased levels of the apoptosis marker CD95 (Moir and Fauci, 2013), and increased expression of apoptosis markers in HIV has been associated with B-cell hyperactivation (Nicholas et al., 2013). Therefore the polyclonal- and pneumococcal-stimulated hyperactivation uncovered in the patient cohort may be indicative of a subtle defect in the HIV patient Q1 compartment, comprising PBs and AMs, despite ART-usage.

Resting memory cells (RMs) found to be depleted in HIV-viraemic individuals (Moir and Fauci, 2013), showed comparable *in vitro* proliferation and activation between patients and controls, as did tissue-like memory cells (data not shown). Other than a decrease in frequency in HIV-viraemic patients (Moir et al., 2008a, Moir et al., 2008b, Moir and Fauci, 2008), the naive B-cell compartment has had few abnormalities reported in the context of HIV (Moir and Fauci, 2013). Hence, it was interesting to find that *in vitro* stimulation with HKD39 resulted in significantly higher CD86 expression in the naive cells of controls compared to patients ($p ≤ 0.010$; fig. 5.10i E). However, proliferation responses (fig. 5.9i) between the naive B-cells of patients and controls yielded no significant differences.

The last phase of the B-cell subset investigation involved quantifying levels of caspases-1, -2, -3, -6, -8, -9 and -10. Because B-cell apoptosis marker expression is increased in HIV (Samuelsson et al., 1997a, Samuelsson et al., 1997b, De Milito et al., 2001, Nicholas et al., 2013), it was hypothesized that an over-expression of caspases would be found in the HIV-infected cohort. However, with this portion of the study only being conducted on five patients, results needed to be interpreted with caution. And while three of the compartments presented (Q1: PBs and AMs, AMs alone and naive B-cells)

had higher un-stimulated and αδdex-stimulated caspase in at least three individuals (fig. 5.11i), this was not statistically significant. Extending this caspase-detection portion of the study to include more numbers would make conclusions drawn more robust. Especially in light of the initial findings of our group which showed statistical power of the αδdex-based immunologic assay requiring a minimum study number of 10 (Darton et al. 2011).

5.4 Conclusion

The overall CD19+ B-cell population studied was separated into B-cell subsets based on the CD10, CD20, CD21 and CD27 markers. These populations comprised mature B-cells, most of which were memory cells. Gating into four quadrants based on FMO controls and a well-established gating strategy (Moir and Fauci, 2013) resulted in subsets of Plasmablasts (PB), Activated Memory (AM), Resting Memory (RM), Naive, and Tissue-Like Memory (TLM) B-cells.

Culture was shown to have no impact on the *in vitro* frequency distribution of B-cell subsets investigated in a healthy group of four individuals. Data presented in this study show αδdex-induced hyperactivation in patient PBs, and pneumococcal-induced hyperactivation in patient AMs. This could represent a subtle defect in these B-cell subsets, in spite of ART-usage.

Lastly, in hypothesizing an increased level of apoptosis in patient B-cell subsets, a pan-caspase probe was incorporated into the study. Only five patient samples (with matched controls) were used for this phase of the study. No significant differences were found between the patients and controls in terms of caspase levels. This could be indicative of ART-control to an extent within this patient cohort, or simply a need for increased study numbers.

CHAPTER SIX: THE EFFECT OF POLYCLONAL AND PNEUMOCOCCAL STIMULATION ON T- AND B-CELLS IN A COHORT OF MGUS PATIENTS

6.1 Introduction

The association of IPD with underlying disease, particularly in the context of compromised immunity, extends to solid tumours, malignancies, and hematologic malignancies (Fukusumi et al., 2017, Kyaw et al., 2005). The present study was interested in investigating the role *in vitro* B-cell responses (with and without T-cell help) play in predisposing myeloma patients to pneumococcal disease. Particularly because aberrant B-cell expansion underpins haematologic malignancies. And these malignancies exist on a progressive spectrum, such that Monoclonal Gammopathy of Undetermined Significance (MGUS) may or may not progress to malignancies (Kyle, 1978, Kyle et al., 2003, Kyle et al., 2010, Kyle et al., 2011, Landgren et al., 2009, Korde et al., 2011, San Miguel, 2015) including Multiple Myeloma (MM), Lymphoproliferative Disorder, AL Amyloidosis, and Waldenstrom's macroglobulinemia (Kyle et al., 2010).

Thus, MGUS is a premalignant condition caused by a disorder in the proliferation of plasma cells resulting in the presence of a monoclonal immunoglobulin- M-protein (Kyle, 1978, Kyle et al., 2003, Kyle et al., 2010, Kyle et al., 2011, Landgren et al., 2009, Korde et al., 2011, San Miguel, 2015). However, the terminology 'Monoclonal Gammopathy of Renal Significance' has been proposed for use when the disease pathology shows a causal relationship between the monoclonal gammopathy and renal damage (Leung et al., 2012). The progression from asymptomatic MGUS and smoldering myeloma to symptomatic myeloma (MM) depends upon the stability of the quiescent clone (San Miguel, 2015).

The pathogenesis of MM involves myelomatous plasma cells interacting with their microenvironment, and genetic lesions. Cytogenic abnormalities have been identified in MM patients, many of which dictate drug resistance and outcome of the disease (San Miguel, 2015). And even though MGUS often precedes MM, it is not known if all MM cases are preceded by MGUS (Landgren et al., 2009).

In terms of clinically detectable parameters, MGUS is characterised by an M-protein detection rate below 3 g/dL, less than 10% bone marrow plasma cells, no related impairment to other tissues/organs, and no other disorder in B-cell proliferation. Advancement to smoldering myeloma involves an increase in M-protein levels and bone marrow plasma cells. Finally, MM patients have detecatable M-protein in their serum and urine, with related impairment of tissues and organs (Kyle et al., 2003, Kyle et al., 2010, Kyle et al., 2011, Mateos and Landgren, 2016).

The leading cause of death in myeloma patients is infection (King, 1980), with a study conducted in Japan finding that over a two-decade period, 34.6% of autopsied MM patients had had pneumonia which was the most common bacterial infection (Oshima et al., 2001). Already in 1954, recurrent bacterial pneumonia was reported in MM patients. Whilst pneumonia episodes promptly responded to antibiotic treatment, there were recurrent episodes caused by the same organism with one patient having 13 bouts. Additionally, the patients in this study showed feeble antibody responses following subcutaneous immunisation with pneumococcal polysaccharides. (Zinneman and Hall, 1954). This same research group also reported an emphasis on pneumonia whilst reviewing the cases of 59 MM patients (Glenchur et al., 1959).

And even in the era of pneumococcal vaccines, MM patients still have a significantly higher risk (p <0.001) of IPD compared to an adult control population. And as some of the reported pneumococcal isolates responsible for infection are contained in PPV23 and PCV13, this warrants an expanded valency conjugate vaccine for this patient group (Wong et al., 2010). Especially as MM patients showed reduced responses to a 14-valent PPV compared to healthy controls, and in some cases no protective antibody concentration (Lazarus et al., 1980). And in more recent times, elderly MM patients still showed suboptimal responses to PPV23 (Karlsson et al., 2013).

The correlation of IPD incidence in patients with chronic illness to advancing age (Kyaw et al., 2005) once again highlighted the need for age-matching

within the MGUS cohort. In addition, Ethnicity has also been shown to play a role in risk of myeloma with a report of a two-fold higher age-adjusted incidence of MM in African-Americans compared to White individuals. This study conducted by Landgren and colleagues (2006) also suggested that this increased MM risk in African-Americans was less likely due to progression of MGUS to MM, but rather due to an initial increased risk of MGUS (Landgren et al., 2006). Black adults have been reported to have higher IPD incidence rates both in a healthy population and in chronically ill cohorts (Kyaw et al., 2005). These studies highlight an interplay of age, ethnicity and comorbidity with IPD, further emphasizing the need for matching of controls to MGUS patients in this portion of the study.

Data gathered and presented in this chapter had two aims based upon the findings within the HIV-infected cohort (chapter's four and five): The first was to assess the effectiveness of *in vitro* T- and B-cell responses in an MGUS cohort to polyclonal stimulation alone, and cognate interactive help thereafter. The second was to use the expanded immunologic assay to study *in vitro* T- and B-cell responses in the MGUS cohort to pneumococcal stimulation using heat-killed S. pneumoniae, D39 strain (HKD39).

6.2 Methods

Patients with Monoclonal Gammopathy of Undetermined Significance (MGUS) were recruited from cohorts under outpatient follow up within the Department of Haematology, STH (section 2.1). Age-, sex- and ethnicity-matched controls were recruited from amongst the staff of the Sheffield Medical School and the Royal Hallamshire Hospital (RHH). Over the two year-long recruitment within this clinic, of the 10 patients who registered interest in participating in this study, five proceeded to donate blood for the study. After informed consent was obtained, blood was drawn and PBMCs were cultured using aseptic technique. The stimulation assay was performed as described in chapter two (section 2.4 and 2.5). The three cell populations of interest in this chapter, CD4+ and CD8+ T-cells and CD19+ B-cells, were gated according to the strategy outlined in fig. 4.3. Table 6.1 details the workflow used for this portion of the study.

Table 6.1: Brief description of the workflow and outcome measures for results presented in chapter six

Aim	Work Flow	Outcome measures	Results presented in figure*:	MGUS cohort number
Investigate differences in T- and B-cell responses between MGUS patients and matched controls, based on our group immunologic assay.	CD4+ T-cell responses to TCR-stimulant; anti-CD3 alone, and in combination with αδdex, and αδdex + anti-CD28 respectively.	CD4+ T-cell frequency, proliferation (based on CFSE proliferation index), and activation (based on CD25 and HLA-DR expression).	6.1 – 6.4	5
	CD8+ T-cell responses to TCR-stimulant; anti-CD3 alone, and in combination with αδdex, and αδdex + anti-CD28 respectively.	CD8+ T-cell frequency, proliferation (based on CFSE proliferation index), and activation (based on CD25 and HLA-DR expression).	6.5 – 6.8	5
	CD19+ B-cell responses to anti-IgD-stimulation using αδdex alone, and in combination with anti-CD3, and anti-CD3 + anti-CD28 respectively.	CD19+ B-cell frequency, proliferation (based on CFSE proliferation index), and activation (based on CD86, CD25 and HLA-DR expression).	6.9 – 6.13	5
Investigate differences in T- and B-cell responses between MGUS patients and matched controls, based on the expanded immunologic assay, including *S. pneumoniae*-stimulation.	CD4+ T-cell responses to D39 strain of *S. pneumoniae* alone, and in combination with anti-CD3, and anti-CD3 + anti-CD28 respectively.	CD4+ T-cell frequency, proliferation (based on CFSE proliferation index), and activation (based on CD25 and HLA-DR expression).	6.1 – 6.4	5
	CD8+ T-cell responses to D39 strain of *S. pneumoniae* alone, and in combination with anti-CD3, and anti-CD3 + anti-CD28 respectively.	CD8+ T-cell frequency, proliferation (based on CFSE proliferation index), and activation (based on CD25 and HLA-DR expression).	6.5 – 6.8	5
	CD19+ B-cell responses to D39 strain of *S. pneumoniae* alone, and in combination with anti-CD3, and anti-CD3 + anti-CD28 respectively.	CD19+ B-cell frequency, proliferation (based on CFSE proliferation index), and activation (based on CD86, CD25 and HLA-DR expression).	6.9 – 6.13	5

* All data was collected by Furaha Asani.

6.3 Results

Table 6.2 outlines the MGUS patient and control characteristics.

Table 6.2: Characteristics of the MGUS cohort recruited for this study, with matched controls. All participants in the MGUS cohort were White.

	MGUS	**Control subjects**
Number	5	5
Mean age (Range)	69.20 (53 – 77)	59.80 (52 – 67)
Sex: Female	2	2
Male	3	3

Using the one-sample Kolmogorov-Smirnov test, some datasets presented in figures 6.1 to 6.13 were ascertained to contain both parametric and non-parametric datasets. Thus the paired-samples *t*-test and the Wilcoxon signed ranks test were respectively used for statistical analyses of these data. Pair-wise comparisons between MGUS patients and age-, sex- and ethnicity-matched controls were conducted. The *p* values shown are two-tailed, testing for differences in both directions. Paired data are presented as spot-line graphs not only to show differences between patints and matched controls, but inter-pair variations. Shaded circles represent one individual, with a line connecting matched patient- control pairs. The graph grid is organised to facilitate comparisons across rows, and down columns. (Patient n = 5).

Stimulation concentrations used were as described in chapter 2: 1µg/ml of αδdex, 0.1µg/ml anti-CD3 alone, and 0.5µg/ml anti-CD3 in combination with 0.5µg/ml anti-CD28 for 96 hr. HKD39 MOI used was 10, for 96 hr. Stimulation conditions are indicated per graph.

Before the *in vitro* proliferation and activation responses of CD4+ T-cells could be analysed, the frequency distribution of CD4+ T-cells in both MGUS patients and matched controls was investigated (fig. 6.1i).
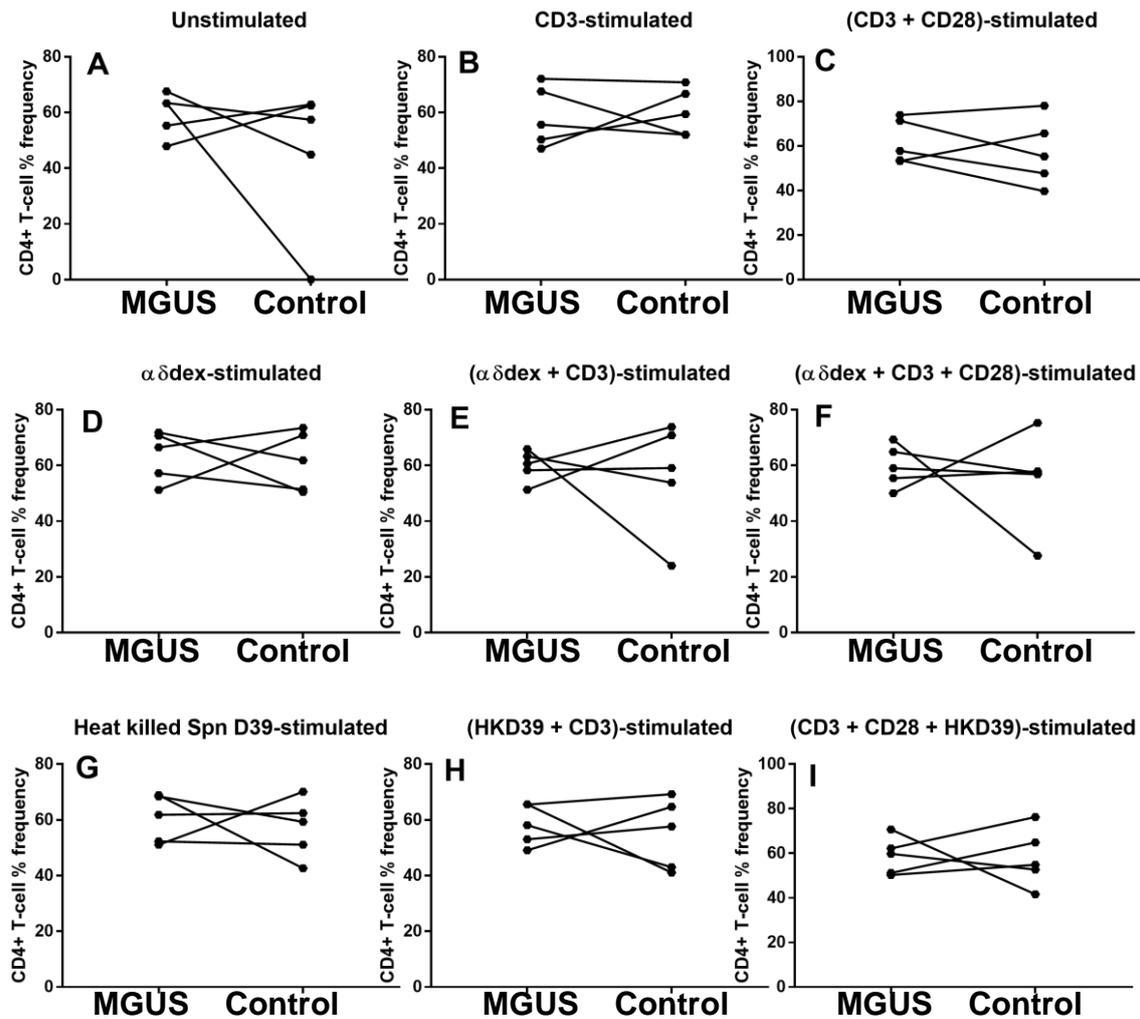
Figure 6.1i: Percentage frequencies of *in vitro* CD4+ T-cells in MGUS patients and matched controls under un-stimulated and stimulated conditions. Dots and lines match each patient-control pair. The paired-samples *t*-test and Wilcoxon signed ranks test were used for parametric and non-parametric datasets respectively. (Patient n = 5). Concentrations of stimulants used: 1µg/ml of αδdex, 0.1µg/ml anti-CD3 alone, and 0.5µg/ml anti-CD3 in combination with 0.5µg/ml anti-CD28. Patient cohort and control cohort tracking data for this graph grid is presented in fig. 6.1ii.

MGUS patients

Control subjects
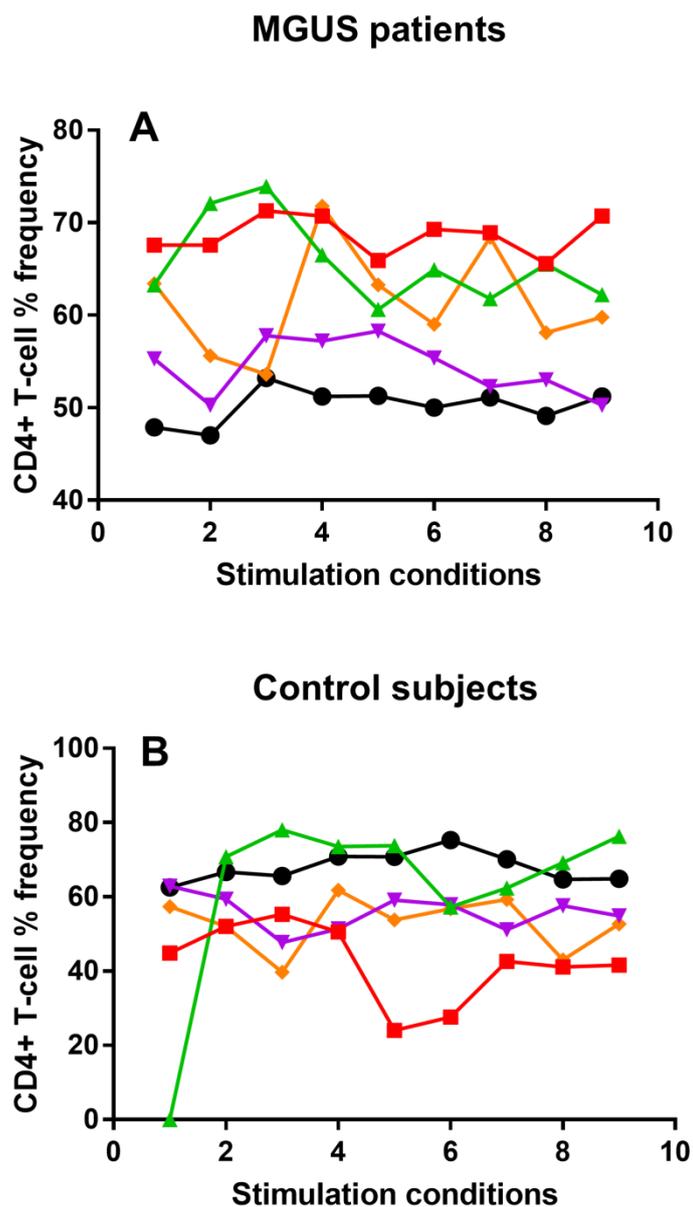
Figure 6.1ii: Tracking data showing the changes in *in vitro* CD4+ T-cell frequencies in MGUS patients (A) and matched controls (B) upon stimulation. Matched patient-control pairs are represented using the same colour across A and B. Conditions: 1; Un-stimulated, 2; CD3-stimulated, 3; (CD3+CD28)-stimulated, 4; αδdex-stimulated, 5; (αδdex +CD3)-stimulated, 6; (αδdex +CD3+CD28)-stimulated, 7; HKD39-stimulated, 8; (HKD39+CD3)-stimulated, 9; (CD3+CD28+HKD39)-stimulated.

While no differences in *in vitro* proliferation (fig. 6.2i) or CD25 expression (fig. 6.3i) was found between the five MGUS patients and matched controls, a difference in HLA-DR expression was uncovered (fig. 6.4i).
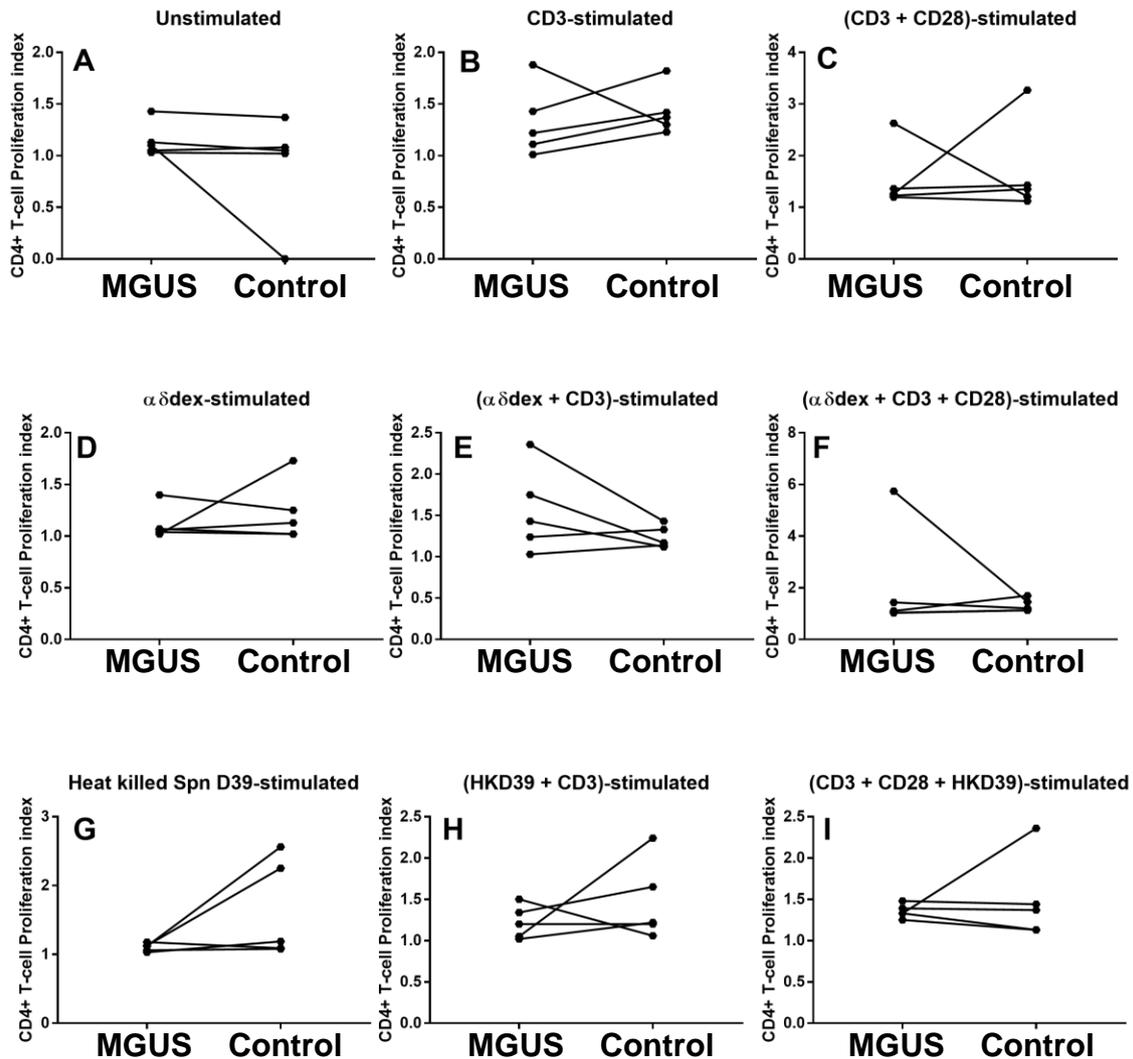
Figure 6.2i: Proliferation of *in vitro* CD4+ T-cells in MGUS patients and matched controls under un-stimulated and stimulated conditions. Dots and lines match each patient-control pair. The paired-samples *t*-test and Wilcoxon signed ranks test were used for parametric and non-parametric datasets respectively. (Patient n = 5). Concentrations of stimulants used: 1µg/ml of αδdex, 0.1µg/ml anti-CD3 alone, and 0.5µg/ml anti-CD3 in combination with 0.5µg/ml anti-CD28. Patient cohort and control cohort tracking data for this graph grid is presented in fig. 6.2ii.

MGUS patients

Control subjects

Figure 6.2ii: Tracking data showing the changes in *in vitro* CD4+ T-cell proliferation in MGUS patients (A) and matched controls (B) upon stimulation. Matched patient-control pairs are represented using the same colour across A and B. Conditions: 1; Un-stimulated, 2; CD3-stimulated, 3; (CD3+CD28)-stimulated, 4; αδdex-stimulated, 5; (αδdex +CD3)-stimulated, 6; (αδdex +CD3+CD28)-stimulated, 7; HKD39-stimulated, 8; (HKD39+CD3)-stimulated, 9; (CD3+CD28+HKD39)-stimulated.
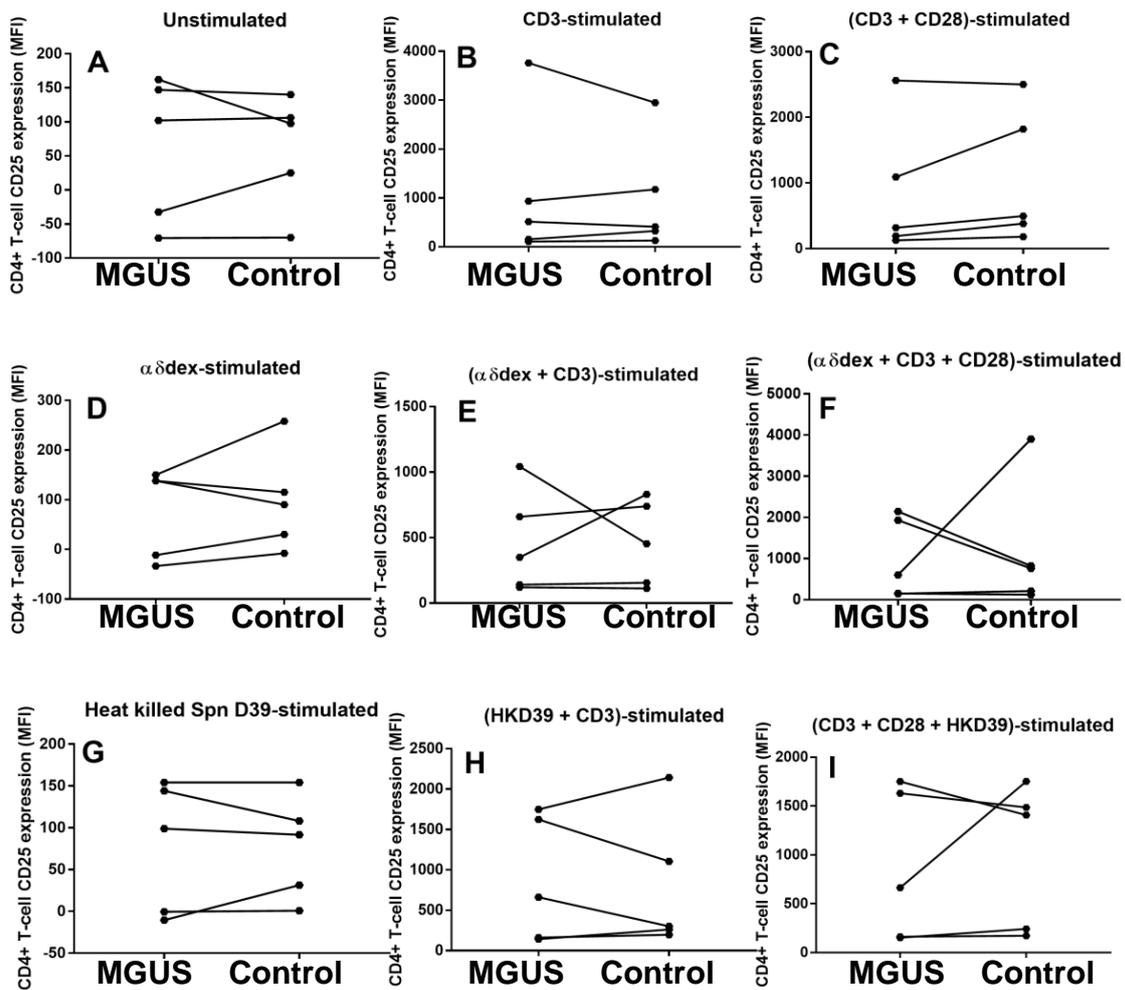
Figure 6.3i: CD25 expression on *in vitro* CD4+ T-cells in MGUS patients and matched controls under un-stimulated and stimulated conditions. Dots and lines match each patient-control pair. The paired-samples *t*-test and Wilcoxon signed ranks test were used for parametric and non-parametric datasets respectively. (Patient n = 5). Concentrations of stimulants used: 1µg/ml of αδdex, 0.1µg/ml anti-CD3 alone, and 0.5µg/ml anti-CD3 in combination with 0.5µg/ml anti-CD28. Patient cohort and control cohort tracking data for this graph grid is presented in fig. 6.3ii.

MGUS patients

Control subjects

Figure 6.3ii: Tracking data showing the changes in *in vitro* CD4+ T-cell CD25 expression in MGUS patients (A) and matched controls (B) upon stimulation. Matched patient-control pairs are represented using the same colour across A and B. Conditions: 1; Un-stimulated, 2; CD3-stimulated, 3; (CD3+CD28)-stimulated, 4; αδdex-stimulated, 5; (αδdex +CD3)-stimulated, 6; (αδdex +CD3+CD28)-stimulated, 7; HKD39-stimulated, 8; (HKD39+CD3)-stimulated, 9; (CD3+CD28+HKD39)-stimulated.

Figure 6.4i: HLA-DR expression on *in vitro* CD4+ T-cells in MGUS patients and matched controls under un-stimulated and stimulated conditions. Dots and lines match each patient-control pair. The paired-samples *t*-test and Wilcoxon signed ranks test were used for parametric and non-parametric datasets respectively. (Patient n = 5). Concentrations of stimulants used: 1µg/ml of αδdex, 0.1µg/ml anti-CD3 alone, and 0.5µg/ml anti-CD3 in combination with 0.5µg/ml anti-CD28. Patient cohort and control cohort tracking data for this graph grid is presented in fig. 6.4ii.
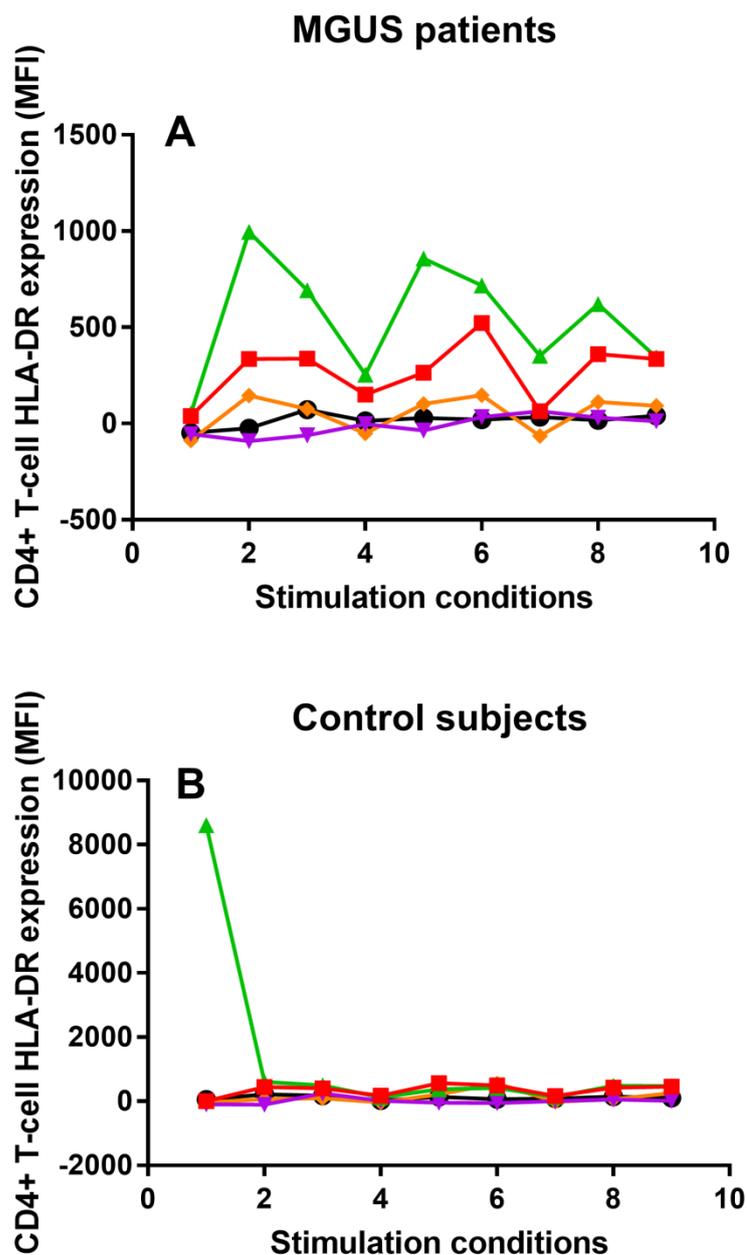
Figure 6.4ii: Tracking data showing the changes in *in vitro* CD4+ T-cell HLA-DR expression in MGUS patients (A) and matched controls (B) upon stimulation. Matched patient-control pairs are represented using the same colour across A and B. Conditions: 1; Un-stimulated, 2; CD3-stimulated, 3; (CD3+CD28)-stimulated, 4; αδdex-stimulated, 5; (αδdex +CD3)-stimulated, 6; (αδdex +CD3+CD28)-stimulated, 7; HKD39-stimulated, 8; (HKD39+CD3)-stimulated, 9; (CD3+CD28+HKD39)-stimulated.

Following the analysis of *in vitro* responses in CD4+ T-cells in this study cohort, CD8+ T-cells were investigated beginning with frequency distribution (fig. 6.5i).

Figure 6.5i: Percentage frequencies of *in vitro* CD8+ T-cells in MGUS patients and matched controls under un-stimulated and stimulated conditions. Dots and lines match each patient-control pair. The paired-samples *t*-test and Wilcoxon signed ranks test were used for parametric and non-parametric datasets respectively. (Patient n = 5). Concentrations of stimulants used: 1µg/ml of αδdex, 0.1µg/ml anti-CD3 alone, and 0.5µg/ml anti-CD3 in combination with 0.5µg/ml anti-CD28. Patient cohort and control cohort tracking data for this graph grid is presented in fig. 6.5ii.

MGUS patients

Control subjects

Figure 6.5ii: Tracking data showing the changes in *in vitro* CD8+ T-cell frequencies in MGUS patients (A) and matched controls (B) upon stimulation. Matched patient-control pairs are represented using the same colour across A and B. Conditions: 1; Un-stimulated, 2; CD3-stimulated, 3; (CD3+CD28)-stimulated, 4; αδdex-stimulated, 5; (αδdex +CD3)-stimulated, 6; (αδdex +CD3+CD28)-stimulated, 7; HKD39-stimulated, 8; (HKD39+CD3)-stimulated, 9; (CD3+CD28+HKD39)-stimulated.

However, differences were uncovered for proliferation (fig. 6.6i) and activation in terms of CD25 expression (fig. 6.7i).

Figure 6.6i: Proliferation of *in vitro* CD8+ T-cells in MGUS patients and matched controls under un-stimulated and stimulated conditions. Dots and lines match each patient-control pair. The paired-samples *t*-test and Wilcoxon signed ranks test were used for parametric and non-parametric datasets respectively. (Patient n = 5; Where * $p \leq 0.050$). Concentrations of stimulants used: 1µg/ml of αδdex, 0.1µg/ml anti-CD3 alone, and 0.5µg/ml anti-CD3 in combination with 0.5µg/ml anti-CD28. Patient cohort and control cohort tracking data for this graph grid is presented in fig. 6.6ii.

MGUS patients

Control subjects

Figure 6.6ii: Tracking data showing the changes in *in vitro* CD8+ T-cell proliferation in MGUS patients (A) and matched controls (B) upon stimulation. Matched patient-control pairs are represented using the same colour across A and B. Conditions: 1; Un-stimulated, 2; CD3-stimulated, 3; (CD3+CD28)-stimulated, 4; αδdex-stimulated, 5; (αδdex +CD3)-stimulated, 6; (αδdex +CD3+CD28)-stimulated, 7; HKD39-stimulated, 8; (HKD39+CD3)-stimulated, 9; (CD3+CD28+HKD39)-stimulated.

Activation responses also yielded differences between MGUS patients and controls (fig. 6.7i).
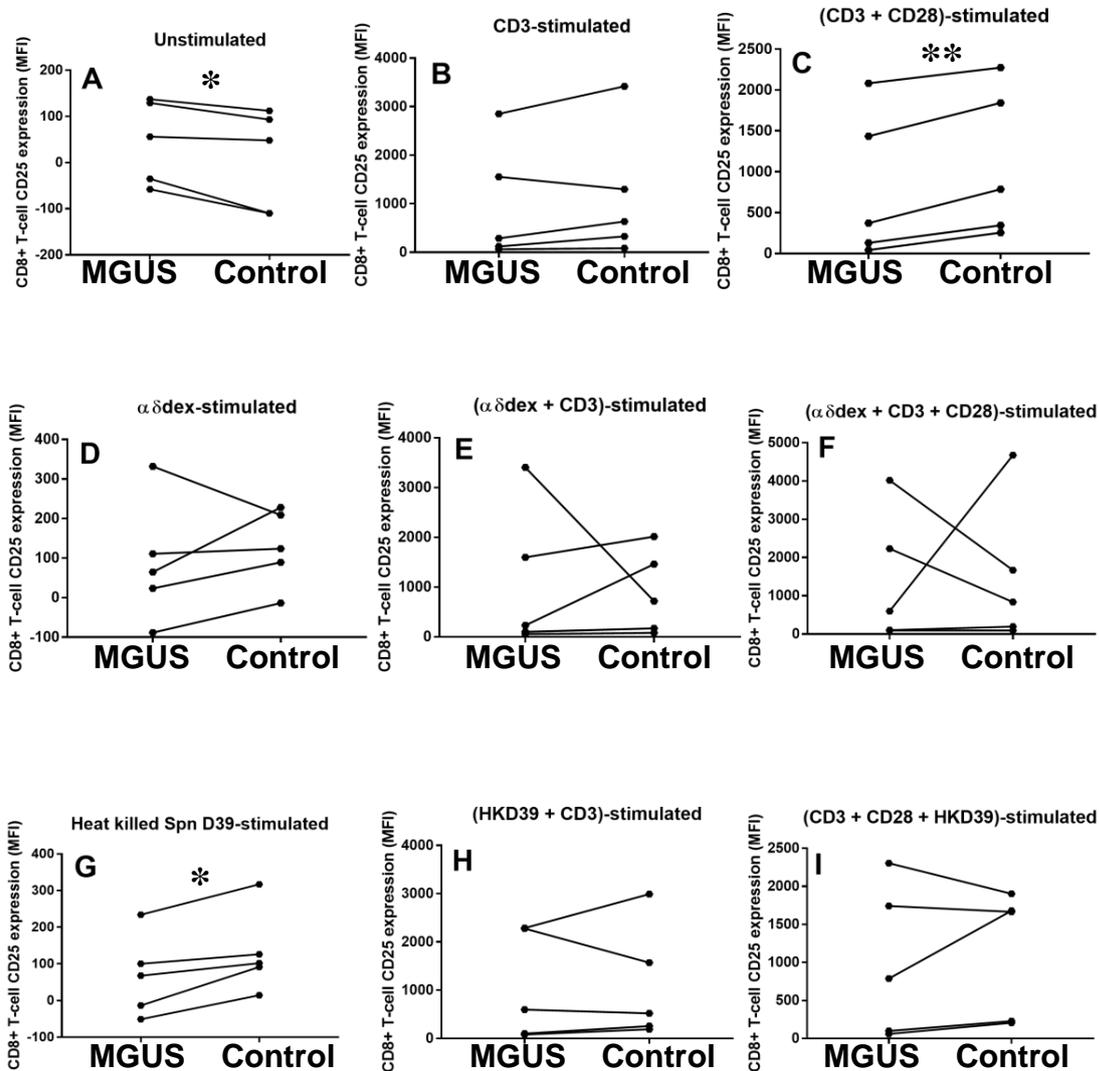
Figure 6.7i: CD25 expression on *in vitro* CD8+ T-cells in MGUS patients and matched controls under un-stimulated and stimulated conditions. Dots and lines match each patient-control pair. The paired-samples *t*-test and Wilcoxon signed ranks test were used for parametric and non-parametric datasets respectively. (Patient n = 5; Where * $p \leq 0.050$; ** $p \leq 0.010$). Concentrations of stimulants used: 1μg/ml of αδdex, 0.1μg/ml anti-CD3 alone, and 0.5μg/ml anti-CD3 in combination with 0.5μg/ml anti-CD28. Patient cohort and control cohort tracking data for this graph grid is presented in fig. 6.7ii.
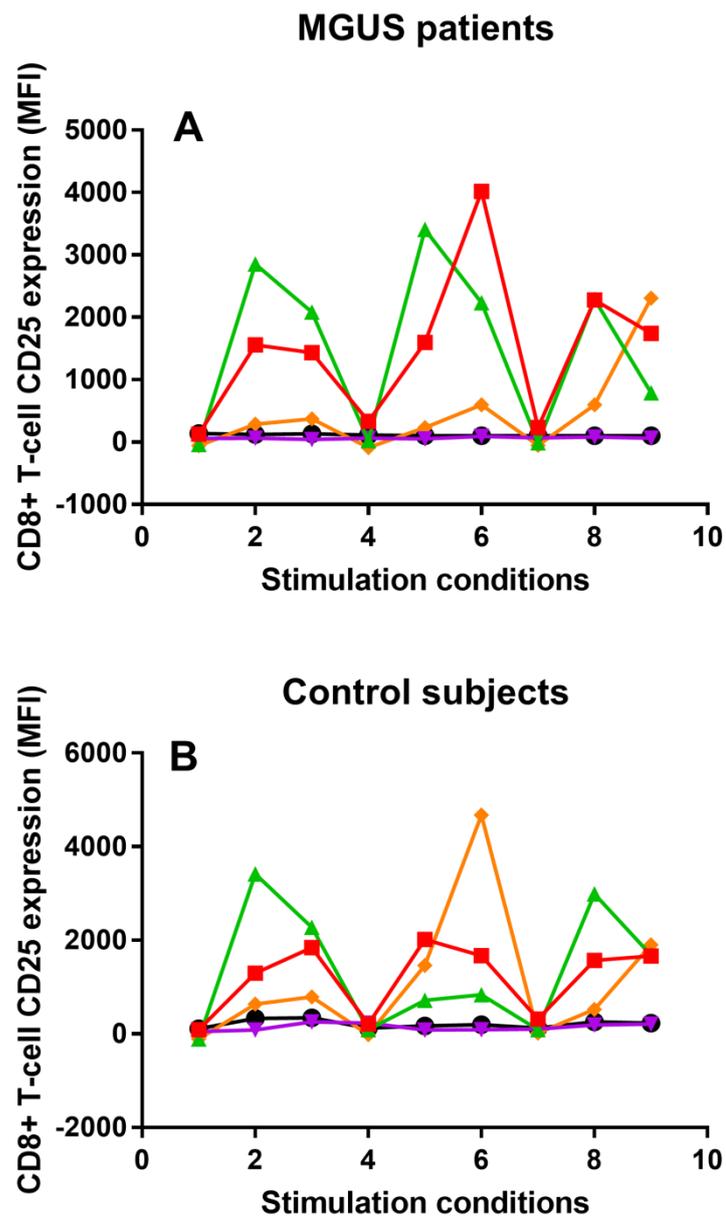
Figure 6.7ii: Tracking data showing the changes in *in vitro* CD8+ T-cell CD25 expression in MGUS patients (A) and matched controls (B) upon stimulation. Matched patient-control pairs are represented using the same colour across A and B. Conditions: 1; Un-stimulated, 2; CD3-stimulated, 3; (CD3+CD28)-stimulated, 4; αδdex-stimulated, 5; (αδdex +CD3)-stimulated, 6; (αδdex +CD3+CD28)-stimulated, 7; HKD39-stimulated, 8; (HKD39+CD3)-stimulated, 9; (CD3+CD28+HKD39)-stimulated.

A paralleled response in terms of HLA-DR expression was not found, however (fig. 6.8i).
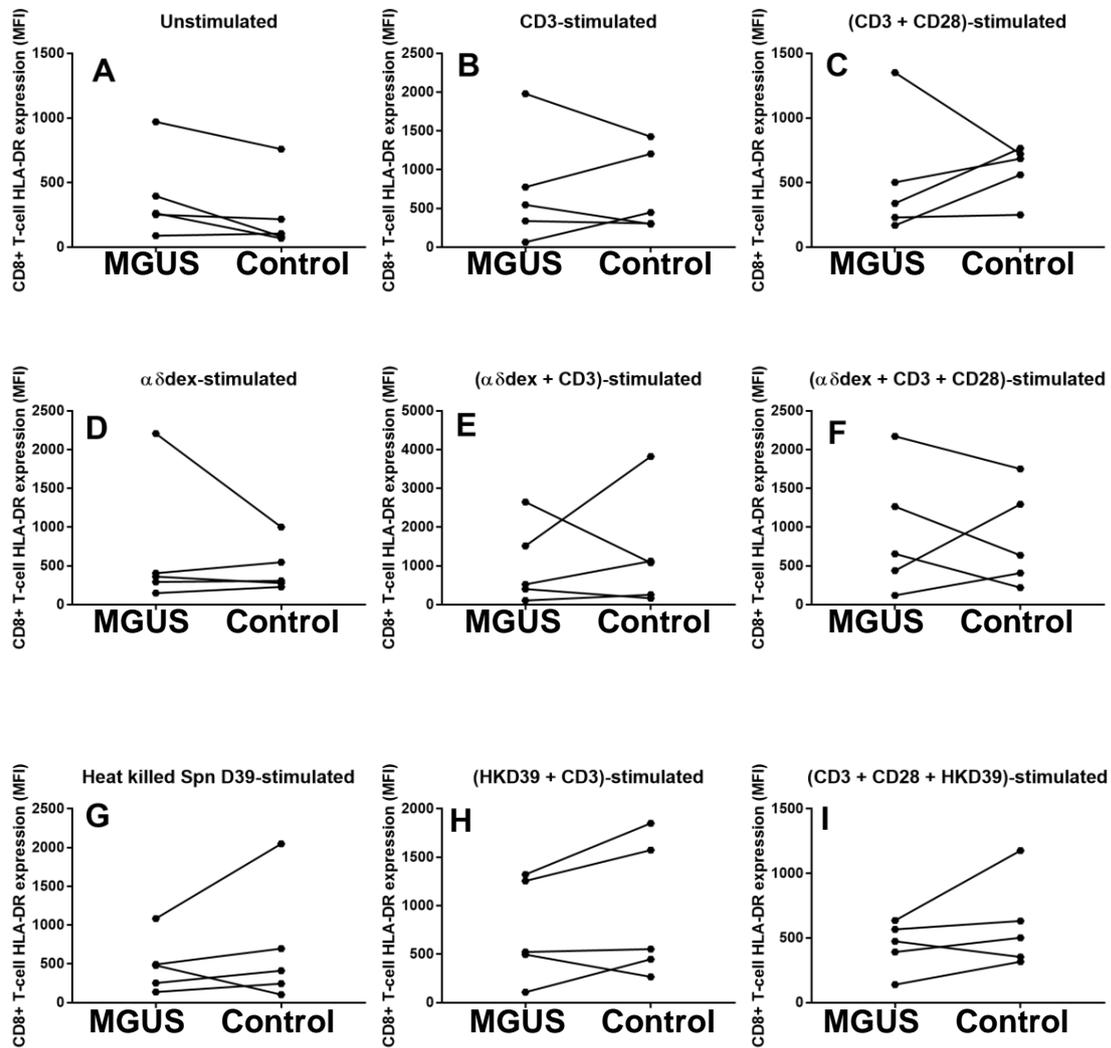
Figure 6.8i: HLA-DR expression on *in vitro* CD4+ T-cells in MGUS patients and matched controls under un-stimulated and stimulated conditions. Dots and lines match each patient-control pair. The paired-samples *t*-test and Wilcoxon signed ranks test were used for parametric and non-parametric datasets respectively. (Patient n = 5). Concentrations of stimulants used: 1µg/ml of αδdex, 0.1µg/ml anti-CD3 alone, and 0.5µg/ml anti-CD3 in combination with 0.5µg/ml anti-CD28. Patient cohort and control cohort tracking data for this graph grid is presented in fig. 6.8ii.
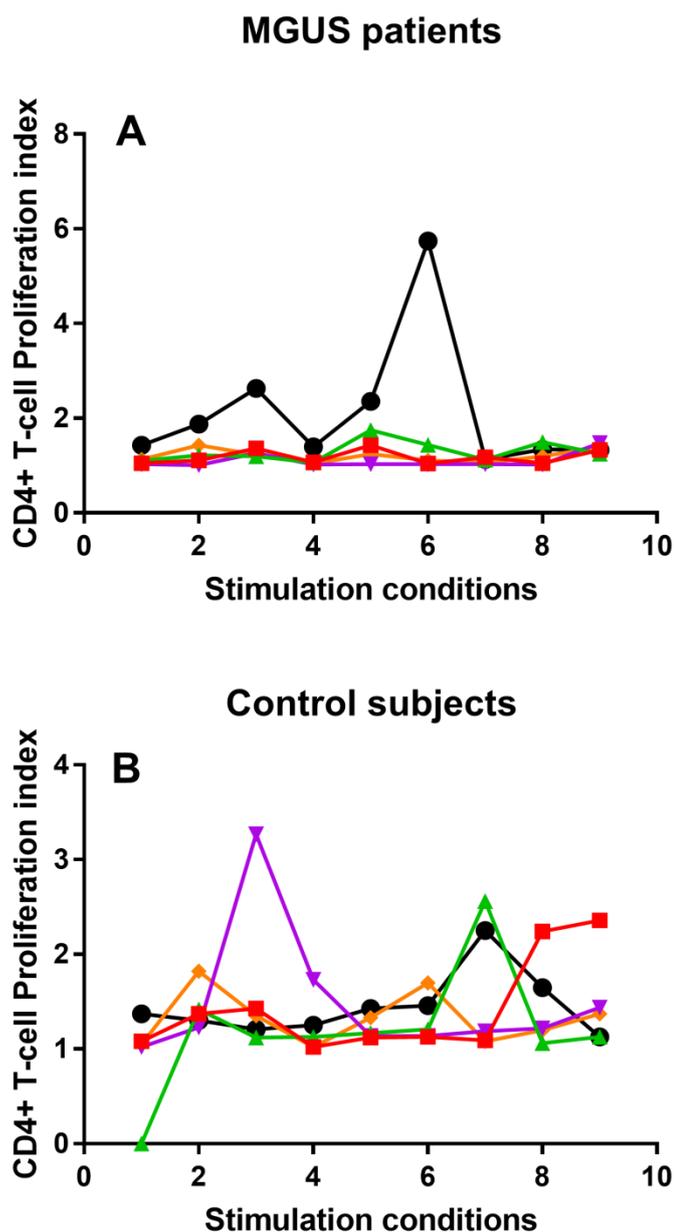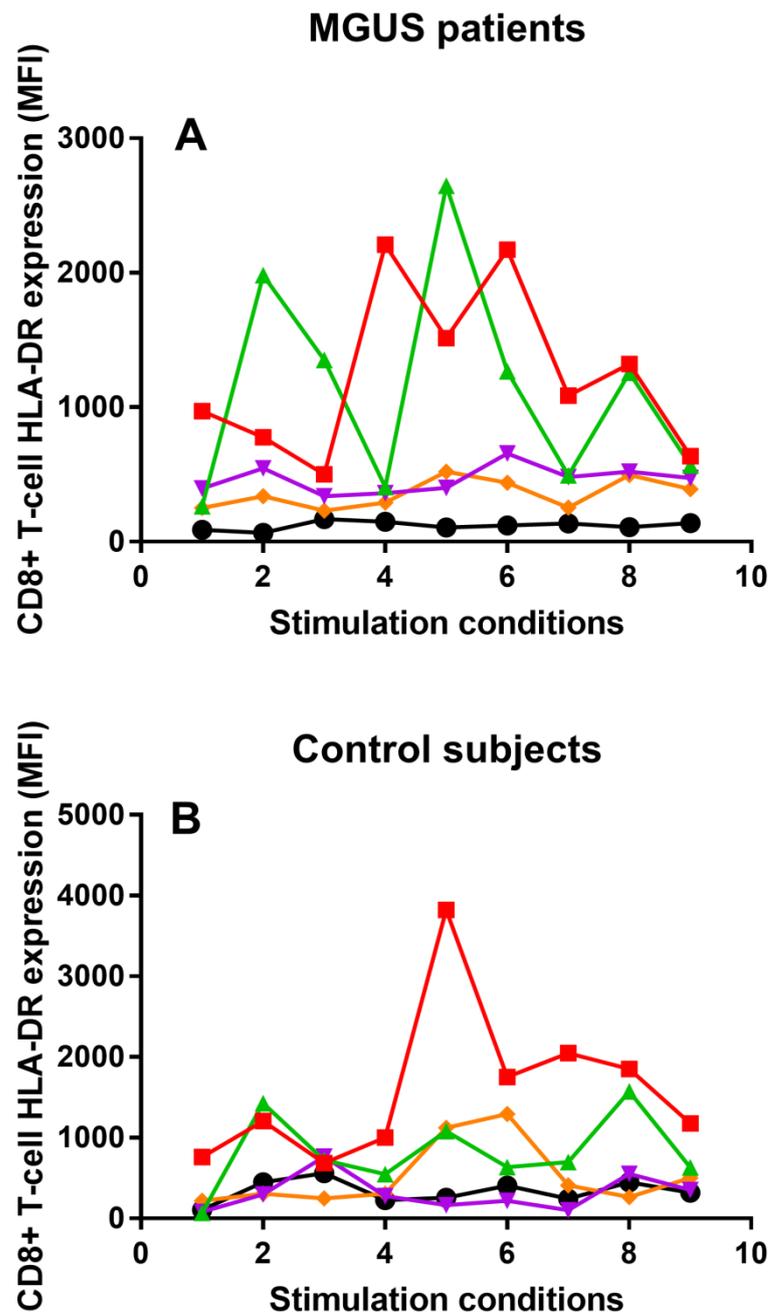
Figure 6.8ii: Tracking data showing the changes in *in vitro* CD8+ T-cell HLA-DR expression in MGUS patients (A) and matched controls (B) upon stimulation. Matched patient-control pairs are represented using the same colour across A and B. Conditions: 1; Un-stimulated, 2; CD3-stimulated, 3; (CD3+CD28)-stimulated, 4; αδdex-stimulated, 5; (αδdex +CD3)-stimulated, 6; (αδdex +CD3+CD28)-stimulated, 7; HKD39-stimulated, 8; (HKD39+CD3)-stimulated, 9; (CD3+CD28+HKD39)-stimulated.

The third cell population to be investigated was CD19+ B-cells. Once again, frequency distribution (fig. 6.9i) was investigated prior to proliferation and activation responses.
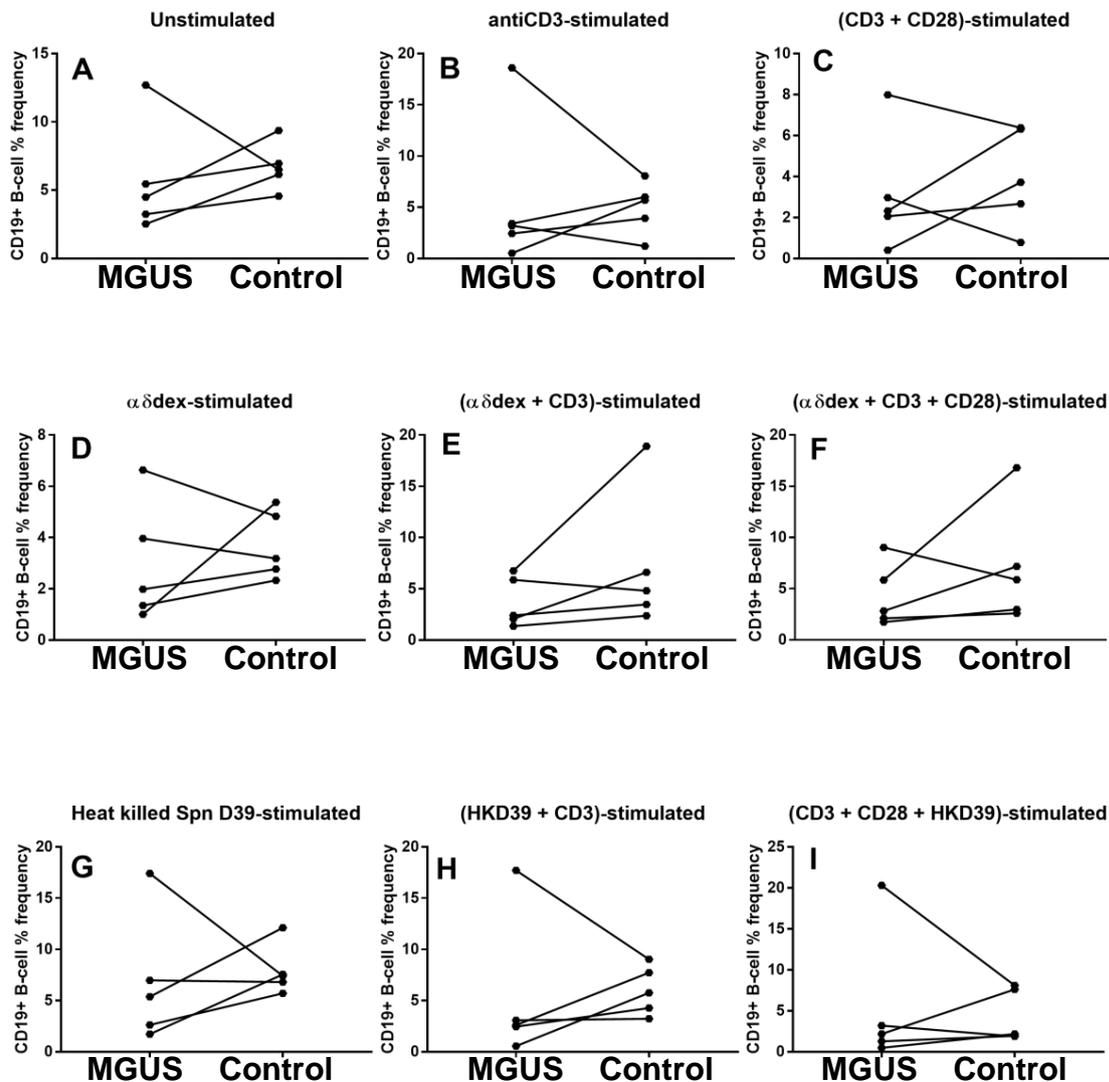
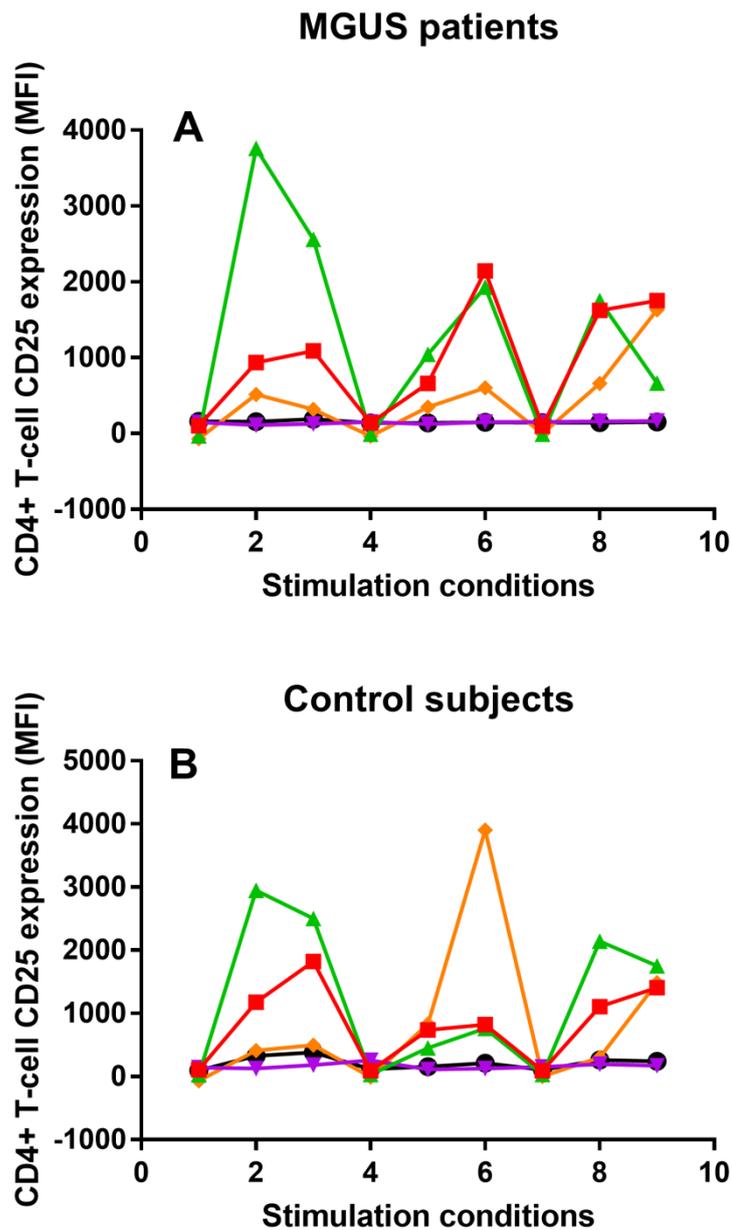**Figure 6.9i: Percentage frequencies of *in vitro* CD19+ B-cells in MGUS patients and matched controls under un-stimulated and stimulated conditions.** Dots and lines match each patient-control pair. The paired-samples *t*-test and Wilcoxon signed ranks test were used for parametric and non-parametric datasets respectively. (Patient n = 5). Concentrations of stimulants used: 1µg/ml of αδdex, 0.1µg/ml anti-CD3 alone, and 0.5µg/ml anti-CD3 in combination with 0.5µg/ml anti-CD28. Patient cohort and control cohort tracking data for this graph grid is presented in fig. 6.9ii.

MGUS patients

Control subjects
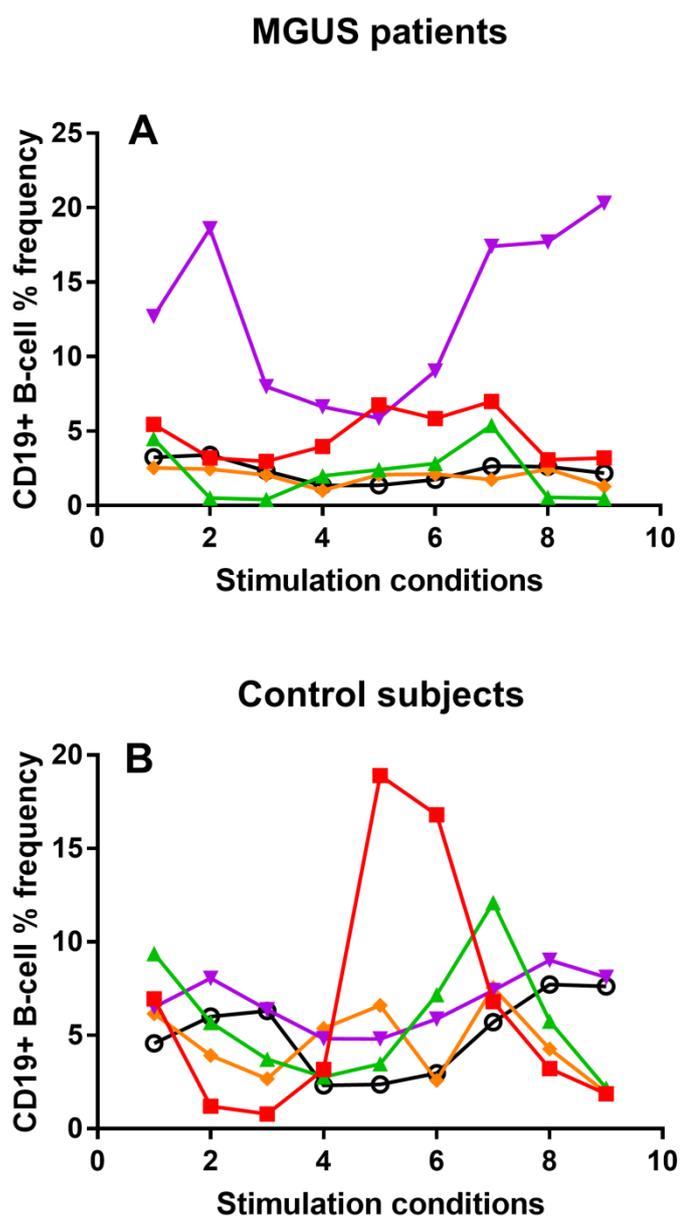
Figure 6.9ii: Tracking data showing the changes in *in vitro* CD19+ B-cell frequencies in MGUS patients (A) and matched controls (B) upon stimulation. Matched patient-control pairs are represented using the same colour across A and B. Conditions: 1; Un-stimulated, 2; CD3-stimulated, 3; (CD3+CD28)-stimulated, 4; αδdex-stimulated, 5; (αδdex +CD3)-stimulated, 6; (αδdex +CD3+CD28)-stimulated, 7; HKD39-stimulated, 8; (HKD39+CD3)-stimulated, 9; (CD3+CD28+HKD39)-stimulated.

In parallel, comparable responses between MGUS patients and matched controls were found for proliferation (fig. 6.10i).
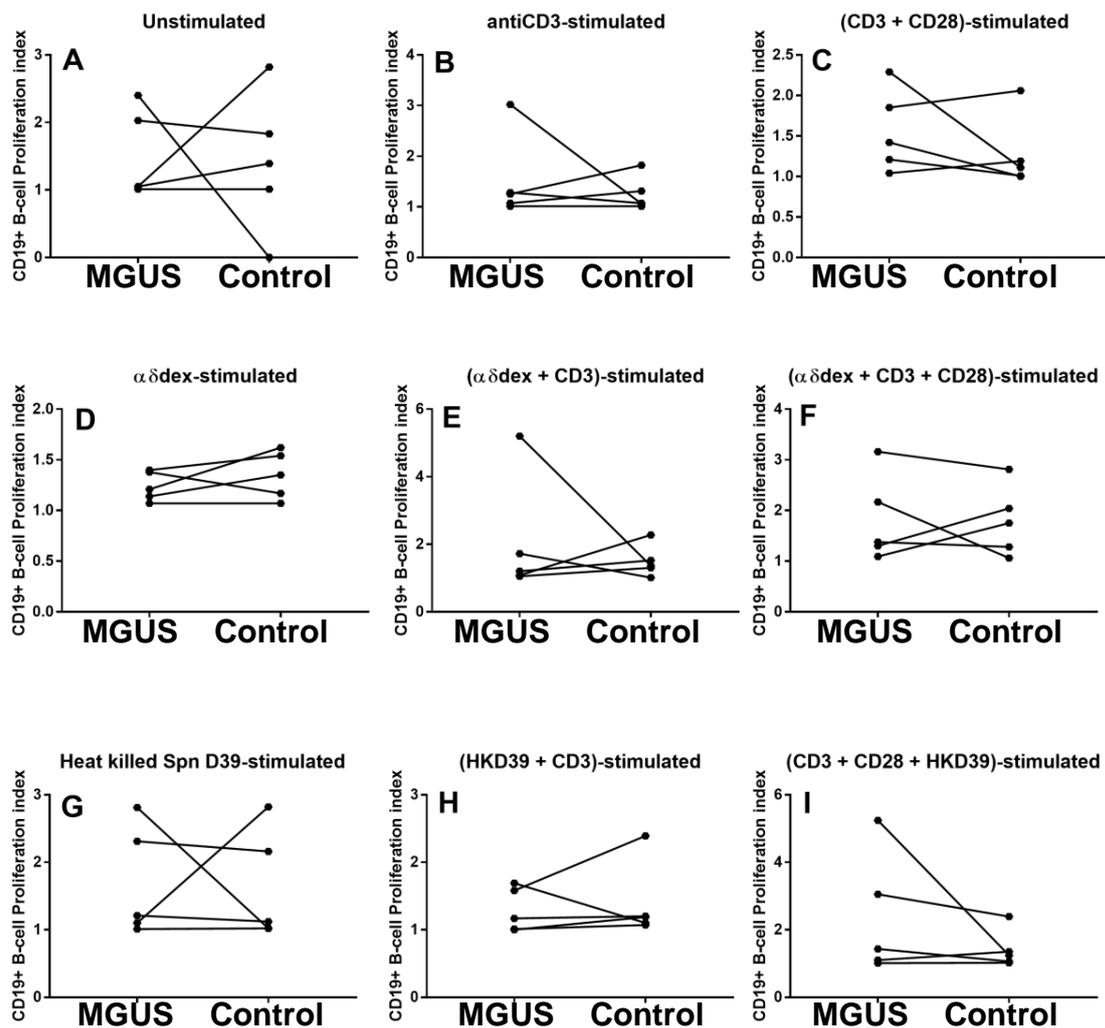
Figure 6.10i: Proliferation of *in vitro* CD19+ B-cells in MGUS patients and matched controls under un-stimulated and stimulated conditions. Dots and lines match each patient-control pair. The paired-samples *t*-test and Wilcoxon signed ranks test were used for parametric and non-parametric datasets respectively. (Patient n = 5). Concentrations of stimulants used: 1µg/ml of αδdex, 0.1µg/ml anti-CD3 alone, and 0.5µg/ml anti-CD3 in combination with 0.5µg/ml anti-CD28. Patient cohort and control cohort tracking data for this graph grid is presented in fig. 6.10ii.
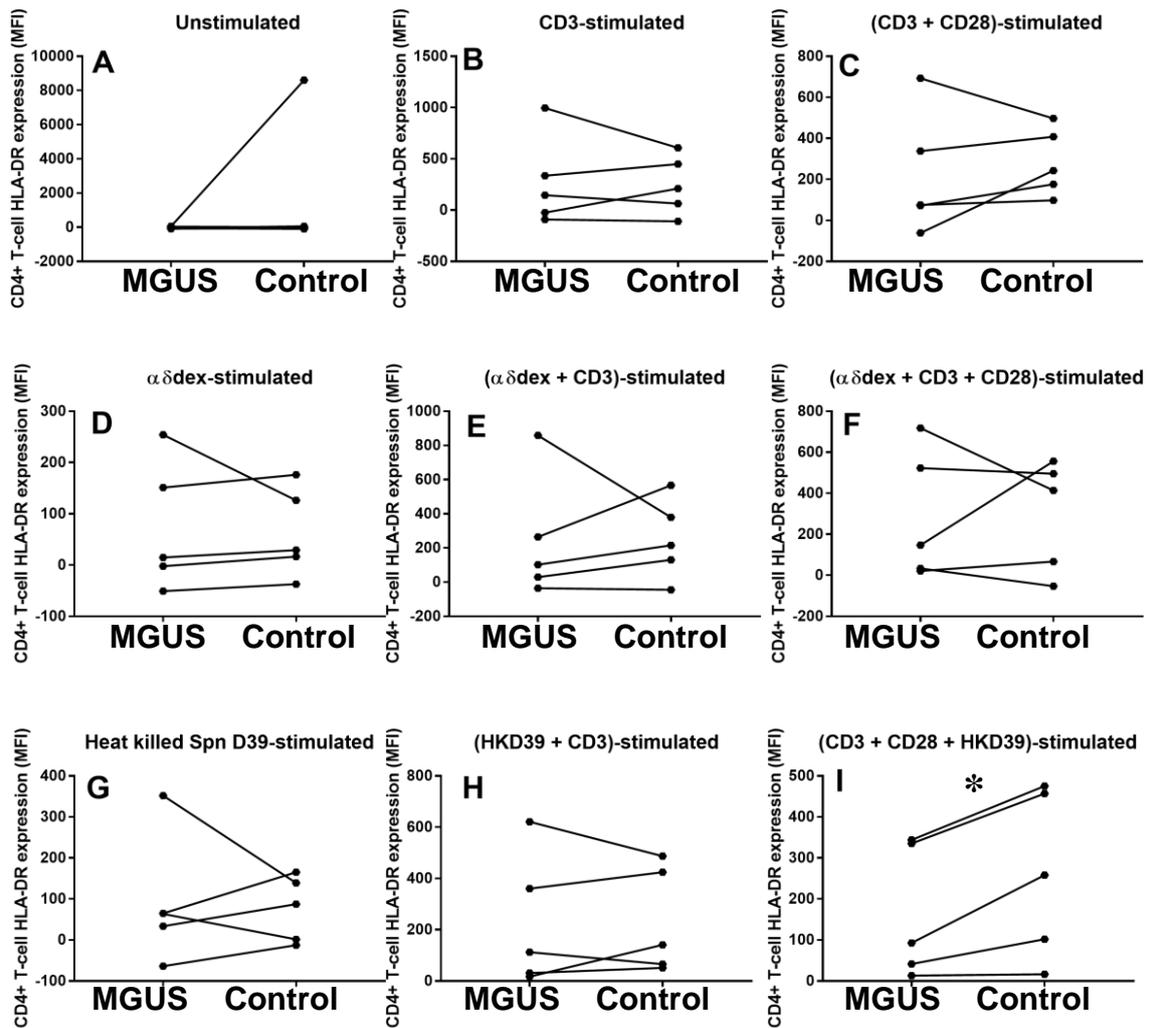
MGUS patients

Control subjects
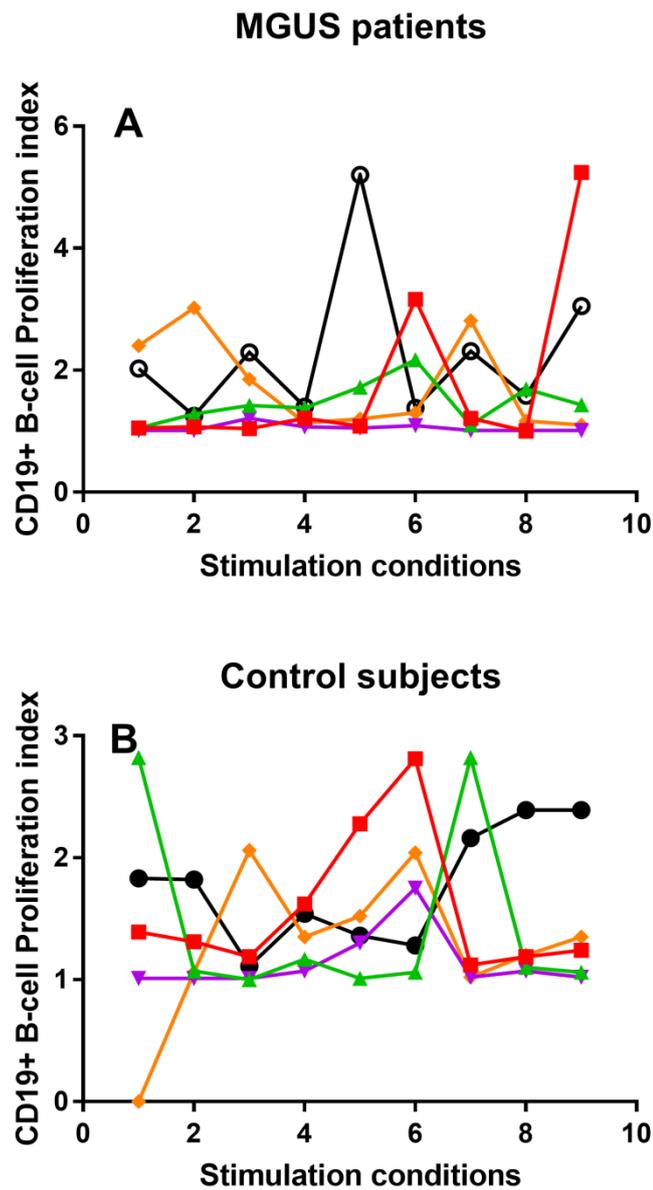
Figure 6.10ii: Tracking data showing the changes in *in vitro* CD19+ B-cell proliferation in MGUS patients (A) and matched controls (B) upon stimulation. Matched patient-control pairs are represented using the same colour across A and B. Conditions: 1; Un-stimulated, 2; CD3-stimulated, 3; (CD3+CD28)-stimulated, 4; αδdex-stimulated, 5; (αδdex +CD3)-stimulated, 6; (αδdex +CD3+CD28)-stimulated, 7; HKD39-stimulated, 8; (HKD39+CD3)-stimulated, 9; (CD3+CD28+HKD39)-stimulated.

Further, *in vitro* CD25 expression was comparable between MGUS patients and controls (fig. 6.11i).
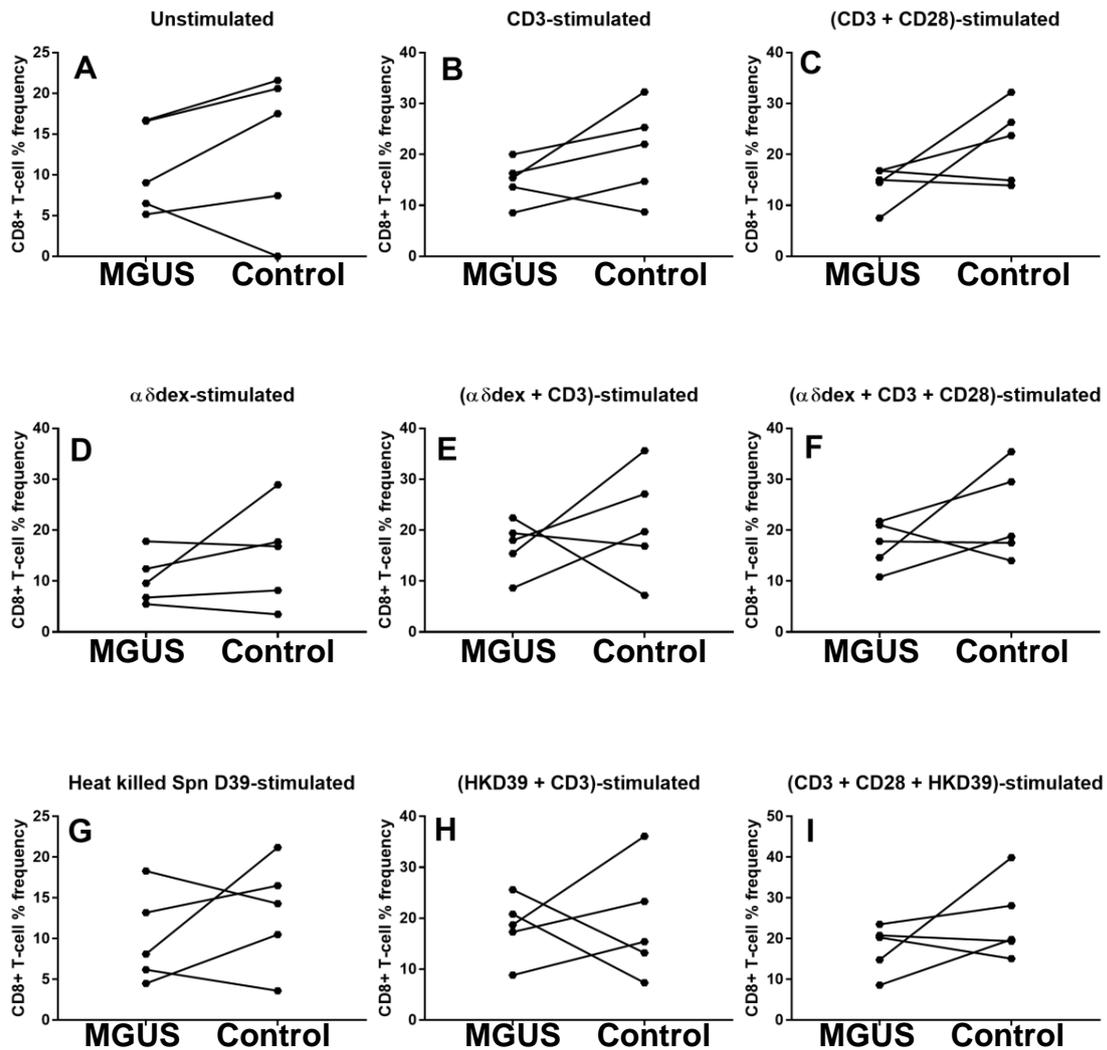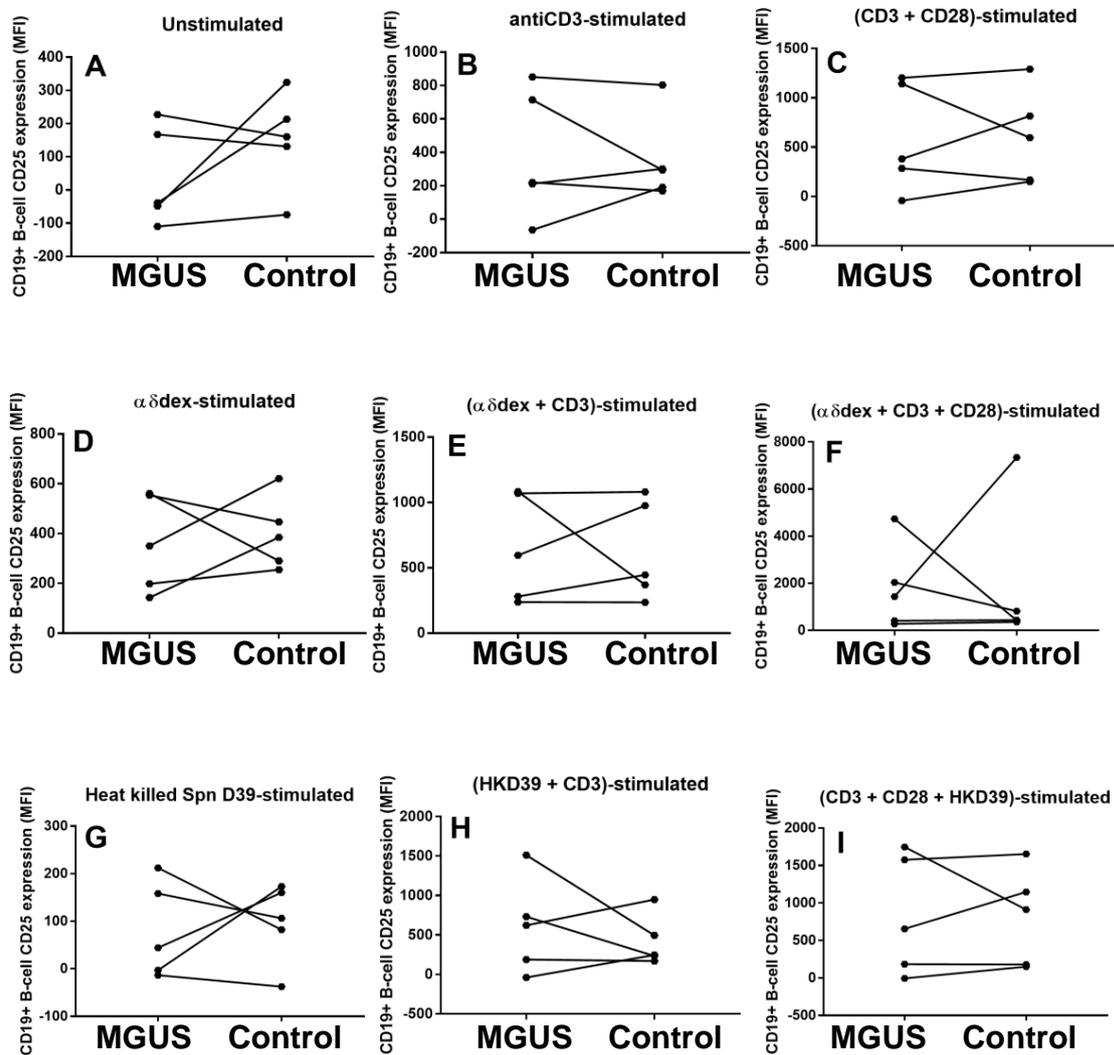

Figure 6.11i: CD25 expression on *in vitro* CD19+ B-cells in MGUS patients and matched controls under un-stimulated and stimulated conditions. Dots and lines match each patient-control pair. The paired-samples *t*-test and Wilcoxon signed ranks test were used for parametric and non-parametric datasets respectively. (Patient n = 5). Concentrations of stimulants used: 1µg/ml of αδdex, 0.1µg/ml anti-CD3 alone, and 0.5µg/ml anti-CD3 in combination with 0.5µg/ml anti-CD28. Patient cohort and control cohort tracking data for this graph grid is presented in fig. 6.11ii.
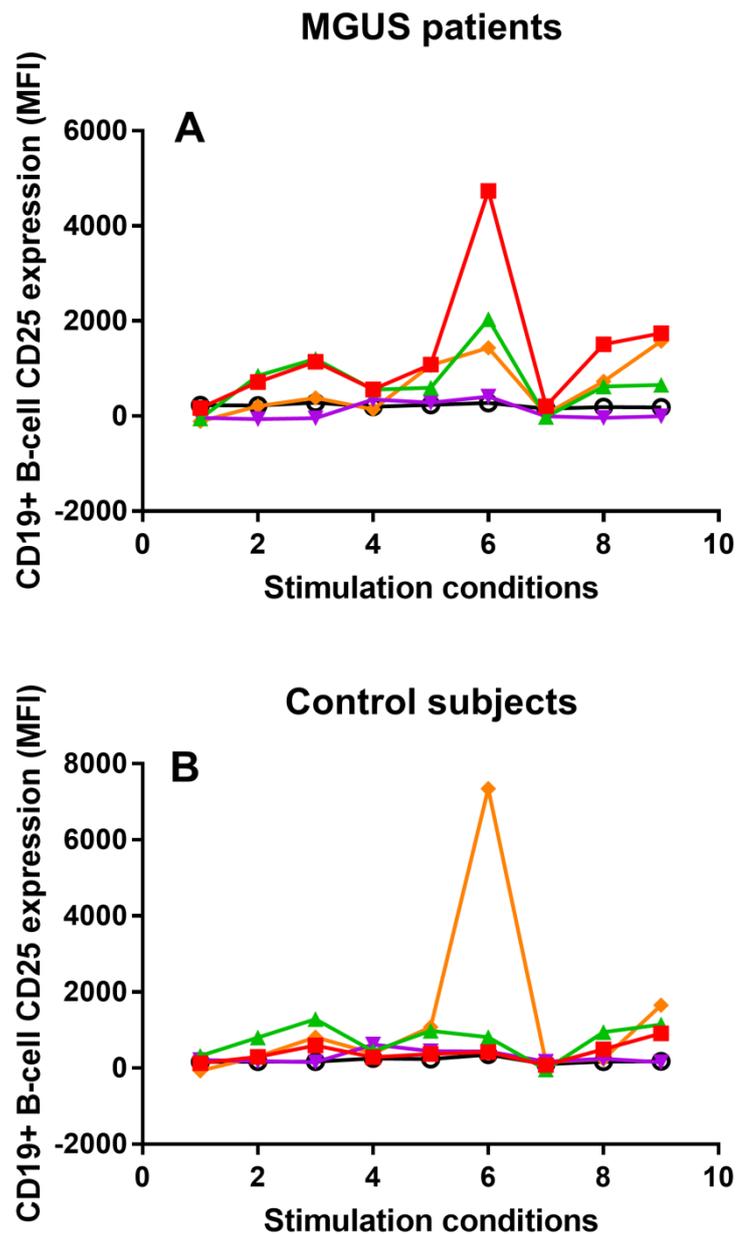
Figure 6.11i: Tracking data showing the changes in *in vitro* CD19+ B-cell CD25 expression in MGUS patients (A) and matched controls (B) upon stimulation. Matched patient-control pairs are represented using the same colour across A and B. Conditions: 1; Un-stimulated, 2; CD3-stimulated, 3; (CD3+CD28)-stimulated, 4; αδdex-stimulated, 5; (αδdex +CD3)-stimulated, 6; (αδdex +CD3+CD28)-stimulated, 7; HKD39-stimulated, 8; (HKD39+CD3)-stimulated, 9; (CD3+CD28+HKD39)-stimulated.

Two more CD19+ B-cell activation markers, CD86 (fig. 6.12i) and HLA-DR (fig. 6.13i) were analysed for any differential responses between patients and controls.
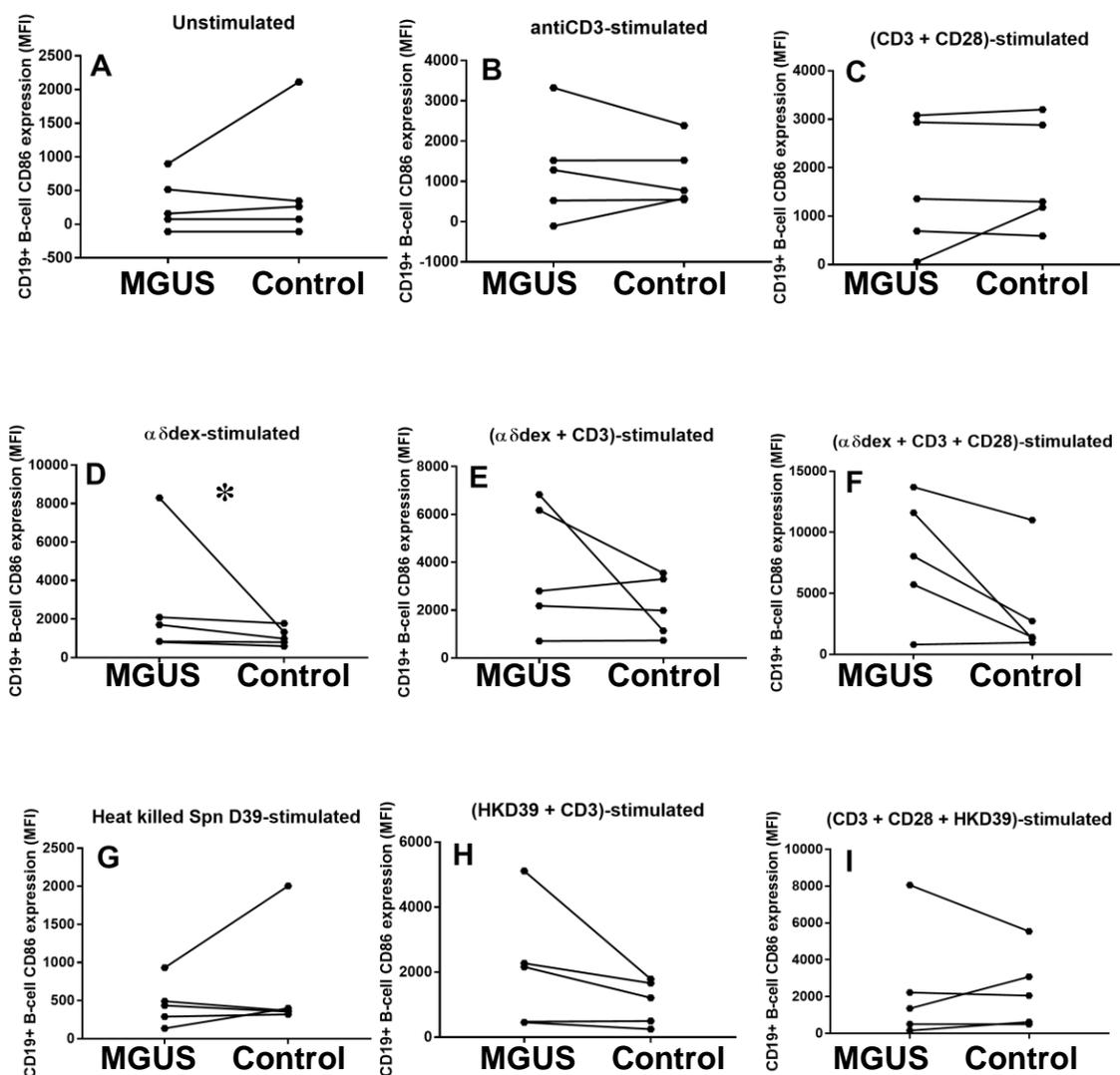
Figure 6.12i: CD86 expression on *in vitro* CD19+ B-cells in MGUS patients and matched controls under un-stimulated and stimulated conditions. Dots and lines match each patient-control pair. The paired-samples *t*-test and Wilcoxon signed ranks test were used for parametric and non-parametric datasets respectively. (Patient n = 5; Where * $p \leq 0.050$). Concentrations of stimulants used: 1µg/ml of αδdex, 0.1µg/ml anti-CD3 alone, and 0.5µg/ml anti-CD3 in combination with 0.5µg/ml anti-CD28. Patient cohort and control cohort tracking data for this graph grid is presented in fig. 6.12ii.
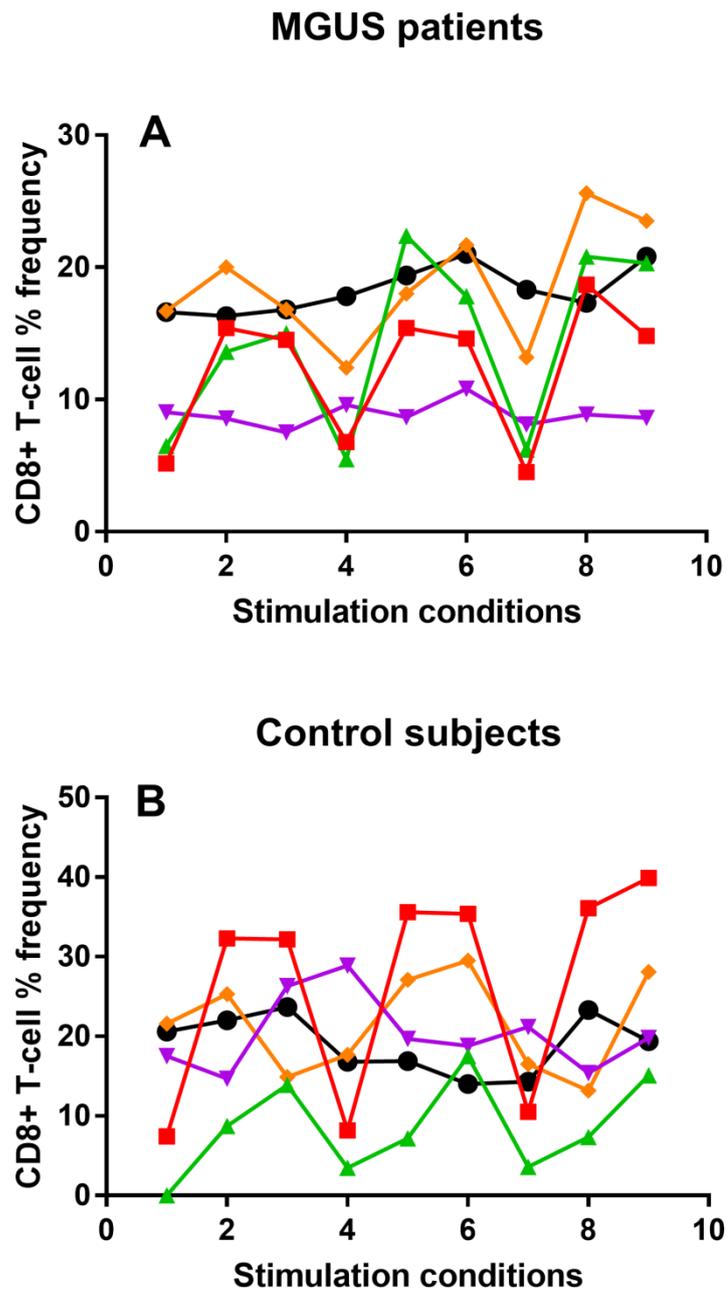
MGUS patients

Control subjects
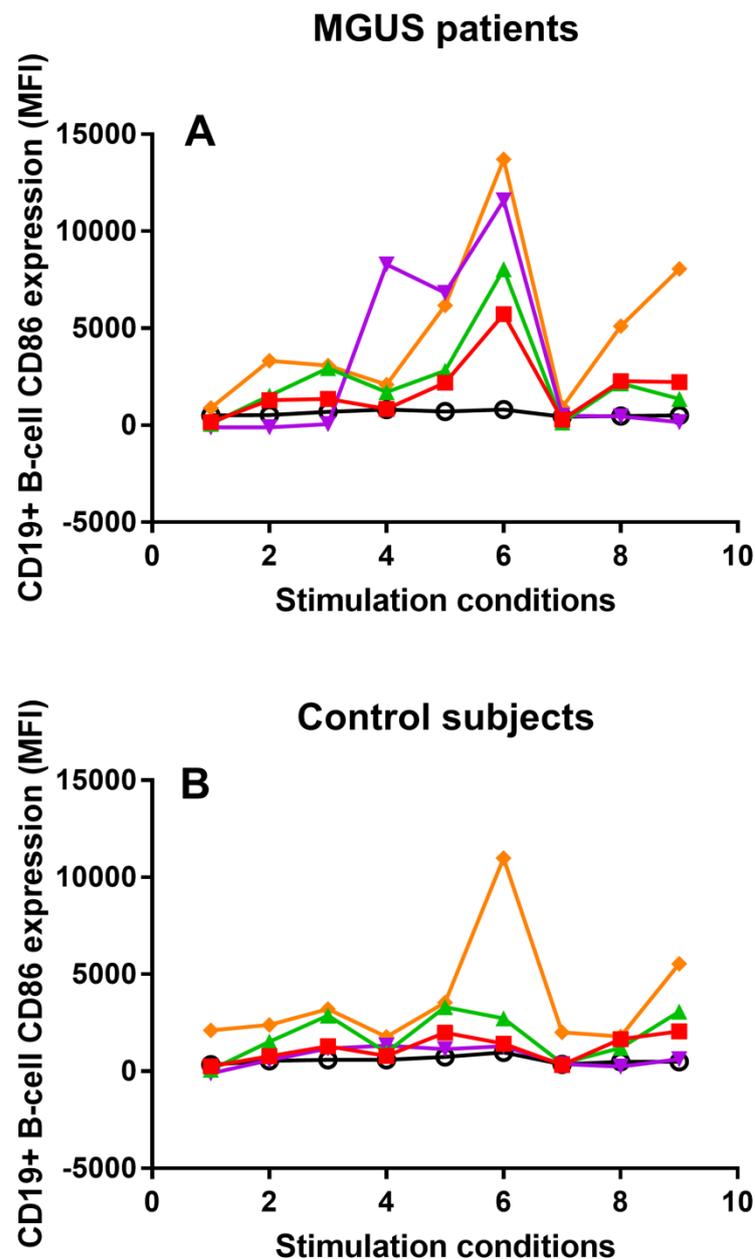
Figure 6.12ii: Tracking data showing the changes in *in vitro* CD19+ B-cell CD86 expression in MGUS patients (A) and matched controls (B) upon stimulation. Matched patient-control pairs are represented using the same colour across A and B. Conditions: 1; Un-stimulated, 2; CD3-stimulated, 3; (CD3+CD28)-stimulated, 4; αδdex-stimulated, 5; (αδdex +CD3)-stimulated, 6; (αδdex +CD3+CD28)-stimulated, 7; HKD39-stimulated, 8; (HKD39+CD3)-stimulated, 9; (CD3+CD28+HKD39)-stimulated.
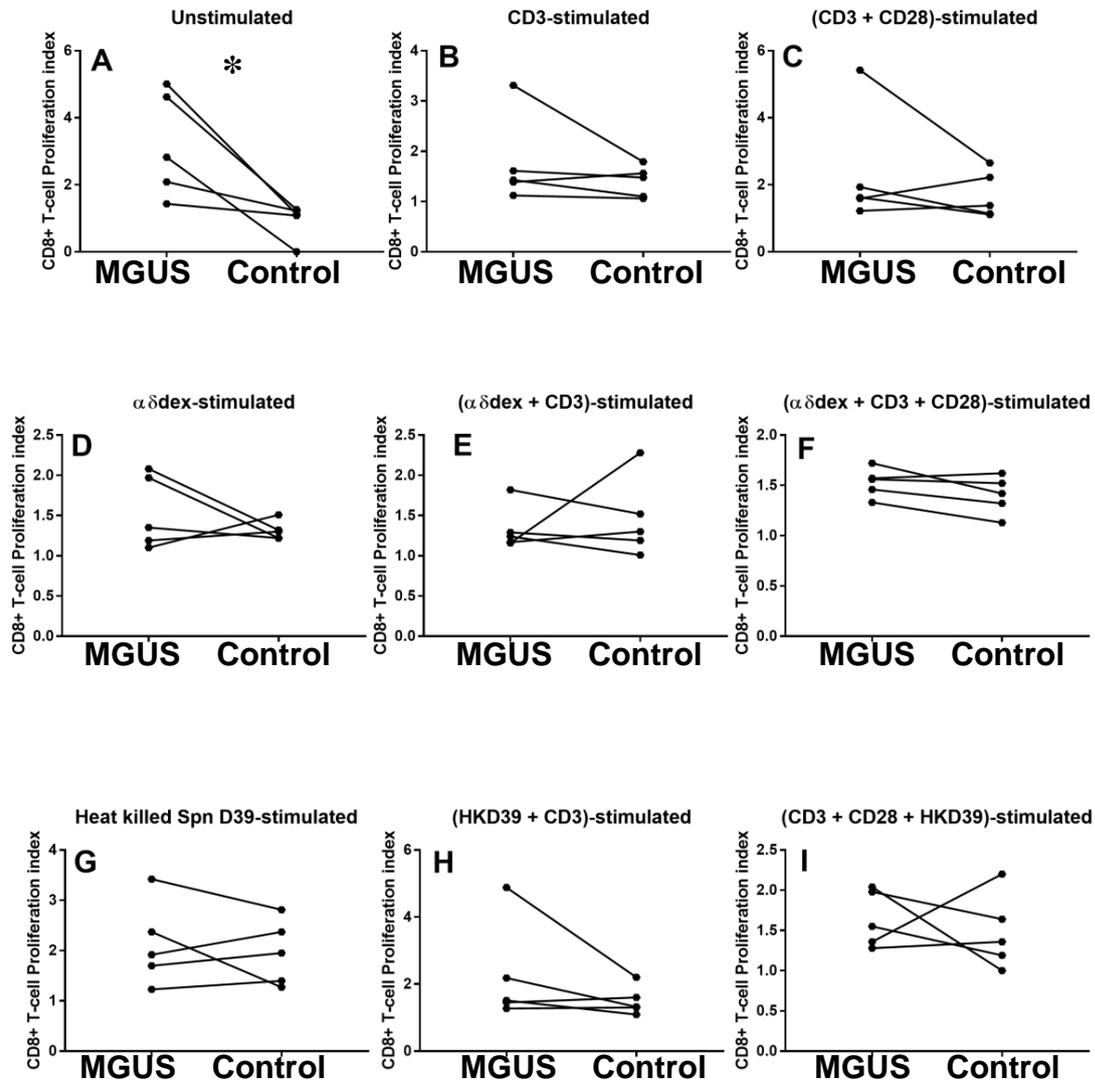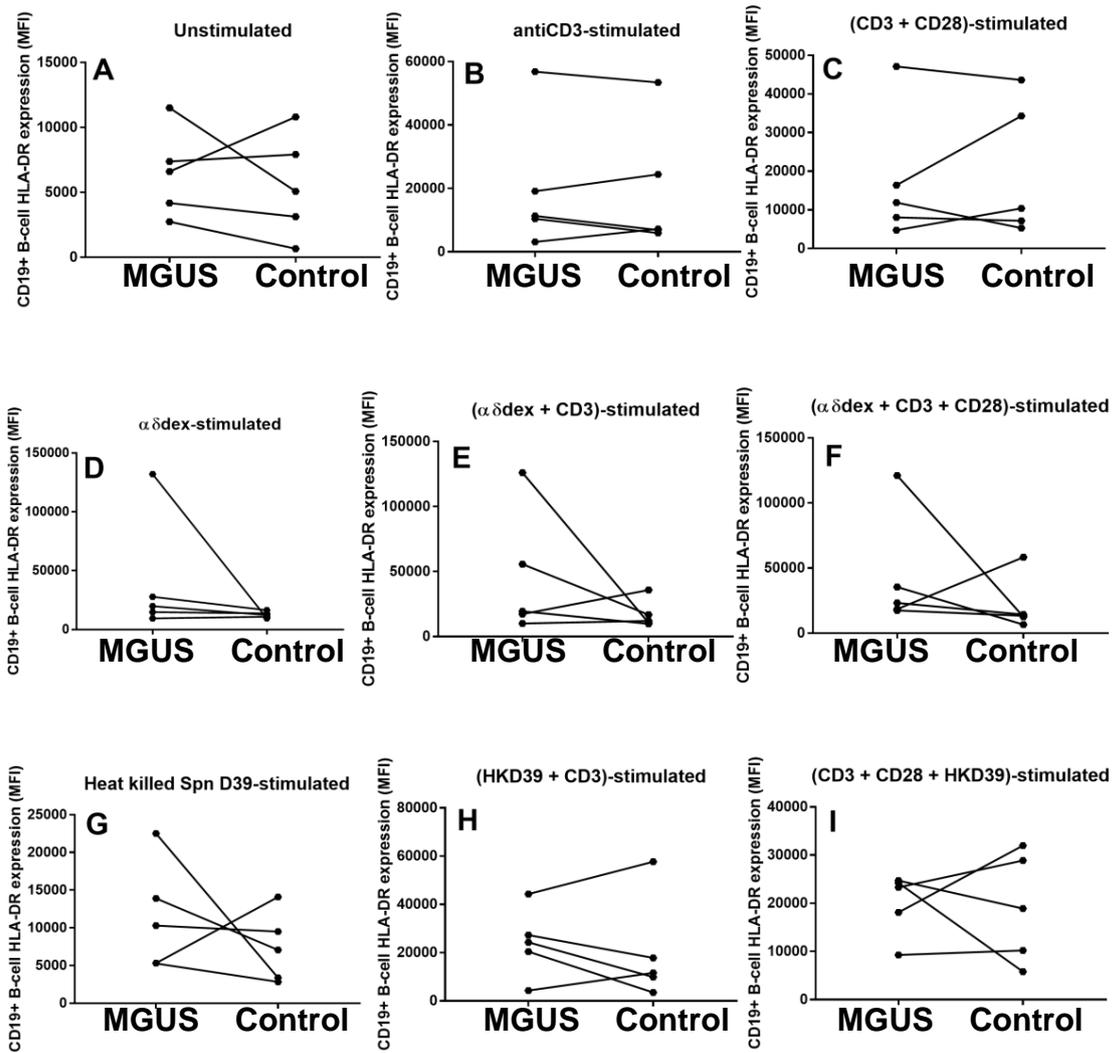
Figure 6.13i: HLA-DR expression on *in vitro* CD19+ B-cells in MGUS patients and matched controls under un-stimulated and stimulated conditions. Dots and lines match each patient-control pair. The paired-samples *t*-test and Wilcoxon signed ranks test were used for parametric and non-parametric datasets respectively. (Patient n = 5). Concentrations of stimulants used: 1µg/ml of αδdex, 0.1µg/ml anti-CD3 alone, and 0.5µg/ml anti-CD3 in combination with 0.5µg/ml anti-CD28. Patient cohort and control cohort tracking data for this graph grid is presented in fig. 6.13ii.

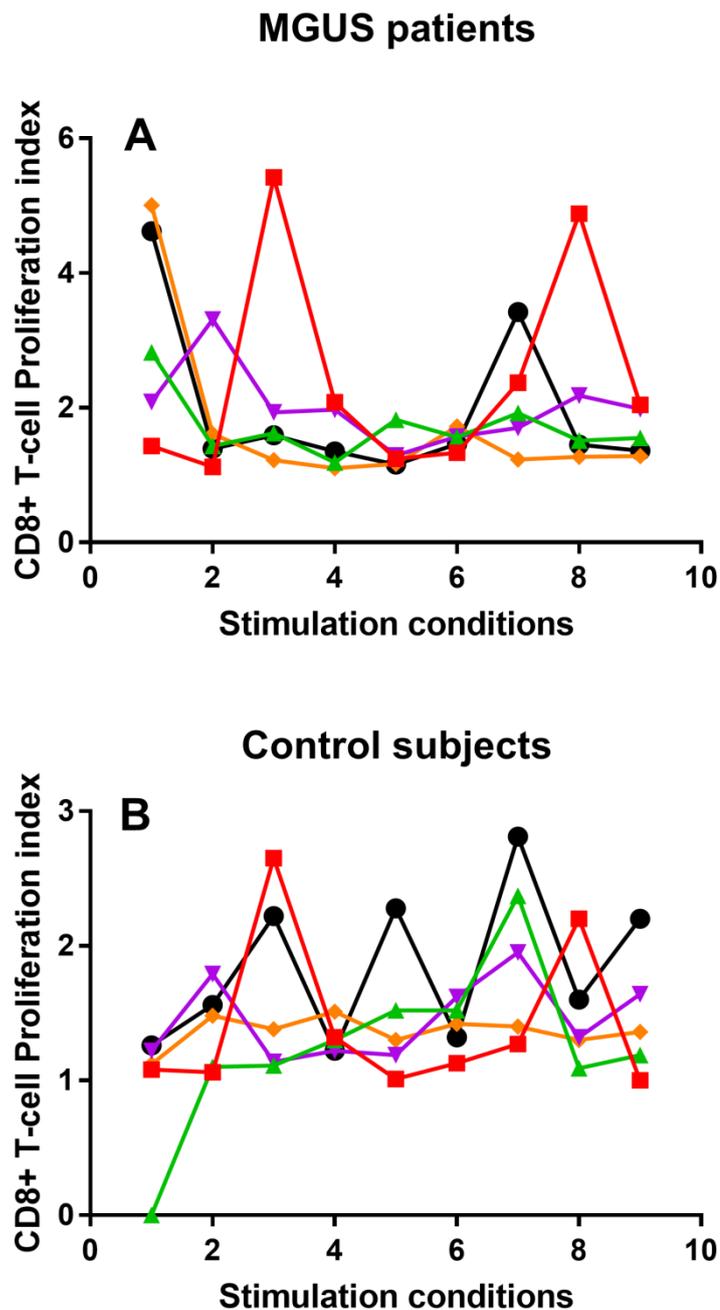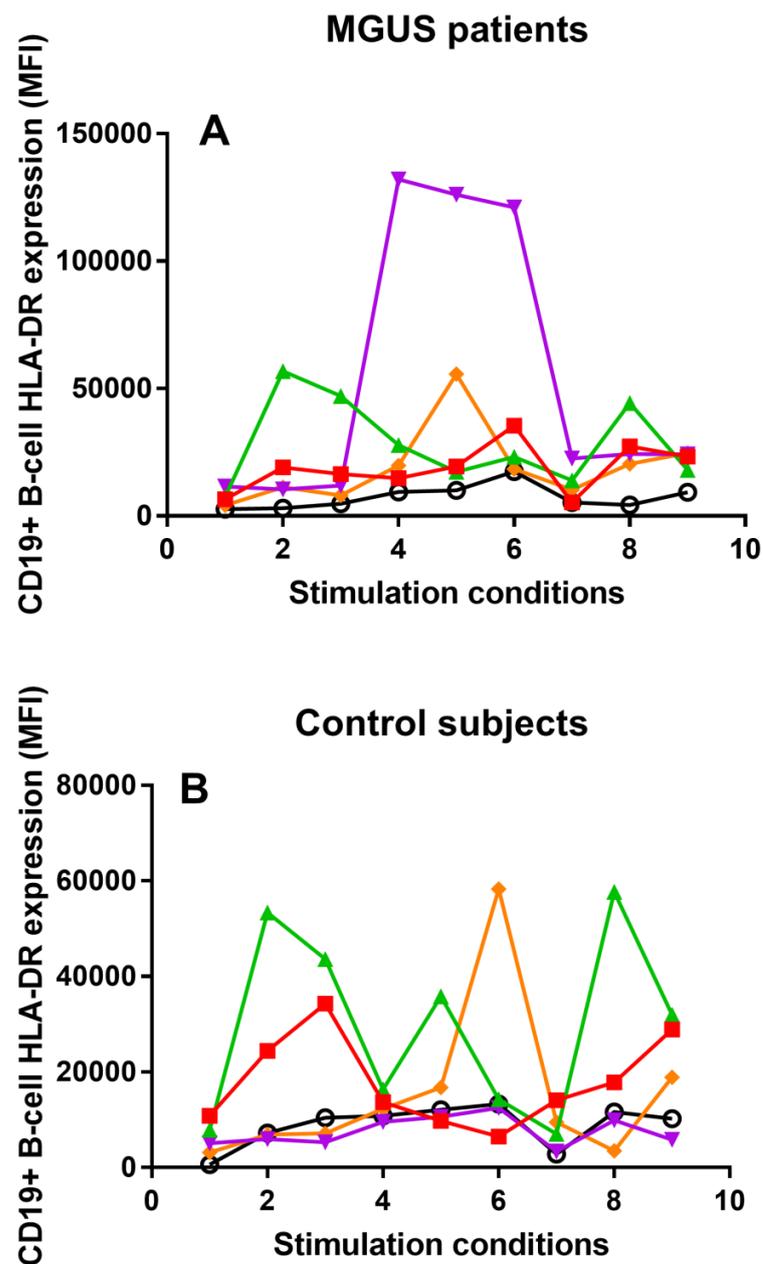**Figure 6.13ii: Tracking data showing the changes in *in vitro* CD19+ B-cell HLA-DR expression in MGUS patients (A) and matched controls (B) upon stimulation.** Matched patient-control pairs are represented using the same colour across A and B. Conditions: 1; Un-stimulated, 2; CD3-stimulated, 3; (CD3+CD28)-stimulated, 4; αδdex-stimulated, 5; (αδdex +CD3)-stimulated, 6; (αδdex +CD3+CD28)-stimulated, 7; HKD39-stimulated, 8; (HKD39+CD3)-stimulated, 9; (CD3+CD28+HKD39)-stimulated.

6.4 Discussion of Findings

Hypothesizing that patients from different points on the myeloma spectrum would likely have variable *in vitro* T- and B-cell responses to polyclonal and pneumococcal stimulation, recruitment was focused on MGUS patients. In a cohort comprising five MGUS patients and age-, sex- and ethnicity-matched controls, no differential responses were found for CD4+ T-cell frequency (fig. 6.1i), proliferation (fig. 6.2i), or CD25 expression (fig. 6.3i). It is important to note that the immunologic assay based on αδdex had previously been powered at a sample size of 10 (Foster et al., 2009, Foster et al., 2010, Darton et al., 2011). Therefore results presented in this chapter need to be interpreted with caution. Furthermore, because MGUS falls at the beginning of the myeloma spectrum, the five patients studied would show different outcomes: some may respond more like controls than others. Interestingly, *in vitro* TCR stimulation and CD28 co-stimulation of CD4+ T-cells, in the presence of HKD39, elicited significantly higher HLA-DR expression levels in controls, compared to patients ($p \leq 0.050$; fig. 6.4i I).

And while no significantly different responses between MGUS patients and controls were found for CD8+ T-cell frequency distribution (fig. 6.5i) or HLA-DR expression (fig. 6.8i), proliferation (fig. 6.4i) and CD25 expression (fig. 6.5i) yielded differences. The MGUS patients had significantly higher *in vitro* CD8+ T-cell proliferation than controls under un-stimulated conditions ($p \leq 0.050$; fig. 6.6i A) which became comparable to control responses upon stimulation (fig. 6.6i). This echoes the findings of Halapi and colleagues, showing significant CD8+ T-cell expansions ($p < 0.001$) in MGUS patients (Halapi et al., 1997). Further, the MGUS patients also expressed significantly higher *in vitro* levels of CD25 on CD8+ T-cells under un-stimulated conditions ($p \leq 0.050$; fig. 6.7i A) compared to controls. However, upon stimulation with anti-CD3 and CD28-costimulation, it was control CD8+ T-cells that expressed higher levels of CD25 *in vitro* ($p \leq 0.010$; fig. 6.7i C). In addition, stimulation with HKD39 also led to higher *in vitro* levels of CD25 on CD8+ T-cells of controls compared to patients ($p \leq 0.050$; fig. 6.7i G).

To investigate if defects could be detected within the CD19+ B-cell population of MGUS patients, frequency distribution of B-cells, proliferation, and activation were studied. No significant differences were found between MGUS patients and controls for *in vitro* CD19+ B-cell frequency distribution (fig. 6.9i), proliferation (fig. 6.10i), CD25 expression (fig. 6.11i), or HLA-DR expression (fig. 6.13i). Further, the significance emerging after αδdex-stimulation in terms of CD86 expression within the MGUS patient cohort ($p \leq 0.050$; fig. 6.12i D) was most likely due to one outlier patient data point.

6.5 Conclusion

In a cohort of five MGUS patients and age-, sex- and ethnicity-matched controls, differential T-cell responses were detected. Control CD4+ T-cells stimulated by anti-CD3 and costimulated by anti-CD28 in the presence of HKD39 expressed higher levels of HLA-DR, compared to patients. The CD8+ T-cell subset also yielded differential responses. MGUS patients had higher *in vitro* proliferation of CD8+ T-cells and CD25 expression, both under un-stimulated conditions. Upon stimulation with anti-CD3 and anti-CD28, and with HKD39 alone, control CD8+ T-cells expressed higher CD25 levels compared to patients. No significant differences were found for the B-cell parameters measured, between MGUS patients and controls. Only in the case of αδdex-stimulated CD86 expression which was likely due to one outlier data point. It cannot be concluded that within this cohort of five MGUS patients a defect in B-cells was detected. However, this should not rule out the possibility of such a defect existing within this patient group, or within other patient groups that fall in the symptomatic myeloma spectrum. An increase in sample size of MGUS patients (n ≥ 10), and investigation within other myeloma patient groups would shed more light on T- and B-cell defects in this immunocompromised group, which potentially contributes to their predisposition to pneumococcal disease.

CHAPTER SEVEN: DISCUSSION

Because a discussion of the main findings was provided in each results chapter, the aim of this overall discussion chapter is to provide a summary of the findings within this research project. Also, to outline some methodological criticisms which may have impacted on data collection and interpretation. Finally, to detail the future direction this work could take to provide deeper insight, as well as the clinical implications of the main findings.

This project aimed to investigate T- and B-cell responses in HIV-infected individuals and MGUS patients to polyclonal- and pneumococcal-stimulation, compared to matched controls, with the aim of uncovering subtle defects *in vitro* in patients which could be responsible for their higher risk of developing pneumococcal disease.

7.1 Main findings

7.1.1 Chapter 3- The effect of age, sex and ethnicity on T- and B-cell responses

Chapter three reports reproducibility in the immunologic stimulation assay that our group developed (Foster et al., 2009). The main findings highlighted in this chapter however are that age significantly correlates with *in vitro* CD4+ T-cell activation upon stimulation with αδdex and anti-CD3. There is a significant reduction in the *in vitro* un-stimulated CD86 expression on CD19+ B-cells with advancing age that disappears upon stimulation with αδdex alone and in combination with T-cell help. A limitation to this portion of the study was the small numbers amongst individuals older than 40 years.

Sex was also shown to impact *in vitro* B-cell responses, with males showing significantly higher B-cell activation (in terms of CD86 expression) upon stimulation with αδdex alone and in combination with T-cell help. No differences between females and males was found for T-cell activation.

Finally, strong ethnicity-based variations were found in *in vitro* T-cell responses. White individuals showed higher un-stimulated T-cell activation (in terms of CD25 expression) compared to Black individuals which persisted after anti-CD3-stimulation alone and with anti-CD28 costimulation. Interestingly, αδdex-stimulation elicited higher B-cell proliferation in Black compared to White individuals, which was absent under un-stimulated conditions and which disappeared upon T-cell help. Further, White individuals once more exhibited higher B-cell activation in the presence of T-cell help.

The implications of these findings are that age, sex and ethnicity are factors that need to be strictly accounted for in case-control studies.

7.1.2 Chapter 4- T- and B-cell responses in HIV-infected individuals following polyclonal and pneumococcal stimulation

There were three cell populations of interest to be studied in the HIV-infected cohort: CD4+ and CD8+ T-cells, and CD19+ B-cells. Based on finding defective B-cell responses in previous sufferers of IPD (Darton et al., 2011) and MenC disease (Foster et al., 2009) as well as MenC adolescent vaccine failures (Foster et al., 2010), this portion of the study hypothesized that immunocompromised patients would likely also exhibit defective B-cell responses that increase their likelihood of developing pneumococcal disease.

The *in vitro* work conducted on 16 HIV-infected individuals and matched controls did indeed reveal strong anti-CD3-stimulated hyperactivation in the patient CD8+ T-cell population. Further, T-cell-helped pneumococcal-stimulation induced higher B-cell proliferation in patients. In the context of pneumococcal disease, this CD19+ B-cell proliferation was noteworthy in light of the B-cell subset perturbations that have been reported in viraemic HIV (Moir and Fauci, 2013). The results in this portion of the study indicated

hyperactivation of CD8+ T-cells and aberrant proliferation of CD19+ B-cells in HIV-infected individuals inspite of ART-usage and viral suppression.

The association of defective B-cell responses to an increased risk of pneumococcal disease (Foster et al., 2009; Darton et al., 2011), the 35-fold increased likelihood of HIV patients developing pneumococcal disease compared to their uninfected counterparts even in the HAART era (Heffernan et al., 2005), and B-cell subset perturbations in viraemic HIV (Moir and Fauci, 2013) necessitated further investigation into B-cell subset responses within the 16 HIV-infected individuals in the present study.

7.1.3 Chapter 5- B-cell subset responses in HIV-infected individuals following polyclonal and pneumococcal stimulation

Chapter five demonstrates that even with ART-usage and viral suppression, hyperactivation after αδdex-stimulation occurs particularly within the plasmablast B-cell subset population of HIV-infected. Further, higher *in vitro* CD86 expression under un-stimulated conditions was uncovered in the patient activated memory B-cells, which persisted upon pneumococcal-stimulation. Because caspase levels correlate with B-cell exhaustion in HIV-viraemic patients (Nicholas et al., 2013) the present study hypothesized an increase in caspase levels within the patient group. While most of the patients did show higher un-stimulated and αδdex-stimulated caspase levels compared to controls, these were not significant (patient n = 5). Nonetheless, the hyperactivation in plasmablasts and activated memory B-cells represent a subtle defect uncovered in 16 ART-using, virally-suppressed HIV-infected individuals.

7.1.4 Chapter 6- The effect of polyclonal and pneumococcal stimulation on T- and B-cells in a cohort of MGUS patients

To investigate the effectiveness of T- and B-cell responses to the immunologic stimulation assay in a second immunocompromised patient group, MGUS patients were recruited with matched controls. Before data

analysis was conducted, it was clear that conlusions would have to be drawn with caution due to the small numbers within the study (patient n = 5). Despite these small numbers however, a strong CD3-stimulated and CD28-costimulated higher *in vitro* expression of CD25 was found on the CD8+ T-cells of controls, compared to the patients. While numbers would have to be increased before conclusively stating that this represents a defect in MGUS patients CD8+ T-cell responses, the strength of the significance ($p \leq 0.010$) suggests that further study is warranted. The results however do suggest that in the case of the MGUS patients, a defect is present in T-cells, rather than B-cells. This could pose a significant problem during the cytotoxic effector arm of immune responses (Andersen et al., 2006).

7.2 Methodological criticisms

7.2.1 Chapter 3- The effect of age, sex and ethnicity on T- and B-cell responses

One of the areas in which variability could have been introduced into this portion of the study lies within the recruitment of individuals for studying the effects of age, sex and ethnicity on T- and B-cell responses. Due to the fact that individuals were recruited across a number of years for the age and sex studies (due to incorporating data previously collected by James Wing; a member of our group), there was room for human error to be introduced first from two different individuals handling sample acquisition and data processing. The day-to-day variability in the assay would have further added a margin of error to these two studies, and to the ethnicity study.

7.2.2 Chapter 4- T- and B-cell responses in HIV-infected individuals following polyclonal and pneumococcal stimulation

Pre-handling data, one of the points at which error could have been introduced into this portion of the study was during control recruitment. Controls were recruited under the assumption of HIV-uninfected status at the

time of bleed. Had any of these controls been infected, this would have counteracted any difference to be seen in their particular patient-control pair. In order to minimise day-to-day variability in the assay and enable the usage of statistical paired testing, patient-control pairs were bled on the same day, usually within one hour of each other. From then on samples were handled in the same way.

It is possible however that error was introduced during the flow cytometry protocol. Firstly, antibodies produced from the same clone and across different lots can exhibit bioactivity variation, even when produced by the same company (Li et al., 2010). Thus, the use of different antibody lots within the time frame of this project could have introduced variability. Second, compensation in multi-colour flow cytometry can introduce another margin of error into data (Roederer, 2002). To circumvent this, the FACSDiva™ software package was used in conjunction with compensation controls and optimised voltages. The third point at which error could have been introduced was at the point of flow cytometry gating, which can be subjective. The use of fluorescence-minus-one (FMO) controls per experiment should have minimised this error however.

7.2.3 Chapter 5- B-cell subset responses in HIV-infected individuals following polyclonal and pneumococcal stimulation

Much like chapter four, errors could have been introduced into this portion of the study during patient recruitment and the flow cytometry protocol. Specifically as the gating strategy used in chapter five was more detailed, and called for the separation of plasmablasts and activated memory cells based on 'high' and 'intermediate' levels of CD27 expression. The use of FMO controls and consultation with technical staff at the Flow Cytometry Core Facility at Sheffield Medical School during optimisation of the gating strategy should have minimised these errors.

7.2.4 Chapter 6- The effect of polyclonal and pneumococcal stimulation on T- and B-cells in a cohort of MGUS patients

The points raised for the patients recruitment and flow cytometry protocol within the HIV cohort are applicable to the MGUS cohort.

7.3 Future work and clinical considerations

7.3.1 Chapter 3- The effect of age, sex and ethnicity on T- and B-cell responses

The sex-based variability in B-cell activation seen in this study may have implications on the influence of sex in vaccine responses. Particularly as sex-differential effects of vaccines have been reported, perhaps with a future for personalised vaccines that will account for these differences (Flanagan and Plebanski, 2017). Importantly also, the ethnicity-based influence on T-cell activation uncovered in this study may contribute towards the ongoing debate on the influence of ethnicity on disease susceptibility and treatment outcomes (Feller et al., 2014).

One way this study can be taken forward is to include more numbers per age, sex and ethnicity study groups. More ethnicities could also be included. Furthermore, to expand these functional studies, more parameters other than the markers used in the present study could be included.

7.3.2 Chapter 4- T- and B-cell responses in HIV-infected individuals following polyclonal and pneumococcal stimulation

While much is known about the polyclonal hyperactivation of T- and B-cells in HIV-viraemic patients (Meyaard et al., 1992, Appay and Sauce, 2008, Day et al., 2006, Nicholas et al., 2013), the present study sought to elucidate why even in the era of HAART, HIV-infected individuals are still 35-fold more likely to develop IPD than uninfected individuals (Heffernan et al., 2005,

Westerink et al., 2012). Results in chapter four demonstrate that even with ART-usage and viral suppression, hyperactivation of T- and B-cells still persists. Most notably in the context of pneumococcal disease, the results showing increased B-cell proliferation in patients upon T-cell-helped pneumococcal-stimulation. The CD3-stimulated hyperactivation in the patient CD8+ T-cell population also has implications regarding T-cell exhaustion (Haas et al., 2011, Okoye and Picker, 2013, Mauricio Rueda et al., 2012, Ott et al., 1997). In conjunction with studies into improved adjuvantion for pneumococcal vaccines specifically for HIV-infected individuals, it would be beneficial to study mechanisms in which hyperactivation inspite of ART-usage can be dampened.

A transcriptomics study to investigate gene expression changes (Lowe et al., 2017) between HIV-infected individuals and matched controls after *in vitro* polyclonal- and pneumococcal-stimulation, compared to *ex vivo* samples, may provide more clues about mechanisms underlying pneumococcal disease development. Additionally, an expanded cohort in which nasal swabs are included to ascertain carriage/colonisation could strengthen conclusions drawn. Lastly, extending this study to include HIV-infected individuals (and controls) with known history of pneumococcal vaccination and comparing the effectiveness of their T- and B-cell responses to their unvaccinated counterparts may provide important information regarding how vaccine adjuvants can be improved.

7.3.3 Chapter 5- B-cell subset responses in HIV-infected individuals following polyclonal and pneumococcal stimulation

Plasmablasts and activated memory B-cells in HIV viraemia arise as a result of HIV-induced immune activation (Moir and Fauci, 2013). While HAART has been found to normalise B-cell subsets in asymptomatic individuals (Fogli et al., 2012), results in chapter five suggest that a subtle defect in B-cell subsets still persists despite ART-usage. These results may have clinical implications in terms of which B-cell subsets can be targeted to suppress hyperactivation in the context of pneumococcal vaccine-induced immunity.

Plasmablast responses have been speculated to be predictive for later immunity, most probably deriving from memory B-cells and circulating in peripheral blood 6 – 7 days post-infection or immunisation (Fink, 2012). The polyclonal-induced hyperactivation in PBs and antigen-specific activation in AMs of HIV-infected individuals in the present study have implications on anti-pneumococcal immunity. This hyperactivation could trend both PBs (Nicholas et al., 2013) and AMs in the patients to exhaustion (Moir and Fauci, 2017). These results suggest that the PB and AM B-cell subsets may play a significant role in the increased likelihood of HIV-infected individuals developing pneumococcal disease.

There is still the need for these results to be reproduced however. In addition, for the numbers in the cohort to be increased. It would be interesting to see if this expanded cohort of patients would show significantly higher caspase levels compared to controls. It may also be useful to include a cohort of viraemic patients and study how their responses differ to ART-users.

7.3.4 Chapter 6- The effect of polyclonal and pneumococcal stimulation on T- and B-cells in a cohort of MGUS patients

A study across the spectrum of haematological malignancies (including asymptomatic and symptomatic patients) may highlight T- and B-cell defects in patients. This may provide more clarity on how these patients' immunity to pneumococcal disease can be boosted.

7.4 Overall considerations

Work conducted in this project uncovered a subtle *in vitro* defect in the B-cell subsets of ART-using, virally suppressed HIV-infected individuals, which presented as a hyperactivation response. Particularly, the plasmablast and activated memory B-cell subsets which showed αδdex-stimulated and HKD39-stimulated hyperactivion, respectively. Conversley, *in vitro* hypoactivation in polyclonally-stimulated CD8+ T-cells of MGUS patients was uncovered. Both these patient groups are known to have a higher risk of developing pneumococcal disease. Thus, results presented in this thesis suggest that immunocompromised individuals may exhibit either hyper- or hypoactivation responses to polyclonal-stimulation. If these *in vitro* responses mimic those *in vivo*, these may represent subtle defects which put these immunocompromised patients at risk of developing pneumococcal disease.

ABDULLAH, M., CHAI, P.-S., CHONG, M.-Y., TOHIT, E. R. M., RAMASAMY, R., PEI, C. P. & VIDYADARAN, S. 2012. Gender effect on in vitro lymphocyte subset levels of healthy individuals. *Cellular Immunology,* 272**,** 214-219.

AIDSINFO. 2017. *FDA-Approved HIV Medicines* [Online]. Available: https://aidsinfo.nih.gov/understanding-hiv-aids/fact-sheets/21/58/fda-approved-hiv-medicines [Accessed 7 September 2017].

ALONSODEVELASCO, E., VERHEUL, A. F. M., VERHOEF, J. & SNIPPE, H. 1995. STREPTOCOCCUS-PNEUMONIAE - VIRULENCE FACTORS, PATHOGENESIS, AND VACCINES. *Microbiological Reviews,* 59**,** 591-&.

AMMANN, A. J., SCHIFFMAN, G., ABRAMS, D., VOLBERDING, P., ZIEGLER, J. & CONANT, M. 1984. B-CELL IMMUNODEFICIENCY IN ACQUIRED IMMUNE-DEFICIENCY SYNDROME. *Jama-Journal of the American Medical Association,* 251**,** 1447-1449.

AMSTAD, P. A., YU, G., JOHNSON, G. L., LEE, B. W., DHAWAN, S. & PHELPS, D. J. 2001. Detection of caspase activation in situ by fluorochrome-labeled caspase inhibitors. *Biotechniques,* 31**,** 608-+.

ANDERSEN, M. H., SCHRAMA, D., STRATEN, P. T. & BECKER, J. C. 2006. Cytotoxic T cells. *Journal of Investigative Dermatology,* 126**,** 32-41.

ANDREWS, N. J., WAIGHT, P. A., GEORGE, R. C., SLACK, M. P. E. & MILLER, E. 2012. Impact and effectiveness of 23-valent pneumococcal polysaccharide vaccine against invasive pneumococcal disease in the elderly in England and Wales. *Vaccine,* 30**,** 6802-6808.

APPAY, V. & SAUCE, D. 2008. Immune activation and inflammation in HIV-I infection: causes and consequences. *Journal of Pathology,* 214**,** 231-241.

AUTRAN, B., CARCELAIN, G., LI, T. S., BLANC, C., MATHEZ, D., TUBIANA, R., KATLAMA, C., DEBRE, P. & LEIBOWITCH, J. 1997. Positive effects of combined antiretroviral therapy on CD4(+) T cell homeostasis and function in advanced HIV disease. *Science,* 277**,** 112-116.

AVERY, O. T. & DUBOS, R. 1931. The protective action of a specific enzyme against type III pneumococcus infection in mice. *Jour Exp Med,* 54**,** 73-89.

AVERY, O. T. & GOEBEL, W. F. 1929. Chemo-immunological studies on conjugated carbohydrate-proteins II. Immunological specificity of synthetic sugar-protein antigens. *Journal of Experimental Medicine,* 50**,** 533-550.

BARRETTC.E 1971. BACTERIAL INFECTION AND SICKLE CELL ANEMIA - ANALYSIS OF 250 INFECTIONS IN 166 PATIENTS AND A REVIEW OF LITERATURE. *Medicine,* 50**,** 97-&.

BEGEMANN, M. & POLICAR, M. 2001. Pneumococcal vaccine failure in an HIV-infected patient with fatal pneumococcal sepsis and HCV-related cirrhosis. *Mount Sinai Journal of Medicine,* 68**,** 396-399.

BOGAERT, D., DE GROOT, R. & HERMANS, P. W. M. 2004. Streptococcus pneumoniae colonisation: the key to pneumococcal disease. *Lancet Infectious Diseases,* 4**,** 144-154.

BOHLER, T., BAUMLER, C., HERR, I., GROLL, A., KURZ, M. & DEBATIN, K. M. 1997. Activation of the CD95 system increases with disease progression in human immunodeficiency virus type 1-infected children and adolescents. *Pediatric Infectious Disease Journal,* 16**,** 754-759.

BOOY, R., HODGSON, S., CARPENTER, L., MAYONWHITE, R. T., SLACK, M. P. E., MACFARLANE, J. A., HAWORTH, E. A., KIDDLE, M., SHRIBMAN, S., ROBERTS, J. S. C. & MOXON, E. R. 1994. EFFICACY OF HAEMOPHILUS-INFLUENZAE TYPE-B CONJUGATE VACCINE PRP-T. *Lancet,* 344**,** 362-366.

BREIMAN, R. F., KELLER, D. W., PHELAN, M. A., SNIADACK, D. H., STEPHENS, D. S., RIMLAND, D., FARLEY, M. M., SCHUCHAT, A. & REINGOLD, A. L. 2000. Evaluation of effectiveness of the 23-valent pneumococcal capsular polysaccharide vaccine for HIV-infected patients. *Archives of Internal Medicine,* 160**,** 2633-2638.

BROUWER, M. C., DE GANS, J., HECKENBERG, S. G. B., ZWINDERMAN, A. H., VAN DER POLL, T. & VAN DE BEEK, D. 2009. Host genetic susceptibility to pneumococcal and meningococcal disease: a systematic review and meta-analysis. *Lancet Infectious Diseases,* 9**,** 31-44.

BROUWER, M. C. & VAN DE BEEK, D. 2009. Genetics in Meningococcal Disease: One Step Beyond. *Clinical Infectious Diseases,* 48**,** 595-597.

BRUNSWICK, M., FINKELMAN, F. D., HIGHET, P. F., INMAN, J. K., DINTZIS, H. M. & MOND, J. J. 1988. PICOGRAM QUANTITIES OF ANTI-IG ANTIBODIES COUPLED TO DEXTRAN INDUCE B-CELL PROLIFERATION. *Journal of Immunology,* 140**,** 3364-3372.

BRYANT, K. A., BLOCK, S. L., BAKER, S. A., GRUBER, W. C., SCOTT, D. A. & GRP, P. C. V. I. S. 2010. Safety and Immunogenicity of a 13-Valent Pneumococcal Conjugate Vaccine. *Pediatrics,* 125**,** 866-875.

CDC. 2012. *Pneumococcal Disease* [Online]. Centers for Disease Control and Prevention. Available: http://www.cdc.gov/vaccines/pubs/pinkbook/pneumo.html [Accessed 30 November 2013].

CHAPLIN, D. D. 2010. Overview of the immune response. *Journal of Allergy and Clinical Immunology,* 125**,** S3-S23.

CHENG, A., CHANG, S.-Y., TSAI, M.-S., SU, Y.-C., LIU, W.-C., SUN, H.-Y. & HUNG, C.-C. 2016. Long-term immune responses and comparative effectiveness of one or two doses of 7-valent pneumococcal conjugate vaccine (PCV7) in HIV-positive adults in the era of combination antiretroviral therapy. *Journal of the International Aids Society,* 19.

CLOYD, M. W., CHEN, J. J. Y., ADEQBOYEGA, P. & WANG, L. 2001. How does HIV cause depletion of CD4 lymphocytes? A mechanism involving virus signaling through its cellular receptors. *Current Molecular Medicine (Hilversum),* 1**,** 545-550.

COHEN, M. S., CHEN, Y. Q., MCCAULEY, M., GAMBLE, T., HOSSEINIPOUR, M. C., KUMARASAMY, N., HAKIM, J. G., KUMWENDA, J., GRINSZTEJN, B., PILOTTO, J. H. S., GODBOLE, S. V., MEHENDALE, S., CHARIYALERTSAK, S., SANTOS, B. R., MAYER, K. H., HOFFMAN, I. F., ESHLEMAN, S. H., PIWOWAR-MANNING, E., WANG, L., MAKHEMA, J., MILLS, L. A., DE BRUYN, G., SANNE, I., ERON, J., GALLANT, J., HAVLIR, D., SWINDELLS, S., RIBAUDO, H., ELHARRAR, V., BURNS, D., TAHA, T. E., NIELSEN-SAINES, K., CELENTANO, D., ESSEX, M., FLEMING, T. R. & TEAM, H. S. 2011. Prevention of HIV-1 Infection with Early Antiretroviral Therapy. *New England Journal of Medicine,* 365**,** 493-505.

COLLINS, A. M., EL BATRAWY, S., GORDON, S. B. & FERREIRA, D. M. 2013. Increased IgG but normal IgA anti-pneumococcal protein antibodies in lung of HIV-infected adults. *Vaccine,* 31**,** 3469-3472.

CONNORS, M., KOVACS, J. A., KREVAT, S., GEABANACLOCHE, J. C., SNELLER, M. C., FLANIGAN, M., METCALF, J. A., WALKER, R. E., FALLOON, J., BASELER, M., STEVENS, R., FEUERSTEIN, I., MASUR, H. & LANE, H. C. 1997. HIV infection induces changes in CD4(+) T-cell phenotype and depletions within the CD4(+) T-cell repertoire that are not immediately restored by antiviral or immune-based therapies. *Nature Medicine,* 3**,** 533-540.

COOPER, D., YU, X., SIDHU, M., NAHM, M. H., FERNSTEN, P. & JANSEN, K. U. 2011. The 13-valent pneumococcal conjugate vaccine (PCV13) elicits cross-functional opsonophagocytic killing responses in humans to Streptococcus pneumoniae serotypes 6C and 7A. *Vaccine,* 29**,** 7207-7211.

CRUM-CIANFLONE, N. F., ROEDIGER, M., HULLSIEK, K. H., GANESAN, A., LANDRUM, M., WEINTROB, A., AGAN, B., MEDINA, S., RAHKOLA, J., HALE, B., JANOFF, E. N. & INFECT DIS CLINICAL RES PROGRAM, H. I. 2010. The association of ethnicity with antibody responses to pneumococcal vaccination among adults with HIV infection. *Vaccine,* 28**,** 7583-7588.

D'ORSOGNA, L. J., KRUEGER, R. G., MCKINNON, E. J. & FRENCH, M. A. 2007. Circulating memory B-cell subpopulations are affected differently by HIV infection and antiretroviral therapy. *Aids,* 21**,** 1747-1752.

DARTON, T. C., WING, J. B., LEES, A., HEATH, A. W. & READ, R. C. 2011. Adult Survivors of Invasive Pneumococcal Disease Exhibit Defective B Cell Function. *Clinical Infectious Diseases,* 52**,** 1133-1136.

DAY, C. L., KAUFMANN, D. E., KIEPIELA, P., BROWN, J. A., MOODLEY, E. S., REDDY, S., MACKEY, E. W., MILLER, J. D., LESLIE, A. J., DEPIERRES, C., MNCUBE, Z., DURAISWAMY, J., ZHU, B., EICHBAUM, Q., ALTFELD, M., WHERRY, E. J., COOVADIA, H. M., GOULDER, P. J. R., KLENERMAN, P., AHMED, R., FREEMAN, G. J. & WALKER, B. D. 2006. PD-1 expression on HIV-specific T cells is associated with T-cell exhaustion and disease progression. *Nature,* 443**,** 350-354.

DE MILITO, A. 2004. B lymphocyte dysfunctions in HIV infection. *Current Hiv Research,* 2**,** 11-21.

DE MILITO, A., MORCH, C., SONNERBORG, A. S. & CHIODI, F. 2001. Loss of memory (CD27) B lymphocytes in HIV-1 infection. *Aids,* 15**,** 957-964.

DONKOR, E. S., BISHOP, C. J., GOULD, K. A., HINDS, J., ANTONIO, M., WREN, B. & HANAGE, W. P. 2011. High Levels of Recombination among Streptococcus pneumoniae Isolates from the Gambia (vol 2, e00040, 2011). *Mbio,* 2.

ECDC. 2007. *Report on the status of communicable diseases in the EU and EEA/EFTA countries* [Online]. ECDC. Available: http://www.ecdc.europa.eu/en/publications/Publications/0706_SUR_Annual_Epidemiologic al_Report_2007.pdf [Accessed 28 December 2013].

ECDC. 2010. *Surveillance report* [Online]. ECDC. Available: http://www.ecdc.europa.eu/en/publications/Publications/1011_SUR_Annual_Epidemiologic al_Report_on_Communicable_Diseases_in_Europe.pdf [Accessed 28 December 2013].

ECDC. 2013. *Surveillance report* [Online]. ECDC. Available: http://www.ecdc.europa.eu/en/publications/Publications/annual-epidemiological-report-2013.pdf [Accessed 28 December 2013].

ELMORE, S. 2007. Apoptosis: A review of programmed cell death. *Toxicologic Pathology,* 35**,** 495-516.

EVRARD, B., DOSGILBERT, A., JACQUEMOT, N., DEMEOCQ, F., GILLES, T., CHASSAGNE, J., BERGER, M. & TRIDON, A. 2010. CFSE flow cytometric quantification of lymphocytic proliferation in extracorporeal photopheresis: Use for quality control. *Transfusion and Apheresis Science,* 42**,** 11-19.

FARESJO, T. & FARESJO, A. 2010. To Match or Not to Match in Epidemiological Studies-Same Outcome but Less Power. *International Journal of Environmental Research and Public Health,* 7**,** 325-332.

FAUCI, A. S. 1993. IMMUNOPATHOGENESIS OF HIV-INFECTION. *Journal of Acquired Immune Deficiency Syndromes and Human Retrovirology,* 6**,** 655-662.

FEIKIN, D. R., JAGERO, G., AURA, B., BIGOGO, G. M., OUNDO, J., BEALL, B. W., KARANI, A., MORPETH, S., NJENGA, M. K. & BREIMAN, R. F. 2010. High rate of pneumococcal bacteremia in a prospective cohort of older children and adults in an area of high HIV prevalence in rural western Kenya. *Bmc Infectious Diseases,* 10.

FEIKIN, D. R., SCHUCHAT, A., KOLCZAK, M., BARRETT, N. L., HARRISON, L. H., LEFKOWITZ, L., MCGREER, A., FARLEY, M. M., VUGIA, D. J., LEXAU, C., STEFONEK, K. R., PATTERSON, J. E. & JORGENSEN, J. H. 2000. Mortality from invasive pneumococcal pneumonia in the era of antibiotic resistance, 1995-1997. *American Journal of Public Health,* 90**,** 223-229.

FELLER, L., BALLYRAM, R., MEYEROV, R., LEMMER, J. & AYO-YUSUF, O. A. 2014. Race/ethnicity in biomedical research and clinical practice. *SADJ : journal of the South African Dental Association = tydskrif van die Suid-Afrikaanse Tandheelkundige Vereniging,* 69**,** 272-4.

FINK, K. 2012. Origin and function of circulating plasmablasts during acute viral infections. *Frontiers in Immunology,* 3.

FLANAGAN, K. L. & PLEBANSKI, M. 2017. Sex-differential heterologous (non-specific) effects of vaccines: an emerging public health issue that needs to be understood and exploited. *Expert Review of Vaccines,* 16**,** 5-13.

FOGLI, M., TORTI, C., MALACARNE, F., FIORENTINI, S., ALBANI, M., IZZO, I., GIAGULLI, C., MAGGI, F., CAROSI, G. & CARUSO, A. 2012. Emergence of Exhausted B Cells in Asymptomatic HIV-1-Infected Patients Naive for HAART is Related to Reduced Immune Surveillance. *Clinical & Developmental Immunology*.

FOSTER, R. A., CARLRING, J., LEES, A., BORROW, R., RAMSAY, M., KACSMARSKI, E., MILLER, E., MCKENDRICK, M. W., HEATH, A. W. & READ, R. C. 2010. Functional T-Cell Deficiency in Adolescents Who Experience Serogroup C Meningococcal Disease despite Receiving the Meningococcal Serogroup C Conjugate Vaccine. *Clinical and Vaccine Immunology,* 17**,** 1104-1110.

FOSTER, R. A., CARLRING, J., MCKENDRICK, M. W., LEES, A., BORROW, R., READ, R. C. & HEATH, A. W. 2009. Evidence of a Functional B-Cell Immunodeficiency in Adults Who Experience Serogroup C Meningococcal Disease. *Clinical and Vaccine Immunology,* 16**,** 692-698.

FRASCA, D., DIAZ, A., ROMERO, M., LANDIN, A. M. & BLOMBERG, B. B. 2011. Age effects on B cells and humoral immunity in humans. *Ageing Research Reviews,* 10**,** 330-335.

FRENCH, N., GORDON, S. B., MWALUKOMO, T., WHITE, S. A., MWAFULIRWA, G., LONGWE, H., MWAIPONYA, M., ZIJLSTRA, E. E., MOLYNEUX, M. E. & GILKS, C.

F. 2010. A Trial of a 7-Valent Pneumococcal Conjugate Vaccine in HIV-Infected Adults. *New England Journal of Medicine,* 362**,** 812-822.

FUKUSUMI, M., CHANG, B., TANABE, Y., OSHIMA, K., MARUYAMA, T., WATANABE, H., KURONUMA, K., KASAHARA, K., TAKEDA, H., NISHI, J., FUJITA, J., KUBOTA, T., SUNAGAWA, T., MATSUI, T., OISHI, K. & ADULT, I. P. T. S. G. 2017. Invasive pneumococcal disease among adults in Japan, April 2013 to March 2015: disease characteristics and serotype distribution. *Bmc Infectious Diseases,* 17.

GAREY, K. W. 2004. The role of matching in epidemiologic studies. *American Journal of Pharmaceutical Education,* 68.

GENO, K. A., GILBERT, G. L., SONG, J. Y., SKOVSTED, I. C., KLUGMAN, K. P., JONES, C., KONRADSEN, H. B. & NAHM, M. H. 2015. Pneumococcal Capsules and Their Types: Past, Present, and Future. *Clinical Microbiology Reviews,* 28**,** 871-899.

GEPPERT, T. D. & LIPSKY, P. E. 1987. ACCESSORY CELL INDEPENDENT PROLIFERATION OF HUMAN-T4 CELLS STIMULATED BY IMMOBILIZED MONOCLONAL-ANTIBODIES TO CD3. *Journal of Immunology,* 138**,** 1660-1666.

GIEFING-KROELL, C., BERGER, P., LEPPERDINGER, G. & GRUBECK-LOEBENSTEIN, B. 2015. How sex and age affect immune responses, susceptibility to infections, and response to vaccination. *Aging Cell,* 14**,** 309-321.

GLENCHUR, H., ZINNEMAN, H. H. & HALL, W. H. 1959. A REVIEW OF 51 CASES OF MULTIPLE MYELOMA - EMPHASIS ON PNEUMONIA AND OTHER INFECTIONS AS COMPLICATIONS. *Archives of Internal Medicine,* 103**,** 173-183.

GLENNIE, S. J., SEPAKO, E., MZINZA, D., HARAWA, V., MILES, D. J. C., JAMBO, K. C., GORDON, S. B., WILLIAMS, N. A. & HEYDERMAN, R. S. 2011. Impaired CD4 T Cell Memory Response to Streptococcus pneumoniae Precedes CD4 T Cell Depletion in HIV-Infected Malawian Adults. *Plos One,* 6.

GOLDBLATT, D. 2000. Conjugate vaccines. *Clinical and Experimental Immunology,* 119**,** 1-3.

GORDON, S. B., IRVING, G. R. B., LAWSON, R. A., LEE, M. E. & READ, R. C. 2000. Intracellular trafficking and killing of Streptococcus pneumoniae by human alveolar macrophages are influenced by opsonins. *Infection and Immunity,* 68**,** 2286-2293.

GORDON, S. B., KAYHTY, H., MOLYNEUX, M. E., HAIKALA, R., NURKKA, A., MUSAYA, J., ZIJLSTRA, E. E., LINDELL, D. & FRENCH, N. 2007. Pneumococcal conjugate vaccine is immunogenic in lung fluid of HIV-infected and immunocompetent adults. *Journal of Allergy and Clinical Immunology,* 120**,** 208-210.

GORDON, S. B., MALAMBA, R., MTHUNTHAMA, N., JARMAN, E. R., JAMBO, K., JERE, K., ZIJLSTRA, E. E., MOLYNEUX, M. E., DENNIS, J. & FRENCH, N. 2008. Inhaled delivery of 23-valent pneumococcal polysaccharide vaccine does not result in enhanced pulmonary mucosal immunoglobulin responses. *Vaccine,* 26**,** 5400-5406.

GOUGEON, M. L. & MONTAGNIER, L. 1993. APOPTOSIS IN AIDS (VOL 260, PG 1269, 1993). *Science,* 260**,** 1709-1709.

GRANAT, S. M., OLLGREN, J., HERVA, E., MIA, Z., AURANEN, K. & MAKELA, P. H. 2009. Epidemiological Evidence for Serotype-Independent Acquired Immunity to Pneumococcal Carriage. *Journal of Infectious Diseases,* 200**,** 99-106.

GREENWOOD, B. 1999. The epidemiology of pneumococcal infection in children in the developing world. *Philosophical Transactions of the Royal Society of London Series B-Biological Sciences,* 354**,** 777-785.

GROUX, H., TORPIER, G., MONTE, D., MOUTON, Y., CAPRON, A. & AMEISEN, J. C. 1992. ACTIVATION-INDUCED DEATH BY APOPTOSIS IN CD4+ T-CELLS FROM HUMAN-IMMUNODEFICIENCY-VIRUS INFECTED ASYMPTOMATIC INDIVIDUALS. *Journal of Experimental Medicine,* 175**,** 331-340.

HAAS, A., ZIMMERMANN, K. & OXENIUS, A. 2011. Antigen-Dependent and -Independent Mechanisms of T and B Cell Hyperactivation during Chronic HIV-1 Infection. *Journal of Virology,* 85**,** 12102-12113.

HADDY, T. B., RANA, S. R. & CASTRO, O. 1999. Benign ethnic neutropenia: What is a normal absolute neutrophil count? *Journal of Laboratory and Clinical Medicine,* 133**,** 15-22.

HALAPI, E., WERNER, A., WAHLSTROM, J., OSTERBORG, A., JEDDITEHRANI, M., YI, Q., JANSON, C. H., WIGZELL, H., GRUNEWALD, J. & MELLSTEDT, H. 1997. T cell repertoire in patients with multiple myeloma and monoclonal gammopathy of undetermined significance: clonal CD8(+) T cell expansions are found preferentially in patients with a low tumor burden. *European Journal of Immunology,* 27**,** 2245-2252.

HALASA, N. B., SHANKAR, S. M., TALBOT, T. R., ARBOGAST, P. G., MITCHEL, E. F., WANG, W. C., SCHAFFNER, W., CRAIG, A. S. & GRIFFIN, M. R. 2007. Incidence of invasive pneumococcal disease among individuals with sickle cell disease before and after the introduction of the pneumococcal conjugate vaccine. *Clinical Infectious Diseases,* 44**,** 1428-1433.

HARABUCHI, Y., FADEN, H., YAMANAKA, N., DUFFY, L., WOLF, J. & KRYSTOFIK, D. 1994. NASOPHARYNGEAL COLONIZATION WITH NONTYPABLE HAEMOPHILUS-INFLUENZAE AND RECURRENT OTITIS-MEDIA. *Journal of Infectious Diseases,* 170**,** 862-866.

HARALAMBIEVA, I. H., OVSYANNIKOVA, I. G., KENNEDY, R. B., LARRABEE, B. R., PANKRATZ, V. S. & POLAND, G. A. 2013. Race and sex-based differences in cytokine immune responses to smallpox vaccine in healthy individuals. *Human Immunology,* 74**,** 1263-1266.

HARALAMBIEVA, L. H., SALK, H. M., LAMBERT, N. D., OVSYANNIKOVA, I. G., KENNEDY, R. B., WARNER, N. D., PANKRATZ, V. S. & POLAND, G. A. 2014. Associations between race, sex and immune response variations to rubella vaccination in two independent cohorts. *Vaccine,* 32**,** 1946-1953.

HART, M., STEEL, A., CLARK, S. A., MOYLE, G., NELSON, M., HENDERSON, D. C., WILSON, R., GOTCH, F., GAZZARD, B. & KELLEHER, P. 2007. Loss of discrete memory B cell subsets is associated with impaired immunization responses in HIV-1 infection and may be a risk factor for invasive pneumococcal disease. *Journal of Immunology,* 178**,** 8212-8220.

HAZENBERG, M. D., HAMANN, D., SCHUITEMAKER, H. & MIEDEMA, F. 2000. T cell depletion in HIV-I infection: how CD4(+) T cells go out of stock. *Nature Immunology,* 1**,** 285-289.

HAZENBERG, M. D., OTTO, S. A., VAN BENTHEM, B. H. B., ROOS, M. T. L., COUTINHO, R. A., LANGE, J. M. A., HAMANN, D., PRINS, M. & MIEDEMA, F. 2003. Persistent immune activation in HIV-1 infection is associated with progression to AIDS. *Aids,* 17**,** 1881-1888.

HEFFERNAN, R. T., BARRETT, N. L., GALLAGHER, K. M., HADLER, J. L., HARRISON, L. H., REINGOLD, A. L., KHOSHNOOD, K., HOLFORD, T. R. & SCHUCHAT, A. 2005. Declining incidence of invasive Streptococcus pneumoniae infections among persons with AIDS in an era of highly active antiretroviral therapy, 1995-2000. *Journal of Infectious Diseases,* 191**,** 2038-2045.

HERZENBERG, L. A., TUNG, J., MOORE, W. A., HERZENBERG, L. A. & PARKS, D. R. 2006. Interpreting flow cytometry data: a guide for the perplexed. *Nature Immunology,* 7**,** 681-685.

HILLER, N. L., AHMED, A., POWELL, E., MARTIN, D. P., EUTSEY, R., EARL, J., JANTO, B., BOISSY, R. J., HOGG, J., BARBADORA, K., SAMPATH, R., LONERGAN, S., POST, J. C., HU, F. Z. & EHRLICH, G. D. 2010. Generation of Genic Diversity among Streptococcus pneumoniae Strains via Horizontal Gene Transfer during a Chronic Polyclonal Pediatric Infection. *Plos Pathogens,* 6.

HULSPAS, R., O'GORMAN, M. R. G., WOOD, B. L., GRATAMA, J. W. & SUTHERLAND, D. R. 2009. Considerations for the Control of Background Fluorescence in Clinical Flow Cytometry. *Cytometry Part B-Clinical Cytometry,* 76B**,** 355-364.

HUNG, C. C., CHANG, S. Y., SU, C. T., CHEN, Y. Y., CHANG, S. F., YANG, C. Y., LIU, W. C., WU, C. H. & CHANG, S. C. 2010. A 5-year longitudinal follow-up study of serological responses to 23-valent pneumococcal polysaccharide vaccination among patients with HIV infection who received highly active antiretroviral therapy*. *Hiv Medicine,* 11**,** 54-63.

IAC. 2013. *Pneumococcal Vaccines (PCV13 and PPSV23)* [Online]. St Paul, MN: IAC. Available: http://www.immunize.org/askexperts/experts_pneumococcal_vaccines.asp#ppsv23 [Accessed 10 December 2013].

INGLE, G. S., CHAN, P., ELLIOTT, J. M., CHANG, W. S., KOEPPEN, H., STEPHAN, J. P. & SCALES, S. J. 2008. High CD21 expression inhibits internalization of anti-CD19 antibodies and cytotoxicity of an anti-CD19-drug conjugate. *British Journal of Haematology,* 140**,** 46-58.

ISAACMAN, D. J., MCINTOSH, E. D. & REINERT, R. R. 2010. Burden of invasive pneumococcal disease and serotype distribution among Streptococcus pneumoniae isolates in young children in Europe: impact of the 7-valent pneumococcal conjugate vaccine and considerations for future conjugate vaccines. *International Journal of Infectious Diseases,* 14**,** E197-E209.

JAGER, K. J., ZOCCALI, C., MACLEOD, A. & DEKKER, F. W. 2008. Confounding: What it is and how to deal with it. *Kidney International,* 73**,** 256-260.

JAMBO, K. C., BANDA, D. H., KANKWATIRA, A. M., SUKUMAR, N., ALLAIN, T. J., HEYDERMAN, R. S., RUSSELL, D. G. & MWANDUMBA, H. C. 2014. Small alveolar macrophages are infected preferentially by HIV and exhibit impaired phagocytic function. *Mucosal Immunology,* 7**,** 1116-1126.

JAMBO, K. C., SEPAKO, E., FULLERTON, D. G., MZINZA, D., GLENNIE, S., WRIGHT, A. K., HEYDERMAN, R. S. & GORDON, S. B. 2011. Bronchoalveolar CD4(+) T cell responses to respiratory antigens are impaired in HIV-infected adults. *Thorax,* 66**,** 375-382.

JCVI. 2011. *Joint Committee on Vaccination and Immunisation advice on the pneumococcal vaccination programme for people aged 65 years and older* [Online]. GOV.UK. Available: https://www.gov.uk/government/publications/joint-committee-on-vaccination-and-immunisation-advice-on-the-pneumococcal-vaccination-programme-for-people-aged-65-years-and-older [Accessed 13 February 2018].

JCVI. 2013. *JCVI statement on the wider use of pneumococcal conjugate vaccines* [Online]. GOV.UK. Available: https://www.gov.uk/government/publications/jcvi-statement-on-the-wider-use-of-pneumococcal-conjugate-vaccines [Accessed 13 February 2018].

JEDRZEJAS, M. J. 2001. Pneumococcal virulence factors: Structure and function. *Microbiology and Molecular Biology Reviews,* 65**,** 187-+.

KARLSSON, J., HOGEVIK, H., ANDERSSON, K., ROSHANI, L., ANDRÉASSON, B. & WENNERÅS, C. 2013. Pneumococcal vaccine responses in elderly patients with multiple myeloma, Waldenstrom's macroglobulinemia, and monoclonal gammopathy of undetermined significance. *Trials in Vaccinology,* 2**,** 31 - 38.

KERNEIS, S., LAUNAY, O., TURBELIN, C., BATTEUX, F., HANSLIK, T. & BOELLE, P.-Y. 2014. Long-term Immune Responses to Vaccination in HIV-Infected Patients: A Systematic Review and Meta-Analysis. *Clinical Infectious Diseases,* 58**,** 1130-1139.

KERR, A. R., PATERSON, G. K., RIBOLDI-TUNNICLIFFE, A. & MITCHELL, T. J. 2005. Innate immune defense against pneumococcal pneumonia requires pulmonary complement component C3. *Infection and Immunity,* 73**,** 4245-4252.

KING, K. 1980. Septicaemia in patients with haematological malignant disease. Med J Aust.

KLATT, N. R., FUNDERBURG, N. T. & BRENCHLEY, J. M. 2013. Microbial translocation, immune activation, and HIV disease. *Trends in Microbiology,* 21**,** 6-13.

KLUGMAN, K. P., MADHI, S. A., HUEBNER, R. E., KOHBERGER, R., MBELLE, N., PIERCE, N. & VACCINE TRIALISTS, G. 2003. A trial of a 9-valent pneumococcal conjugate vaccine in children with and those without HIV infection. *New England Journal of Medicine,* 349**,** 1341-1348.

KOPPE, U., SUTTORP, N. & OPITZ, B. 2012. Recognition of Streptococcus pneumoniae by the innate immune system. *Cellular Microbiology,* 14**,** 460-466.

KORDE, N., KRISTINSSON, S. Y. & LANDGREN, O. 2011. Monoclonal gammopathy of undetermined significance (MGUS) and smoldering multiple myeloma (SMM): novel biological insights and development of early treatment strategies. *Blood,* 117**,** 5573-5581.

KROON, F. P., VAN DISSEL, J. T., RAVENSBERGEN, E., NIBBERING, P. H. & VAN FURTH, R. 2000. Enhanced antibody response to pneumococcal polysaccharide vaccine after prior immunization with conjugate pneumococcal vaccine in HIV-infected adults. *Vaccine,* 19**,** 886-894.

KUMASHI, P., GIRGAWY, E., TARRAND, J. J., ROLSTON, K. V., RAAD, II & SAFDAR, A. 2005. Streptococcus pneumoniae bacteremia in patients with cancer - Disease characteristics and outcomes in the era of escalating drug resistance (1998-2002). *Medicine,* 84**,** 303-312.

KUPPER, L. L., KARON, J. M., KLEINBAUM, D. G., MORGENSTERN, H. & LEWIS, D. K. 1981. MATCHING IN EPIDEMIOLOGIC STUDIES - VALIDITY AND EFFICIENCY CONSIDERATIONS. *Biometrics,* 37**,** 271-291.

KYAW, M. H., ROSE, C. E., FRY, A. M., SINGLETON, J. A., MOORE, Z., ZELL, E. R., WHITNEY, C. G. & ACTIVE BACTERIAL CORE, S. 2005. The influence of chronic illnesses on the incidence of invasive pneumococcal disease in adults. *Journal of Infectious Diseases,* 192**,** 377-386.

KYLE, R. A. 1978. MONOCLONAL GAMMOPATHY OF UNDETERMINED SIGNIFICANCE - NATURAL-HISTORY IN 241 CASES. *American Journal of Medicine,* 64**,** 814-826.

KYLE, R. A., BUADI, F. & RAJKUMAR, S. V. 2011. Management of Monoclonal Gammopathy of Undetermined Significance (MGUS) and Smoldering Multiple Myeloma (SMM). *Oncology-New York,* 25**,** 578-586.

KYLE, R. A., CHILD, J. A., ANDERSON, K., BARLOGIE, B., BATAILLE, R., BENSINGER, W., BLADE, J., BOCCADORO, M., DALTON, W., DIMOPOULOS, M., DJULBEGOVIC, B., DRAYSON, M., DURIE, B., FACON, T., FONSECA, R., GAHRTON, G., GREIPP, P., HAROUSSEAU, J. L., HARRINGTON, D., HUSSEIN, M., JOSHUA, D., LUDWIG, H., MORGAN, G., OKEN, M., POWLES, R., RICHARDSON, P., ROODMAN, D., SAN MIGUEL, J., SHIMIZU, K., SHUSTIK, C., SIROHI, B., SONNEVELD, P., TRICOT, G., TURESSON, I., VAN NESS, B., VESOLE, D., WEBER, D., WESTIN, J., WHEATLEY, K. & INT MYELOMA WORKING, G. 2003. Criteria for the classification of monoclonal gammopathies, multiple myeloma and related disorders: a report of the International Myeloma Working Group. *British Journal of Haematology,* 121**,** 749-757.

KYLE, R. A., DURIE, B. G. M., RAJKUMAR, S. V., LANDGREN, O., BLADE, J., MERLINI, G., KROEGER, N., EINSELE, H., VESOLE, D. H., DIMOPOULOS, M., SAN MIGUEL, J., AVET-LOISEAU, H., HAJEK, R., CHEN, W. M., ANDERSON, K. C., LUDWIG, H., SONNEVELD, P., PAVLOVSKY, S., PALUMBO, A., RICHARDSON, P. G., BARLOGIE, B., GREIPP, P., VESCIO, R., TURESSON, I., WESTIN, J., BOCCADORO, M. & INT MYELOMA WORKING, G. 2010. Monoclonal gammopathy of undetermined significance (MGUS) and smoldering (asymptomatic) multiple myeloma: IMWG consensus perspectives risk factors for progression and guidelines for monitoring and management. *Leukemia,* 24**,** 1121-1127.

LANDGREN, O., GRIDLEY, G., TURESSON, I., CAPORASO, N. E., GOLDIN, L. R., BARIS, D., FEARS, T. R., HOOVER, R. N. & LINET, M. S. 2006. Risk of monoclonal gammopathy of undetermined significance (MGUS) and subsequent multiple myeloma among African American and white veterans in the United States. *Blood,* 107**,** 904-906.

LANDGREN, O., KYLE, R. A., PFEIFFER, R. M., KATZMANN, J. A., CAPORASO, N. E., HAYES, R. B., DISPENZIERI, A., KUMAR, S., CLARK, R. J., BARIS, D., HOOVER, R. & RAJKUMAR, S. V. 2009. Monoclonal gammopathy of undetermined significance (MGUS) consistently precedes multiple myeloma: a prospective study. *Blood,* 113**,** 5412-5417.

LANE, H. C., MASUR, H., EDGAR, L. C., WHALEN, G., ROOK, A. H. & FAUCI, A. S. 1983. ABNORMALITIES OF B-CELL ACTIVATION AND IMMUNOREGULATION IN PATIENTS WITH THE ACQUIRED IMMUNODEFICIENCY SYNDROME. *New England Journal of Medicine,* 309**,** 453-458.

LANIE, J. A., NG, W.-L. N., KAZMIERCZAK, K. M., ANDRZEJEWSKI, T. M., DAVIDSEN, T. M., WAYNE, K. J., TETTELIN, H., GLASS, J. I. & WINKLER, M. E. 2007. Genome sequence of Avery's virulent serotype 2 strain D39 of Streptococcus pneumoniae and comparison with that of unencapsulated laboratory strain R6. *Journal of Bacteriology,* 189**,** 38-51.

LAZARUS, H. M., LEDERMAN, M., LUBIN, A., HERZIG, R. H., SCHIFFMAN, G., JONES, P., WINE, A. & RODMAN, H. M. 1980. PNEUMOCOCCAL VACCINATION - THE RESPONSE OF PATIENTS WITH MULTIPLE-MYELOMA. *American Journal of Medicine,* 69**,** 419-423.

LEE, H. Y., ANDALIBI, A., WEBSTER, P., MOON, S. K., TEUFERT, K., KANG, S. H., LI, J. D., NAGURA, M., GANZ, T. & LIM, D. J. 2004. Antimicrobial activity of innate immune molecules against Streptococcus pneumoniae, Moraxella catarrhalis and nontypeable Haemophilus influenzae. *Bmc Infectious Diseases,* 4.

LEUNG, N., BRIDOUX, F., HUTCHISON, C. A., NASR, S. H., COCKWELL, P., FERMAND, J.-P., DISPENZIERI, A., SONG, K. W., KYLE, R. A. & INT KIDNEY MONOCLONAL, G. 2012. Monoclonal gammopathy of renal significance: when MGUS is no longer undetermined or insignificant. *Blood,* 120**,** 4292-4295.

LEVESQUE, M. C., MOODY, M. A., HWANG, K.-K., MARSHALL, D. J., WHITESIDES, J. F., AMOS, J. D., GURLEY, T. C., ALLGOOD, S., HAYNES, B. B., VANDERGRIFT, N. A., PLONK, S., PARKER, D. C., COHEN, M. S., TOMARAS, G. D., GOEPFERT, P. A., SHAW, G. M., SCHMITZ, J. E., ERON, J. J., SHAHEEN, N. J., HICKS, C. B., LIAO, H.-X., MARKOWITZ, M., KELSOE, G., MARGOLIS, D. M. & HAYNES, B. F. 2009. Polyclonal B Cell Differentiation and Loss of Gastrointestinal Tract Germinal Centers in the Earliest Stages of HIV-1 Infection. *Plos Medicine,* 6.

LI, F., VIJAYASANKARAN, N., SHEN, A., KISS, R. & AMANULLAH, A. 2010. Cell culture processes for monoclonal antibody production. *Mabs,* 2**,** 466-479.

LIAO-CHAN, S., DAINE-MATSUOKA, B., HEALD, N., WONG, T., LIN, T., CAI, A. G., LAI, M., D'ALESSIO, J. A. & THEUNISSEN, J. W. 2015. Quantitative Assessment of Antibody

Internalization with Novel Monoclonal Antibodies against Alexa Fluorophores. *Plos One,* 10.

LINGAPPA, J. R., DUMITRESCU, L., ZIMMER, S. M., LYNFIELD, R., MCNICHOLL, J. M., MESSONNIER, N. E., WHITNEY, C. G. & CRAWFORD, D. C. 2011. Identifying Host Genetic Risk Factors in the Context of Public Health Surveillance for Invasive Pneumococcal Disease. *Plos One,* 6.

LIPSITCH, M., WHITNEY, C. G., ZELL, E., KAIJALAINEN, T., DAGAN, R. & MALLEY, R. 2005. Are anticapsular antibodies the primary mechanism of protection against invasive pneumococcal disease? *Plos Medicine,* 2**,** 62-68.

LONGO, D. M., LOUIE, B., MATHI, K., POS, Z., WANG, E., HAWTIN, R. E., MARINCOLA, F. M. & CESANO, A. 2012. Racial differences in B cell receptor signaling pathway activation. *Journal of Translational Medicine,* 10.

LOWE, R., SHIRLEY, N., BLEACKLEY, M., DOLAN, S. & SHAFEE, T. 2017. Transcriptomics technologies. *Plos Computational Biology,* 13.

LU, Y.-J., GROSS, J., BOGAERT, D., FINN, A., BAGRADE, L., ZHANG, Q., KOLLS, J. K., SRIVASTAVA, A., LUNDGREN, A., FORTE, S., THOMPSON, C. M., HARNEY, K. F., ANDERSON, P. W., LIPSITCH, M. & MALLEY, R. 2008. Interleukin-17A mediates acquired immunity to pneumococcal colonization. *Plos Pathogens,* 4.

LUND, E. 1960. Laboratory diagnosis of Pneumococcus infections. *Bulletin of the World Health Organization,* 23**,** 5-13.

LYONS, A. B. & PARISH, C. R. 1994. DETERMINATION OF LYMPHOCYTE DIVISION BY FLOW-CYTOMETRY. *Journal of Immunological Methods,* 171**,** 131-137.

MAARTENS, G., CELUM, C. & LEWIN, S. R. 2014. HIV infection: epidemiology, pathogenesis, treatment, and prevention. *Lancet,* 384**,** 258-271.

MACLEOD, C. M. & KRAUSS, M. R. 1950. RELATION OF VIRULENCE OF PNEUMOCOCCAL STRAINS FOR MICE TO THE QUANTITY OF CAPSULAR POLYSACCHARIDE FORMED INVITRO. *Journal of Experimental Medicine,* 92**,** 1-9.

MALASPINA, A., MOIR, S., KOTTILIL, S., HALLAHAN, C. W., EHLER, L. A., LIU, S. Y., PLANTA, M. A., CHUN, T. W. & FAUCI, A. S. 2003. Deleterious effect of HIV-1 plasma viremia on B cell costimulatory function. *Journal of Immunology,* 170**,** 5965-5972.

MARGOLICK, J. B., DONNENBERG, A. D., MUNOZ, A., PARK, L. P., BAUER, K. D., GIORGI, J. V., FERBAS, J. & SAAH, A. J. 1993. CHANGES IN LYMPHOCYTE-T AND NON-LYMPHOCYTE-T SUBSETS FOLLOWING SEROCONVERSION TO HIV-1 - STABLE CD3+ AND DECLINING CD3- POPULATIONS SUGGEST REGULATORY RESPONSES LINKED TO LOSS OF CD4 LYMPHOCYTES. *Journal of Acquired Immune Deficiency Syndromes and Human Retrovirology,* 6**,** 153-161.

MARGOLICK, J. B., MUNOZ, A., DONNENBERG, A. D., PARK, L. P., GALAI, N., GIORGI, J. V., OGORMAN, M. R. G. & FERBAS, J. 1995. FAILURE OF T-CELL HOMEOSTASIS PRECEDING AIDS IN HIV-1 INFECTION. *Nature Medicine,* 1**,** 674-680.

MARTINEZ-PICADO, J. & DEEKS, S. G. 2016. Persistent HIV-1 replication during antiretroviral therapy. *Current Opinion in Hiv and Aids,* 11**,** 417-423.

MATEOS, M.-V. & LANDGREN, O. 2016. MGUS and Smoldering Multiple Myeloma: Diagnosis and Epidemiology. *Cancer treatment and research,* 169**,** 3-12.

MAURICIO RUEDA, C., ANDREA VELILLA, P., CHOUGNET, C. A., JULIO MONTOYA, C. & TERESA RUGELES, M. 2012. HIV-Induced T-Cell Activation/Exhaustion in Rectal Mucosa Is Controlled Only Partially by Antiretroviral Treatment. *Plos One,* 7.

MCLEOD, J. W. & GORDON, J. 1922. Production of hydrogen peroxide by bacteria. *Biochemical Journal,* 16**,** 499-506.

MCMICHAEL, A. J., BORROW, P., TOMARAS, G. D., GOONETILLEKE, N. & HAYNES, B. F. 2010. The immune response during acute HIV-1 infection: clues for vaccine development. *Nature Reviews Immunology,* 10**,** 11-23.

MEHR, S. & WOOD, N. 2012. Streptococcus pneumoniae - a review of carriage, infection, serotype replacement and vaccination. *Paediatric Respiratory Reviews,* 13**,** 258-264.

MELEGARO, A. & EDMUNDS, W. J. 2004. Cost-effectiveness analysis of pneumococcal conjugate vaccination in England and Wales. *Vaccine,* 22**,** 4203-4214.

MELEGARO, A., EDMUNDS, W. J., PEBODY, R., MILLER, E. & GEORGE, R. 2006. The current burden of pneumococcal disease in England and Wales. *Journal of Infection,* 52**,** 37-48.

MEYAARD, L., OTTO, S. A., JONKER, R. R., MIJNSTER, M. J., KEET, R. P. M. & MIEDEMA, F. 1992. PROGRAMMED DEATH OF T-CELLS IN HIV-1 INFECTION. *Science,* 257**,** 217-219.

MICHELOUD, D., ALVARO-MECA, A., JENSEN, J., DIAZ, A. & RESINO, S. 2012. Trend of Pneumonia Incidence Among Children Infected With HIV in the Era of Highly Active Antiretroviral Therapy. *Pediatric Infectious Disease Journal,* 31**,** 599-601.

MIIRO, G., KAYHTY, H., WATERA, C., TOLMIE, H., WHITWORTH, J. A. G., GILKS, C. F. & FRENCH, N. 2005. Conjugate pneumococcal vaccine in HIV-infected Ugandans and the effect of past receipt of polysaccharide vaccine. *Journal of Infectious Diseases,* 192**,** 1801-1805.

MILLAR, E. V., WATT, J. P., BRONSDON, M. A., DALLAS, J., REID, R., SANTOSHAM, M. & O'BRIEN, K. L. 2008. Indirect effect of 7-valent pneumococcal conjugate vaccine on pneumococcal colonization among unvaccinated household members. *Clinical Infectious Diseases,* 47**,** 989-996.

MILLER, E., ANDREWS, N. J., WAIGHT, P. A., SLACK, M. P. E. & GEORGE, R. C. 2011. Herd immunity and serotype replacement 4 years after seven-valent pneumococcal conjugate vaccination in England and Wales: an observational cohort study. *Lancet Infectious Diseases,* 11**,** 760-768.

MIZUMA, H., LITWIN, S. & ZOLLAPAZNER, S. 1988. B-CELL ACTIVATION IN HIV INFECTION - RELATIONSHIP OF SPONTANEOUS IMMUNOGLOBULIN SECRETION TO VARIOUS IMMUNOLOGICAL PARAMETERS. *Clinical and Experimental Immunology,* 71**,** 410-416.

MOIR, S., BUCKNER, C. M., HO, J., WANG, W., CHEN, J., WALDNER, A. J., POSADA, J. G., KARDAVA, L., O'SHEA, M. A., KOTTILIL, S., CHUN, T.-W., PROSCHAN, M. A. & FAUCI, A. S. 2010. B cells in early and chronic HIV infection: evidence for preservation of immune function associated with early initiation of antiretroviral therapy. *Blood,* 116**,** 5571-5579.

MOIR, S. & FAUCI, A. S. 2008. Pathogenic mechanisms of B-lymphocyte dysfunction in HIV disease. *Journal of Allergy and Clinical Immunology,* 122**,** 12-19.

MOIR, S. & FAUCI, A. S. 2009. B cells in HIV infection and disease. *Nature Reviews Immunology,* 9**,** 235-245.

MOIR, S. & FAUCI, A. S. 2013. Insights into B cells and HIV-specific B-cell responses in HIV-infected individuals. *Immunological Reviews,* 254**,** 207-224.

MOIR, S. & FAUCI, A. S. 2017. B-cell responses to HIV infection. *Immunological Reviews,* 275**,** 33-48.

MOIR, S., HO, J., MALASPINA, A., WANG, W., DIPOTO, A. C., O'SHEA, M. A., ROBY, G., KOTTILIL, S., ARTHOS, J., PROSCHAN, M. A., CHUN, T.-W. & FAUCI, A. S. 2008a. Evidence for HIV-associated B cell exhaustion in a dysfunctional memory B cell compartment in HIV-infected viremic individuals. *Journal of Experimental Medicine,* 205**,** 1797-1805.

MOIR, S., MALASPINA, A., HO, J., WANG, W., DIPOTO, A. C., O'SHEA, M. A., ROBY, G., MICAN, J. M., KOTTILIL, S., CHUN, T.-W., PROSCHAN, M. A. & FAUCI, A. S. 2008b. Normalization of B cell counts and subpopulations after antiretroviral therapy in chronic HIV disease. *Journal of Infectious Diseases,* 197**,** 572-579.

MOIR, S., MALASPINA, A., OGWARO, K. M., DONOGHUE, E. T., HALLAHAN, C. W., EHLER, L. A., LIU, S. Y., ADELSBERGER, J., LAPOINTE, R., HWU, P., BASELER, M., ORENSTEIN, J. M., CHUN, T. W., MICAN, J. A. M. & FAUCI, A. S. 2001. HIV-1 induces phenotypic and functional perturbations of B cells in chronically infected individuals. *Proceedings of the National Academy of Sciences of the United States of America,* 98**,** 10362-10367.

MOIR, S., MALASPINA, A., PICKERAL, O. K., DONOGHUE, E. T., VASQUEZ, J., MILLER, N. J., KRISHNAN, S. R., PLANTA, M. A., TURNEY, J. E., JUSTEMENT, J. S., KOTTILIL, S., DYBUL, M., MICAN, J. M., KOVACS, C., CHUN, T. W., BIRSE, C. E. & FAUCI, A. S. 2004. Decreased survival of B cells of HIV-viremic patients mediated by altered expression of receptors of the TNF superfamily. *Journal of Experimental Medicine,* 200**,** 587-599.

MORRIS, L., BINLEY, J. M., CLAS, B. A., BONHOEFFER, S., ASTILL, T. P., KOST, R., HURLEY, A., CAO, Y. Z., MARKOWITZ, M., HO, D. D. & MOORE, J. P. 1998. HIV-1 antigen-specific and -nonspecific B cell responses are sensitive to combination antiretroviral therapy. *Journal of Experimental Medicine,* 188**,** 233-245.

MURPHY, K. 2012. *Janeway's Immunobiology,* New York, Garland Science, Taylor & Francis Group, LLC.

MUSHER, D. M., GROOVER, J. E., REICHLER, M. R., RIEDO, F. X., SCHWARTZ, B., WATSON, D. A., BAUGHN, R. E. & BREIMAN, R. F. 1997. Emergence of antibody to capsular polysaccharides of Streptococcus pneumoniae during outbreaks of pneumonia: Association with nasopharyngeal colonization. *Clinical Infectious Diseases,* 24**,** 441-446.

NEDELEC, Y., SANZ, J., BAHARIAN, G., SZPIECH, Z. A., PACIS, A., DUMAINE, A., GRENIER, J.-C., FREIMAN, A., SAMS, A. J., HEBERT, S., SABOURIN, A. P., LUCA, F., BLEKHMAN, R., HERNANDEZ, R. D., PIQUE-REGI, R., TUNG, J., YOTOVA, V. & BARREIRO, L. B. 2016. Genetic Ancestry and Natural Selection Drive Population Differences in Immune Responses to Pathogens. *Cell,* 167**,** 657-+.

NHS. 2012. *Pneumococcal infections* [Online]. UK: National Health Service. Available: http://www.nhs.uk/conditions/Pneumococcal-infections/Pages/Introduction.aspx [Accessed 30 November 2013].

NHS. 2016a. *Pneumococcal Vaccine* [Online]. National Health Service. Available: https://www.nhs.uk/conditions/vaccinations/pneumococcal-vaccination/ [Accessed 13 February 2018].

NHS. 2016b. *Who should have the pneumococcal vaccine?* [Online]. National Health Service. Available: https://www.nhs.uk/conditions/vaccinations/when-is-pneumococcal-vaccine-needed/#babies-and-the-pneumococcal-vaccine [Accessed 13 February 2018].

NICHOLAS, K. J., ZERN, E. K., BARNETT, L., SMITH, R. M., LOREY, S. L., COPELAND, C. A., SADAGOPAL, S. & KALAMS, S. A. 2013. B Cell Responses to HIV Antigen Are a Potent Correlate of Viremia in HIV-1 Infection and Improve with PD-1 Blockade. *Plos One,* 8.

NOGUCHI, A., KANEKO, T., NAITOH, K., SAITO, M., IWAI, K., MAEKAWA, R., KAMIGAKI, T. & GOTO, S. 2014. Impaired and imbalanced cellular immunological status assessed in advanced cancer patients and restoration of the T cell immune status by adoptive T-cell immunotherapy. *International Immunopharmacology,* 18**,** 90-97.

O'BRIEN, K. L., WOLFSON, L. J., WATT, J. P., HENKLE, E., DELORIA-KNOLL, M., MCCALL, N., LEE, E., MULHOLLAND, K., LEVINE, O. S., CHERIAN, T. & HIB PNEUMOCOCCAL GLOBAL BURDEN, D. 2009. Burden of disease caused by Streptococcus pneumoniae in children younger than 5 years: global estimates. *Lancet,* 374**,** 893-902.

OBUKHANYCH, T. V. & NUSSENZWEIG, M. C. 2006. T-independent type II immune responses generate memory B cells. *Journal of Experimental Medicine,* 203**,** 305-310.

OKOYE, A. A. & PICKER, L. J. 2013. CD4+T-cell depletion in HIV infection: mechanisms of immunological failure. *Immunological Reviews,* 254**,** 54-64.

OSHIMA, K., KANDA, Y., NANNYA, Y., KANEKO, M., HAMAKI, T., SUGURO, M., YAMAMOTO, R., CHIZUKA, A., MATSUYAMA, T., TAKEZAKO, N., MIWA, A., TOGAWA, A., NIINO, H., NASU, M., SAITO, K. & MORITA, T. 2001. Clinical and pathologic findings in 52 consecutively autopsied cases with multiple myeloma. *American Journal of Hematology,* 67**,** 1-5.

OTT, M., EMILIANI, S., VANLINT, C., HERBEIN, G., LOVETT, J., CHIRMULE, N., MCCLOSKEY, T., PAHWA, S. & VERDIN, E. 1997. Immune hyperactivation of HIV-1-infected T cells mediated by Tat and the CD28 pathway. *Science,* 275**,** 1481-1485.

OVERTURF, G. D. 2003. Prevention of invasive pneumococcal infection in sickle cell disease: On the threshold of a new era of successes? *Journal of Pediatrics,* 143**,** 423-425.

PARADISO, P. 2009. Essential criteria for evaluation of pneumococcal conjugate vaccine candidates. *Vaccine,* 27**,** C15-C18.

PARISH, C. R. 1999. Fluorescent dyes for lymphocyte migration and proliferation studies. *Immunology and Cell Biology,* 77**,** 499-508.

PEARCE, N. 2016. Analysis of matched case-control studies. *Bmj-British Medical Journal,* 352.

PECANHA, L. M. T., SNAPPER, C. M., FINKELMAN, F. D. & MOND, J. J. 1991. DEXTRAN-CONJUGATED ANTI-IG ANTIBODIES AS A MODEL FOR T-CELL-INDEPENDENT TYPE-2 ANTIGEN-MEDIATED STIMULATION OF IG SECRETION INVITRO .1. LYMPHOKINE DEPENDENCE. *Journal of Immunology,* 146**,** 833-839.

PEDERSEN, R. H., LOHSE, N., OSTERGAARD, L. & SOGAARD, O. S. 2011. The effectiveness of pneumococcal polysaccharide vaccination in HIV-infected adults: a systematic review. *Hiv Medicine,* 12**,** 323-333.

PELTOLA, H., KILPI, T. & ANTTILA, M. 1992. RAPID DISAPPEARANCE OF HAEMOPHILUS-INFLUENZAE TYPE-B MENINGITIS AFTER ROUTINE CHILDHOOD IMMUNIZATION WITH CONJUGATE VACCINES. *Lancet,* 340**,** 592-594.

PERFETTO, S. P., CHATTOPADHYAY, P. K., LAMOREAUX, L., NGUYEN, R., AMBROZAK, D., KOUP, R. A. & ROEDERER, M. 2006. Amine reactive dyes: An effective tool to discriminate live and dead cells in polychromatic flow cytometry. *Journal of Immunological Methods,* 313**,** 199-208.

PERFETTO, S. P., CHATTOPADHYAY, P. K., LAMOREAUX, L., NGUYEN, R., AMBROZAK, D., KOUP, R. A. & ROEDERER, M. 2010. Amine-reactive dyes for dead cell discrimination in fixed samples. *Current protocols in cytometry,* Chapter 9**,** Unit 9.34-Unit 9.34.

PERICONE, C. D., OVERWEG, K., HERMANS, P. W. M. & WEISER, J. N. 2000. Inhibitory and bactericidal effects of hydrogen peroxide production by Streptococcus pneumoniae on other inhabitants of the upper respiratory tract. *Infection and Immunity,* 68**,** 3990-3997.

PFIZER. 2013a. *Frequently asked questions about Prevnar 13 for pediatric use* [Online]. Pfizer Inc. Available: http://www.pfizer.com/files/health/vaccines/about_prevnar13_faqs.pdf [Accessed 29 December 2013].

PFIZER. 2013b. *Indications and Important Safety Information for Prevnar 13*® [Online]. USA: Pfizer Inc. Available: http://adult.prevnar13.com/ [Accessed 9 December 2013].

PFIZER. 2017. *Pneumococcal polysaccharide vaccine solution for injection in a vial*
Pneumococcal Polysaccharide Vaccine [Online]. Available: https://www.medicines.org.uk/emc/files/pil.1061.pdf [Accessed 13 February 2018].

PFIZER. 2018. *Prevenar 13 suspension for injection*
Pneumococcal polysaccharide conjugate vaccine (13 valent, adsorbed) [Online]. Available: https://www.medicines.org.uk/emc/files/pil.453.pdf [Accessed 13 February 2018].

PHE. 2013. *Immunisation procedures: the green book, chapter 4* [Online]. GOV.UK. Available: https://www.gov.uk/government/publications/immunisation-procedures-the-green-book-chapter-4 [Accessed 13 February 2018].

PHE. 2016. *HIV in the UK 2016 Report* [Online]. Public Health England. Available: https://www.gov.uk/government/uploads/system/uploads/attachment_data/file/602942/HIV_in_the_UK_report.pdf [Accessed 5 July 2017].

PILISHVILI, T., LEXAU, C., FARLEY, M. M., HADLER, J., HARRISON, L. H., BENNETT, N. M., REINGOLD, A., THOMAS, A., SCHAFFNER, W., CRAIG, A. S., SMITH, P. J., BEALL, B. W., WHITNEY, C. G., MOORE, M. R. & ACTIVE BACTERIAL CORE, S. 2010. Sustained Reductions in Invasive Pneumococcal Disease in the Era of Conjugate Vaccine. *Journal of Infectious Diseases,* 201**,** 32-41.

PRECIADO-LLANES, L., WING, J. B., FOSTER, R. A., CARLRING, J., LEES, A., READ, R. C. & HEATH, A. W. 2015. Contact-dependent suppression of CD4 T-cell activation and proliferation by B cells activated through IgD cross-linking. *Immunology,* 144**,** 444-452.

REDDY, M., EIRIKIS, E., DAVIS, C., DAVIS, H. M. & PRABHAKAR, U. 2004. Comparative analysis of lymphocyte activation marker expression and cytokine secretion profile in stimulated human peripheral blood mononuclear cell cultures: an in vitro model to monitor cellular immune function. *Journal of Immunological Methods,* 293**,** 127-142.

REHE, G. T., KATONA, I. M., BRUNSWICK, M., WAHL, L. M., JUNE, C. H. & MOND, J. J. 1990. ACTIVATION OF HUMAN LYMPHOCYTES-B BY NANOGRAM CONCENTRATIONS OF ANTI-IGM-DEXTRAN CONJUGATES. *European Journal of Immunology,* 20**,** 1837-1842.

RIVES FERREIRO, M. T., MENENDEZ SUSO, J. J., CALDERON LLOPIS, B., DE JOSE GOMEZ, M. I., ALVARADO ORTEGA, F. & RUZA TARRIO, F. J. 2008. Pneumococcal conjugate vaccine failure in HIV-infected child. Clinical case. *Anales de pediatria (Barcelona, Spain : 2003),* 69**,** 59-62.

ROBINSON, K. A., BAUGHMAN, W., ROTHROCK, G., BARRETT, N. L., PASS, M., LEXAU, C., DAMASKE, B., STEFONEK, K., BARNES, B., PATTERSON, J., ZELL, E. R., SCHUCHAT, A., WHITNEY, C. G. & NETW, A. B. E. I. P. 2001. Epidemiology of invasive Streptococcus pneumoniae infections in the United States, 1995-1998 - Opportunities for prevention in the conjugate vaccine era. *Jama-Journal of the American Medical Association,* 285**,** 1729-1735.

RODGER, A. J., CAMBIANO, V., BRUUN, T., VERNAZZA, P., COLLINS, S., VAN LUNZEN, J., CORBELLI, G. M., ESTRADA, V., GERETTI, A. M., BELOUKAS, A., ASBOE, D., VICIANA, P., GUTIERREZ, F., CLOTET, B., PRADIER, C., GERSTOFT, J., WEBER, R., WESTLING, K., WANDELER, G., PRINS, J. M., RIEGER, A., STOECKLE, M., KUEMMERLE, T., BINI, T., AMMASSARI, A., GILSON, R., KRZNARIC, I., RISTOLA, M., ZANGERLE, R., HANDBERG, P., ANTELA, A., ALLAN, S., PHILLIPS, A. N., LUNDGREN, J. & GRP, P. S. 2016. Sexual Activity Without Condoms and Risk of HIV

Transmission in Serodifferent Couples When the HIV-Positive Partner Is Using Suppressive Antiretroviral Therapy. *Jama-Journal of the American Medical Association,* 316**,** 171-181.

ROEDERER, M. 2002. Multiparameter FACS analysis. *Current protocols in immunology,* Chapter 5**,** Unit 5.8-Unit 5.8.

ROEDERER, M., DUBS, J. G., ANDERSON, M. T., RAJU, P. A. & HERZENBERG, L. A. 1995. CD8 NAIVE T-CELL COUNTS DECREASE PROGRESSIVELY IN HIV-INFECTED ADULTS. *Journal of Clinical Investigation,* 95**,** 2061-2066.

ROSE, S. & VAN DER LAAN, M. J. 2009. Why Match? Investigating Matched Case-Control Study Designs with Causal Effect Estimation. *International Journal of Biostatistics,* 5.

ROY, S., HILL, A. V. S., KNOX, K., GRIFFITHS, D. & CROOK, D. 2002. Association of common genetic variant with susceptibility to invasive pneumococcal disease. *British Medical Journal,* 324**,** 1369-1369.

RUSSELL, F. M., CARAPETIS, J. R., SATZKE, C., TIKODUADUA, L., WAQATAKIREWA, L., CHANDRA, R., SEDUADUA, A., OFTADEH, S., CHEUNG, Y. B., GILBERT, G. L. & MULHOLLAND, E. K. 2010. Pneumococcal Nasopharyngeal Carriage following Reduced Doses of a 7-Valent Pneumococcal Conjugate Vaccine and a 23-Valent Pneumococcal Polysaccharide Vaccine Booster. *Clinical and Vaccine Immunology,* 17**,** 1970-1976.

SACHSENBERG, N., PERELSON, A. S., YERLY, S., SCHOCKMEL, G. A., LEDUC, D., HIRSCHEL, B. & PERRIN, L. 1998. Turnover of CD4(+) and CD8(+) T lymphocytes in HIV-1 infection as measured by Ki-67 antigen. *Journal of Experimental Medicine,* 187**,** 1295-1303.

SAIFUDDIN, M., SPEAR, G. T., CHANG, C. H. & ROEBUCK, K. A. 2000. Expression of MHC class II in T cells is associated with increased HIV-1 expression. *Clinical and Experimental Immunology,* 121**,** 324-331.

SAMUELSSON, A., BROSTROM, C., VANDIJK, N., SONNERBORG, A. & CHIODI, F. 1997a. Apoptosis of CD4(+) and CD19(+) cells during human immunodeficiency virus type 1 infection - correlation with clinical progression, viral load, and loss of humoral immunity. *Virology,* 238**,** 180-188.

SAMUELSSON, A., SONNERBORG, A., HEUTS, N., COSTER, J. & CHIODI, F. 1997b. Progressive B cell apoptosis and expression of Fas ligand during human immunodeficiency virus type 1 infection. *Aids Research and Human Retroviruses,* 13**,** 1031-1038.

SAN MIGUEL, J. F. 2015. Introduction to a series of reviews on multiple myeloma. *Blood,* 125**,** 3039-3040.

SANTOSHAM, M., WOLFF, M., REID, R., HOHENBOKEN, M., BATEMAN, M., GOEPP, J., CORTESE, M., SACK, D., HILL, J., NEWCOMER, W., CAPRIOTTI, L., SMITH, J., OWEN, M., GAHAGAN, S., HU, D., KLING, R., LUKACS, L., ELLIS, R. W., VELLA, P. P., CALANDRA, G., MATTHEWS, H. & AHONKHAI, V. 1991. THE EFFICACY IN NAVAJO INFANTS OF A CONJUGATE VACCINE CONSISTING OF HAEMOPHILUS-INFLUENZAE TYPE-B POLYSACCHARIDE AND NEISSERIA-MENINGITIDIS OUTER-MEMBRANE PROTEIN COMPLEX. *New England Journal of Medicine,* 324**,** 1767-1772.

SCOTT, J. A. G. 2007. The preventable burden of pneumococcal disease in the developing world. *Vaccine,* 25**,** 2398-2405.

SHIRAI, A., COSENTINO, M., LEITMANKLINMAN, S. F. & KLINMAN, D. M. 1992. HUMAN-IMMUNODEFICIENCY-VIRUS INFECTION INDUCES BOTH POLYCLONAL AND VIRUS-SPECIFIC B-CELL ACTIVATION. *Journal of Clinical Investigation,* 89**,** 561-566.

SIMELL, B., AURANEN, K., KAYHTY, H., GOLDBLATT, D., DAGAN, R., O'BRIEN, K. L. & PNEUMOCOCCAL CARRIAGE, G. 2012. The fundamental link between pneumococcal carriage and disease. *Expert Review of Vaccines,* 11**,** 841-855.

SIMELL, B., KILPI, T. M. & KAYHTY, H. 2002. Pneumococcal carriage and otitis media induce salivary antibodies to pneumococcal capsular polysaccharides in children. *Journal of Infectious Diseases,* 186**,** 1106-1114.

STARSKA, K., GLOWACKA, E., KULIG, A., LEWY-TRENDA, I., BRYS, M. & LEWKOWICZ, P. 2011. The role of tumor cells in the modification of T lymphocytes activity - the expression of the early CD69(+), CD71(+) and the late CD25(+), CD26(+), HLA/DR+ activation markers on T CD4(+) and CD8(+) cells in squamous cell laryngeal carcinoma. Part I. *Folia Histochemica Et Cytobiologica,* 49**,** 579-592.

TINCATI, C., BELLISTRI, G. M., ANCONA, G., MERLINI, E., D'ARMINIO MONFORTE, A. & MARCHETTI, G. 2012. Role of in vitro stimulation with lipopolysaccharide on T-cell

activation in HIV-infected antiretroviral-treated patients. *Clinical & developmental immunology,* 2012**,** 935425-935425.

TITANJI, K., CHIODI, F., BELLOCCO, R., SCHEPIS, D., OSORIO, L., TASSANDIN, C., TAMBUSSI, G., GRUTZMEIER, S., LOPALCO, L. & DE MILITO, A. 2005. Primary HIV-1 infection sets the stage for important B lymphocyte dysfunctions. *Aids,* 19**,** 1947-1955.

TROTTER, C. L., STUART, J. M., GEORGE, R. & MILLER, E. 2008. Increasing hospital admissions for pneumonia, England. *Emerging Infectious Diseases,* 14**,** 727-733.

TROTTER, C. L., WAIGHT, P., ANDREWS, N. J., SLACK, M., EFSTRATIOU, A., GEORGE, R. & MILLER, E. 2010. Epidemiology of invasive pneumococcal disease in the pre-conjugate vaccine era: England and Wales, 1996-2006. *Journal of Infection,* 60**,** 200-208.

TRZCINSKI, K., THOMPSON, C. M., SRIVASTAVA, A., BASSET, A., MALLEY, R. & LIPSITCH, M. 2008. Protection against nasopharyngeal colonization by Streptococcus pneumoniae antigen-specific CD4(+) T cells. *Infection and Immunity,* 76**,** 2678-2684.

TSACHOURIDOU, O., SKOURA, L., ZEBEKAKIS, P., MARGARITI, A., GEORGIOU, A., DANIILIDIS, M., MALISIOVAS, N. & METALLIDIS, S. 2015. The controversial impact of B cells subsets on immune response to pneumococcal vaccine in HIV-1 patients. *International Journal of Infectious Diseases,* 38**,** 24-31.

TU, W. & RAO, S. 2016. Mechanisms Underlying T Cell Immunosenescence: Aging and Cytomegalovirus Infection. *Frontiers in Microbiology,* 7.

USUF, E., BOTTOMLEY, C., ADEGBOLA, R. A. & HALL, A. 2014. Pneumococcal Carriage in Sub-Saharan Africa-A Systematic Review. *Plos One,* 9.

UTSUYAMA, M., HIROKAWA, K., KURASHIMA, C., FUKAYAMA, M., INAMATSU, T., SUZUKI, K., HASHIMOTO, W. & SATO, K. 1992. DIFFERENTIAL AGE-CHANGE IN THE NUMBERS OF CD4+CD45RA+ AND CD4+CD29+ T-CELL SUBSETS IN HUMAN PERIPHERAL-BLOOD. *Mechanisms of Ageing and Development,* 63**,** 57-68.

WANG, Y., TIAN, Y., JIANG, B., WEISER, J. & SHEN, H. 2014. Streptococcus pneumoniae specific Th17 memory immunity provides cross protection against invasive pneumococcal diseases in mice. *Journal of Immunology,* 192.

WESTERINK, M. A. J., SCHROEDER, H. W., JR. & NAHM, M. H. 2012. Immune Responses to pneumococcal vaccines in children and adults: Rationale for age-specific vaccination. *Aging and Disease,* 3**,** 51-67.

WHEATLEY, A. K., KRISTENSEN, A. B., LAY, W. N. & KENT, S. J. 2016. HIV-dependent depletion of influenza-specific memory B cells impacts B cell responsiveness to seasonal influenza immunisation. *Scientific Reports,* 6.

WHITNEY, C. G., FARLEY, M. M., HADLER, J., HARRISON, L. H., BENNETT, N. M., LYNFIELD, R., REINGOLD, A., CIESLAK, P. R., PILISHVILI, T., JACKSON, D., FACKLAM, R. R., JORGENSEN, J. H., SCHUCHAT, A. & ACTIVE BACTERIAL CORE, S. 2003. Decline in invasive pneumococcal disease after the introduction of protein-polysaccharide conjugate vaccine. *New England Journal of Medicine,* 348**,** 1737-1746.

WHITNEY, C. G., FARLEY, M. M., HADLER, J., HARRISON, L. H., LEXAU, C., REINGOLD, A., LEFKOWITZ, L., CIESLAK, P. R., CETRON, M., ZELL, E. R., JORGENSEN, J. H., SCHUCHAT, A. & ACTIVE BACTERIAL CORE, S. 2000. Increasing prevalence of multidrug-resistant Streptococcus pneumoniae in the United States. *New England Journal of Medicine,* 343**,** 1917-1924.

WHITNEY, C. G., PILISHVILI, T., FARLEY, M. M., SCHAFFNER, W., CRAIG, A. S., LYNFIELD, R., NYQUIST, A.-C., GERSHMAN, K. A., VAZQUEZ, M., BENNETT, N. M., REINGOLD, A., THOMAS, A., GLODE, M. P., ZELL, E. R., JORGENSEN, J. H., BEALL, B. & SCHUCHAT, A. 2006. Effectiveness of seven-valent pneumococcal conjugate vaccine against invasive pneumococcal disease: a matched case-control study. *Lancet,* 368**,** 1495-1502.

WHO. 2008. *23-Valent pneumococcal polysaccharide vaccine:WHO position paper* [Online]. World Health Organization. Available: http://www.who.int/wer/2008/wer8342.pdf [Accessed 15 December 2013].

WHO. 2013a. *Bacterial meningitis (including Haemophilus influenzae type b (Hib), Neisseria meningitidis, andStreptococcus pneumoniae)* [Online]. World Health Organisation. Available: http://apps.who.int/immunization_monitoring/diseases/meningitis_surveillance/en/index.html [Accessed 29 December 2013].

WHO. 2013b. *Pneumonia* [Online]. World Health Organisation. Available: http://www.who.int/mediacentre/factsheets/fs331/en/ [Accessed 29 December 2013].

WILEN, C. B., TILTON, J. C. & DOMS, R. W. 2012. HIV: cell binding and entry. *Cold Spring Harbor perspectives in medicine,* 2.

WILLOCKS, L. J., VITHAYATHIL, K., TANG, A. & NOONE, A. 1995. PNEUMOCOCCAL VACCINE AND HIV-INFECTION - REPORT OF A VACCINE FAILURE AND REAPPRAISAL OF ITS VALUE IN CLINICAL-PRACTICE. *Genitourinary Medicine,* 71**,** 71-72.

WING, J. B., SMART, L., BORROW, R., FINDLOW, J., FINDLOW, H., LEES, A., READ, R. C. & HEATH, A. W. 2012. Correlation of Group C Meningococcal Conjugate Vaccine Response with B- and T-Lymphocyte Activity. *Plos One,* 7.

WONG, A., MARRIE, T. J., GARG, S., KELLNER, J. D., TYRRELL, G. J. & GRP, S. 2010. Increased risk of invasive pneumococcal disease in haematological and solid-organ malignancies. *Epidemiology and Infection,* 138**,** 1804-1810.

WRIGHT, A. K. A., BANGERT, M., GRITZFELD, J. F., FERREIRA, D. M., JAMBO, K. C., WRIGHT, A. D., COLLINS, A. M. & GORDON, S. B. 2013. Experimental Human Pneumococcal Carriage Augments IL-17A-dependent T-cell Defence of the Lung. *Plos Pathogens,* 9.

ZHANG, Z., CLARKE, T. B. & WEISER, J. N. 2009. Cellular effectors mediating Th17-dependent clearance of pneumococcal colonization in mice. *Journal of Clinical Investigation,* 119**,** 1899-1909.

ZINNEMAN, H. H. & HALL, W. H. 1954. RECURRENT PNEUMONIA IN MULTIPLE MYELOMA AND SOME OBSERVATIONS ON IMMUNOLOGIC RESPONSE. *Annals of Internal Medicine,* 41**,** 1152-1163.